DEVELOPMENT OF BIOPOLYMERS AND THEIR MODIFIED FORMS AS SUSTAINABLE SORBENT MATERIALS

A Thesis Submitted to the College of

Graduate and Postdoctoral Studies

In Partial Fulfillment of the Requirements

For the Degree of Doctor of Philosophy

In the Department of Chemistry

University of Saskatchewan

Saskatoon

By

LEILA DEHABADI

Permission To Use

In presenting this thesis in partial fulfillment of the requirements for a Postgraduate degree from the University of Saskatchewan, I agree that the Libraries of this University may make it freely available for inspection. I further agree that permission for copying of this thesis in any manner, in whole or in part, for scholarly purposes may be granted by Dr. Wilson who supervised my thesis work or, in his absence, by the Head of the Department of Chemistry or the Dean of the College in which my thesis work was done. It is understood that any copying or publication or use of this thesis or part of it for financial gain shall not be allowed without my written permission. It is also understood that due recognition shall be given to me and to the University of Saskatchewan in any scholarly use which may be made of any material in my thesis. Requests for permission to copy or to make other use of material in this thesis in whole or part should be addressed to:

Head of the Department of Chemistry
University Of Saskatchewan
110 Science Place
Saskatoon, Saskatchewan
S7N 5C9 Canada

Dean
College of Graduate and Postdoctoral Studies
University of Saskatchewan
116 Thorvaldson Building, 110 Science Place
Saskatoon, Saskatchewan S7N 5C9
Canada

Acknowledgements

In The Name of GOD

I would like to express my sincere appreciation to my supervisor Dr. Lee D. Wilson, to whom am greatly indebted by the support and guidance he accorded me throughout the course of my PhD program.

My fervent thanks to the Department of Chemistry for the opportunity to do research and further my scientific career. I wish to thank gratefully to the Dr. Keith Brown for the opportunity to train and work on the NMR spectrometer; the University of Saskatchewan for the Graduate Teaching Fellowship; and the support provided by the Government of Saskatchewan through the Minstry of Agriculture (Agriculture Development Fund; ADF) for this research.

I am grateful to members of my PhD advisory committee, Drs. M. Soledade C. Pedras, Ian Burgess and Lifeng Zhang for their expert guidance.

I wish to thank Drs. Sammynaiken and J. Maley, and K. Thoms (Saskatchewan Structural Sciences Center (SSSC)) for their technical support.

To my colleagues in the Lab; Dr. Mohamed, Dr. Abdalla Karoyo, and Mohamad Mahaninia, Dr. Inimfon Udoetok, Henry Agbovi, Michael Danquah , Chen Xue, for their help and support.

Dedications

This thesis is dedicated to my parents.

Thank you for your love and support.

Abstract

The production of ethanol in the biofuels industry requires methods to remove water from mixtures to improve biofuel quality. To address the large energy footprint of conventional distillative separation of biofuels and water, new materials and methods are required to reduce GHG emissions and to develop more sustainable industrial processing. The overall goal of this research focuses on the sorption properties of biopolymers and their modified forms as adsorbents for fractionation of chemical mixtures such as water/ethanol in binary systems. The short term goals of this thesis are related to the synthesis, characterization, and evaluation of the sorption properties of biopolymers and their modified forms. Moreover, a long term goal relates to the development of biopolymer materials with tunable adsorptive properties for the fractionation of binary water-ethanol (W-E) mixtures. Biopolymers such as starch (linear and branched) and cellulose were modified with variable amounts of epichlorohydrin (EPI) as a cross-linker for the enhancement of physicochemical properties related to sorption processes. The characterization of materials included Thermogravimetry Analysis (TGA), Infrared spectroscopy (FT-IR) and NMR spectroscopy. These methods provided support that incorporation of incremental levels of cross-linker with the biopolymers resulted in variable structure and physicochemical properties related to sorption. This thesis describes four leading edge contributions related to the objectives of this study: i) The development of biopolymers and their modified forms for the controlled uptake of ethanol in binary W-E systems, ii) Evaluation of the adsorption properties using dye probes, nitrogen adsorption, and the use of quantitative NMR (qNMR) spectroscopy as a convenient and rapid analytical tool to quantify uptake of both water and ethanol content in binary solvent systems, iii) Evaluation of biomass and its biopolymer components for the fractionation of W-E mixtures, and iv) Evaluation of the role of solvent effects on the adsorption properties of biopolymers. Based

on the results herein, the biopolymer adsorbents displayed preferential uptake of water over ethanol in binary W-E solutions. The adsorptive solvent uptake selectivity ($R_{selectivity}$; $Q_m(W)/Q_m(E)$) of water over ethanol for a given sorbent material requires an understanding of hydration phenomena, biopolymer structure, and textural properties of adsorbent materials. This thesis contributes to a molecular-level understanding of the solvent fractionation properties of biopolymers and their modified forms, along with the development of green strategies for biofuel separation. The isotherm modeling results show that the monolayer adsorption capacity (Q_m) of ethanol and water by cellulose biopolymer materials along with its cross-linked forms cover a range (Q_m= 1.13−2.44 g/g) of values. The parameters indicate heterogeneous adsorption behaviour, in agreement with the Sips exponential fitting parameter ($n_s \neq 1$). The $R_{selectivity}$ values (($Q_m(W)/Q_m(E)$) obtained at saturative conditions are variable (1.10 to 2.03) and further illustrate that cellulose materials display molecular selective solvent fractionation in binary W−E solutions. By comparison, the Q_m values for starch and its cross-linked forms varied from 0.01 to 2.70 $g \cdot g^{-1}$ for water and ethanol in binary mixtures according to the Sips isotherm model. The $R_{selectivity}$ (Q_m (W)/Q_m(E)) values of starch-EPI adsorbents for water (W) and ethanol (E) in the binary mixtures range from 3.8 to 80. As well, the isotherm results show that the monolayer adsorption capacity (Q_m; $g.g^{-1}$) of biomass such as miscanthus with water Q_m (W) and ethanol Q_m (E) fractions were determined by the best-fit Sips model isotherm parameters for raw Miscanthus (Q_m (W) =8.93 and Q_m (E) =4.15 $g.g^{-1}$) and pretreated Miscanthus (Q_m (W) =4.73 and Q_m (E) =3.22, $g.g^{-1}$). The fractionation properties of Miscanthus revealed variable $R_{selectivity}$ ($Q_m(W)$/ $Q_m(E)$) values: raw Miscanthus ($R_{selectivity}$=3:1); pretreated Miscanthus ($R_{selectivity}$ = 1.5:1), and lignin isolates ($R_{selectivity}$ = 1: 5.4). The solvent interactions of biopolymers impact their biodegradability, recyclability and tunable physicochemical properties for various applications that employ composite materials,

pharmaceutical delivery systems, paper production, fibers and biofuel production. Studies of the hydration properties of these materials were carried out that include dielectric absorption, Raman spectroscopy and Differential Scanning Calorimetry (DSC) to determine the structural and thermodynamic properties that reveal differences in biopolymer-solvent interactions that depend on the nature of the system.

Table of Contents

List of Tables

List of schemes

List of Figures

List of Abbreviations and Symbols

AC……. Activated Carbon

AM……. Amylose

AP……. Amylopectin

CE……. Cellulose

D_2O…….Deuterium oxide

DMSO-d_6……Deuterated dimethyl sulfoxide

DTG……..Differential Thermogravimmetry

E…….. Ethanol

EPI……...Epichlorohydrin

FT-IR…… Fourier Transform Infrared

FWHM..……Full-width at half-maximum

GCO……..... GC-Olfactometry

HLB…….. Hydrophile-Lipophile balance

IUPAC ……International Union of Pure and Applied Chemistry

KF…….. Karl Fischer

LOD……. Limit of Detection

mM…….. Millimolar

NCMs……... Nanocomposite Membranes

NMR…….. Nuclear Magnetic Resonance

PFO……. Pseudo- First -Order

PHP…… Phenolphthalein

PNP…… Para-nitrophenol

PSO……. Pseudo- Second- Order

PS……. Polysaccharide

PV ……..Pervaporation

qNMR…….. Quantitative NMR

RT……... Repetition Time

SEM…….Scanning Electron Microscopy

TGA……..Thermogravimetry Analysis

THF…… Tetrahydrofuran

UV-Vis……Ultraviolet-Visible

W…… Water

λ ……Deformation ratio

V_m……...Molar Volume

$\mu_{l,c}$ ……..Activity of the solvent

$\mu_{l,u}$ ……Activity of the non-cross-linked polymer

V_0 ……Swelling equilibrium

V_c ……..Polymer volume fraction

Q……..Equilibrium volume swelling degree

C_0……...Initial concentration of adsorbate

C_e…….Equilibrium concentration of adsorbate

Q_e……...Sorption capacity

N……....Number of nuclei

I……..Integral area

M…….Molar mass

K_d……partition coefficient

V_i…….Volume of pores

S_i……...Surface area of pores

$\bar{x}$……..Distance of particle surface

θ……Local volume fraction of water

$\bar{q}$……Water flux

D……...Diffusion coefficient

V_{excess}……...Excess volume of water

$\bar{v}$ ……Average velocity

$\bar{n}$ …….Normal vector

t ……Thickness of the adsorption layer

γ ……Surface tension

μ…………………………………………………………………………...Chemical potential

CHAPTER 1

1 Introduction

1.1 Bioethanol

One of the most fundamental parts of our universe is energy. Energy is defined as the ability to do work and it takes on many forms. On the earth, the most common sources of energy used by industry are based on fossil fuels. Since the source of fossil fuels is limited, other alternative sources[1] of energy such as hydro, wind, biofuels, solar, and geothermal energy[1,2] should be explored for future use. Among these sources, biofuels have drawn great attention recently because it is considered economically viable and more environmentally sustainable. The term 'biofuel' is widely used to refer to any fuel derived from renewable resources. Bioethanol is an example of a biofuel that can be blended with other hydrocarbon-based fuels. As an advantage, the mixing of ethanol with gasoline results in fuel with lower emissions of carbon monoxide. Also, the presence of volatile organic compounds in bioethanol may mitigate some of the negative effects of the hydrocarbon-based fuels when they are mixed. Therefore, bioethanol is an excellent gasoline blending component.[1,3]

The main source of bioethanol is the fermentation of sugar, starch, or cellulosic biomaterials.[1−4] Generally, the two main groups of cellulosic materials utilized for bioethanol production are waste residues and dedicated crops. Some of the commonly used waste residues are municipal waste, forestry residues (from logging or milling) and agricultural residues (corn stover, wheat straw, etc.). Examples of dedicated crops are perennial herbaceous crops, and switch grass or woody crops.[5,6] The fermentation process leads to production of water-ethanol mixtures containing 8−12 wt % ethanol in water, along with carbon dioxide.[7] The presence of water in mixed gasoline or ethanol fuels causes problems due to the occurrence of phase separation in the mixtures.[1] Anhydrous ethanol, also known as absolute ethanol, is a clear, colourless liquid containing at least 99.5% ethanol by volume at 15.6˚C. The ethanol favourable for use as additive in fuels must contain less than 0.5 wt % amount of water. Therefore, there is an incentive to develop methods for removal of water from ethanol for eventual use in fuel mixtures.[2] The conversion of biomass into anhydrous ethanol by fermentation involves three stages: (i) At the first stage, biomass is converted into fermentable forms of sugar; (ii) the fermentation of produced sugars that yields a mixture with 10-12% ethanol by weight; and finally, (iii) the produced anhydrous ethanol is separated and purified.[1] Unfortunately, the separation of ethanol from mixtures that contain high

water content after the fermentation process is neither economical nor environmentally friendly.[4] Various techniques are widely used for water/ethanol separation but they come with drawbacks, due to the energy inputs and the production of unwanted by-products.[2] Therefore, there is a need to develop alternative separation techniques, especially with regard to reducing the energy footprint of such chemical separations. The following section describes the common separation techniques for water/ethanol mixture in brief.

1.2 Existing methods for separation of water-ethanol

The ethanol-water mixture produced through fermentation of sugars or biomaterials has an azeotrope at 78˚C. By their nature, azeotropic mixtures cannot be effectively separated using a conventional distillation process. During the production of anhydrous ethanol, the separation of the diluted aqueous ethanol via distillation takes place up to its azeotropic composition (95.6 wt.% ethanol).[1] For separation of this azeotropic composition, several techniques have been used such as pervaporation, adsorptive distillation, azeotropic distillation, extractive distillation, and reactive distillation.[1] Pervaporation (PV) is a special membrane-based technique used widely for separation of organic solvents because of its ease of operation, energy-conserving nature, and its effectiveness.[8] Another method used for the separation of water from ethanol is adsorptive distillation.[9] This method is limited because the azeotropic mixtures cannot be completely separated, without the use of adsorbents such as molecular sieves, chloride salts, and silicagel.[9] Heterogeneous azeotropic distillation is one of the most-often used methods for the separation of a mixture that includes the ethanol–water azeotrope. This separation process requires high external energy input which is the big disadvantage of this method.[10] Extractive distillation has been proven as a promising ethanol-water separation technology because of its low energy consumption, but its efficiency does not justifies its wide usage.[11] Reactive distillation is a traditional method and, due to its potential for profit (e.g. enhanced overall rates by overcoming very low reaction equilibrium constants and ease of separations), selectivity improvements (which reduce excess raw materials usage and by-product formation), reduced energy input, and the reduction or elimination of solvents, it is a better distillation technique. However, the drawback of the reactive distillation process is the difficulty in separation of residual water from the products.[12] For instance, a study by Dirk-Faitakis and Chuang revealed that the use of this method for the removal of water from an ethanol/water mixtures removed approximately 90% of the water, but led to the production of

a mixture consisting of ethanol and other by-products. Therefore, this method cannot produce ethanol with high purity.[13]

Among all methods mentioned above for the separation of water and ethanol, the higher amount of energy consumption during the separation process is a shortcoming or limitation of these techniques (*cf.* Table 1.1) that affect the overall sustability of biofuel production.

Table 1.1 Energy requirement for separation of water and ethanol.[14]

Purification (Wt.%)	Energy Input (kJ/kg Ethanol)	Process Method
8.0-99.5	10376	Distillation
95.0-99.5	3305	Azeotrope Distillation
95.0-99.5	423	Pervaporation

Adsorption processes are an alternative technique that can be considered as a low-energy option due to its simpler design and easier operation.[15,16] Adsorption refers to the accumulation of large number of molecular species (adsorbate) at the surface of liquid or solid phase (adsorbent). Various adsorption techniques are employed for water-ethanol separation that include fixed-bed adsorbents, as well as adsorptive dehydration.[17] The efficiency of an adsorption process is related to the adsorbate's chemical and structural properties including the textural properties and surface chemistry of the adsorbent. Delgado *et al.*[18] investigated the separation of ethanol–water mixtures using selective adsorbents in cyclic column adsorption processes. This method looks appealing due to separation of pure ethanol with low demand of energy.

During an adsorption process, the existence of favourable adsorbate-adsorbent interactions determines the effectiveness of the process. For example, adsorbents with different structural and chemical properties and even different shapes behave differently toward adsorbates. To gain a better grasp of the adsorption process, familiarity with the physicochemical properties of various types of adsorbents is essential. These properties detect whether the adsorbate is able to interact with the adsorbent and requires due attention. A favourable adsorbent must possess properties such

as good thermal stability and high surface area, where higher surface area offers more active sites for uptake of materials of interest. In addition, the chemical functionalities on the surface of the adsorbent play an important role in their adsorptive properties. Silica materials like zeolite and molecular sieves are inorganic adsorbents that adsorb water preferentially, based on the differences in the molecular sizes and physical properties of water and ethanol.[19] A molecular sieve contains small pores with a uniform size, which enable selective adsorption of the water over ethanol; since the latter cannot enter the pores of the sieve with a diameter of 4 Å. However, the downside of this adsorbent is its expensive cost. Activated carbon (AC) is one of the most commonly used adsorbents due to its unique properties (e.g. high surface area and functionality). Activated carbon with different particle sizes can be used as a promising adsorbent for water uptake.[120-27] However, the high cost of activated carbon motivates the search for alternative sources of adsorbents such as biomaterials originating from local agriculture in order to separate mixtures.[28] The use of bio-based adsorbents such as starch for separation of water from ethanol was first introduced by Beery *et al.*[17] Another attempt to utilize starch-based adsorbents was carried out in a bid to replace the commercialized adsorbent 3Å zeolite.[29] These studies have illustrated the feasibility of adsorption process for the separation of water/ethanol mixtures in the vapor phase. However, studies on use of bio-based adsorbents for the separation of water/ethanol mixtures in the liquid media are not well established. Previous studies have demonstrated that starch and cellulose based materials have affinity for separation of water from ethanol in liquid phase due to hydrogen bonding (*cf.* Scheme 1.1) that results in the formation of stable complexes.[17,30] Beery *et al.*[17] showed that the adsorption capacity of several types of starchy materials (e.g., white corn grits, amylase-modified yellow corn grits) was comparable to that of inorganic adsorbents like silica when the water concentrations is above 10%.The following sections provide further details on application of polysaccharide-based materials as adsorbent.

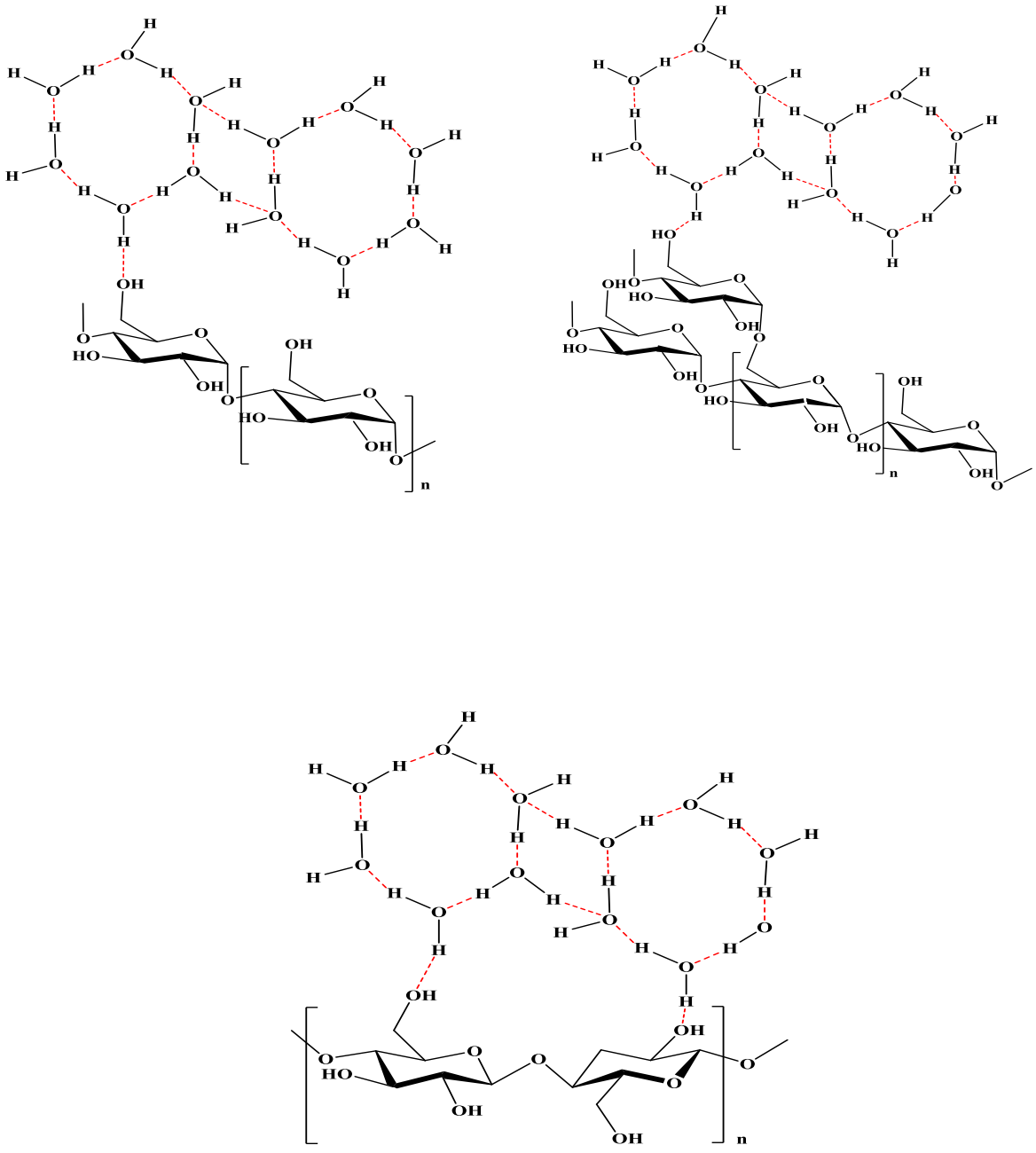

Scheme 1.1 Hydrogen bonding interactions between solvent-biopolymer and solvent-solvent systems, where the dashed lines represent hydrogen bonding.

1.3 Polysaccharide as adsorbent materials

Polysaccharides are biopolymers composed of long chains of monosaccharide units bound via glycosidic linkages that exist as linear or branched forms.[31] Often, the repeating units consist of six carbons with the following general formula: $(C_6H_{10}O_5)_n$, where $40 \leq n \leq 3000$.[32] Examples of polysaccharides include starch, glycogen, cyclodextrin, cellulose, and chitin. They possess specific properties that make them amorphous or insoluble in water based on their structure.[33] Recently, a number of approaches have been considered to develop the low-cost and more effective adsorbents using natural polymers. Among these, polysaccharides such as chitin,[33,34] starch,[35,36] and their derivatives,[37,38] cyclodextrin[39-41] deserve consideration due to their physio-chemical properties. These types of biopolymer are used as adsorbent materials because of their thermal stability, high reactivity/selectivity affinity towards polar compounds depending on functionality (hydroxyl, amine) of the polymer chains. Undoubtedly, as mentioned before, activated carbon had been the most common adsorbent for wastewater treatment throughout the world.[37] The high adsorptive capacity of activated carbon toward pollutants, especially metal ions, make it an effective industrial adsorbent. Its adsorptive capacity relates to the unique structural characteristics such as its unique porosity and surface area. However, some disadvantages of activated carbon include its non-selective uptake and high-cost. In addition, the treatment for regeneration of activated carbon can be costly. These challenges with the use of activated carbon has triggered the demand for alternative materials where greater interest on the development of new adsorbents using polysaccharide biopolymers.

Polysaccharides are good alternatives for activated carbon because they are highly abundant, low cost, where such adsorbents require little processing because of their functionality.[33] The efficiency of polysaccharides as sorbent materials is dependent on their physicochemical properties and are discussed in the following section.

1.3.1 Polysaccharides and their physicochemical properties

Cellulose, chitosan and starch are highly abundant biomaterials on the earth, where the differences between them lie in their functionality and composition. For instance, the repeating unit of starch and cellulose is the glucopyranose unit, where cellulose is more rigid than starch due to strong intra/inter molecular hydrogen bonding network within its structure. The greater flexibility of native starch relative to cellulose is affirmed by the presence of both amylopectin and

amylose in its structure.[33,42] Chitosan is a partially deacetylated form of chitin that is produced commercially at low cost. The difference between chitosan and cellulose/starch is based on their sources and the functionality at C2 of the glucopyranose unit. Chitosan is animal based and possess an $-NH_2$ or $-NHCOCH_3$ group at C2 while cellulose and starch are majorly plant based polysaccharides and has an -OH group at C2 (*cf.* Scheme 1.1). Biopolymers possess many advantages like non-toxicity, biocompatibility, biodegradability, high reactivity, chelation ability that make them excellent materials to be used as adsorbent in large-scale in industries.[33] The physicochemical properties of polysaccharides are mainly attributed to: (1) high hydrophilicity due to the presence of hydroxyl functional groups of glucose units; (2) presence of variable functionalities like acetamido, primary amino and/or hydroxyl groups; (3) flexible structure of the biopolymer chain. Since the detailed discussion about the properties of all type of polysaccharides is not possible, the following section describes the sources, structure, composition and physicochemical properties of the starch and cellulose with greater detail due to their relevance to the objectives of this thesis research.

1.3.2 Sources, structure and composition of polysaccharides

1.3.2.1 Starch

Starch is a promising biopolymer material for adsorption applications because of its low cost and abundance. It is a major source of energy in many plants and has functional utility for various applications.[43] Starch mainly forms granules and the morphology, composition, and structure of starch in each plant is distinct from other species and governed by genetic and environmental factors. Starch functionality is controlled by its components, amylose and amylopectin, as well as the arrangement of these components inside of the granular structure.[44] The unique properties of starch such as linear *vs* branched starch, molecular weight and composition gives it versatile potential for use as a raw material for diverse applications in textiles, adhesives, and various food industries.[45,46] Starch can be sourced from cereal grains (e.g., maize, rice, wheat, barley, oats, and sorghum) and root crops (e.g., sweet potatoes, cassava, arrowroot, and yam). However, the mainstream sources for starch are corn, potato, rice, and wheat, which are widely used as foods throughout the world. But in tropical regions starches are sourced from other plants such as tapioca (cassava) and cowpea. Starch contains two types of polysaccharide components: amylose (linear) and amylopectin (branched), where both polymers contain α-D-

glucose units. In amylose, all units are linked via α-(1 → 4) glycosidic linkages; whereas in amylopectin, another type of linkage occurs via α-(1 → 6) after approximately every 20 units. (*cf.* Figure 1.1).

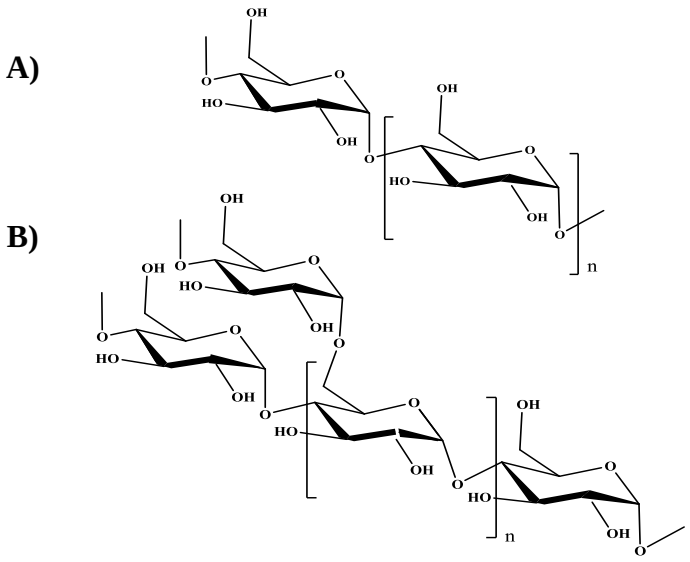

Figure 1.1 Molecular structure of starch: A) Amylose and B) Amylopectin.

The molecular properties of amylopectin and amylose such as size, shape, structure and polydispersity are governed by the origin of plant species. The length of amylopectin units are relatively short compared to amylose molecules where they are typically *ca.* 18–25 units long.[47,48] In amylopectin, the chains with short units tend to cluster together, where the units of clusters are interconnected by longer chains. In a classification offered by Peat *et al.*[49], chain type A is defined as unsubstituted, chain type B are substituted by other chains, and type C caries the sole reducing end group. However, type B in most of the cases can be further subdivided into other B-chains. The B-chains can be classified according to their positions in the cluster structure model as suggested by Hizukuri.[50] This classification of chain (type B) cannot be used for amylose since it has no clusters.[51]

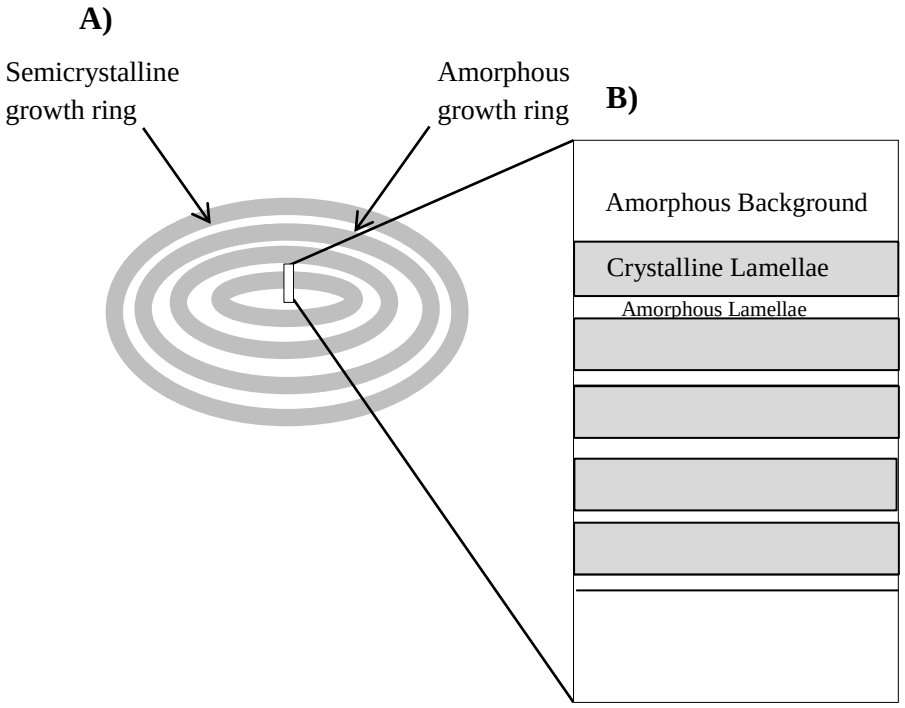

Figure 1.2 Starch granule structure, A) amorphous and semi-crystalline growth rings and B) amorphous and crystalline lamellae.[52]

Another notable aspect of starch is that it is deposited as semi-crystalline granules where periodicity of the alternating amorphous and crystalline domains result in a hierarchical structure (Figure 1.2). The native starch granules contain amorphous and crystalline domains arranged in alternating concentric rings. The degree of crystallinity is a major factor that governs the properties of starch.[53]

As mentioned above, starch granules are not perfect crystals but semi-crystals where crystalline and amorphous regions exist concurrently and the degree of crystallinity varies between 15 to 50% depending on the origin and the method of preparation. The crystallinity of starch depends on the moisture content as well. For example, when moisture content reaches to *ca.* 27% the maximum crystallinity is observable and a minimum of 8% moisture content is necessary for obtaining diffraction pattern.[54]

For starches rich with amylopectin content, the crystallinity originates from intertwining of the outer chains of amylopectin in the form of double helices. This combination along with variable moisture content results in formation of the crystalline lamellae. Although, amylose has no significant effect on crystallinity of normal and waxy starches due to higher amylopectin

content, it may contribute to the change in crystallinity when its content is much higher than that of amylopectin.[55-57]

The average length of starch biopolymers can vary widely, ranging from 20–100 μm, depending on its source. For instance, the average granule size of potato starch ranges from 1 to 20 μm for small and 20 to 110 μm for large granules, while in corn starch, the size varies from 1 to 7 μm for small and from 15 to 20 μm for large granules. Rice starch has a relatively smaller granule size, ranging from 3 to 5 μm in size. For wheat starch, the average diameter ranges from 10 to 35 μm for large granules and 1–10 μm for the small granules. With respect to the shape, potato starch granules are oval and irregular, cornstarch granules are angular, and rice starch granules are pentagonal and angular. Wheat starch is granules are disk-like or lenticular in shape as well as roughly spherical or polygonal depending on the diameter.[58] In addition to the main sources of starch indicated earlier, there are mutant genotypes of some cereals that contain starches with a higher content of either amylose or amylopectin; the latter is called waxy. Native starch granules are insoluble in water and, when heated in water, granules absorb water and swell. Furthermore, starch can be modified physically or chemically to produce a wide range of modified starches.[46, 59]

1.3.2.2 Cellulose

The cell walls of plants and other organisms are mainly composed of cellulose.[60] Rayon is a textile produced from cellulose. Hence raw material for textile production and feedstock for rayon are used synonymously. Figure 1.3 depicts cellulose and its structure.

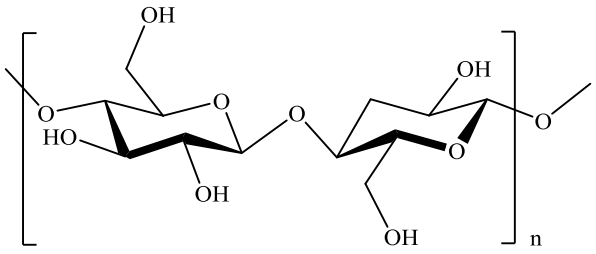

Figure 1.3 The repeat structural unit of the cellulose biopolymer.

The fibril structure of cellulose possesses both amorphous and crystalline domains with a crystallinity degree ranging between 40-60 %. The degree of crystallinity in the cellulose may indicate the accessibility of the hydroxyl groups, where the amorphous region offers more accessible hydroxyl groups compared to the crystalline region.[61] The accessibility of the hydroxyl groups of the cellulose can be assigned as follows: C6-OH >> C2-OH > C3-OH.[62,63] Existing intermolecular hydrogen bonds between adjacent cellulose strands are one of the main characteristics that cause cellulose to exist in a variety of polymorph forms.[64] Cellulose, as a natural polymorph, can be classified into Type I and Type II crystal structures. In cellulose Type I (with parallel arrangement of the chains), the hydrogen bonds form just between chains of the same sheet.[64,65] Whereas, in cellulose Type II (with an anti-parallel arrangement of chains) the hydrogen bonds can also be formed between sheets to create a three-dimensional (3D) network.[66] Since cellulose has hydrophilic properties, hydration plays a key role, mainly through the dissociation and reformation of intra- and intermolecular hydrogen bonds, which can alter the cellulose structure.[67] Starch and cellulose based adsorbents can serve as a possible alternative for the production of green materials due to their low cost, availability and renewability. They can be used in ways that produce smaller amounts of wastes (e.g., byproducts) which ultimately decrease the environmental impact.[68] However, to make these polysaccharides efficient adsorbents, various forms of modifications are required and are discussed in the following section.

1.3.3 Polysaccharide modification

Generally, biomaterials can be modified using many techniques and methods to improve adsorptive capacity of the adsorbents. These modifications can be conducted using chemical or physical treatment. The modified biomaterials have variations in their textural properties, surface chemistry, surface area and the Hydrophile-Lipophile Balance (HLB).[69] The strategies for modification usually include cross-linking, etherification, esterification and oxidation, cationization, grafting and composite formation etc. These modification strategies have been shown to improve the adsorptive properties of polysaccharides. Among all the types of modifications, cross-linking is most common due to ease of reaction and availability of much different types of cross-linkers. The following section describes detailed information on why using cross-linking can be a versatile method for modification of polysaccharides to prepare the new adsorbents.

1.3.4 Cross-linking of polysaccharides

Cross-linking of polysaccharides with various linkers is one of the techniques used to modify both physical and chemical properties of adsorbents. Cross-linking results in changes to the solubility, hydrophobicity, and solvent swelling properties. The alteration of the properties of adsorbents can eventually lead to enhancement of their adsorption capacity due to increasing the surface area via the pillaring effect (*cf.* Scheme 1.2)[70] and creation of favourable functional groups on the surface of the polysaccharides. In addition, cross-linking of polysaccharides may alter the mechanical stability of adsorbents. Several methods are available for cross-linking polysaccharides by using different cross-linkers at different conditions to achieve covalent bonding between polymer chains. Cross-linking can occur by chemical (covalent or ionic) or physical means (hydrogen bonding, hydrophobic/van der Waals interactions), where the structural and physicochemical properties of the polymer can be altered significantly.[71] Cross-linkers not only give favourable functionalities to the polymers but also alter their structural properties (e.g., surface area, pore size, and rigidity). When polymers are modified via cross-linking in order to prepare adsorbents, the length of the cross-linker chain can alter the structural properties (e.g., spacing between chains), and the number of the functionalities on the cross-linkers can change the chemical properties (e.g., polarity) of the prepared adsorbents.[70] Cross-linking can increase the surface area of the material since the process leads to exposure of functional groups such as amine and hydroxyl groups. By exposing these functional groups, the sorption of adsorbates on the surface of the biomaterials can occur. Additionally, due to the "pillaring effect", sorption can also take place at the internal sites where intraparticle diffusion can play a role and particle size controls the accessibility of these active sites for adsorption (Scheme 1.2).[70]

As mentioned above, the type of functional groups is one of the major elements to determine the required technique for cross-linking. Cross-linking might occur via polymerization of monomers with suitable functionalities (using condensation), or through covalent bonding between polymer chains (by irradiation). Another technique for cross-linking is irradiation using high-energy ionizing radiation. In this process of cross-linking, the polymers absorb radiation energy so that chemical bonds are broken and free radicals are formed, which results in new chemical bonds upon reaction of the free radical sites. This high-energy ionizing radiation can be supplied by sources like an electron beam (e-beam), gamma radiation, or X-rays.[72] All these modifications alter the

chemical structure of the polymer during the cross-linking process. However, the chemical cross-linking is beneficial since it offers greater diversity for introducing the functionalities. In the chemical cross-linking process, the numerous chemical cross-linkers can react with the functional groups present in carbohydrates, and can provide materials with substantial improvements in their textural and surface chemical properties.[73] Cross-linkers such as glutaraldehyde (GLU) and epichlorohydrin (EPI) have been employed widely for cross-linking of carbohydrates. Since epichlorohydrin was used as a cross-linker in this research, the rest of this section provides more details corresponding to this cross-linker.

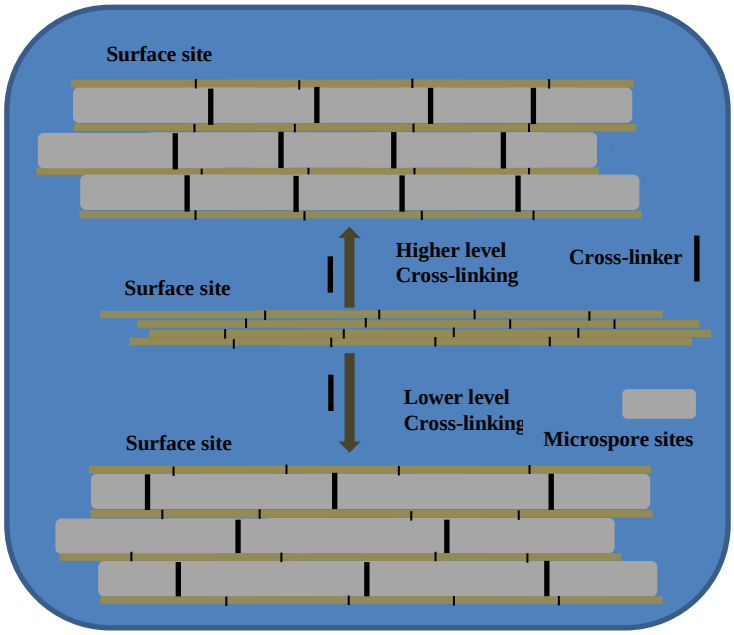

Scheme 1.2 Schematic illustration of the pillaring effect in cross-linked biopolymers.[70]

EPI is one of the most common cross-linkers used for modification of polysaccharides since its reaction can occur in aqueous environments at moderate temperature that offers a water-based reaction pathway.[74] Though EPI is toxic, cross-linking with polysaccharides results in the formation of non-toxic products, where excess or unreacted EPI can be removed through solvent washing thus supporting sustainable and green chemistry.[75]

The mechanism of reaction with EPI was studied by Jyothi *et al.*[76] using determination of the unreacted EPI molecules. The cross-linking of starch using EPI occurs through a series of steps. Depending on the reaction conditions, different functional groups can react either with one or two molecules of EPI. The cross-linking reaction is influenced by a variety of factors such as starch

concentration, viscosity, heating rate, temperature, and amount of shear, as well as solubility with other dissolved solutes and polymers.[71]Hirsch *et al.*[77]reported that time, temperature, concentration and mole ratio of the reactants are the main factors that affect the cross-linking reaction. The study of Kuniak *et al.*[78] reported that EPI can react with starch via glycerol monoether substituent by controlling the time, temperature and mole ratio of the reactants. According to earlier literature, the reaction of EPI with starch in an alkali condition leads to the formation of glycerol monoethers and diethers.[79,80]

Diverse cross-linkers have been employed to modify cellulose via hydroxyl groups under alkali conditions.[81] For instance, cross-linking of cellulose using adipic dihydrazide was used to produce gels with various physicochemical properties.[82] Berger *et al.*[83,84] classified cellulose and starch gels prepared via cross-linking as physical and chemical gels. Based on his classification, chemical gels are irreversible covalent links, while physical gels are formed by various reversible links. Application of formaldehyde-based dimethylol dihydroxy-ethylene urea (DMDHEU) as cross-linker agent for preparing press-durable agents was considered to produce wrinkle resistant cellulosic fabrics in the textile industry. Also, employing of polycarboxylic acids as cross-linking agents was reported in the 1960s.[85] In general, EPI is a commonly used cross-linker for modification of properties of cellulosic materials.[86]

After reviewing the examples of single component polysaccharides and their modified forms as adsorbents, an investigation of properties of biomass materials which contain multi-component polysaccharides is essential. The following section will describe some useful information on structural and physio-chemical properties such materials in greater detail.

1.3.5 Biomass adsorbents

Recently, there has been increasing interest in the use of cheaper and more recyclable adsorbents. Biomass is available abundantly material from wastes of the agricultural industry and have the capability to be used as low-cost adsorbents. Biomass adsorbents possess complex structures and are mainly composed of polysaccharides such as cellulose and hemi-cellulose. Depending on their structural composition, the textural properties and surface chemical properties of biomasses may vary. In particular, their adsorptive capability toward water would be of interest due to the presence of abundant oxygen containing groups (e.g., –OH, C=O, C-O-C, etc.) in their biopolymer structures that may serve as potential ligation sites, make them suitable as desiccants.

Many studies have been conducted in ethanol dehydration using various biomass materials such as corn,[87,88] corn meal,[89,90] corn grits,[16,91] cellulose materials,[92, 93] and starch.[94,95]

Miscanthus (commonly known as elephant grass) is one of the main biomass sources for the preparation of activated carbons, but it has the potential for use as an adsorbent material in its native form. Miscanthus is a low-cost, abundant, and renewable material with about 20 species found in nature. Miscanthus belongs to the *Gramineae* family and mainly can be found in east and Southeast Asia, the Pacific islands, and other regions. Among several crops used for energy generation (e.g., corn, wheat, or soy), Miscanthus, with its unique ability to self-fertilize, yields incredibly high output. The dry matter in this plant yields 2 tons per acre each year, where its high yield production can continuously last up to 20 years. In addition, it has great environmental adaptability as well as low water and fertilizer requirements, which affords its survival in variable climatic environments. Miscanthus can be considered as a typical energy crop because of high energy content and low moisture content after harvest.[96] Miscanthus consists of three major biopolymer components with variable composition: cellulose (40 to 60 w_t %), hemicellulose (20 to 40 w_t %), and lignin (10 to 30 w_t %). It can be inferred that the structure and physicochemical properties of such biopolymers are variable in nature depending on their composition.[97] Another aspect of this plant is that it has a low mineral content compared to other biomass resources. This aspect makes Miscanthus one of the top energy crops.[98] As mentioned above, while Miscanthus recently has gained attention either for energy production or as a precursor to generate activated carbon, research on its potential as an adsorbent is limited.[99] Different types of Miscanthus have been used as adsorbents for treatment of waterborne contaminants. In one study, the Chinese Reed (*Miscanthus sinensis*) was employed for the removal of Cr (III) from wastewater in which the variable parameters were studied using a batch mode adsorption method.[100] Osman *et al.*[101] proposed an application of Miscanthus for adsorption of heavy metal from aqueous solution. Their results revealed a high removal capacity up to 88% occurs for variable types of Miscanthus.

The study of the properties of the adsorbent/adsorbate systems cannot solely and completely reveal the entire factors that govern the adsorption process because the media in which adsorption takes place also plays a critical role. For this reason, the following section offers some important information about the interactions between adsorbate/adsorbent system and solvent to gain better insight on the adsorption process.

1.3.6 Biopolymer solvent interactions

Hydration phenomena of polymers are related to the interaction of water with natural and synthetic polymers due to the unique physicochemical properties of water. Hydration plays a key role in the adsorption process due to the microenvironment effects and adsorbate for binding at adsorption sites, along with alteration of the morphology of the polymer in a solvent phase (ionization processes) as a result of its variable HLB.[102] In one study, Mohamed *et al.*[103] demonstrated variable tertiary structures (morphology) of polymer materials upon cross-linking of β-CD with diisocyanates under thermodynamic *vs.* kinetic conditions. The study revealed that materials with variable solvent accessibility can be obtained due to the type of cross-linker and the degree of cross-linking was correlated to the variable HLB of the final polymer.

In the hydration process, water molecules can be divided into two forms: "bound water" and "unbound water." Bound water is divided into freezing and non-freezing components, whereas; unbound water is divided into trapped and bulk contributions. Generally, hydration is measured by determining the amount of bound water interacting with the solute. This term can be defined as "non-bulk" water because it is more closely associated with the solute rather than the solvent. The freezing point for unbound water is the same as normal water (< 0 °C depending on cooling rate).[104] However, some water is likely to take a longer time to freeze, up to 24 h in some cases. In the reversible transition, bound freezable water undergoes fusion at a lower temperature compared to normal water, which exhibits a reduced enthalpy of fusion (melting).[105]

One way to distinguish bound water from other types is its relative tendency to freeze. Calorimetry measurement may not be a good assessment of the level of hydration. In hydration phenomena, an alternative way to determine the bound water is by the use of relaxation methods in the NMR spectroscopy. Since the NMR relaxation times strongly depend on the mobility of the molecules, particularly on their rotational motion, proton spin-lattice (T_1) and proton spin-spin relaxation times (T_2) parameters can be used for determining the exchange kinetics between free and bound states of water molecules onto the adsorbent if only intramolecular dipole-dipole interactions of the water molecules are present as a relaxation mechanism. It is notable that the time resolution for the NMR technique is combination of dynamic and steady state while other methods (e.g., GC) may run at steady state. One of the best methods to differentiate among the types of hydration are calorimetric methods such as DSC, where the enthalpy of the phase change is determined.[106,107] Thermogravimetric methods also offer an assessment of biopolymers with

bound water, which is based on measurement of weight loss changes due to differences in the desorption profile of bound solvent as a function of temperature. The investigation of the hydration on cross-linked polysaccharides is sometimes challenging due to the presence of the biopolymer branches or cross-linked domains. This leads to a more low-density water structure and stronger binding of the water micro-pools.[108] Alternative methods for defining bound and unbound water are based on bound water being divided into non-freezing and freezing.[109]

Practically, the effects of water on polysaccharide adsorption properties are complex and become even more complicated when other materials (e.g., adsorbates, buffers, etc.) are present. Water molecules may compete for adsorption through intramolecular and intermolecular hydrogen bonding.[110] The entropic changes that occur when water interacts via hydrogen bonding are high (up to about 20.8 kJ mol^{-1} or more at 25 ˚C for a totally "frozen" molecule) and this must be compensated for through the formation of stronger, or extra, hydrogen bonds.[111] The uniqueness of the physicochemical properties of water[112] contribute to the remarkable hydration properties of adsorbents in aqueous solution[113] and governs the hydration phenomena in physical and biological processes.[114] In biopolymers, the role of hydration effects can be understood by their tertiary and quaternary structures, in agreement with the relative surface accessibility of the hydrophilic groups in the presence of water. Thus, an understanding of hydration and role of water molecules in an adsorption process is essential for understanding the binding affinity and molecular selectivity of adsorbates in aqueous solution. Due to the existence of abundant hydroxyl groups of cellulose, hydration occurs at the biopolymer surface.[115] Hydration of cellulose can be affected by the textural properties (e.g., surface area and pore structure) because of the variable functional group accessibility of the polar groups (hydrogen bond donors and acceptors).[116]

1.3.7 Solvent swelling

The increase in the volumes of a biopolymer due to the uptake of a liquid or gas species is referred to as swelling. It usually leads to an alteration of the mechanical properties of the resulting biopolymer. Swelling is a significant property of biomaterials that affects adsorption processes. Swelling depends mainly on three factors: (1) affinity and accessibility of the solvent to the polysaccharide (2) The length of the chains between cross-links and (3) porosity based on surface area and electronic surface charge of the material lead to counter ion accumulation.These three factors can be altered by cross-linking of an adsorbent material. Cross-linking can reduce or

increase the 3-D nature of a polymer network, thus affecting the adsorptive properties of the polysaccharide material in a solvent. The swelling properties of the polysaccharides can be determined based on the entropy of mixing of a polymer network within the aqueous medium, where the enthalpy of water-polymer interaction and elastic restoring force of the polymer network occur.[117,118] Starch is known to swell in aqueous solutions and its structural modification may result in alteration of its swelling properties. The properties of polysaccharides like cellulose and starch are highly influenced by their structure and composition since they can affect the water molecule dynamics and diffusion ability into the system. For example, altering the amylose/amylopectin ratio is one of the major factor that plays a role in the swelling properties of starch materials due to variable chain length distribution between amylose and amylopectin.[119] Other properties such as molecular weight distribution, and the degree branching of amylopectin are also known to influence the functional and swelling properties of starch.[119,120]

The presence of free hydroxyl groups in the amorphous region of cellulose favours strong attraction to many solvents and components in a solution environment. During the adsorption process in aqueous solution, the hydrogen bonds of the amorphous region in anhydrous cellulose constantly start to break and these hydrogen bonds in the cellulose start to replace with the hydrogen bonds between hydroxyl groups of cellulose and water. When absorbed water within the biopolymer structure of cellulose reaches the saturation point, water molecules continue to enter the pores of the cellulose fibril to form another layer of adsorbed water (*i.e.* capillary water), which is called free water.[121] Therefore, the swelling properties not only offer valuable information about the structure of the adsorbent materials but also can provide an account for the mode of interactions in variable adsorbent/adsorbate systems.

There are wide ranging forces which affect the swelling of biomaterials. These include osmotic repulsive forces, Brownian motion, van der Waals force and electrostatic force.[122,123] The study by Geffert *et. al* [124] has shown that the swelling of cellulosic materials occur via two steps; i) the filling and activation of empty and collapsed swelling centers with water, and ii) an increase in volume due to actual water uptake.

Capillarity is another factor that has shown to influence swelling properties. Sweijen *et al.*[125]developed a grain-scale modeling technique to produce the capillary pressure–saturation curves for swelling granular materials. By using this model, they could study the effects of porosity change and swelling on the capillary pressure–saturation curve.

Equilibrium swelling is method for characterization of native and modified polymer networks. The idea of equilibrium swelling was first presented by Frenkel, and further developed by Flory and Rehner.[126] The Flory-Rehner theory has been considered for evaluation of the swelling degree of a polymer network swollen to equilibrium in a solvent. In this model, swelling equilibrium from a competition between two forces; i) the entropy of mixing, and ii) rubbery retractive forces is evaluated. Equilibrium swelling is achieved when these two forces balance each other. In Flory-Rehner theory, separability of the mixing and elastic free energies has been calculated separately and it has been assumed that they are considered independent. The difference of the total free energy ΔF, associated with the change of volume induced by swelling, can be presented as:

$$\Delta F = \Delta F_{dil} + \Delta F_{el} \qquad \text{Equation 1.1}$$

Where ΔF_{dil}, is the variation of the 'osmotic' free energy corresponding to the dilution of the polymer network chains and ΔF_{el}, is the variation of the elastic free energy. These two terms are dependent on the conformation of the polymer chains, separately. To assess this point, the experimental data indicated that the variation of the reduced dilation modulus (experimentally available) vs the square of the deformation ratio (λ) is expressed by eq. 1.2.

$$\frac{\lambda}{V_m} \ln\left(\mu_{l,c} \big/ \mu_{l,u}\right) = f\left(\lambda^2\right) \qquad \text{Equation 1.2}$$

V_m is the molar volume of the swelling solvent, $\mu_{l,c}$ is the activity of solvent for the swollen cross-linked polymer, and $\mu_{l,u}$ is the corresponding activity for the unmodified polymer at the same concentration of solvent (the ratio $\mu_{l,c}/\mu_{l,u}$ shows the elastic contribution to solvent activity). The deformation ratio (λ) is described by eq. 1.3 and 1.4.

$$\lambda = \left(\frac{V_c}{V_0}\right)^{1/3} \qquad \text{Equation 1.3}$$

$$\lambda = \frac{V}{V_0} = Q \qquad \text{Equation 1.4}$$

V_0 and V_c are the swelling equilibrium and polymer volume fractions where cross-linking took place, respectively. V is the volume of the isotropically swollen material and V_0 the volume in the dry state, and Q is the degree of volume swelling at equilibrium .

The swelling kinetic equations of particle that is submerged into sufficient water can be used for description of the water diffusion into structure of polymer by assuming an incompressibility of both polymer and water.[127] If one assumes an arbitrary shaped particle, there is a need to introduce a parameter for water uptake onto the particle surface. This assumptions and equations can be applied to a spherical particle. Consider a particle with an arbitrary shape filling an area indicated by Ω(0). When t > 0, the area can be expressed by Ω(t). So, at each point $\bar{x} \in \Omega(t)$ where $\bar{x}$ is the distance of particle surface. The local volume fraction of water can be signified as $\theta(\bar{x},t)$, where applying $\theta_0 \leq \theta(\bar{x},t) \leq \theta_{max}$ and constraining the system to $\theta(\bar{x}, t)$, where θ_{max} and θ_0 are the maximum and initial constant values for θ, respectively. The boundary of the area can be denoted as $\partial\,\Omega(t)$ at which $\theta = \theta_b$ where θ_b indicates the value of θ at the boundary. The boundary has an outward normal vector $\bar{n}$ and a velocity $\bar{v}$. Diffusion into a particle is described by the following set of equations:

$$\frac{\partial \theta}{\partial t} + div\,\bar{q} = 0 \qquad \text{For } \bar{x} \in \Omega(t) \text{ and } t > 0 \qquad \text{Equation 1.5a}$$

$$\bar{q} = -D\nabla\theta$$

$$\theta \big| \partial\Omega(t) = \partial_b \qquad \text{For } t > 0 \qquad \text{Equation 1.5b}$$

$$\theta \big| t = 0 = \theta_0 \qquad \text{Equation 1.5c}$$

$\bar{q}$ denotes the water flux and D is a diffusion coefficient which is independent from time. For simplification of calculation, it can be assumed that the diffusion process occurs linearly (when D is a constant), despite water diffusion into a dry particle is non-linear. During swelling, a moving boundary, $\partial\,\Omega(t)$, can be defined to account for growing the particle size when water enters to the

boundary. For a given small surface of $\partial\,\Omega(t)$, with an area A, the growth in particle volume in space from time t to time t+Δt results (θ=1) which means that an excess volume of water (V_{excess}) is placed inside the particle close to the boundary, that must diffuse into the particle. This volume can be expressed as eq. 1.6:

$$V_{excess} = (1-\theta_b)(\bar{v}.\bar{n})\,A\Delta t \qquad \text{Equation 1.6}$$

As this volume of water diffuses into the particle, the following equation also can be used to express the term, V_{excess}, by eq. 1.7.

$$V_{excess} = -D\left[-\bar{n}.\nabla\theta\,|\,\partial\Omega(t)\right]A\Delta t = D(\nabla\theta.\bar{n})\,A\Delta t \qquad \text{Equation 1.7}$$

By combining eq. 1.2 and 1.3, the volume balance can be calculated using eq. 1.8.

$$D(\nabla\theta\,|\,\partial\Omega(t).\bar{n}) = (1-\theta_b)(\bar{v}.\bar{n}) \qquad \text{Equation 1.8}$$

The volume balance relates to the water flux at the boundary and the speed of the boundary growth. equation 1.4 takes volume conservation into account across a moving boundary. Fasano *et al.*[128] used equation 1.4 to investigate the effect of water absorption by a spherical particle. These sets of equations can be employed to address water diffusion in an arbitrary domain and its subsequent relationship to swelling. Based on the discussion above, the swelling of biopolymers is related to uptake and the molar volume of the solvent, adsorbent porosity and surface functionality. This thesis research aims at the modification of biopolymers to improve the aforementioned properties to enhance efficient swelling in water.

1.4 References

1. Kumar, S.; Singh, N.; Prasad, R. *Sustain. Energy Rev.* **2010,** *14,* 1830-1844.
2. Frolkova, A. K.; Raeva, V. M. *Theo. Found. Chem. Eng.* **2010,** *44,* 545-556.
3. Delgado, J.A.; Águeda, V.I.; Uguina, M.A.; Sotelo, J.L.; García-Sanz, A.; García, A. *Sep. Purif. Technol.* **2015,** *149,* 370–380.
4. Jeong, J. S.; Jang, B. U.; Kim, Y. R.; Chung, B. W.; Choi, G. W. *J. Chem. Eng.* **2009,** *26,* 1308-1312.
5. Blanco-Canqui, H. *Soil Sci. Soc. Am. J.* **2016,** *80,* 845–858.
6. Hahn-Hagerdal, B.; Galbe, M.; Gorwa-Grauslund, M. F.; Liden, G.; Zacchi, G. *Trends Biotechnol.* **2006,** *24,* 549-556.
7. Sun, N.; Okoye, C.; Niu, C. H.; Wang, H. *Inter. J. Green Energy* **2007,** *4,* 623-634.
8. Magalad, V. T.; Gokavi, G. S.; Nadagouda, M. N.; Aminabhavi, T. M. *J. Phys. Chem. C* **2011,** *115,* 14731–14744.
9. Chang, H.; Yuan, X-G.; Tian, H.; Zeng, A-W. *Ind. Eng. Chem. Res.* **2006,** *45,* 3916-3921.
10. Lei, Z.; Biaohua, C.; Ding, Z. Special Distillation Processes, Elsevier, 1st ed. **2005,** 1-370.
11. Dai, Ch.; Lei, Zh.; Xi, X.; Zhu, J.; Chen, B. *Ind. Eng. Chem. Res.* **2014,** *53,* 15786−15791.
12. Hassan, H. Z.; Mohamad, A. A.; Alyousef, Y.; Al-Ansary, H. A. *Renew. Sustain. Energy Rev.* **2015,** *45,* 600–609.
13. Dirk-Faitakis, C. B.; Chuang, K. T. *Ind. Eng. Chem. Res*. **2004,** *43,* 762-768.
14. Ladisch, M. R. *Science,* **1979,** 270, 898-900.
15. Dabrowski, A. *Adv. Colloid Interface Sci.* **2001,** *93,* 135-224.
16. Banat, I.; Makkar, R.; Cameotra, S. *Appl. Microbiol. Biotechnol.* **2000,** *53,* 495–508.
17. Beery, K. E.; Ladisch, M. R. *Ind. Eng. Chem. Res.* **2001,** *40,* 2112-2115.
18. Delgado, J. A.; Uguina, M. A.; Sotelo, J. L.; Águeda, V. I.; García, A.; Roldán, A. *Chem. Eng. J.* **2012,** *180,* 137–144.
19. Simo, M.; Sivashanmugam, S.; Brown, C. J.; Hlavacek, V. *Ind. Eng. Chem. Res.* **2009,** *48,* 9247–9260.
20. Baskan, M. B.; Pal, A. *Water Air Soil Pollut.* **2014,** *225,* 1798-1087.
21. Zhao, W.; Huang, X.; Wang, Y.; Sun, S.; Zhao, C. *Carbohydr. Polym.* **2016,** *150,* 201–208.
22. Ai, L.; Zeng, Y. *Chem. Eng. J.* **2013,** *215–216,* 269–278.
23. Song, Z.; Chen, L.; Hu, J.; Richards, R. *Nanotechnology* **2009,** *20(27),* 275707- 275716.

24. Faghihi, A.; Vakili, M. H.; Hosseinzadeh, G.; Farhadian, M.; Jafari, Z. *Desalin.Water Treat.* **2016,** *57,* 1-16.
25. Sumesh, E.; Bootharaju, M. S.; Pradeep, A.T. *J. Hazard. Mater.* **2011,** *189,* 450-457.
26. Sadegh, H. *Science, Technology and Development* **2015,** *34(3),* 195-214.
27. Ghaedi, M.; Golestani Nasab, A.; Khodadoust, S.; Rajabi, M.; Azizian, S. *J. Ind. Eng. Chem.* **2014,** *20,* 2317–2324.
28. De Gisi, S.; Lofrano, G.; Grassi, M.; Notarnicola, M. *SM&T,* **2016,** 9, 10–40.
29. Hsu, Sh-H.; Hsu, W-Ch.; Chung, T-W.; Lia, Ch-Ch. *J. Taiwan Inst. Chem. Eng.* **2013,** *44,* 952–956.
30. Okewale, A. O.; Igbokwe, P. K.; Ogbuagu, J. O. *Int. J. Eng. Innov. Technol.* **2013,** *2(9),* 36 – 42.
31. Shi, L. *Int. J. Biol. Macromol.* **2016,** *92,* 37-48.
32. Pathania, D.; Sharma, R.; Kalia, S. *Adv. Mat. Lett.* **2012,** *3(2),* 259-264.
33. Crini, G. *Prog. Polym. Sci.* **2005,** *30(1),* 38-70.
34. Dutta, K.P.; Dutta, J.; Tripathi, V. S. *JSIR.* **2004,** *63,* 20-31.
35. Synowiecki, J.; Al-Khateeb N. A. *Crit. Rev. Food Sci. Nutr.* **2003,** *43,* 145–71.
36. Kumar, M. N. V. R. *React. Funct. Polym.* **2000,** *46,* 1–27.
37. Babel, S.; Kurniawan, T. A. *J. Hazardous Mat.* **2003,** *B97,* 219–243.
38. Varma, A. J.; Deshpande, S.V.; Kennedy, J. F. *Carbohydr. Polym.* **2004,** *55,* 77–93.
39. Singh, M.; Sharma, R.; Banerjee, U.C. *Biotechnol. Adv.* **2002,** *20,* 341–59.
40. Crini, G.; *J. Sep. Sci.* **2002,** *25,* 789–813.
41. Del Valle, E.M.M. *Proc. Biochem.* **2004,** *39,* 1033–46.
42. Chandra, R.; Rustgi, R. *Prog. Polym. Sci.* **1998,** *23,* 1273–335.
43. Alcazar-Alay, S. C.; Meireles, M. A. A. *Food Sci. Technol. Campinas* **2015,** *35(2),* 215-236.
44. Paredes-Lopez, O.; Bello-Perez, L. A.; Lopez, M. G. *Food Chemistry*, **1994,** *50,* 411-417.
45. Laya, C-H.; Kuo S-Y.; Sen, B.; Chen, C-C.; Chang, J-Sh.; Lin, C-Y. *Int. J. Hydrogen Energy* **2012,** *37,* 2050–2057.
46. Singh, S.; Gamlath, S.; Wakeling, L. *Int. J. Food Sci. Tech.* **2007,** *42,* 916–929.
47. Yoshimoto, Y.; Tashiro, J.; Takenouchi, T.; Takeda, Y. *Cereal Chem.* **2000,** *77,* 279–285.
48. Hizukuri, S. *Carbohydr. Res.* **1985,** *141,* 295–305.
49. Peat, S.; Whelan, W. J.; Thomas, G. J. *J. Chem. Soc. Chem. Commun.* **1952,** *0,* 4546-4548.

50. Hizukuri, S. *Carbohydr. Res.* **1986,** *147,* 342–347.
51. Bertoft, E. Analyzing starch structure. In Starch in food: Structure, function and applications, A. C. Eliasson ed., Woodhead Publishing, Cambridge, England. **2004,** 1-607.
52. Waigh, T. A.; Jenkins, P. J.; Donald, A. M. *Faraday Discuss.* **1996,** *103,* 325-337.
53. Bertoft, E. *Agronomy* **2017,** *56(7),* 1-29.
54. Imberty, A.; Perez, S. *Biopolymers* **1988,** *27,* 1205–1221.
55. Hoover, R. *Carbohydr. Polym.* **2001,** *45,* 253–267.
56. Matveev, Y. I.; van Soest, J. J. G.; Nieman, C.; Wasserman, L. A.; Protserov, V.; Ezernitskaja, M.; Yuryev, V.P. *Carbohydr. Polym.* **2001,** *44,* 151–160.
57. Tester, R. F.; Debon, S. J. J.; Sommerville, M. D. *Carbohydr. Polym.* **2000,** *42,* 287–299.
58. Singh, N.; Singh, J.; Kaur, L.; Sodhi, N. S.; Gill, B. S. *Food Chem.* **2003,** *81,* 219–231.
59. Perez1, S.; Bertoft, E. *Starch/Stärke* **2010,** *62,* 389–420.
60. Somerville, C.; Bauer, S.; Brininstool, G.; Facette, M.; Hamann, T.; Milne, J.; Osborne, E.; Paredez, A.; Persson, S.; Raab, T.; Vorwerk, S.; Youngs, H. *Science* **2004,** *306,* 2206-2211.
61. Prestwich, G. D.; Marecak, D. M.; Marecek, J. F.; Vercruysse, K. P.; Ziebell, M. R. *J. Control. Release* **1998,** *53,* 93–103.
62. Liu, L.; Liu, D. R.; Wang, M.; Du, G. C.; Chen, J. *Eur. Polym. J.* **2007,** *43,* 2672–2681.
63. Tejado, A.; Antal, M.; Liu, X.; van de Ven, T.G.M. *Ind. Eng. Chem. Res.* **2011,** *50,* 5907–5913.
64. Kocherbitov, V.; Ulvenlund, S.; Kober, M.; Jarring, K.; Arnebrant, T. *J. Phys. Chem. B* ***2008,*** *112,* 3728–3734.
65. Nishiyama, Y.; Sugiyama, J.; Chanzy, H.; Langan, P. *J. Am. Chem. Soc.* **2003,** *125(47),* 14300–14306.
66. Langan, P.; Nishiyama, Y.; Chanzy, H. A. *J. Am. Chem. Soc.* **1999,** *121,* 9940–9946.
67. Zhou, S.; Tashiro, K.; Hongo, T.; Shirataki, H.; Yamane, C.; Li, T. *Macromolecules* **2001,** *34,* 1274–1280.
68. Song, J. H.; Murphy, R. J.; Narayan R.; Davies, G. B. H. Ph. *Trans. R. Soc. B* **2009,** *364,* 2127–2139.
69. Udoetok, I. A.; Wilson, L. D.; Headley, J. V. *Materials* **2016,** *9,* 645-661.
70. Mohamed, M. H.; Udoetok, I. A.; Wilson, L. D.; Headley, J. V. *RSC Adv.* **2015,** *5,* 82065-82077.

71. Patil, S. V.; Jadge, D. R. *Am. Pharmaceut. Rev.* **2008,** *6,* 1-10.
72. Maitra, J.; Shukla, K. *AJMS* **2014,** *4(2),* 25-31.
73. Reddy, N.; Reddy, R.; Jiang, Q. *Trends Biotechnol.* **2015,** *33(6),* 362-369.
74. Holmberg, L.; Lindberg, B.; Lindqvist, B. *Carbohydr. Res.* **1995,** *272(2),* 203-211.
75. Khasreen, M. M.; Banfill, P. F.G.; Menzies, G. F. *Sustainability* **2009,** *1,* 674-701.
76. Jyothi, A. N.; Moorthy, S. N.; Rajasekharan, K. N. *Starch/Stärke* **2006,** *58,* 292–299.
77. Hirsch, J. B.; Kokini, J. L. *Cereal Chem.* **2002,** *79,* 102-107.
78. Kuniak, L.; Marchessault, R. H. *Starch/Stärke* **1972,** *24,* 110–116.
79. Hamerstrand, G. E.; Hofreiter, B. T.; Mehltretter, C. L. *Cereal Chem.* **1960,** 37, 519.
80. Roberts, H. T. Starch: Chemistry and Technology, Ed.; R. L. Whistler, Academic Press, New York, **1965,** 482-491.
81. Jin, Y.; Yamanaka, J.; Sato, S.; Miyata, I.; Yomota, C.; Yonese, M. *J. Control. Release* **2001,** *73,* 173–81.
82. Prestwich, G.D.; Marecak, D.M.; Marecek, J.F.; Vercruysse, K.P.; Ziebell, M.R. *J. Control. Release* **1998,** *53,* 93–103.
83. Berger, J.; Reist, M.; Mayer, J. M.; Felt, O.; Peppas, N. A.; Gurny, R. *Eur. J. Pharma. Biopharm.* **2004,** *57,* 35–52.
84. Berger, J.; Reist, M.; Mayer, J. M.; Felt, O.; Peppas, N. A.; Gurny, R. *Eur. J. Pharma. Biopharm.* **2004,** *57,* 19–34.
85. Yang, Ch. Q. Chen, D. Guan, J.; He, Q. *Ind. Eng. Chem. Res.* **2010,** *49,* 8325–8332.
86. Nur hasanah, A.; Elyani, I.; Sriwidodo, S.; Muchtaridi, M.; Muhtadi, A.; Musfiroh, I. *Int. J. Chem. Sci.* **2015,** *13(3),* 1227-1237. .
87. Chang, H.; Yuan, X. G.; Tian, H.; Zeng, A-W. *Chem. Eng. Technol.* **2006,** *29(4),* 454- 461.
88. Quintero, J. A.; Cardona, C. A. *Ind. Eng. Chem. Res.* **2009,** *48,* 6783–6788.
89. Hong, J.; Voloch, M.; Ladisch, M. R.; Tsao, G.T. *Biotechnol. Bioeng.* **1982,** *24(3),* 725-730.
90. Bienkowski, P. R.; Barthe, A.; Voloch, M.; Neuman, R. N.; Ladisch, M. R. *Biotechnol. Bioeng. Symp.* **1983,** *13,* 629-647.
91. Benson, T. J.; George, C. E. *Adsorption* **2005,** *11,* 697-701.
92. Quintero, J. A.; Cardona, C. A. *Ind. Eng. Chem. Res.* **2009,** *48(14),* 6783–6788.
93. Boonfung, C.; Rattanaphanee, P. *World Acad Sci Eng Technol* **2010,** *4(11),* 716-719.

94. Sun, J.; Wang, W.; Wang, P.; Lv, H.; Luo, X.; Gao, H. *Adsorpt. Sci. Technol.* **2013,** *31,* 829-843.

95. Liu, H.; Tian, Y.; Lu, X. *Energ. Source Part A* **2015,** 37, 2422-2428.

96. Murphy, F.; Devlin, G.; McDonnell, K. *Renew. Sust. Energ. Rev.* **2013,** *23,* 412–420.

97. Xiao, L-P.; Sun, Z-J.; Shi, Z-J.; Xu, F.; Sun, R. C. *Bioresources* **2011,** *6(2),* 1576-1598.

98. Brosse, N.; Dufour, A.; Meng, X.; Sun, Q.; Ragauskas, A. *Biofuels, Bioprod. Bioref.* **2012,** *6,* 580–598.

99. Namasivayam, C.; Holl, W. H. *Holz. Roh. Werkst.* **2004,** *62,* 74–80.

100. Mischnicka, P.; Momcilovic, D. *Adv .Carbohydr. Chem. Biochem.* **2010,** *64,* 117–210.

101. Osman, A. I.; Ahmed, A. T.; Johnston, Ch. R.; Rooney, D.W. *Environ. Prog. Sustain. Energy* **2017,** *0,* 1-10.

102. Koopmans, C.; Ritter, H. *Macromolecules* **2008,** *41,* 7418-7422.

103. Mohamed, M. H.; Wilson, L. D.; Headley, J. V. *Microporous Mesoporous Mater.* **2015,** *214,* 23-31.

104. Moster A. L.; Mitchell, B. S. *J. Appl. Polym. Sci.* **2009,** *113,* 243–50.

105. Hatakeyama, T.; Tanaka, M.; Hatakeyama, H. *J. Biomater. Sci. Polym. Ed.* **2010,** *21(14),* 1865-75.

106. Dehabadi, L.; Udoetok, I.; Wilson, L. D. *J. Therm. Anal. Calorim.* **2016,** *126,* 1851–1866.

107. Li, W.; Zheng, Y.; Cheng, R. *Polymer* **2008,** *49,* 4740-4744.

108. Grossutti, M.; Dutcher, J. R. *Biomacromolecules* **2016,** *17,* 1198−1204.

109. Wolfe, J.; Bryant G.; Koster, K. L. *Cryo Letters* **2002,** *23,* 157-166.

110. Kirschner, K. N.; Woods, R. J. *PNAS.* **2001,** *98,* 10541-10545.

111. Buléon, A.; Colonna, P.; Planchot, V.; Ball, S. *Int. J. Biol. Macromol.* **1998,** *23,* 85-112.

112. Loftsson, T.; Brewster, M. E. *Int. J. Pharm.* **2008,** *354,* 248–254.

113. Oleinikova, A.; Brovchenko, I. *J. Phys. Chem. B* **2012,** *116(50),* 14650–14659.

114. Levy, R. M.; Zhang, L. Y.; Gallicchio, E.; Felts, A. K. *J. Am. Chem. Soc.* **2003,** *125,* 9523–9530.

115. Lindman, B.; Medronho, B.; Theliander, H. *Nord Pulp Papers J.* **2015,** *30,* 2–3.

116. Khazraji, A. C.; Robert, S. *J. Nanomater.* **2013,** *2013,* 1–9.

117. Desam, G. P.; Li, J.; Chen, G.; Campanella, O.; Narsimhan, G. *J. Food Eng.* **2018,** *222,* 237-249.

118. Blazek, J.; Copeland, L. *Carbohydr. Polym.* **2008,** *71,* 380–387.

119. Viksø-Nielsen, A.; Blennow, A.; Jørgensen, K.; Kristensen, K. H.; Jensen, A.; Møller, B. L. *Biomacromolecules* **2001,** *2,* 836-843.

120. Desse, M.; Fraiseau, D.; Mitchell, J.; Budtova, T. *Soft Matter,* **2010,** *6,* 363–369.

121. Kimura, S.; Kondo, T. *J. Plant Res.* **2002,** *115,* 297–302.

122. Grim, R. E. Clay mineralogy, 2nd ed.; McGraw-Hill: New York, **1968.**

123. Schreyer-Bennethum, L.; *Comput. Geotech.* **2007,** *34,* 267–278.

124. Geffert, A.; Vacek, O.; Jankech, A.; Geffertová, J.; Milichovský, M. *BioRes.* **2017,** *12(3),* 5017-5030.

125. Sweijen, T.; Nikooee, E.; Hassanizadeh, S. M.; Chareyre, B. *Transp. Porous Med.* **2016,** *113,* 207–226.

126. Flory, P. J. Principles of Polymer Chemistry, 1st ed.; Cornell University Press, Ithaca, NewYork, **1953.**

127. Sweijen, T.; van Duijn, C. J.; Hassanizadeh, S. M. *Chem. Eng. Sci.* **2017,** *172* 407–413.

128. Fasano, A.; Mikelic, A. *Interf. Free Bound.* **2002,** *4 (3),* 239– 261.

CHAPTER 2

2 Methodology

2.1 Overview of techniques for detection of water and ethanol

Important aspects of an analytical method include the limit of detection (LOD) and its relative sensitivity for discrimination between two or more components (resolution). Herein, the application of different techniques for detection and quantification of water-ethanol is discussed.

Gas chromatography (GC) is an important analytical technique for the detection of compounds that can be vapourized without thermal decomposition. Since the ethanol is volatile, quantitative analyses are possible using GC.[1,2] (The LOD for ethanol was found to be 0.1 ppm). Typically, GC can be used for testing the purity of a sample, separating the different components and relative amounts of different components of a mixture. Weatherly *et al.*[3] examined the response range for water and ethanol using GC, by considering the thermal conductivity detection (TCD), and barrier ionization detection (BID) techniques. Validation of these methods was accomplished by using standard reference materials. In addition, Tiscione *et al.*[4] employed GC with flame-ionization detection (HS-GC–FID) for quantification of ethanol since its automation can be obtained with acceptable sensitivity, and accuracy.

High Performance Liquid Chromatography (HPLC) is a promising analytical technique, that differs from GC, where LC employs a liquid as the mobile phase.[5,6] Although HPLC can be employed more widely for compound analysis, it is considered a more expensive method relative to GC due to the level of solvent consumption. (The LOD of ethanol was found to be 0.02μM for ethanol in water).[7] Both HPLC and GC method require time for chemical separation to occur which may be on the order of 15-20 minutes. Sharma *et al.*[8] suggested the HPLC method for the determination of variety of alcohols. This method is advantageous due to the use of pure water as a mobile phase. Yarita *et al.*[9] reported a unique HPLC method referred to as reversed-phase column high-performance liquid chromatography (RP-HPLC). RP-HPLC was used to produce higher resolution signals for the separation of organic compounds that has been used successfully for ethanol determination in alcoholic beverages.

The Karl Fischer (KF) titration is a useful technique for the determination of water content by use of coulometric or volumetric titration.[10] Fregolente *et al.*[11] reported the application of this method to evaluate the presence of water in biodiesel and diesel fuel samples. The advantage of

this method lies in its high selectivity towards water. Furthermore, this method is laborious and the reagents can be expensive, especially in the case of large sample volumes.

Infrared (IR) spectroscopy is a technique based on the absorption of infrared radiation. This equipment is fairly inexpensive, where the analysis of samples using this method is simple and fast. Generally, this method can be employed as a complementary method and for identification of functional groups within a molecule. [12,13] Application of the IR technique for detection of water and/or ethanol can be considered difficult due to overlap of spectral signatures which poses problems for water-cosolvent mixtures. However, Laakso *et al.*[14] used a low-resolution FT-IR spectrometry for measurement of ethanol in human breath. Sharma *et al.*[8] indicated a very strong peak for C-O, stretching at *ca.* 1015.3 and 1044.2 cm^{-1}, for methanol and ethanol, respectively and this absorption of vibrational stretching frequency for C-O of alcohols was used for quantification purposes. In cases where water is present in the mixture, the C-O group signal of alcohols can be measured using Horizontal Attenuated Total Reflectance (HATR-FTIR) with a zinc-selenide crystal.

Among the various types of spectroscopic methods, Nuclear magnetic resonance (NMR) spectroscopy is a potential quantitative technique that allows for measurement of the composition of mixtures in cases where well-resolved spectral signatures are required.[15]

2.2 Quantitative NMR spectroscopy (qNMR)

NMR spectroscopy is a suitable technique for elucidation of chemical structure and composition of materials. Quantitative NMR refers to the use of NMR spectroscopy for the determination of the concentration of one or more chemical species in solution. Proton NMR spectroscopy as a useful tool for quantitative analysis was first employed in 1963 by Jungnickel and Forbes for calculating the intra-molecular proton ratios of an organic substance.[16] Another study by Hollis proved the application of quantitative NMR (qNMR) for analyzing the fraction of aspirin and caffeine in mixtures.[17] The use of GC and qNMR together was employed by Gonçalves *et al.*[18] to quantify the level of ethanol (%) in a pharmaceutical formulation of indinavir sulfate. In this research study, ethanol was quantified by ^{1}H NMR and compared with estimates obtained by GC results. It was reported that the disparity between the ethanol content (%) obtained by these two methods is insignificant, affirming the suitability of ^{1}H NMR spectroscopy as an alternative method for detection and quantification of ethanol in pharmaceutical mixtures. The qNMR method

is considered more advantageous since it requires relatively small amounts of sample and shorter analysis time. Another study on application of qNMR technique for determination of alcohol content was reported by Isaac-Lam by using a low-field 45 MHz NMR spectrometer.[19,20] The use of a benchtop NMR spectrometer promoted features of this method for its ease and cost of operation when compared to high-field NMR instrumentation.[21] Recently, there has been progress in the use of qNMR in analytical chemistry since it can be used with or without any specific internal standard. [22] However, the applications of qNMR with other nuclei (e.g., ^{31}P and ^{13}C) are restricted due to their low sensitivity/natural abundance. Nevertheless, recent progress in the development of high-field magnets has enabled quantitative analysis of samples at low concentration.[23] qNMR spectroscopy has found a deserved place in environmental science. Reliable results by qNMR relate to the acquisition, processing parameters and referencing techniques. Based on the mode of application, reference compounds are classified as internal and external standards, where appropriate choice enables reliable estimation of the analyte concentration. Attention to sample preparation and experimental procedures can reduce systematic errors and provide better accuracy and precision.

Since the signal intensity of the spectrum (I_x) in NMR spectroscopy is directly proportional to the number of nuclei (N_x) corresponding to a particular resonance, it can be employed as a quantitative technique for detection of relative analyte levels in solution. Even though this technique requires a high-level of operational skill, it is practical for analytical measurements of samples.[23] Since the spectrometer constant of all resonances in a NMR spectrum remains the same, quantitative measurements are possible *in situ* without the need of chemical separations as for the case of chromatography (GC and HPLC). However, factors like pulse excitation, repetition time, broad-band decoupling, digital resolution and data processing via integration errors affect the measured values. Generally, there are two ways by which quantitative analysis is possible through the use of qNMR spectroscopy. The two strategies outlined below relate to relative and absolute quantitation are discussed in sections 2.2.1 and 2.2.2, respectively.

2.2.1 Relative quantitation method

A facile qNMR method involves the measurement of relative quantitation, where the molar ratio for two compounds x and y (M_x and M_y) can be calculated by equation 2.1.[24]

$$\frac{M_x}{M_y} = \frac{I_x}{I_y} \cdot \frac{N_y}{N_x} \qquad \text{Equation 2.1}$$

The terms I and N represent integral area and number of nuclei, respectively.

2.2.2 Absolute quantification method

There are two analytical methods for the determination of the absolute concentration of analytes. In cases where all components present in the NMR spectrum, along with impurities, can be measured quantitatively, the composition can be assessed from mass-balance consideration by additivity of components to the total overall composition (100%). This method has limitations when resonances from the impurities overlap with species of interest or other impurities. In cases when quantifying the purity of one of the main components, it can be calculated directly from the NMR spectrum using equation 2.2. [24]

$$P_x = \frac{I_x}{I_{std}} \cdot \frac{N_{std}}{N_x} \cdot \frac{M_x}{M_{std}} \cdot \frac{W_{std}}{W} \cdot P_{std} \qquad \text{Equation 2.2}$$

In this equation, I, N, M, W and P are terms corresponding to the integral area, number of nuclei, molar mass, gravimetric weight and purity of analyte (x) and standard (std), respectively.

2.2.3 Referencing method in quantitative NMR

In this method, addition of a standard reference compound in solution with known concentration is necessary to determine a NMR "response factor" per nuclide under specified experimental conditions. This technique can be used directly since there is no need to add standard reference material to each sample, also known as "Concentration Conversion Factor" (CCF). For example, an internal standard is identified at a known concentration of a reference compound that is dissolved in a known volume of analyte solution for quantitative analysis. Different reference compounds such as tetramethyl silane (TMS), and tetrahydrofuran (THF) are widely used as internal standards for qNMR analysis. The solubility and chemical interaction of an internal standard with the analyte are the two most significant conditions that enable estimation of the analyte concentration.[23-25] In one study, the minimum detection limits (MDL) for proton

measurements in water ranged from 3 to 10 µg/g.[26] Various parameters affect the accuracy and precision of qNMR technique such as recycle delay, pulse sequence, and acquisition time, where detailed aspects of these parameters are outlined in the experimental section in the Appendix A, chapter 2.

2.3 Sorption

The term *sorption* is generally used for describing the combined process of absorption and adsorption. These processes involve a substance (adsorbate and absorbate) to be adsorbed onto and/or absorbed within a substrate, as shown in Figure 2.1. While the absorption involves the uptake of adsorbates from the bulk phase into the network of the adsorbent (phase transfer),[27] adsorption is the attraction of the adsorbate from the bulk phase onto the surface of the adsorbent.[28] Whereas, absorption is a volume-driven phenomenon, adsorption is a surface-driven phenomenon.

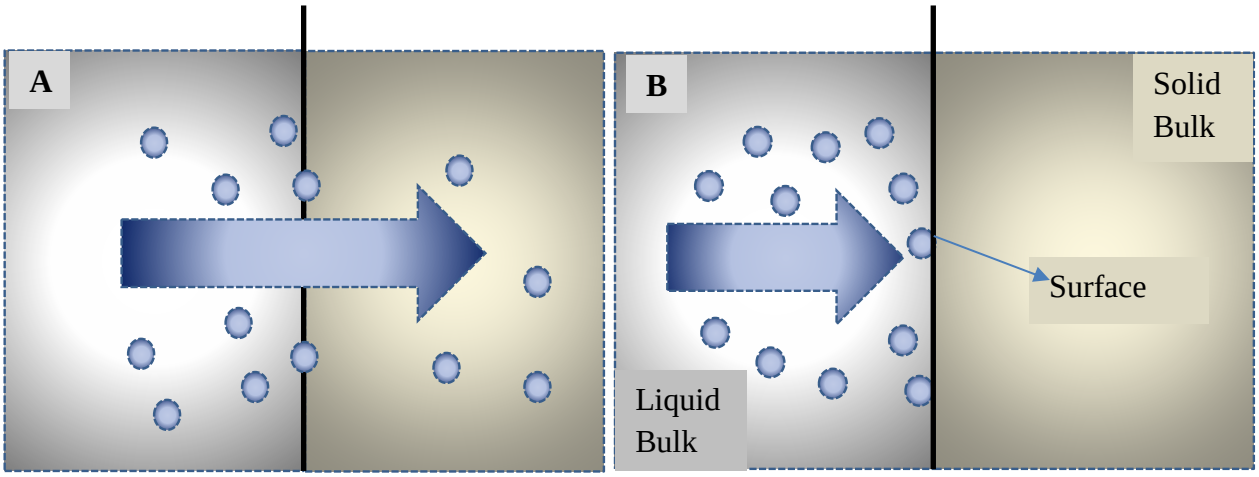

Figure 2.1 A) Gas-Solid Absorption and B) Liquid-Solid Adsorption process. Solid line denotes the solid-medium phase boundary.

2.3.1 Absorption and adsorption processes

Sorption is an accepted term that represents a combination of two phenomena, absorption and adsorption. During adsorption process, the adsorbate species from the bulk phase binds to the surface of adsorbent while absorption takes place within the interior phase of the sorbent.
Absorption as a physical process can be estimated according to the "Nernst distribution law" since the absorbed substance is uniformly distributed in the bulk of the other.[29] This law suggests distribution of a solute (solid or liquid) in non-miscible solvents. This law can be represented using following equation 2.3, where C_1 is concentration of "X" in solvent 1, C_2 is concentration of "X" in solvent 2, and K_d is a constant called the partition coefficient (distribution constant).

$$\frac{C_1}{C_2} = K_d \qquad \text{Equation 2.3}$$

In general, the adsorption process is categorized by: (i) physisorption, and (ii) chemisorption. Physisorption involves non-covalent interactions between the adsorbate and the adsorbent by physical forces such as van der Waals interactions, surface charge interaction (e.g., electrostatic forces), dipolar (e.g., hydrogen bonding), and π-π interactions. Chemisorption describes covalent bonding interactions, Metal-ligand binding, ion-ion interactions between the adsorbate and adsorbent. The interaction between the adsorbate and adsorbent is driven by multiple intermolecular forces such as van der Waals and/or hydrogen bonding. These interactions that result in physical adsorption are weak and reversible, where the process has an enthalpy of desorption *ca.* 20-40 kJ/mol. The nature of the physical adsorption can be understood according to the polarity of the interacting species. Indeed, polarity of the interacting species plays an important role in physisorption as a driving force. Physisorption also occurs via solvent driven association such as the hydrophobic effect, where the apolar adsorbate resides on the surface of the sorbent leading to an overall increase in the entropy of the solvent (water) medium.[30] By contrast, chemisorption occurs via strong interactions that result in irreversible adsorption between the adsorbate-adsorbent system. The driving force for chemical adsorption is valence force that is similar to processes related to covalent bond formation, where sharing of electrons occurs for the adsorbate-adsorbent system. Chemisorption is characterized by large exothermic heats of

adsorption in the range 100-400 kJ/mol. By contrast physisorption is often characterized by heats of adsorption that lie below 100 kJ/mol.

Among the methods mentioned above for the separation of water and ethanol, adsorption-based processes are among the most attractive and simple techniques chiefly due to their lower energy consumption requirements.[31,32] Various adsorption techniques are employed for water-ethanol separation that include fixed-bed adsorbents, as well as adsorptive dehydration.[31] Hu *et al.*[33] used two types of Chinese cornmeal as adsorbent for packing a fixed bed for separation of ethanol and water. Their results indicated that the adsorption capacity of water mainly depends on the vapor velocity, temperature, and the particle-size distribution of cornmeal in the fixed bed. Determining the efficiency of an adsorption process can be estimated by the chemical and structural properties of the adsorbate such as the porosity and surface chemistry of the adsorbent and by adsorption techniques including batch and column methods.[34]Adsorption, as mentioned above, can be defined as the accumulation of substrates (the adsorbate) on a surface of the adsorbent in contact with the air/water phase. Although the term adsorption can be used to refer to the same process in air or water media, the mechanism of this process differs for these two conditions due to medium effects. Since the separation of water-ethanol takes place in their liquid form, the solvent-solvent interactions compete with the solid-solvent adsorption processes. Therefore, distinguishing between adsorption in solution *vs.* gas phase systems seems necessary for developing a better understanding of the process.

2.3.2 Solution *vs.* gas-based adsorption

Adsorption occurs onto an adsorbent when the adsorbate is in the form of a gas or liquid. The difference between gas phase and liquid phase adsorption is shown by the illustrated processes in Figure 2.2.

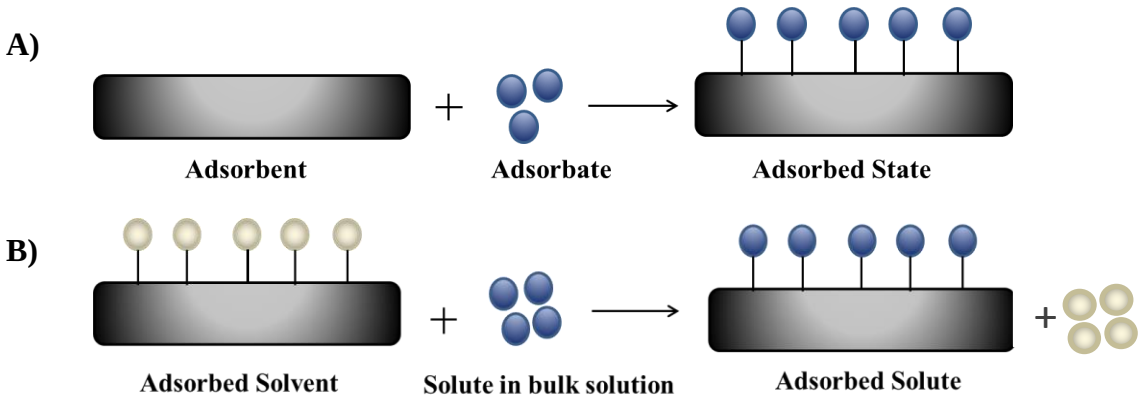

Figure 2.2 Chemical adsorption processes using a solid substrate with an adsorbate in various phases: A) gas adsorption,[32] and B) solution-based adsorption.[35]

In solid-gas adsorption, the process involves noncovalent binding of the gas to a vacant sorption site on the adsorbent surface. Thus, the sorption capacity of the adsorbent can be considered as the amount of adsorbate bound onto the adsorbent surface.[36] For liquid-phase adsorption, all sorption sites are occupied by either a solvent or solute molecule in contrast to gas-phase adsorption. Thus, the adsorption process is the replacement of solvent molecules by the solute, along with the role of solute-solvent interactions. As a result, all models for liquid-phase adsorption account for the solute and solvent activities together.[35]

2.3.3 Solution-phase adsorption

Liquid-phase adsorption on solid adsorbents occurs via equilibrium or dynamic processes. As briefly mentioned before, an adsorption process can be carried out using batch and column methods. The focus of this discussion will concentrate on the batch technique. Batch studies at equilibrium have some benefits, such as easy access to sorption sites at the interior of the adsorbent. In this method, the solid adsorbents are placed in the solution phase, which consists of the adsorbate/solvent, adsorbate species, and the solvent medium, where the adsorbent surface interacts with the ensemble until equilibrium occurs between the bound and unbound sites of the adsorbent. At equilibrium, the maximum sorption capacity (Q_m) can be determined graphically via a plot of sorption capacity (Q_e) *vs.* equilibrium or total concentration and analyzed using a suitable isotherm model.[37] For liquid-phase adsorption process, Q_e is a function of the mole fraction of the solute relative to the specific surface area of the adsorbent. Assuming that the ideal-dilute solution condition governs the adsorption process, Q_e can be estimated using mass-balance considerations,

the initial concentration of adsorbate (C_0), equilibrium concentration of adsorbate (C_e), mass of the adsorbent (m) and volume of solution (V) according to Equation 2.4.

$$Q_e = \frac{(C_0 - C_e)}{m} \times W_{Solution} \qquad \text{Equation 2.4}$$

2.3.4 Dye-based adsorption method

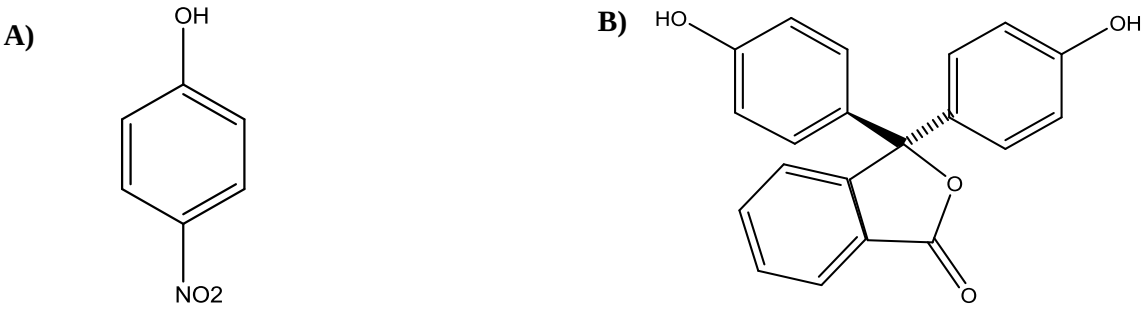

Figure 2.3 The molecular structure of A) *p*-nitrophenol (PNP) and B) phenolphthalein (PHP) in their non-ionized forms.

At equilibrium conditions, the uptake of an adsorbate by an adsorbent system can be determined using mass-balance considerations provided that the fraction of free or bound adsorbate can be determined. In the case of adsorbates that contain chromophores, the decrease in the concentration of the unbound species (C_e) can be measured using the optical absorbance properties of the adsorbate, according to the Beer-Lambert law. For dyes such as *p*-nitrophenol (PNP) and phenolphthalein (PHP), the observed colour can be induced by hydrogen bonding with water (as solvent) that reduces the energy gap for the $\pi \rightarrow \pi^*$ electronic transition. When adsorption of dyes takes place in the bonding sites of the adsorbent, the adsorbate is no longer dispersed in the bulk solvent but exists in a bound state by interaction with the adsorbent. PNP will exhibit a distinct yellow colour in the presence of the solvent; therefore, this dye-based technique can be coupled with batch equilibrium and/or kinetic studies for studying the adsorption process since the optical density can be related to the concentration of unbound dye in solution.[38] Based on the

assumption of large molar absorptivity coefficients for various dyes, the UV-Vis method is considered sensitive to dye concentration over the μM to mM range. In addition, these dyes can be employed to estimate the sorption capacity of adsorbent materials to estimate textural properties, analogous to the use of the nitrogen adsorption method. Thus, the ability to measure free or bound dye in a heterogeneous sorption process enables evaluation of the binding affinity, sorption site accessibility, and even surface area of the adsorbent.[39] Furthermore, it is well established that dyes can exist in various ionization states (cationic, anionic, or neutral forms) depending on the pH and nature of the dye. In the case of solvent (water and ethanol) adsorption, the major reason for adsorption studies that employ model dyes such as *p*-nitrophenol (PNP) and phenolphthalein (PHP) relate to the insight provided on the textural and surface chemical properties of adsorbents. The properties are dependent on the nature of the dye-adsorbent system according to the type of adsorbent-adsorbate interactions. PNP is an aromatic dye with a pK_a of 7.14. The pH of the PNP solution can be adjusted using a buffer, depending on adsorption conditions required. It should be noted that some ionization occurs near the pK_a value so the pH conditions need to be adjusted to control the degree of ionization of such adsorbate species, according to the Henderson-Hasselbalch equation.[40] At pH conditions well below the pK_a, the dye exists in its non-ionized form; whereas, the dye will exist as an anion species above its pK_a. The sorption properties of phenolphthalein (PHP) were reported by Bertau and Jorg using amylose-based polysaccharides. The degree of decolorization is related to the relative accessibility of the –OH groups of the polysaccharide to afford decolorization of PHP. The sorption process resulted in variable decolourization of phenolphthalein (PHP) because of the formation of noncovalent complexes.[41] A noticeable change in the molar absorptivity of PHP is evidenced by complex formation according to a decolourization from pink to transparent in alkaline solution, especially for adsorption onto β-cyclodextrin and its polymer forms.[42] PHP is a special category of dye since the binding with -OH groups, especially in the case of β-cyclodextrin, leads to a shift in pK_a of the dye to result in optical transparency *vs.* a strong absorbance *ca.* 500 nm above its pK_a value. In some ways, the shift in pK_a above is analogous to the colour change observed in acid-base titrations on going from colourless to pink upon titration with a base as PHP goes from below to above its pK_a of the dianion species. PHP is considered as a reporter dye with "on-off" properties according to its bound and unbound states, especially in the case of adsorption by polysaccharides for the reasons of pK_a shift described above. [43]Analogous decolourization effects were observed for the adsorption of PHP in the presence of

cellulose and its cross-linked forms.[44] The nature of the active sites of adsorbents involved in the adsorption process can be inferred by studying model dyes such as PHP. A greater understanding of the role of solvent polarity and the H-bonding ability of a solvent can be inferred by studying the adsorption of a model dye (PHP) with adsorbent systems of interest. This can provide insight on the role of solvent adsorption for species with variable polarity, such as water *vs.* ethanol. The relative water solubility of PHP is 400 mg/L at 20 °C.[45] The hydrophilic character of adsorbates is a consideration in the sorption process due to the role of hydrophobic effects and the availability of suitable binding sites on the adsorbent surface.[46] In summary, the application of the dye-adsorption method using adsorbents provides more detailed information about structural and surface chemical properties of the adsorbents by accounting for the role of surface chemistry and textural properties in the overall mechanism of adsorption.[47]

The adsorption process can be studied through graphs referred to as adsorption isotherms, defined as a graph with the amounts of adsorbate bound onto the surface of an adsorbent (ordinate) and concentration of the adsorbate (abscissa) at constant temperature and pressure. The adsorption isotherm profiles are categorized according to the nature of the adsorption process. The shape of the adsorption isotherm is an informative tool for understanding the size of the pores on the surface of the adsorbents. The following discussion outlines the various categories of adsorption isotherm in more detail.

2.3.5 Adsorption isotherms

According to the International Union of Pure and Applied Chemistry (IUPAC), there are six general types of adsorption isotherms.[48] Each isotherm type is governed by the surface area and the pore diameter of the adsorbent material. Pore sizes can be classified according to their relative diameter:

1. Macropores: Possess pore diameters larger than 50 nm.
2. Mesopores: Possess pores within the range of 2-50 nm.

The hysteresis loop is associated with the secondary pore filling process of capillary condensation. For this range, the pores are large enough to fit more than gas molecules and capillary condensation may occur.

3. Micropores: Possess pore diameters of 2 nm and less. Typically, pores of such small dimensions afford adsorption of one gas molecule within the cross-sectional area to accommodate the gas that lead to formation of adsorbed monolayers similar to the Type I isotherm.

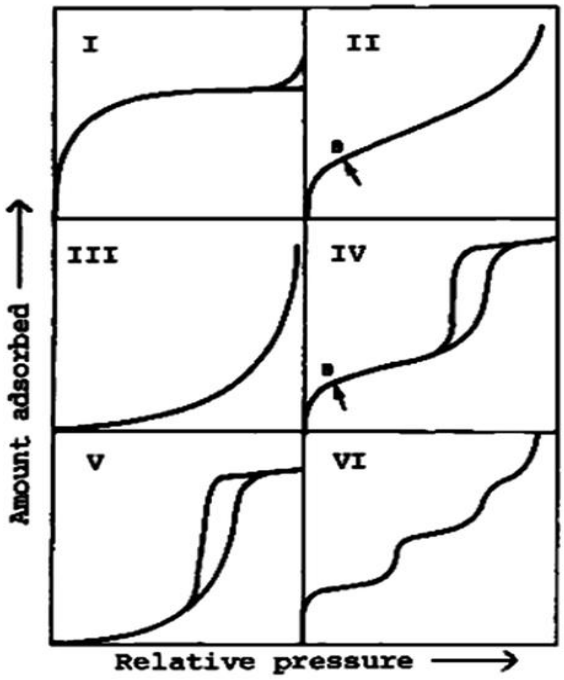

Figure 2.4 Variable types of sorption isotherms (IUPAC report) for gas adsorption. (Figure is reprinted with permission from ref. 48).

Type I

This isotherm type shows a monotonic increase in uptake, which reaches a specific sorption capacity at the plateau region. Adsorbents in this category are usually microporous materials with a very small cross-sectional area such as activated carbon or zeolites.[48]

Type II

This isotherm type shows two extremes in terms of pore size dimensions representative of large macropores. The surface area of the pores is large enough to allow formation of multilayer adsorption with no limitations.

Type III

This isotherm type is observed when strong adsorbate-adsorbate interactions exist and the binding of adsorbate molecules with one another exceeds the interaction between the adsorbate and adsorbent.

Type IV

Mesoporous materials tend to follow the Type IV isotherm profile, which describes multi-layer adsorption processes. This isotherm suggests the occurrence of capillary condensation in the case where a hysteresis loop for the adsorption-desorption profile is observed.

Type V

The Type V isotherm curve is analogous to Type III but the interactions between the adsorbates are weaker in this case. This isotherm type shows finite sorption sites by a plateau. The presence of a hysteresis loop suggests that the agglomerated particles desorb cooperatively as a collective group.

Type VI

This type of curve represents a step-wise multilayer adsorption profile. Initially, one sorption site is filled and another site will be occupied thereafter. This type of isotherm reveals that the required energy to adsorb at one site should differ sufficiently from other sites for preferential filling to take place.

2.3.6 Classification of adsorption isotherm models

2.3.6.1 Langmuir isotherm

Irving Langmuir developed this isotherm a century ago to explain the adsorption behaviour of hydrogen gas on a palladium surface using a simple kinetic model.[49] He applied several assumptions to create this model. The first assumption dealt with the nature of the materials. He assumed a homogeneous surface that results in sorption sites on the material surface with similar energy of adsorption if each site can be treated independently. Secondly, he supposed monolayer coverage for adsorption, which means one layer of adsorbates on the surface. Lastly, he assumed that the adsorbate gas should behave like an ideal gas so that interaction between the gases within the monolayer could be neglected.

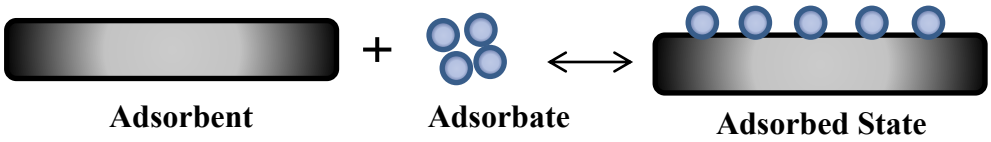

Figure 2.5 Langmuir model of gas adsorption onto a solid adsorbent.

$$Q_e = \frac{Q_m K_L C_e}{1 + K_L C_e} \qquad \text{Equation 2.5}$$

Q_e (mmol/g or mg/g) is the sorption capacity or amount of material adsorbed per gram of substrate. Q_m (mmol/g or mg/g) is defined as the maximum adsorption capacity of the material at saturation and K_L is the equilibrium adsorption constant for the adsorbent/adsorbate system.

2.3.6.2 Freundlich isotherm

According to the Freundlich isotherm model, the heat of adsorption for all sorption sites is not absolutely uniform to account for surface heterogeneities.

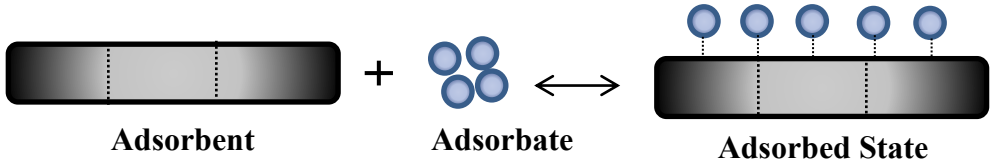

Figure 2.6 The Sips and Freundlich isotherm model of gas, where surface heterogeneity is included.

$$Q_e = K_F C_e^{n_F^{-1}} \qquad \text{Equation 2.6}$$

This model can be described using equation 2.6, where the surface heterogeneity is the parameter $1/n_F$.[50] The major difference between the two models is that the Freundlich model assumes that an infinite amount of adsorbate can be taken up by the adsorbent. On the other hand, the Langmuir model assumes monolayer adsorption that undergoes saturation as soon as each site binds with an adsorbate.[50]

2.3.6.3 Sips isotherm

The Langmuir and Freundlich isotherm models have common assumptions for considering monolayer coverage. However, Freundlich isotherms can account for surface heterogeneity while the Langmuir model assumes monolayer adsorption. By considering the occurrence of surface heterogeneity, the Langmuir isotherm does not account for variable enthalpy of adsorption at the sorption sites and is no longer valid. Thus, application of a general Langmuir-Freundlich isotherm is a great advantage, where the sorption capacity at saturation can be described as a function of the energy distribution for the sorption sites. For cases with distribution of heat of adsorption close to unity, the Langmuir isotherm (unitary heat of adsorption) is preferred, especially if the distribution follows Gaussian behaviour. Based on these rules for combination of the Langmuir and Freundlich isotherm models, the Sips isotherm model was developed.[51]

$$Q_e = \frac{Q_m (K_s C_e)^{n_s}}{1 + (K_s C_e)^{n_s}} \qquad \text{Equation 2.7}$$

In the case where the n_s parameter is not close to the unity, the equation represents the Freundlich isotherm model and reflects surface heterogeneity. Equilibrium constant K_s represents binding affinity of the adsorbate to the sorption sites. A large value of K_s indicates that the sites are readily accessible and adsorption is favoured at the adsorption sites. When the exponent value (n_s) approaches unity, the model converges to the Langmuir isotherm model, where the energy of the sorption site has a singular value. At dilute concentration, the model converges to the Freundlich isotherm. It is important to note that this model assumes monolayer coverage when n_s is equal to unity. The Sips model is very useful for the study of solution-phase adsorption, due to its ability to account for both Langmuir and Freundlich adsorption behaviour. However, the assumptions of the Sips isotherm are not generally applicable under two limiting conditions. Firstly, when there is a strong lateral adsorbate-adsorbate interaction, all previous isotherms assume ideal solutions with zero enthalpy of mixing. One weakness related to the Freundlich and Sips isotherms indicates that the "n_s" parameter enables one to infer the possibility of heterogeneous sites, while lateral interactions between adsorbates can contribute surface heterogeneities. Thus, the assumptions of the Sips isotherm can be violated when the lateral

adsorbate-adsorbate interaction dominates (e.g. Type III isotherm). Secondly, assumptions of the Sips isotherm are violated when multilayer formation occurs.

2.3.6.4 Brunauer-Emmett-Teller (BET) isotherm model

All three previous isotherms (Langmuir, Freundlich, and Sips) primarily considered monolayer coverage; whereas, the BET model takes into account multilayer adsorption. Multilayer adsorption occurs after formation of a monolayer, where the next adsorbed layers are stacked on top of one another through adsorbate-adsorbate interactions.[52] Depending on the strength of the interaction between layers, Type II-V isotherms may be obtained. Specifically, this model can be employed as a useful tool for providing thermodynamic information such as the enthalpy of adsorption/desorption. Determination of the sorption capacity of the substrate at the first monolayer is possible if the BET model follows a Type II or IV isotherm.

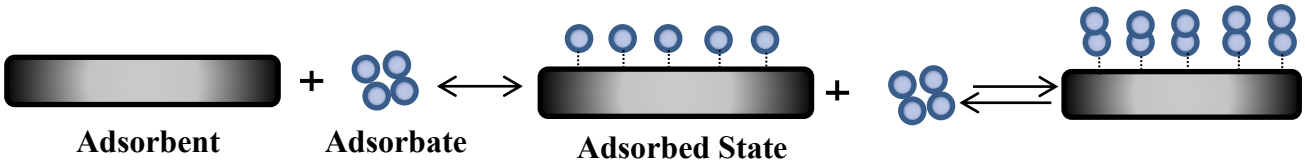

Figure 2.7 BET model of physical adsorption for gas. The dashed lines represent bonding between the adsorbate and the adsorbent surface.

In this model, the constant term c (*cf.* Equation 2.8) is considered a function of the enthalpy for adsorption on the first layer and enthalpy of condensation for the gas. A larger value of c suggests a large enthalpy for adsorption of adsorbates with the adsorbent, and this implies that adsorption of a species onto the adsorbent surface does not occur favourably. This leads to adsorption of molecules on the surface of the adsorbent, where additional species are able to adsorb onto the existing bound layer of adsorbate instead of the adsorbent surface directly. Unlike the other isotherms, the initial concentration (C_0) of the adsorbate is required. The BET isotherm model predicts the saturation accurately when an amount of adsorbate is bound to the surface of the adsorbent. The BET model assumes that the formation of multiple layers of adsorbate continues until the adsorbate is completely adsorbed onto the adsorbent surface and condensation occurs.

$$\frac{n_a}{n_m} = \frac{C\left(P/P_0\right)}{\left(1-P/P_0\right)\left(1+(C-1)\,P/P_0\right)} \qquad \text{Equation 2.8}$$

Where P and p_0 are equilibrium and the saturation pressure of adsorbates, respectively, n_a is adsorbed gas quantity, the n_m represents the monolayer capacity, and C is BET constant. As outlined above in the description of isotherms, the following discussion of intermolecular interactions can provide further insight on the magnitude of the isotherm parameters by relating the thermodynamic factors to molecular-level processes for the adsorbate-adsorbate systems of interest. Generally, the thermodynamics of the adsorption processes describe the behavior of the adsorbent-adsorbate system as a function of state variables (P, T, concentration) for the adsorption process. Although thermodynamics is just a continuum description of the chemical state of systems, limitations on the prediction of microscopic details or elementary processes on the atomic scale but one may correlate free surface energy to chemical potential. Changes in Gibbs energy of surface processes during adsorption have been related to chemical potentials by Gibbs surface excess.[53]

Equation 2.9 and 2.10 consider the differential change of the Gibbs Energy (dG) for a thermodynamic system during any change of state:

$$dG = \left[\frac{\partial G}{\partial P}\right]_{T,A} dP + \left[\frac{\partial G}{\partial T}\right]_{P,A} dT + \left[\frac{\partial G}{\partial A}\right]_{P,T} dA + \left[\frac{\partial G}{\partial n_i}\right]_{P,A,T} dn_i \qquad \text{Equation 2.9}$$

$$\left[\frac{\partial G}{\partial P}\right]_{T,A} = +V \qquad \left[\frac{\partial G}{\partial T}\right]_{P,A} = -S \qquad \left[\frac{\partial G}{\partial A}\right]_{P,T} = \gamma$$

$$dG = VdP - SdT + \gamma dA + \sum_i \mu_i d n_i \qquad \text{Equation 2.10}$$

P is pressure, T is temperature, A is surface area, γ is surface tension, V is the system volume, μ is chemical potential, and S is entropy. In the adsorption process, the surface tension [γ ; N/m] at the interface of the adsorbent and solvent is equivalent to the surface energy [Nm/m^2], which is a key driving force for all surface phenomena. The Gibbs surface excess can be related to an isotherm models such as Langmuir. The adsorption isotherm describes how much adsorbate will adsorb for a given set of state variables. As described in the isotherm section, the value of adsorption can be recast as surface coverage (θ), defined as the fraction of occupied/accessible sites, or by the total volume taken up by the sum of adsorbed particles in the first monolayer.

The use of the BET method as a static technique employs a sorption isotherm for calculating the surface area of adsorbents.[54] A derivate equation of the BET expression can be used to calculate the surface area of adsorbents according to the equation 2.11.

$$\frac{P}{\left(P_0 - P\right)n_a} = \frac{1}{n_m C} + \frac{(C-1)}{n_m C} \times \frac{P}{P_0} \qquad \text{Equation 2.11}$$

The parameters (n_m and C) of the BET equation can be obtained by plotting the adsorption isotherm typically at a relative pressure (P/P_0) range of 0.05-0.35 due to existence of a linear relationship. Through the n_m value, the surface area can be calculated using molecular cross-sectional area (A) through equation 2.12:

$$S_{total} = \frac{n_m N A}{V} \qquad \text{Equation 2.12}$$

Where N is Avogadro's number and V is the molar volume of the adsorbate. Then, the specific surface area (m^2/g) can be calculated by dividing the total surface area by the sample weight (g).

$$S_{total} = \frac{S_{BET}}{\text{Sample Mass}} \qquad \text{Equation 2.13}$$

The method of Barrett, Joyner, and Halenda (BJH) is a well-known procedure for calculating the pore size distribution of a material from experimental isotherms according to the Kelvin model of pore filling. The BJH equation can be expressed by equation 2.14. [55]

$$V_{ads}(x_k) = \sum_{i=1}^{k} \Delta V_i\left(r_i \le r_c(x_k)\right) + \sum_{i=k+1}^{n} \Delta S_i t_i\left(r_i > r_c(x_k)\right) \qquad \text{Equation 2.14}$$

V_{ads} (x_k) is the volume of adsorbate at relative pressure (x_k),V_i is pore volume, S_i represents the pore surface area of pores, and t is the thickness of the adsorption layer.

As briefly outlined above, the adsorption isotherm can be used for calculation of surface area and pore size distribution. Furthermore, the shape of an obtained isotherm using these models can be employed as a tool for the interpretation of an adsorption process. The following section will provide useful information on types and application of the hysteresis of adsorption/desorption curves for characterization of the textural properties (e.g porosity and surface area) of a material.

2.3.7 Hysteresis in solid-gas adsorption/desorption curves

A typical nitrogen gas-adsorption isotherm can be obtained by plotting Q_e *vs.* the relative pressure (P/P_0). For instance, depending on the pore shape, cylindrical pores often display type H1 profiles, while ink-bottle pores have type H2 profiles.[48] Gas absorbed into the structure of the adsorbent undergoes condensation. The desorption process takes place after the condensation step and occur in the solution state. Therefore, the amount of heat (enthalpy of adsorption) evolved during this processes are different. The desorption branch generally differs from the isotherm branch of adsorption due to the difference for the enthalpy of adsorption *vs*. desorption. Based on this difference, hysteresis loops have been described based on gas adsorption results, where this technique can provide useful information on the adsorption-desorption process. (*cf*. Figure 2.8)

Type H1

The H1 type of hysteresis is possible when nitrogen gas adsorbs onto the walls of the pores prior to formation of multilayers until the pore volume is fully occupied. Cylindrical pores are associated with this type of hysteresis as the filling of the pores occurs uniformly within the pore and allows a steep asymptote profile when condensation occurs.

Type H2

The H2 hysteresis is related to ink-bottle pores due to difficulties in the filling for some of the pores. Although the adsorption into the pores is similar to H1, attenuation of capillary condensation is the reason behind this hysteresis loop. The IUPAC types of profiles note that desorption isotherms are governed by other factors that can also affect the isotherm shape, such as the presence of network pores within a material. However, the desorption curve does not follow the original/initial desorption branch of the hysteresis profile.

Type H3

The H3 hysteresis loop exists in the isotherm due to adsorbate-adsorbate interaction following the completion of the monolayer coverage. For example, thin slit-like capillaries can promote this type of hysteresis.[56]

Type H4

This type of isotherm is distinguished by the high adsorption affinity of the adsorbent, which indicates microporosity that allows for strong adsorbent-adsorbate interactions.[48] The desorption-isotherm branch looks like the H3 type and the pore structure is almost slit-shaped.

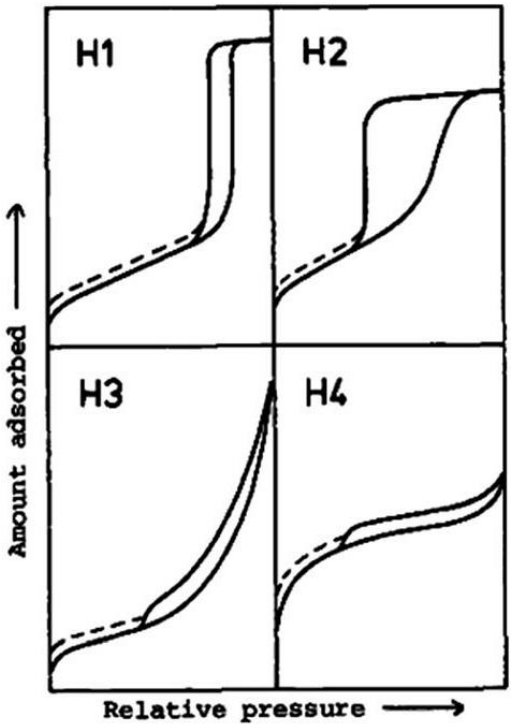

Figure 2.8 The four general hysteresis loops detected for nitrogen adsorption and desorption as defined by IUPAC. (Figure is reprinted with permission from ref. 48)

Isotherm types and models are useful analyzing tools for understanding of the adsorption process under variable conditions. One of the main factors governing the adsorption process is the adsorbent itself. Adsorbents with different structural and chemical properties and even different shapes behave differently toward adsorbates. To gain a better grasp of the adsorption process, familiarity with the physicochemical properties of various types of adsorbents is essential.

2.4 Knowledge gaps and hypotheses

The applications of biomaterial sorbents, especially cellulose and starch have gained increasing attention in recent years due to interest in the development of sustainable alternative sorbent materials. However, research on these materials for the purpose of water-ethanol adsorptive separation is sparsely reported in terms of liquid phase separation. Modification of these biomaterials to alter their chemical and textural properties can be done by a variety of synthetic methods. Although, there have been many studies on the modification of cellulose and starch by various types of surface functionalization, limited studies have examined the effect of cross-linking degree in a systematic fashion.[57,58] The structural characterization of these materials is necessary

for understanding the role of cross-linking and its extent on the adsorptive properties of a modified adsorbent to improve the adsorption capacity. Meanwhile, there is a variety of native forms of biomass available that can be employed as an adsorbent in controlled uptake of chemical species and separations from aqueous solution. The adsorptive capacity of biomass can be enhanced in a parallel manner as for the case of biopolymers by synthetic modification. In addition, detection of water/ethanol has been carried out commonly using GC and LC techniques, as outlined above. However, it is necessary to find other techniques due to limitations such as thermal degradation and such as longer run times for separation and quantitative analysis. The development of alternative methods may provide abundant opportunities for future research such as quantitative NMR (qNMR) could be employed for detection of water/ethanol without the necessity of chromatographic separation. The use of qNMR offers *in situ* detection (assuming there is no spectral overlap with the NMR signatures of interest) with shorter analysis times (*ca.* 1 min for data acquisition).

This PhD thesis research addresses various knowledge gaps and hypotheses (H):

- Biopolymers such as cellulose, starch, and their modified forms are capable of separating/removing of components from a mixture. (H1)
- Modification using cross-linking can alter the textural properties (surface area and porosity) and surface chemistry of starch and cellulose biopolymers. (H2)
- Quantitative proton NMR spectroscopy is a suitable quantitative method for determination of water and ethanol in binary mixtures. (H3)
- Biomass such as Miscanthus and its modified forms that contain varying amounts of cellulose and lignin biopolymers are suitable for adsorptive separation/removal of components from a mixture. (H4)
- The adsorption process is highly influenced by hydration phenomena. (H5)

2.5 Research objectives

The overall objectives of this research are focused on the sorption properties of biopolymers and their modified forms for the fractionation of water/ethanol in binary mixtures. The short-term objectives are related to the synthesis of modified biopolymers and their structural

characterization, along with the evaluation of the sorption properties of the biopolymers and their modified forms.

The overall objectives proposed in this thesis research can be further organized by dividing it into various projects:

Project 1) To synthesize and characterize the biopolymers modified with variable cross-linking, including starch and cellulose. Studies of the dye uptake properties using *p*-nitrophenol at equilibrium conditions and a study of the solvent swelling properties in neat solvents (water and ethanol). This project is outlined in Chapter 3.

Projects 2 and 3) To develop an NMR method for *in-situ* quantitative analysis of water and ethanol in binary mixtures. Characterize the structural and physicochemical properties of polysaccharide materials containing different types of starch and cellulose. To study the adsorption properties of materials using various characterization methods included UV-vis/ IR/ thermal gravimetric analysis. These projects are outlined in Chapters 4 and 5.

Project 4) To evaluate the relative water selective adsorption behaviour of biomaterials by the quantitative NMR (qNMR) method. Evaluate the potential utility of native and treated biomass components of Miscanthus for the fractionation of water (W) and ethanol (E) in binary W-E mixtures.

Project 5) To study the role of hydration phenomena in starch and cellulose biopolymers (including modified forms) employing thermoanalytical and various spectroscopic techniques in an effort to provide a greater understanding of the adsorption properties of these biopolymers. This project is outlined in Chapter 7.

2.6 Organization of this thesis

This PhD thesis focuses on the study of adsorption-based phenomena of biomaterials and their modified forms, according to the knowledge gaps and hypotheses defined in Chapter 2.

The thesis research is divided into 8 chapters where Chapter 1and 2 provide background information relevant to the studies that follow in the manuscripts outlined in Chapters 3 to 7. The content of the manuscript chapters represent verbatim copies of the published or submitted manuscripts where editing of presentation format was carried out to meet the requirements of the University of Saskatchewan guidelines set forth by the College of Graduate and Postdoctoral Studies (CGSPS). The literature review of the research is contained within the introduction section

of each manuscript chapter in order to address the specific objectives of knowledge gaps. The manuscripts in Chapters 3–7 are either published peer-reviewed or under review (Chapter 7), as outlined below.

Manuscript 1: **Dehabadi**, **L.;** Wilson, L. D. Polysaccharide-based materials and their adsorption properties in aqueous solution. *Carbohydr. Polym.* **2014,** *113,* 471–479. (Chapter 3)

A hypothesis of this research proposes that biomaterials such as starch and cellulose and their modified forms may be useful as adsorbents in adsorption processes for separation of water and ethanol. The objectives of this project are in line with the first objective of this thesis including synthesis and characterization of polysaccharides (PSs). In this study, PSs such as cellulose and starch with variable amylose and amylopectin content were modified by cross-linking with epichlorohydrin (EPI). Another related objective concerns the evaluation of the textural and adsorptive properties of the polymers using nitrogen gas adsorption-desorption and dye-based probe (*p*-nitrophenol) measurements. Hence, the modified polymers were characterized using spectroscopic (IR and NMR) methods, nitrogen adsorption and thermal gravimetric analysis (TGA). The findings indicate that the cross-linked PS–EPI materials have tunable properties as evidenced by their variable properties compared to the unmodified (native) form. Moreover, the optimum yield of the synthesized polymers was obtained at the reaction temperature (50–54°C). In addition, solvent uptake, nitrogen adsorption, and aqueous dye sorption showed a complex relationship between amylose and amylopectin content in the PS–EPI polymers and their physicochemical properties. Finally, structural variation of the polysaccharide (i.e. branching, molecular weight, and relative amylopectin/amylose content) was confirmed to contribute to the solvent uptake in neat solvents (i.e. water *vs.* ethanol). The uptake properties were observed to depend on the nature of the cross-linking, as evidenced by the dependence on the textural properties and surface chemistry.

Manuscript 2: **Dehabadi, L.; Wilson, L. D.** Nuclear Magnetic Resonance Investigation of the Fractionation of Water–Ethanol Mixtures with Cellulose and Its Cross-Linked Biopolymer Forms. *Energy Fuels,* **2015,** *29 (10),* 6512–6521. (Chapter 4)

Manuscript 3: **Dehabadi, L.; Wilson, L. D.** NMR Investigation of the Fractionation of Water–Ethanol Mixtures with Starch and Its Cross-Linked Forms. *Energy Fuels,* **2016,** *30,* 5684−5692. (Chapter 5)

The hypothesis of these studies proposes that quantitative proton NMR spectroscopy is a suitable technique for quantitative determination of water and ethanol in binary mixtures. Furthermore, cross-linked biomaterials with variable cross-linker ratios could show different adsorption properties towards water and ethanol components in mixtures. The second and third projects (Chapters 4 and 5) cover the second objective of this thesis where the development of a versatile qNMR method for the study of the adsorptive fractionation of water and ethanol by starch and cellulose materials is also investigated in this research.

An overview of the key results obtained from the above mentioned research relates to the water-ethanol fractionation properties of biopolymers such as cellulose and starch (linear amylose *vs.* branched amylopectin) obtained from different biomass sources. As well, the application of the biopolymer adsorbent materials for fractionation of biofuel mixtures is outlined for binary mixtures with variable water and ethanol composition. To develop new adsorbent materials, chemical modification of cellulose and starch (amylose and amylopectin) was conducted via a cross-linking strategy. The fractionation properties were then compared to various native cellulose and starch forms. The qNMR method was shown to be effective as an *in situ* analytical method that allows for measurement of the changes in the ethanol and water mixture concentration (before and after adsorption) in the presence of cellulose, starch and their modified forms. The composition of unbound and bound species was analyzed using a Sips isotherm, because it can provide estimates of the relative uptake of the water fraction *vs.* the ethanol fraction by cellulose and starch after exposure to such mixtures. This allows the exploitation of the unique adsorption properties of these biopolymers, especially in the case of modified cellulose and starch according to cross-linking effects. A study of the isotherms indicated that the cellulose and starch materials could be used to fractionate the components in binary water-ethanol mixtures with a higher adsorption affinity for water over ethanol. The relative solvent selectivity observed from these two studies is reported as 2.5:1 and 80:1(water: ethanol), respectively. These results confirm that biofuel mixtures containing ethanol and water can be enriched without the use of distillation and by means of an adsorption-based approach reported herein in Chapter 4. These studies demonstrate a novel method for the potential refining of biofuels that further illustrate the utility of this green chemistry

adsorption method. This approach offers significant potential savings in the energy consumption during the separation step of biofuels production. The development of a new adsorption-based method for water separation from such mixtures is reported and its advantages over conventional distillation. These reports also lead to a greater understanding of the role of polysaccharide components that are employed for use in chemical separations, as described in Chapter 5.

Manuscript 4: **Dehabadi**, **L.;** Mahaninia, M. H.; Soleimani, M.; Wilson, L. D. Miscanthus biomass for the sustainable fractionation of ethanol-water mixtures. *ASC Sustain. Chem. Eng.* **2017,** *5(4),* 2970–2980. (Chapter 6)

The hypothesis of this research proposed that biomass such as Miscanthus and its modified forms with variable particle sizes might show enhanced water adsorption. The third objective was explored in project 4. The focus of this research was on the potential application of native and treated Miscanthus as a potential biomass adsorbent for fractionation of water and ethanol in binary mixtures, as outlined in Chapter 6. Miscanthus biomass can be prepared to yield a variety of particle sizes. As well, chemical pretreatments were carried out to generate modified cellulosic biomass and lignin. These materials were hypothesized to play a key role in the fractionation of water (W) and ethanol (E) in binary mixtures. In this research, the adsorption properties of cellulose-enriched and lignin materials were evaluated using qNMR spectroscopy to monitor the separation process in binary W-E mixtures. The adsorption capacity results obtained for water and ethanol show that cellulose-enriched materials had lower water uptake compared to the raw Miscanthus biomass (RM), but higher water uptake compared to lignin. This work revealed a solvent selectivity ratio of 3:1 water: ethanol for (RM) in binary W-E solutions. This selectivity ratio is close to that reported for pure cellulose and its cross-linked forms. The key point of this research is that the particle size variation had a minimal impact on the overall adsorption of water and ethanol. By contrast, the impact of chemical treatment was greater according to the content of hydrophilic sites and pore structures of the biomass. According to the data, the regeneration process resulted in a 12% decrease for the relative uptake of water and ethanol. This research contributes to a greater understanding of biomass treatment effects and the deconvolution of biopolymer adsorptive contributions for the fractionation of water-ethanol mixtures. Another contribution of this work relates to the development of advanced biomaterials for the adsorptive processing of beverages, food, and biofuels using sustainable biomaterials.

Manuscript 5: **Dehabadi, L.;** Karoyo, A. H.; Wilson, L. D. Spectroscopic investigation of the fractionation processes of water-ethanol mixtures using biopolymer materials. *ACS Omega* **2018,** Submitted. (Chapter 7)

The overall objectives of this research relate to the use of thermoanalytical and spectroscopic techniques for evaluation of the solvent contribution in the adsorption process of biomaterials and their modified forms with various adsorbates. The final objectives of the thesis related to project 5 are described in Chapter 7. The main objectives of this study focused on the role of hydration effects to gain insight on the adsorption properties of biopolymers. This was achieved through the use of different complementary techniques such as Raman spectroscopy and differential scanning calorimetry (DSC). Also, the measurement of dielectric constant and swelling properties of the various adsorbent materials was shown to provide useful experimental evidence for further understanding the adsorption of water in biopolymers and their cross-linked forms. The importance of this study relates to the relationship between hydration effects and the mechanism of fractionation of water and ethanol. Due to the strong influence of hydration on the properties of biomaterials, a molecular-level understanding of hydration processes is the subject of ongoing interest in food, environmental, and energy science.

2.7 References

1. Campo, E.; Cacho, J.; Ferreira, V. *J. Chromatogr. A* **2007,** *1140,* 180-188.
2. Rodrigues, F.; Caldeira, M.; Camara, J. S. *Anal. Chim. Acta* **2008,** *609(1),* 82-104.
3. Weatherly, C. A.; Woods, R. M.; Armstrong, D.W. *J. Agric. Food Chem.* **2014,** *62(8),* 1832-1838.
4. Tiscione, N. B.; Alford, I.; Yeatman, D. T.; Shan, X. *J. Anal. Toxicol.* **2011,** *35,* 501-511.
5. Yarita, T.; Nakajima, R.; Otsuka, S.; Ihara, T.; Takatsu, A.; Shibukawa, M. *J. Chromatogr. A* **2002,** *976,* 387-391.
6. Alcázar, A.; Jurado, J. M.; Pablos, F.; González, A. G.; Martín, M. J. *Microchem. J.* **2006,** *82(1),* 22-28.
7. Magolan, K. M. Analysis of methanol, ethanol and propanol in aqueous. Ph.D. Thesis, University of North Carolina Wilmington, North Carolina, USA, **2005.**
8. Sharma, K,; Sharma, S.P.; Lahiri, S.C. *J. AOAC Int.* **2009,** *92(2),* 518-526.
9. Yarita, T.; Nakajima, R.; Otsuka, S.; Ihara, T.A.; Takatsu, A.; Shibukawa, M. *J. Chromatogr. A.* **2002,** *976(1-2),* 387-391.
10. Tavcar, E.; Turk, E.; Kreft, S. *J. Anal. Methods Chem.***2012,** *2012,* 1-6.
11. Fregolente, P. B. L.; Wolf Maciel, M. R.; Oliveira, L. S. *Braz. J. Chem. Eng.* **2015,** *32,* 895-901.
12. Lachenmeier, D. W. *Food Chem.* **2007,** *101(2),* 825-832.
13. Pontes, M. J. C.; Santos, S. R. B.; Araújo, M. C. U.; Almeida, L. F.; Lima, R. A. C.; Gaião, E. N.; Souto, U. T. C. P. *Food Res. Int.* **2006,** *39(2),* 182-189.
14. Laakso, O.; Haapala, M.; Jaakkola, P.; Iaaksonen, R.; Nieminen, J.; Pettersson, M.; Räsänen, M.; Himberg, J-J. *J. Anal. Toxicol.* **2000,** *24,* 250-256.
15. Simmler, C.; Napolitano, J. G.; Mcalpine, J. B.; Chen, S. N.; Pauli, G. F. *Curr. Opin. Biotechnol.* **2014,** *25,* 51-59.
16. Jungnickel, J. L.; Forbes, J. W. *Anal. Chem.* **1963,** *35(8),* 938-942.
17. Hollis, D.P. *Anal. Chem.* **1963,** *35,* 1682–1684.
18. Gonçalves, M. I. A.; Andreolli, T. J., Valduga, C. *J. Ann. Magn. Reson.* **2004,** *3(3),* 105-107.
19. Isaac-Lam, M. F. *Int. J. Spectrom.* **2016,** *2016,* 1-8.
20. Isaac-Lam, M. F. *J. Chem. Educ.* **2014,** *91(8),* 1264–1266.
21. Caysa, H. Metz, Mader, H. K. Mueller, T. *J. Exp. Clin. Cancer Res.* **2011,** *30(69),*1-7.

22. Sun, Sh.; Jin, M.; Zhou, X.; Ni, J.; Jin, X.; Liu, H.; Wang, Y. *Molecules* **2017,** *22(9),* 1517-1526.
23. Bharti, S. K.; Roy, R. *Trends Anal. Chem.* **2012,** *35,* 5-26.
24. Malz, F.; Jancke, H. *J. Pharm. Biomed. Anal.* **2005,** *38,* 813-823.
25. Pauli, G.F.; Jaki, B.U.; Lankin, D.C.; *J. Nat. Prod.* **2005,** *68,* 133-138.
26. Creasy, W.R.; McGarvey, D.J.; Rice, J.S.; O'Connor, R.J.; Durst, H.D. Study of Detection Limits and Quantitation Accuracy using 300 MHz NMR (ADA482893), In Proceedings of the 2002 Joint Service Scientific Conference on Chemical and Biological Defense Research, 19-21 November 2002; Berg, D.A., Compiler; U.S. Army Edgewood Chemical Biological Center: Aberdeen Proving Ground, MD, **2003,** UNCLASSIFIED Report.
27. Al-Asheh, S.; Banat, F.; Fara, A. A. *Sep. Sci. Technol.* **2009,** *44,* 3170–3188.
28. Yamamoto, T.; Kim, Y. H.; Kim, B. C.; Endo, A.; Thongprachan, N.; Ohmori, T. *Chem. Eng. J.* **2012,** *181–182,* 443–448.
29. Negi, A. S. A Textbook of Physical Chemistry. New Age International, New Delhi, **2007,** 1-1008.
30. Blokzijl, W.; Engberts, J. B. F. N. *Angew. Chem. Int. Ed. Engl.* **1993,** *32,* 1545-1579.
31. Karunarathne, H. D. S. S.; Amarasinghe, B. M. W. P. K. *Energy Procedia* **2013,** *34,* 83-90.
32. Corma, A. *J. Catal.* **2003,** *216,* 298–312.
33. Hu, X.; Xie, W. *Sep. Sci. Technol.* **2001,** *36(1),* 125–136.
34. Russo, V.; Trifuoggi, M.; Di Serio, M.; Tesser, R. *Chem. Eng. Technol.* **2017,** *40(5),* 799–820.
35. Adamson, A.; Gast, A. Physical Chemistry of Surfaces. Wiley-Interscience, New York, **1997,** 390-420.
36. Mackinnon, M. D.; Boerger, H. *Water Pollut. Res. J. Can.* **1986,** *21,* 496-512.
37. Foo, K.Y.; Hameed, B. H. *Chem. Eng. J.* **2010,** *156 (1),* 2-10.
38. Liu, B.; Yang, F.; Zou, Y.; Peng, Y. *J. Chem. Eng. Data* **2014,** *59,* 1476−1482.
39. Voudrias, E.; Fytianos, K.; Bozani, E. *Global Nest J.* **2002,** *4,* 75-83.
40. Senozan, N. M.; Henry, N. P. *J. Chem. Ed.* **2001,** *78(11),* 1499-1503.
41. Bertau, M.; Jörg, G. *Bio Org. Med. Chem.* **2004,** *12(11),* 2973–2983.
42. Liu, Y.; You, C-C. *J. Phys. Org. Chem.* **2001,** *14,* 11–16.
43. Mohamed, M. H.; Wilson, L. D.; Headley, J. V. *Carbohydr. Polym.* **2010,** *80 (1),* 186−196.
44. Udoetok, I. A.; Dimmick, R. M.; Wilson, L. D.; Headley, J. V. *Carbohydr. Polym.* **2016,** *136,* 329–340.

45. Yalkowsky, S. H.; He, Y.; Jain, P. Handbook of aqueous solubility data. 2nd ed. CRC Press, Boca Raton, Florida, **2010,** 1-1608.
46. Mohamed, M. H.; Wilson, L. D.; Headley, J. V; Peru, K. M. *Energy Fuels* **2015,** *29(6),* 3591 3600.
47. Wilson, L. D.; Mohamed, M. H.; Headley, J. V. *J. Colloid Interface Sci.* **2011,** *357,* 215-222.
48. Kumar, P.; Kim, K-H.; Kwon, E. E.; Szulejko, J. E. *J. Mater. Chem. A* **2016,** *4,* 345-361.
49. Suits, C. G.; Miles, J. M. Irving Langmuir 1881-1957: A Biographical Memoir, National Academy of Sciences Biographical Memoir. **1974,** 214-47.
50. D'Arcy, M.; Bullough, F.; Moffat, C.; Borgomeo, E.; Teh, M.; Vilar, R.; Weiss, D. J. *J. Chem. Educ.* **2014,** *91,* 505−510.
51. Sips, R. *J. Chem. Phys.* **1948,** *16,* 490–495.
52. Brunauer, S.; Emmett, P. H.; Teller, E. *J. Am. Chem. Soc.* **1938,** *60,* 309-319.
53. Fu, Y.; Hansen, R. S.; Bartell, F. E. *J. Phys. Chem.* **1949,** *53(8),* 1141–1152.
54. Determination of the specific surface area of solids by gas adsorption — BET method, 2nd ed. BS ISO 9277: **2010**.
55. Barrett, E.P.; Joyner, L.G.; Halenda, P.P. *J. Am. Chem. Soc.* **1951,** *61,* 373-380.
56. Raghavan, N. S.; Ruthven, D. M. *Chem. Eng. Sci.* **1984,** *39(7-8),* 1201–1212.
57. Zia-Ud-Din, Xiong, H.; Fei, P. *Crit. Rev. Food Sci. Nutr.* **2017,** *57(12),* 2691-2705.
58. Jedvert, K.; Heinze, T. *J. Polym. Eng.* **2017,** *37(9),* 845–860.

CHAPTER 3

MANUSCRIPT 1: Polysaccharide-based materials and their adsorption properties in aqueous solution.

Leila Dehabadi, Lee D. Wilson∗

Description

This thesis project involves the preparation, characterization and assessment of equilibrium sorption properties of polysaccharide-based adsorbents. This research reports on the synthetic modification of various polysaccharides, starch and cellulose, according to a cross-linking strategy with epichlorohydrin (EPI) at variable synthesis conditions (e.g., nature of the biopolymer, stirring rate and temperature). The polysaccharides (PSs) include starch (amylose and amylopectin) and cellulose with variable molecular weight. The modified polysaccharides are designated as PS-EPI with tunable properties, where the structure of the materials and their physicochemical properties were assessed by various characterization methods such as nuclear magnetic resonance (NMR) spectroscopy, thermogravimetric analysis (TGA), infrared (IR) spectroscopy and adsorption isotherms using nitrogen gas or a suitable dye in solution. The dye-based equilibrium sorption properties of the PS-based adsorbents were evaluated using *p*-nitrophenol (PNP) at pH 6 as a model organic compound. The solvent swelling behaviour of the PS-EPI adsorbents were tested in neat solvents using ethanol and water, respectively.

Author's Contribution

The project was conceived by the supervisor (L. D. Wilson) with some input on the types of polysaccharide precursors from L. Dehabadi. The experimental studies related to the preparation and characterization of the materials was carried out by L. Dehabadi along with the first draft of the manuscript. Subsequent editing was carried out by the supervisor and L. Dehabadi prior to publication of this research.

Relation of Manuscript 1 to Overall Objective of this Project

The importance of this research was significant toward developing a series of modified polysaccharide materials with incremental levels of cross-linking. The structural characterization and evaluation of the adsorption properties not only provided the evidence for writing the first manuscript but also served as an initial starting point for future studies and further understanding

of adsorption properties of such modified biopolymers. Particularly, some of the experiments such as the solvent-swelling test provided spectacular vision about textural and surface chemistry of adsorbents. The variable solvent-swelling properties of the PS-EPI materials in water and ethanol solvents indicated the role of polysaccharide's structure in water uptake. In turn, all other experimental results showed trends which supported the hypothesis (H1) introduced in Chapter 1. This hypothesis is further explored in subsequent chapters (3-4) with more focus on the study of starch and cellulose adsorption properties in binary W-E mixtures. The objectives of Chapters 3 and 4 relate to the evaluation of the adsorptive fractionation of W-E binary mixtures using polysaccharides with variable nature (starch *vs.* cellulose) at incremental levels of cross-linking from low to higher values (1:2, 1:3.6 and 1:5.4 PS-EPI mole ratios).

Research Highlights

- Diverse types of polysaccharide–epichlorohydrin (PS–EPI) modified materials were prepared and structurally characterized.
- Modified materials were studied that contain amylose, amylopectin, and cellulose with incremental levels of cross-linking.
- Modified materials displayed variable uptake according to the level of cross-linking and the nature of the polysaccharides.
- Modified materials adsorbed variable amounts of water (up to ~300%) that generally exceeded levels observed for ethanol.
- Modified materials displayed tunable adsorption toward *p*-nitrophenol in aqueous solution according to the type of polysaccharide and the level of cross-linking.

3. Polysaccharide-based materials and their adsorption properties in aqueous solution.

Leila Dehabadi, Lee D. Wilson∗

Department of Chemistry, University of Saskatchewan, 110 Science Place, Saskatoon, Saskatchewan, Canada S7N 5C9.

*Corresponding Author.

Supplementary Information (Appendix A, Chapter 3)

3.1 Abstract

Polysaccharides (PS) of cellulose, soluble corn, and maize-derived starches with variable amylose/amylopectin content were cross-linked with epichlorohydrin (EPI) to form polymeric adsorbents. The properties of the PS–EPI biomaterials were prepared by varying the synthesis conditions (nature of polysaccharide, temperature, and reagent ratios) to afford network polymer materials with tunable properties. The optimized polymers were obtained at a reaction temperature (50–54°C) according to their yield and were characterized using spectroscopic methods (IR and NMR), and thermal gravimetric analysis (TGA). The textural and adsorptive properties of the polymers were evaluated using nitrogen gas and dye-based methods employing *p*-nitrophenol. Solvent uptake, nitrogen adsorption, and aqueous dye sorption showed that the amylose and amylopectin content in the PS–EPI biopolymers displayed a complex relationship with their physicochemical properties. Polymers with greater cross-linking did not show incremental changes in water or dye uptake. Structural variation of the polysaccharide (i.e. branching, molecular weight, and relative amylopectin/amylose content) contributed to the sorption properties by modifying their textural properties and surface chemistry.

3.2 Introduction

Polysaccharides such as starch and cellulose from plant sources are relatively abundant, naturally occurring, nontoxic, inexpensive and economically important biomaterials. They are amenable to chemical modification which make them especially attractive biomaterial platforms to produce value-added materials in technologies such as in drug delivery,[1-3] biomedical devices,[4] tissue engineering scaffolds,[5] dispersions,[6] waste water treatment[7] and bio-refineries.[8] Starch and cellulose are abundant plant-based biopolymers, where the former serves as the plant's main energy reserve while the latter provides structural stability to plant cell walls. Starch may occur as granules (small compact form of starch molecules), which are composed mainly of two biopolymers, where the main component is amylopectin (70-80%), a branched polymer comprised of α-1,4-linked glucose units with α-1,6 branching links. The secondary component is amylose, a linear polymer consisting mainly of α-1,4-linked D-glucose units.[9-12] X-ray structural analysis of starch granules indicates a model of repeating amorphous and crystalline domains.[12] The crystalline domains of starch are associated with amylopectin while the amorphous regions are associated with amylose interspersed with amylopectin.[13] By comparison, cellulose is much more crystalline in nature due to its β-1,4 linked D-glucose units arranged in a linear chain with no coiling or branching.[12] These biopolymer components adopt a relatively linear and rigid conformation where the monomer units undergo extensive intramolecular and intermolecular H-bonding.[9] The tertiary structures of starch and cellulose impact their physicochemical properties. For example, the relative ease with which cellulose chains form stabilizing intra- and intermolecular interactions results in a self-assembled material with high tensile strength and relatively low solubility in water and many organic solvents. These properties, which contribute to its suitable function as a structural component of plant cell walls, limit its industrial use due to material processing challenges. [9] On the other hand, the variable crystalline properties of starch granules due to the amylose and amylopectin content affect its structure and physicochemical properties. As with the case of cellulose, the crystalline domains of starch makes it less soluble in water but the presence of the amorphous regions imparts lower structural rigidity and greater water solubility. This variable affinity of such biopolymers to water is useful in the food industry for improving food texture but may attenuate the sorption properties with xenobiotics due to competitive sorption in aquatic environments.[14] Mixed biopolymers in starch may limit a detailed understanding of their structure and properties but such materials may display unique

physicochemical properties that are nonlinear with respect to their composition. For example, starch with high amylose content is commonly associated with high viscosity due to increased interactions and entanglement of the linear amylose chains.[11] Enhanced interaction between amylose chains is relevant for preparing starch-based derivatives with high thermal and mechanical stability.[15] Starch with high amylopectin content favours swelling whereas starch with high amylose content displays decreased swelling capacity.[11, 16, 17] Swelling is a property closely associated with expansion of the polymer network and is important in drug delivery or for entrapment of guest molecules of a suitable size. Therefore, materials with well-defined swelling properties are important in sorption-based applications. In a recent study, Kyzas *et al.*[18] demonstrated that sorbents that undergo pre-swelling display rapid dye adsorption.

To expand the range of applications of starch and cellulose, cross-linking is a versatile strategy that affords materials with tunable mechanical and chemical properties.[1, 3, 7, 14, 19, 20] The cross-linker introduces intermolecular bridges or cross-links between biopolymer units, which may alter the overall textural properties and surface chemistry of the framework. For example, Dastidar and Netravali [21] cross-linked waxy maize starch to obtain an environmentally friendly resin that has improved toughness and water resistance compared with native starch. Hamdi *et al.* [1] cross-linked soluble starch to form microspheres with controlled particles with narrow size distribution for drug delivery applications. The physicochemical properties of the modified biopolymers may be further varied by the reaction parameters (e.g., temperature, solvent, and prepolymer composition).[19] For example, Ashish *et al.*[22] employed high amylose starch to form biodegradable implants for sustained drug delivery. Kaur *et al.*[20] studied the effects of cross-linker content on the physicochemical properties of starch and attributed their observations to cross-linking of the starch polymer chains. Onofre *et al.*[3] used cross-linked starch with varying amylose/amylopectin content to study the rates of sustained drug release and reported its influence on the degree of cross-linking.

In this study, starch granules (containing varying amylose and amylopectin content) and cellulose were modified by chemical cross-linking with epichlorohydrin at variable reaction conditions. The resulting polysaccharide-epichlorohydrin (PS-EPI) biopolymers were studied by evaluating their sorptive uptake properties in aqueous solutions with a model organic dye adsorbate, *p*-nitrophenol (PNP). The results of this systematic study will contribute to a greater

understanding of the relationship of the sorption properties and structure of such PS-EPI biopolymers in aqueous solutions.

3.3 Experimental:

3.3.1 Preparation of PS-EPI biopolymers

Different sources of starch (corn, maize, high amylose, high amylopectin), natural cellulose fiber from cotton linters, and epichlorohydrin were obtained from Sigma-Aldrich (Oakville, ON, Canada) and used as received. The synthesis of starch-epichlorohydrin biopolymers employed a modified procedure, described elsewhere.[23] Briefly, an aqueous solution of NaOH (2 M) was used to dissolve and ionize the polysaccharide hydroxyl groups prior to the addition of variable amounts of epicholorohydrin (EPI) to produce cross-linked forms. The effect of temperature on the cross-linking reaction was evaluated at 40, 50, 60 and 70°C.

3.3.2 Characterization of PS-EPI biopolymers

The PS-EPI biopolymers products were characterized using ^{13}C solid NMR spectroscopy with a wide-bore (89 mm) 8.6T Oxford superconducting magnet system equipped with a 4mm CP-MAS (cross polarization with magic angle spinning) solids probe. Operating parameters were controlled using an Avance DRX360 console and workstation running TopSpin 1.3 (Bruker Bio Spin Corp; Billerica, MA, USA). Standard pulse programs utilized were included in the TopSpin 1.3 software. Samples were packed in 4mm outer diameter zirconium oxide rotors capped with Teflon MAS rotor caps. Acquisition was carried out using MAS at a rotational speed of 5 kHz, 2-sec recycle delay and 750 μs cross polarization time. The chemical shift of adamantine (δ=38.6 ppm) was used as an internal shift reference.

Fourier Transform Infrared (FT-IR) spectra were obtained with a BIO-RAD FTS-40 spectrophotometer operating in diffuse reflectance mode. Multiple scans were obtained with a 4 cm^{-1} resolution and corrected against spectroscopic grade KBr background and as the sample matrix over the spectral range of 400-4000 cm^{-1}. Thermogravimetry analysis (TGA) was performed using a TGA Q50 (New Castle, DE) operated at a heating rate of 5°C min^{-1} up to a maximum temperature of 500°C under a N_2 (carrier gas) atmosphere.

3.3.3 Solvent swelling properties of PS-EPI biopolymers

The swelling properties of the sorbent materials were studied by use of approximately 40 mg of material that was equilibrated in 6 ml of solvent (either Millipore water or neat ethanol for 48 h). The weight of hydrated polymer (W_S) was determined after tamping dry with filter paper by weighing, and then drying in an oven at 60°C for 12 h to a constant dry weight (W_d). The swelling ratio was calculated using equation 3.1.

$$S_W = \frac{(W_s - W_d)}{W_d} \times 100\% \qquad \text{Equation 3.1}$$

3.3.4 Dye adsorption studies

The textural properties were evaluated using nitrogen adsorption and a dye-based sorption method with UV-vis detection. Aqueous dye solutions of *p*-nitrophenol (PNP) were prepared at pH 6, below the pK_a value (7.14) of PNP.[24] Approximately 20 mg of the powdered and sieved (40 mesh) PS-EPI biopolymers were mixed in 10 ml of solution containing PNP at variable concentration (0.1 to 25 mM) in 10mM potassium phosphate monobasic buffer solution (pH 6) in 4 dram glass vials. The vials were sealed with a parafilm liner between the cap and the glass bottle, followed by equilibration on a horizontal mechanical shaker (Poly Science, Dual Action Shaker) for 24 h at 180 cycles/minute. The samples were then centrifuged (Precision Micro-Semi Micro Centricone, Precision Scientific Co.) at 1800 rpm for 30 min. The UV-Vis absorbance of PNP in the supernatant solutions was measured at λ_{max}= 318 nm using a Varian CARY 100 double beam spectrophotometer at room temperature (295±0.5 K). An absorbance calibration curve was obtained from standard solutions of PNP and the molar absorptivity of PNP (ε=9495 $M^{-1}cm^{-1}$) was determined using the Beer-Lambert relation. The equilibrium concentration (C_e) of PNP in the supernatant solutions was determined and the sorptive uptake (Q_e) of the sorbent material was calculated using equation 3.2, where V is the volume of solution, C_0 is the initial stock concentration (mM), and m is the mass of sorbent.

$$Q_e = \frac{(C_0 - C_e)}{m} \times W_{Solution} \qquad \text{Equation 3.2}$$

The sorptive uptake (%*P*) of PNP from aqueous solution was calculated using equation 3.3.

$$\%P = \frac{(C_0 - C_e)}{C_0} \times 100\% \qquad \text{Equation 3.3}$$

Nitrogen adsorption measurements were obtained using a Micromeritics ASAP 2020 (Norcross, GA) to obtain the surface area and pore structure properties. The surface area was calculated from the adsorption isotherm [11] and the micropore surface area was determined using the de Boer *t*-plot method.[25]

3.4 Results and Discussion

3.4.1 PS-EPI biopolymers synthesis

As indicated above, the molecular structure of native starch and various other biopolymers can be modified by cross-linking with an appropriate linker unit such as epichlorohydrin.[1,3,14,19] Cross-linking EPI with starch or cellulose involves secondary and primary hydroxyl groups; however, a generalized illustration of this process is shown in Scheme 3.1. The PS -EPI biopolymers were prepared at low, medium, and high reactant mole ratios (i.e. 1:2, 1:3.6 and 1:5.4). The temperature conditions for the cross-linking reaction were varied to determine the optimal cross-linking temperature conditions, which were used for all PS-EPI biopolymers preparations.

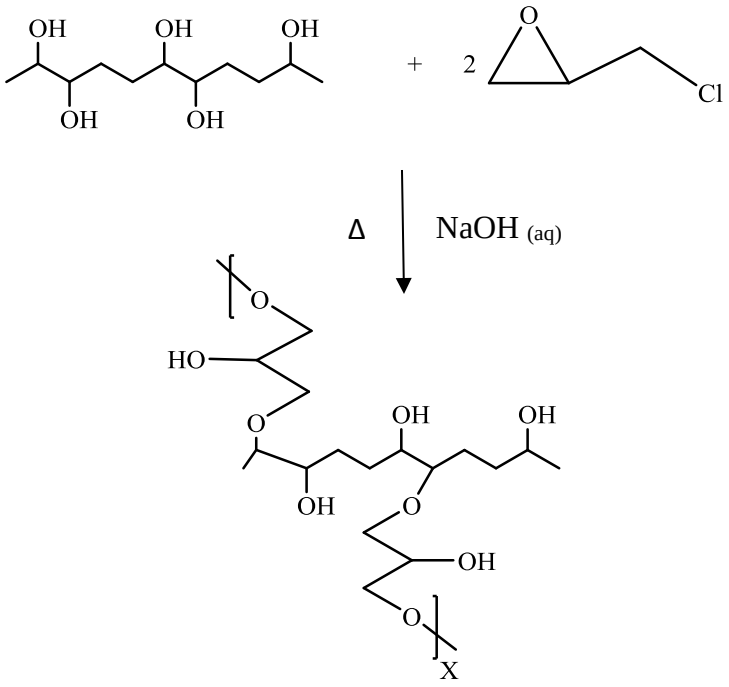

Scheme 3.1 Generalized cross-linking reaction between epichlorohydrin (EPI) with selected hydroxyl groups of a linear polysaccharide (PS).

The cross-linking of starch with epichlorohydrin resulted in variable yield of products (50-98%), which are shown in Tables 3.1 and 3.2, and the PS-EPI biopolymers products were generally water insoluble. In Table 3.1, the greatest yield was obtained with the 1:2 starch-EPI mole ratios and at 50-54°C synthesis conditions. The yields obtained herein are comparable to values (75-95%) reported by Ashish *et al.*[22] where high amylose starch was cross-linked with epicholorohydrin at 50 °C (*cf.* Table 3.1). The yield variability can be attributed to the differences in type of polysaccharide, stirring rate, reagent concentrations, and reaction time. Ashish *et al.* [22] used high amylose starch, which is known to favour cross-linking reactions. In this study, different types of starch were used with amylose/amylopectin (AM/AP) with variable weight ratios (w/w %) to evaluate the effects of composition and branching on the starch-EPI biopolymer properties. The following PS systems were employed: soluble starch (50% AM/AP), corn starch (73% AP/27% AM), and maize starch (98% AP), including cellulose to evaluate the effect of PS structural rigidity.

Table 3.1 Material yield (%) for PS-EPI biopolymers containing soluble starch-EPI at various cross-linking ratios and reaction temperatures (˚C).

PS-EPI biopolymers ID Code	**Mole ratio (PS-EPI)**	**Polysaccharide Composition**	**Yield (%) 40-45˚C**	**Yield (%) 50-54 ˚C**	**Yield (%) 60-64˚C**	**Yield (%) 70-75˚C**
SSE-1	Low (1:2)	~50%(AM/AP)	86	98	66	62
SSE-2	Medium (1:3.6)	~50%(AM/AP)	52	63	48	49
SSE-3	High (1:5.4)	~50%(AM/AP)	56	71	69	37

* Numerical descriptors in the ID code refer to the different mole ratios of PS-EPI, as follows: 1 = Low (1:2 mole ratio); 2 = Medium (1:3.6 mole ratio); and 3 = high (1:5.4 mole ratio)

Table 3.2 Material yield (%) for PS-EPI systems prepared at 50-54 ˚C.

PS-EPI biopolymers	Polysaccharide Composition	PS-EPI biopolymers ID Code*	Yield (%) 50-54 ˚C
Cornstarch-EPI (low)	(73% AP)	CSE-1	95
Cornstarch-EPI (medium)	(73% AP)	CSE-2	53
Cornstarch-EPI (high)	(73% AP)	CSE-3	56
Maize starch-EPI (low)	(98% AP)	MSE-1	71
Maize starch-EPI (medium)	(98% AP)	MSE-2	51
Maize starch-EPI (high)	(98% AP)	MSE-3	45
Low cellulose-EPI (low)	100%	CE-1	58
Cellulose-EPI (medium)	100%	CE-2	42
Cellulose-EPI (high)	100%	CE-3	45
High Amylose corn-based (low)	(98% AM)	AMCE-1	77
High Amylose corn-based (medium)	(98% AM)	AMCE-2	36
High Amylose corn-based (high)	(98% AM)	AMCE-3	51

* Refer to footnotes in Table 3.1 for ID Code descriptors.

3.4.2 FT-IR spectroscopy

The IR spectra of starch and some selected representative modified forms are shown in Figure 3.1. Additional IR results of other systems are provided in (Appendix A3, Figure A3.1). The relative similarity of the IR spectra of starch and its modified forms supports that the primary structure of the polysaccharide was preserved during cross-linking formation, as anticipated. The spectral frequencies are in agreement with those reported elsewhere[7] and the following characteristic IR bands are observed: O-H stretching ~ 3400 cm^{-1}, C-H stretching ~ 2900 cm^{-1}, and C-C stretching ~ 1600 $cm^{-1}$with relatively similar spectral frequencies among the various modified forms prepared herein.[7] The characteristic ring vibrations and the anomeric C-H deformation bands are observed between 900-550 cm^{-1}. Also, the broadening of bands in the range of 900-1400 cm^{-1} are attributed to cross-linking with epichlorohydrin.[26]

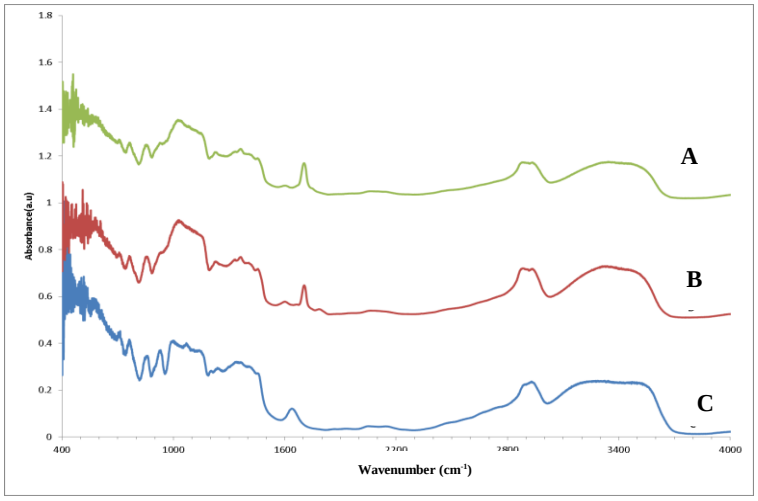

Figure 3.1 FT-IR spectra of starch and its PS-EPI biopolymers. A) SSE-1 synthesized at 60-65°C, B) SSE-1 synthesized at 50-54°C, and C) unmodified starch.

3.4.3 ^{13}C NMR spectroscopy

The PS-EPI biopolymers have limited solubility in various organic solvents such as DMSO, thus, NMR spectra were obtained for selected samples in the solid state using CP-MAS NMR methods, as shown in Figure 3.2. Each glucose monomer of starch contains six C atoms and the spectrum shows four broad ^{13}C NMR lines between 60 and 110 ppm with some overlapping of the various carbon signatures, as observed for amylose-based materials.[23] The results in Figure 3.2, showing intense signals at 72.9, 71.4, 70.0, 63.6 and 61.7 ppm as well as a lower intensity

signal at 100.5 ppm, agree with other reports. [13, 27] There are four ^{13}C signatures for starch, which appear at 100 ppm (anomeric carbon C1), 84 ppm (C4), 70 ppm (C2, C3, and C5), and 61ppm (C6). A comparison of the spectra for the PS-EPI biopolymers indicates greater line broadening relative to starch, and this is understood according the reduced chain dynamics (longer correlation times) of the polysaccharide upon cross-linking, as reported in a previous study of cycloamylose biopolymer cross-linked with epichlorohydrin.[14, 23]

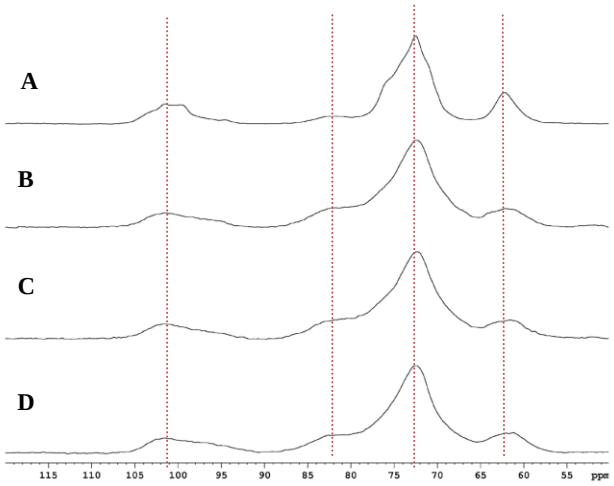

Figure 3.2 ^{13}C CP-MAS NMR spectra of maize starch and selected PS-EPI biopolymers at 295 K. A) MSE, B) MSE-1, C) MSE-2, and D) MSE-3.

3.4.4 Thermogravimetry analysis (TGA)

TGA is a useful method for the quantitative characterization of material composition since it provides a measure of the weight loss due to decomposition, oxidation, or loss of volatile materials, and provides estimates of the relative biopolymers' composition.[13, 23] In this study, TGA results are presented as a first derivative of mass loss with temperature against temperature (DTG plot) to provide information on the decomposition temperature and degree of cross-linking of the biopolymers. A greater degree of cross-linking for amylose-based materials is expected to increase the overall thermal stability of such modified forms.[23] The DTG curves for starch, cellulose and its modified forms are shown in Figure 3.3. The thermal decomposition of these materials occurs over the 200-400°C range; whereas, DTG results for the "as-received" starch and cellulose show decomposition at ~290°C and ~330°C (*cf.* Figures 3.3A and 3.3B). These temperature values agree with reported literature values of 280°C for high amylose corn starch [28] and 330-334°C reported

for cellulose derived from corn cobs.[29] Cross-linking of these biopolymers with epichlorohydrin results in PS-EPI biopolymers with higher decomposition temperatures, providing further support that such materials display greater thermal stability. The PS-EPI biopolymers display an average decomposition temperature of 364 ± 2°C. The difference in thermal stability is evident for starch materials since the starch-EPI biopolymers display higher decomposition temperatures (~+70°C), as compared to cellulose-EPI biopolymers (~ +15°C). Figure 3.3C shows MSE-1 that contains ~98% amylopectin and showed the highest DTG intensity at 364°C. Pratt *et al.*[23] used DTG peak areas to estimate the modified forms composition and the degree of cross-linking. In this case, however, no general trends can be gleaned from DTG intensity results that unequivocally correlate with the AM, AP, or content of EPI of the modified materials. This could mean that the degree of EPI cross-linking is affected by other factors such as steric effects due to branching of the polysaccharide (e.g., AP *vs.* AM), macrocycle effects, and framework structural effects depending on the nature of the polysaccharide and cross-linker. A closer inspection of the DTG curves show that they can be best modeled by a sum of three Gaussian functions centred at 270 °C, 320 °C and 360 °C (refer to Appendix A3, Figure A3.2). Apart from the decomposition temperatures of the PS (270 °C) and the PS-EPI framework (360°C), there is another thermal event at 320°C. A TG/mass spectrometry study of starch-EPI thermal decomposition showed other pathways, aside from polymer dehydration, as the main route of starch-EPI decomposition, which yield secondary degradation products.[30] The presence of other thermal events in the DTG plots can be used to infer the presence of different types of cross-linked materials. Table 3.3 summarizes the relative peak area (%) for the various thermal events of each of the cross-linked materials. Using the peak area under the 360°C event in panel C, it can be related to the degree of cross-linking in descending order: AMCSE-1 > SSE-1≈CSE-1 > MSE-1. This trend is consistent with the relative reactivity of such PS materials with EPI. AMCSE is a linear PS allowing for ease of accessibility of hydroxyl groups to react with EPI; whereas MSE is a branched PS, which may present some steric accessibility of its hydroxyl groups for EPI cross-linking. The relative amount of cross-linking of EPI is estimated from the integrated area of the respective thermal event (at 360°C) corresponding to modified biopolymers' decomposition profile. In panel D, intermediate ratios of EPI were used and the results show a similar trend as in panel C. However, by increasing the amounts of EPI (panel E), the TGA results can no longer be modeled by a simple sum of three Gaussian functions. Instead, the DTG results can be modeled by a minimum of six Gaussian components (Appendix

A3, A3.2) and reveal that cross-linking has resulted in modified biopolymers with heterogeneous domains of intermediate and higher levels of cross-linking.

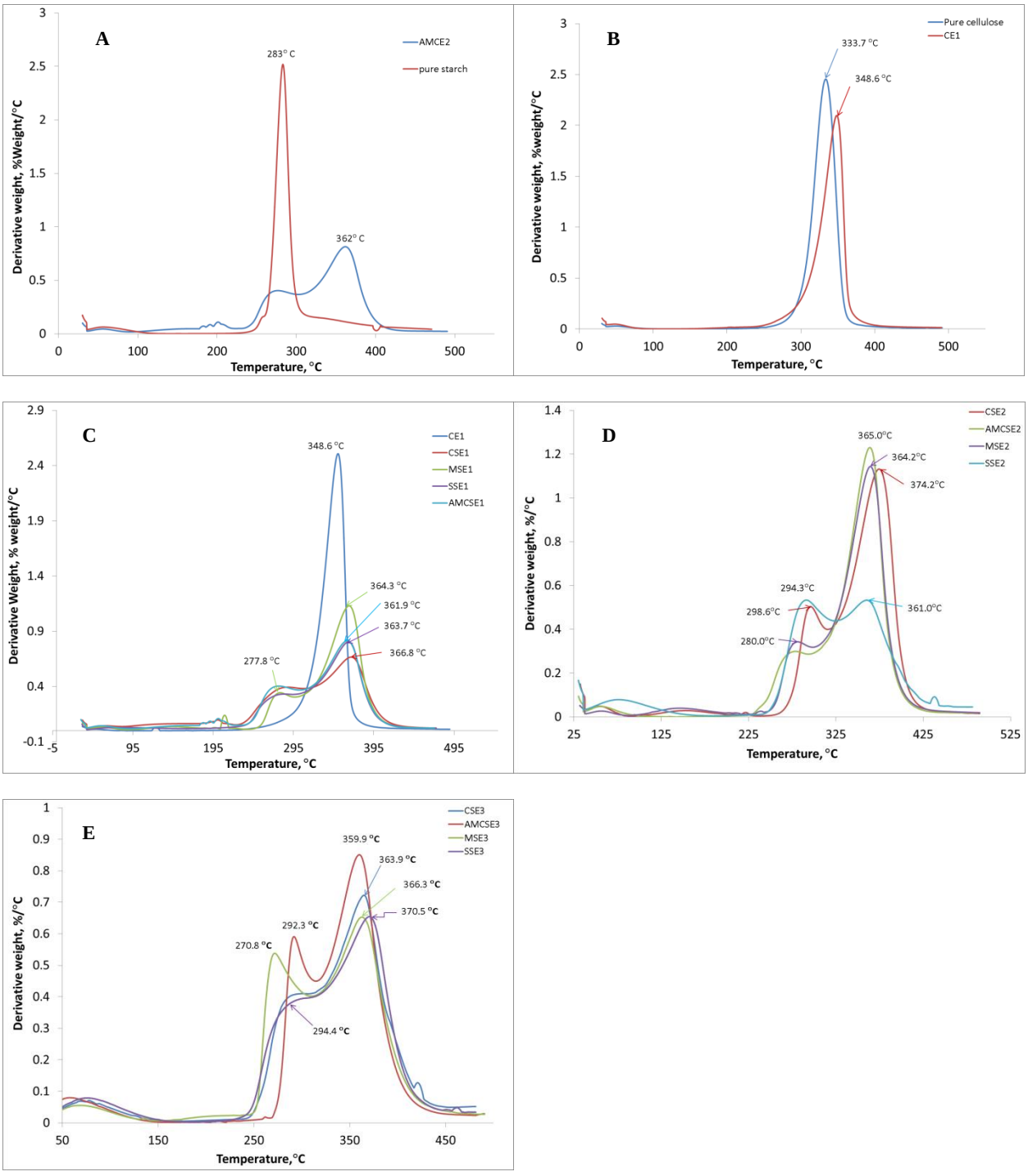

Figure 3.3 First derivative plots of A) pure starch and starch-EPI biopolymer; B) pure cellulose and cellulose-EPI biopolymer and C-E) various PS-EPI biopolymers.

Table 3.3 TGA results for PS-EPI biopolymers prepared at 50-54 °C.

PS-EPI biopolymers ID Code*	Peak Area (270°C)	Peak Area (320°C)	Peak Area (360°C)
CSE-1	25%	21%	53%
CSE-2	30%	39%	30%
CSE-3[a]	21%	9%	69%
MSE-1	12%	57%	30%
MSE-2	14%	57%	28%
MSE-3[a]	11%	27%	61%
AMCSE-1	31%	14%	55%
AMCSE-2	31%	14%	55%
AMCSE-3[a]	15%	32%	52%
SSE-1	29%	16%	54%
SSE-2	39%	10%	51%
SSE-3[a]	16%	27%	58%

***The fitting details found in supporting information.
[a] Areas under the curve were taken from convolution of three Gaussians but the fit was not optimal.

3.4.5 Equilibrium solvent swelling properties

The equilibrium swelling of the unmodified polysaccharides and respective modified forms provide an indication of the relative uptake of the solvent (i.e. water or ethanol) at ambient conditions. Swelling is an important property to measure when assessing the potential of new adsorbent materials since solvent uptake plays a role in the adsorption process, as evidenced by the elementary kinetic steps (e.g., film diffusion, intraparticle diffusion, surface adsorption). For example, Kyzas *et al.*[18] reported the relationship of swelling and dye sorption properties of chitosan derivatives. They describe that pre-swelling of the adsorbents prior to dye adsorption in aqueous solution affects the rate of the adsorption process. The swelling behaviour of the adsorbent materials in water and ethanol [S_w and S_E; Equation 3.1] is presented in Table 3.4. It is noted that the AMCSE modified forms have a greater adsorption capacity for water relative to ethanol; whereas, the MSE biopolymers display the opposite behaviour. The PS-EPI biopolymers display a greater preference for the uptake of water over ethanol. The occurrence of selective solvent uptake by the modified forms of biopolymers depends on several factors: *i*) textural properties (i.e. pore size, pore volume, and surface area), and *ii*) surface chemistry of the modified framework according to the relative accessibility of hydroxyl groups of the sorbent. PS-EPI biopolymers with a pore size less than 4Å will preferentially adsorb water (2.8 Å) due to steric exclusion effects.[17]

In contrast, PS-EPI biopolymers with a pore size exceeding 4Å can retain either species since ethanol has a greater size (4.6 Å).[17] Since the PS-EPI biopolymers synthesized in this study have similar pore sizes and in the range of ~ 21Å -28 Å, steric effects are not anticipated. Solvent selective adsorption may occur depending on the surface chemistry of the framework. In cases where the surface accessibilities of hydroxyl groups vary, the surface chemistry may govern the adsorptive interactions, as evidenced by the variable swelling capacity of the different PS-EPI biopolymers. When the AM units are self-assembled and aligned within the polymer structure, the probability of AM cross-linking with another AM is high (*cf.* Scheme 3.2). By comparison, cross-linking of branched AP with either AM or another unit of AP is expected to result in more pronounced pore domains due to the effects of polysaccharide branching. Comparison of the PS-EPI biopolymers obtained from a common polysaccharide (i.e. CSE-1, CSE-2 and CSE-3) with variable cross-linking shows different water swelling capacity. In the case of modified materials with similar cross-linking (CSE-1 and CSE-2), the water swelling capacity is lower than that for CSE-3. There is no clear correlation between the degree of cross-linking and the swelling properties of the other modified biopolymers; however, the trend in swelling of modified biopolymers with different AP and AM content varies incrementally. The results reveal that AMCSE has the highest swelling capacity in water; whereas, MSE shows the lowest water swelling capacity, in agreement with a previous report.[19] The results indicate that modified biopolymers with high AM content adsorb more water than modified biopolymers with high AP content.

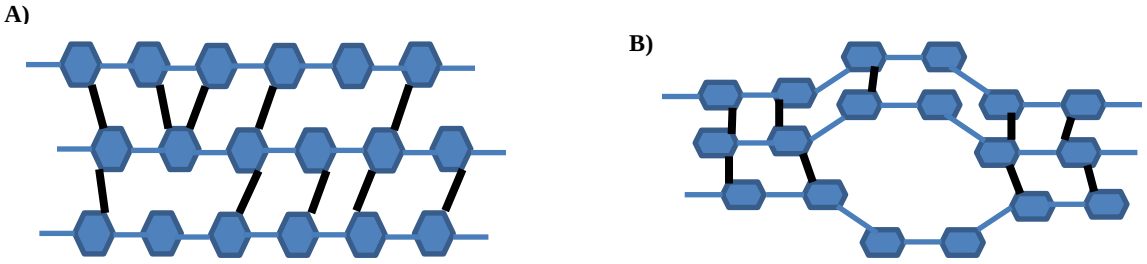

Scheme 3.2 Molecular structure of linear and branched polysaccharides cross-linked with epichlorohydrin (dark line segment): A) Modified linear amylose, and B) Modified branched amylopectin.

Table 3.4 Equilibrium swelling properties in water (S_w) and in ethanol (S_E) of polysaccharides and PS-EPI biopolymers at 295 K.

PS-EPI biopolymers	**S_w (%)[1]**	**S_E (%)[1]**
SSE	35 ± 4	8 ± 3
SSE-1	67 ± 12	13 ±7
SSE-2	117 ± 18	27 ± 3
SSE-3	157 ± 21	8 ± 2
CSE	81 ± 8	13 ± 4
CSE-1	235 ± 9	8 ± 3
CSE-2	269 ± 6	8 ± 4
CSE-3	156 ± 11	1 ± 0.2
MSE	25 ± 5	4 ± 2
MSE-1	52 ± 7	4 ± 1
MSE-2	107 ± 9	3 ± 2
MSE-3	153 ± 9	2 ± 0.5
AMCSE	63 ± 7	1 ± 0.3
AMCSE-1	188 ± 11	2 ± 1
AMCSE-2	307 ± 16	18 ± 4
AMCSE-3	248 ± 12	14 ± 6
CE	166 ± 9	2 ± 0.1
CE-1	244 ± 11	120 ± 14
CE-2	205 ± 9	92 ± 8
CE-3	161 ± 3	15 ± 5

Note: Errors represent standard deviations from triplicate measurements.

3.4.6 Nitrogen gas adsorption

Molecular nitrogen is one of the most common gas adsorbates employed for the study of the textural parameters of adsorbent materials because of ready availability of nitrogen, low cost, and its inert nature.[21] Equation 3.4 describes the relationship between the equilibrium amounts of adsorbed nitrogen (n^o) onto the modified biopolymers against external pressure (p) at constant temperature (T):

$$n^{o} = f\left(\frac{p}{p^{o}}\right)_{T,gas,solid} \qquad \text{Equation 3.4}$$

Where n^0 is a function of the relative equilibrium gas pressure and the saturated vapour pressure (p^0) for the solid-gas adsorption process at isothermal conditions. In addition to nitrogen adsorption, dye-based methods (*vide infra*) have been used to provide complementary estimates of the textural properties of modified materials. Dye probe molecules such as *p*-nitrophenol (PNP) are a suitable probe for the estimation of the surface area and pore structure of adsorbents in aqueous solution, as described elsewhere [31] for modified biopolymers containing amylose.

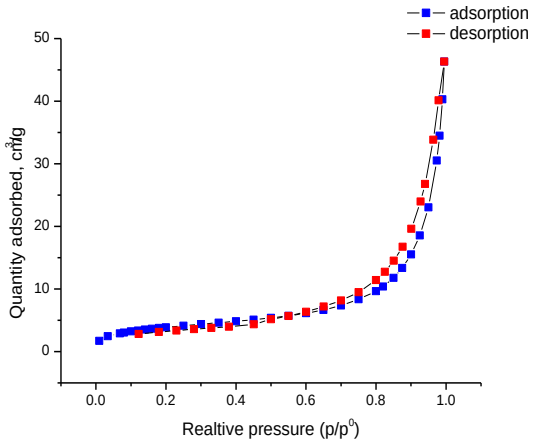

Figure 3.4 Nitrogen adsorption-desorption isotherm for cellulose at 77 K.

Figure 3.4 is consisted with dried cellulose in which all the pores have collapsed. A comparison of the cellulose-EPI and starch-EPI biopolymers suggests that the structure of cellulose-EPI is more rigid than the starch-EPI biopolymer, in agreement with the well-defined mesopore characteristics of cellulose.[32]

3.4.7 Adsorption of PNP in aqueous solution

Figure 3.5 shows 3-D plots representing the percent uptake of PNP from aqueous solution by the polysaccharides and PS-EPI biopolymers at 298 K and pH 6. In all cases, a fixed concentration of dye and dosage of adsorbent were used throughout, as indicated. A comparison of panels A-C for PS-EPI biopolymers with the same EPI content shows that the level of PNP

removal increases as the concentration of PNP increases. This is true for most of the PS-EPI biopolymers but some exceptions were observed for SSE and CSE, where the level of dye uptake decreased for various concentration of PNP; 0.1 mM to 10 mM or from 10 mM to 25 mM. The results suggest that SSE and CSE have fewer adsorption sites compared to the other modified forms. According to panels B and C, the sorption capacities for PNP do not follow a trend for PS-EPI biopolymers, which possess an irregular or non-uniform morphology. In Figure 3.5 A, PS-EPI biopolymers with high amylose (AM PS-EPI) display decreased sorption as the EPI ratio increased; whereas, modified biopolymers with high amylopectin (AP) display high PNP sorption as the EPI ratio is increased. The decrease in PNP sorption capacity in the case of modified AMCSE can be taken as a result of greater cross-linking between AMCSE chains. This results in smaller micropore structures, which hinder access of PNP to the adsorption sites. On the other hand, greater cross-linking of the MSE-EPI biopolymers does not yield micropore structures, due to branching of AMCSE-EPI biopolymers that may provide suitable host sites for PNP. The effect of matching of pore sizes to the guest dimensions, as evidenced by increased adsorption capacity, was reported by Huang *et al.* [33] They report a water-compatible hyper cross-linked polystyrene type resin to adsorb PNP where the pore size matches the molecular size of PNP. Higher levels of cross-linking may contribute steric effects for the uptake of PNP; whereas, intermediate cross-linking does not. The variation in sorptive uptake observed for the intermediate cross-linked biopolymers may reflect the importance of surface chemistry, as noted in other related studies.[24]

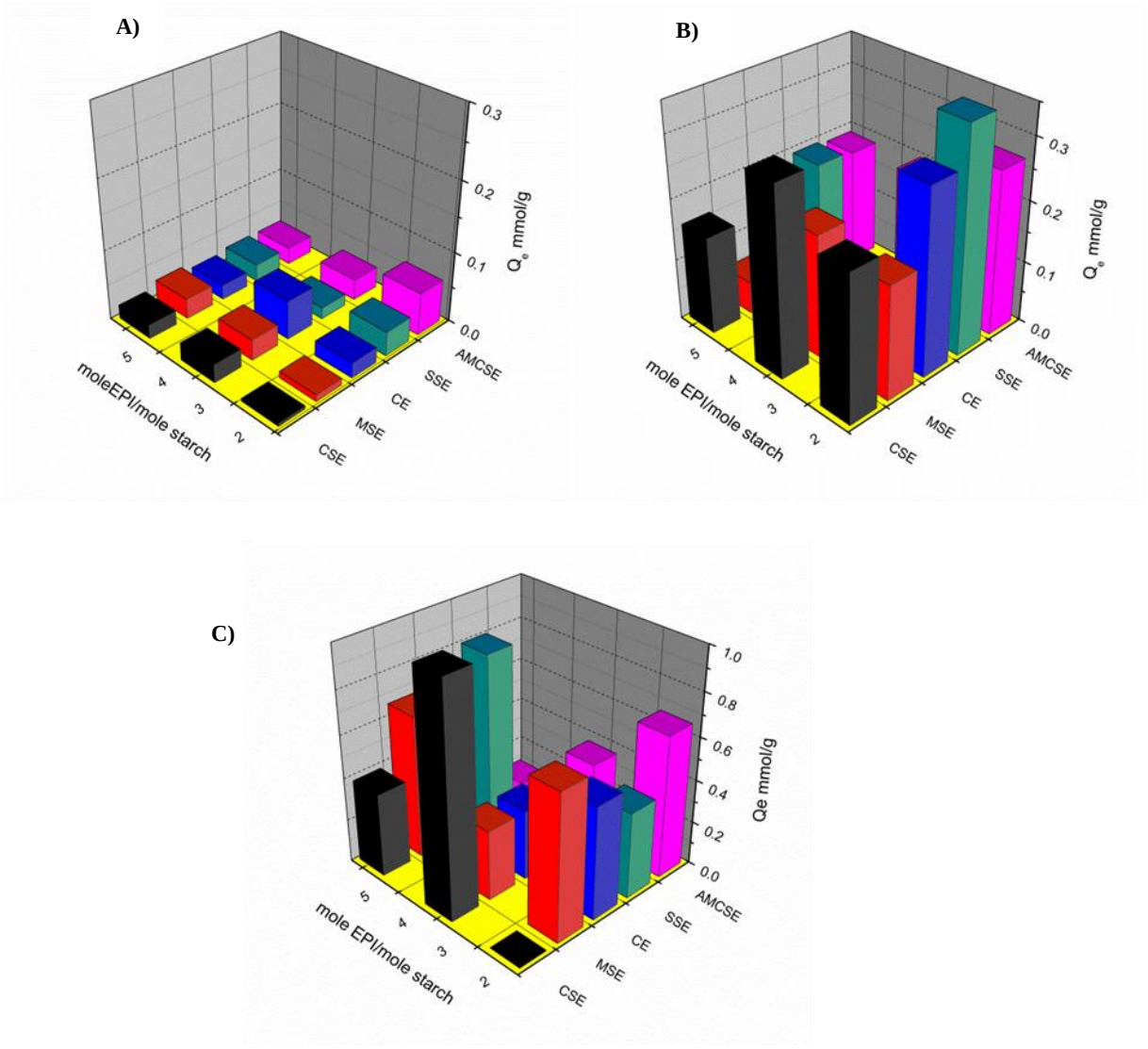

Figure 3.5 Sorptive uptake of PNP with polysaccharides and their respective modified forms with variable cross-linking and dye concentration at pH 6 and 295 K: A) C_o = 0.1 mM PNP, B) C_o = 10 mM PNP, and C) C_o = 25 mM PNP. Panels A and B are scaled along the same z-axis range for comparison purposes.

3.5 Conclusion

In this study, a series of PS-EPI biopolymers were prepared by cross-linking several types of polysaccharides (PS) of variable composition (i.e. amylose, amylopectin, and cellulose) with epichlorohydrin. Cross-linking was carried out at different mole ratios at an optimal temperature of 50°C to afford PS-EPI biopolymers with favourable adsorption properties toward nitrogen gas,

solvents (i.e. water and ethanol), and *p*-nitrophenol in aqueous solution at pH 6. PS-EPI biopolymers with high AM content have relatively high adsorption capacity for water. Differences in dye sorption of modified biopolymers at comparable cross-link density reflect differences in surface properties related to the accessibility of dipolar functional groups, such as hydroxyls, on the modified material's surface. Further studies are underway to ascertain the specific structural role of the modified material's structure and its dependence on the sorptive properties with various adsorbates.

3.6 References

1. Hamdi, G.; Ponchel, G.; Duchêne, D. *J. Microencapsul.* **2001,** *18,* 373-383.
2. Sandra, K. *J. Am. Chem. Soc.* **2009,** *1017,* 13-30.
3. Onofre, F. O.; Wang, Y. J.; *J. Appl. Polym. Sci.* **2010,** *117,* 1558-1565.
4. Marques, A. P.; Reis, R. L.; Hunt, J. A. *Biomaterials* **2002,** *23,* 1471-1478.
5. Gomes, M. E.; Ribeiro, A. S.; Malafaya, P. B.; Reis, R. L.; Cunha, A. M. *Biomaterials* **2001,** *22,* 883-889.
6. Da Silva, P. M. S.; Oliveira, J. C.; Rao, M. A. *J. Texture Stud.* **1997,** *28,* 123-138.
7. Crini, G. *Prog. Polym. Sci.* **2005,** *30,* 38-70.
8. Kamm, B.; Kamm, M. *Appl. Microbiol. Biotechnol.* **2004,** *64,* 137-145.
9. Richardson, S.; Gorton, L. *Anal. Chim. Acta* **2003,** *497,* 27-65.
10. Kubo, A.; Akdogan, G.; Nakaya, M.; Shojo, A.; Suzuki, S. H.; Satoh, H.; Kitamura, S. H. *J. Agric. Food Chem.* **2010,** *58,* 4463-4469.
11. Copeland, L.; Blazek, J.; Salman, H.; Tang, M. C. *Food Hydrocoll.* **2009,** *23,* 1527-1534.
12. Varum, K. M.; Smidsrod, O. Polysaccharides - Structure and Diversity and Functional Versatility, Marcel and Dekker, New York, **2005.**
13. Singh, N.; Singh, J.; Kaur, L.; Singh Sodhi, N.; Singh Gill, B. *Food Chem.* **2003,** *81,* 219-231.
14. Delval, F.; Crini, G.; Bertini, S.; Filiatre, C.; Torri, G. *Carbohydr. Polym.* **2005,** *60,* 67-75.
15. Xie, F.; Yu, L.; Su, B.; Liu, P.; Wang, J.; Hongshen, L.; Chen, L, *J. Cereal Sci.* **2009,** *49,* 371-377.
16. Tester, R. F.; Morrison, W. R. *Cereal Chem.* **1990,** *67,* 551-557.
17. Sasaki, T.; Matsuki, J. *Cereal Chem.* **1998,** *75,* 525-529.

18. Kyzas George, Z.; Bikiaris Dimitrios, N.; Lazaridis Nikolaos, K. *Langmuir* **2008,** *24,* 4791-4799.
19. Ayoub, A. S.; Rizvi, S. S. H. *J. Plast. Film Sheeting* **2009,** *25,* 25-45.
20. Kaur, B.; Ariffin, F.; Bhat, R.; Karim, A. A. *Food Hydrocoll.* **2012,** *26,* 398-404.
21. Ghosh Dastidar, T.; Netravali, A. *ACS Sustainable Chem. Eng.* **2013,** *12,* 1537–1544.
22. Ashish, P.; Khanderao, J.; Deelip, D. *Int. J. Pharm. Pharm. Sci.* **2013,** *5,* 391-397.
23. Pratt, D. Y.; Wilson, L. D.; Kozinski, J. A.; Mohart, A. M. *J. Appl. Polym. Sci.* **2010,** *116,* 2982-2989.
24. a) Mohamed, M. H.; Wilson, L. D.; Headley, J. V.; Peru, K. M. *J. Colloid Interface Sci.* **2011,** *356,* 217-226, and b) Mohamed M. H.; Wilson L. D.; Headley, J. V. *Carbohydr. Polym*. **2010,** *80,* 186-196.
25. Broekhoff, J. C. P.; De Boer, J. H. *J. Catal.* **1968,** *10,* 153-165.
26. Delval, F.; Vebrel, J.; Morcellet, M.; Crini, G. *Polym. Recycl.* **2000,** *5,* 137-143.
27. Šimkovic, I.; Laszlo, J.A.; Thompson, A. R. *Carbohydr. Polym*. **1996,** *30,* 25-30
28. Tian, Y.; Zhu, Y.; Bashari, M.; Hu, X.; Xueming, X.; Zhengyu, J. *Carbohydr. Polym.* **2013,** *91,* 586-589.
29. Azubuike, C.; Okhamafe, A. *Int. J. Recycl. Org. Waste Agric.* **2012,** *1,* 1-7.
30. Šimkovic, I.; Jakab, E. *Carbohydr. Polym.* **2001,** *45,* 53-59.
31. Mohamed, M. H.; Wilson, L. D.; Headley, J. V. *J. Colloid Interface Sci.* **2011,** *357,* 215-222.
32. Julkapli, N. M.; Ahmad, Z.; Akil, H. M. *AIP Conf. Proc.* **2010,** *1202,* 106-111.
33. Huang, J.; Yan, C.; Huang, K. *J. Colloid Interface Sci.* **2009,** *332,* 60-64.

CHAPTER 4

MANUSCRIPT 2: An NMR investigation of the fractionation of water-ethanol mixtures with cellulose and its cross-linked biopolymer forms.

Leila Dehabadi and Lee D. Wilson∗

Description

This research study is directed toward an understanding of the relative adsorption properties of cross-linked biopolymers as adsorbents for the adsorptive uptake of water or ethanol components in binary mixtures. Therefore, this study focused on preparation and characterization of cross-linked biopolymers containing cellulose following the methodology described in the Chapter 3. Quantitative measurement of water or ethanol removal in binary mixtures can be accomplished by using Karl Fischer titrations, gas chromatography (GC) or high performance liquid chromatography (HPLC) to measure the relative ethanol or water content in mixtures, which is often tedious and time-consuming. An alternative and potentially convenient method with rapid quantification of water or ethanol can be carried out using ^{1}H-NMR spectroscopy. Thus, the main goal of this work is to develop a quantitative ^{1}H-NMR technique to directly measure the composition of water and ethanol solvents in binary solutions to enable characterization of the adsorption isotherms of cross-linked biopolymers in the presence of binary solvent systems. The ability to measure multi-component mixtures provides insight on the adsorptive fractionation and potential solvent selectivity of cellulose and modified cellulose adsorbent materials. The fractionation selectivity of cellulose and its modified forms for water (W) and ethanol (E) in binary mixtures varied from 1 to 2.5.

Authors' Contributions

The supervisor (L. D. Wilson) conceived the project concerning the use of quantitative NMR for quantification of water and ethanol in binary mixtures using the adsorbent materials. Dr. Keith Brown and the supervisor contributed investigation of the relaxation time in NMR techniques. L. Dehabadi modified the NMR solvent systems by using a mixture of deuterated dimethyl sulfoxide (DMSO-d_6) with deuterium oxide (D_2O) as solvent for ^{1}H-NMR analysis. The first draft of the manuscript was prepared by L. Dehabadi with subsequent revisions and editing with the supervisor.

Relation of Manuscript 1 to Overall Objective of this Project

As mentioned in Chapter 2 (*cf.* Section 2.4), a knowledge gap related to polysaccharides and their modified forms relates to the limited understanding of the structure and adsorption properties of such materials. Thus, the objective of this work relates to evaluation of the solvent selective uptake of cellulose and its modified forms in binary solvent systems containing ethanol and water. The significance of this work was related to the overall objective of the research project because this research study is demonstrated by the development of a suitable methodology for the quantification of water and ethanol in binary solvent systems. The capability to measure relative changes in water-ethanol composition before and after adsorption enables determination of the adsorption isotherm in such solvent systems. The subsequent use of qNMR enabled the measurement of variable adsorptive uptake of water over ethanol in an incremental manner according to the level of cross-linking of cellulose.

4. An NMR investigation of the fractionation of water-ethanol mixtures with cellulose and its cross-linked biopolymer forms.

Leila Dehabadi and Lee D. Wilson*

Department of Chemistry, University of Saskatchewan, 110 Science Place, Saskatoon, Saskatchewan, Canada S7N 5C9.

*Corresponding Author.

Supplementary Information (Appendix A, Chapter 4)

Graphical abstract

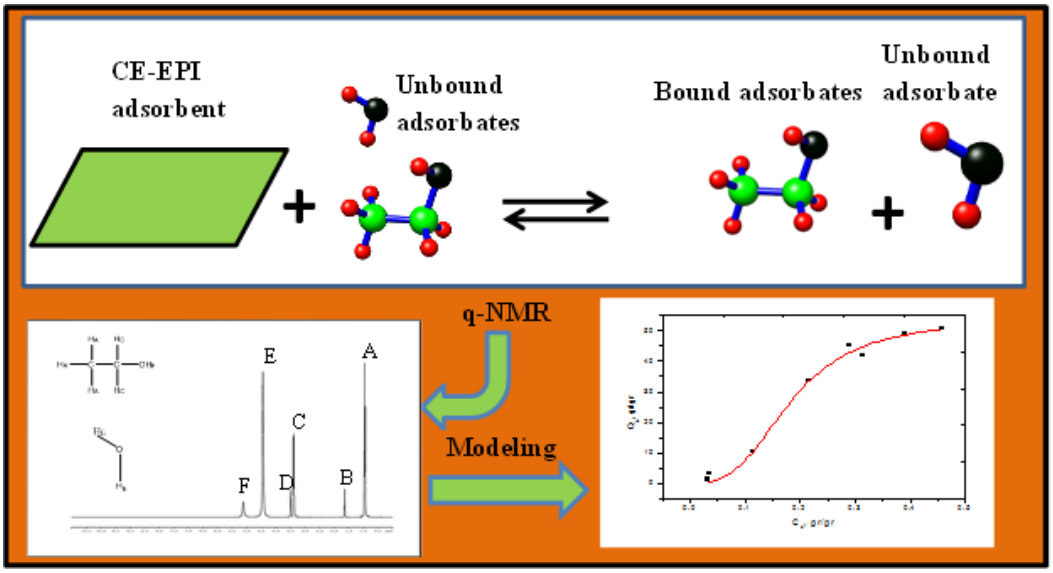

Research Highlights

- Adsorptive uptake properties of cellulose and its cross-linked forms were studied using quantitative ^{1}H-NMR (qNMR) spectroscopy in binary solvent systems.
- Quantitative NMR yields direct analytical estimates of relative solvent uptake in binary solvents.
- Selective uptake of water occurs in ethanol-water binary systems by cellulose and its modified forms.
- Tunable solvent uptake occurs according to the level of cross-linking.
- The contribution of cellulose to selective solvent uptake was assessed.

4.1 Abstract

Cellulose was cross-linked with epichlorohydrin (EPI) at variable composition and the fractionation properties were investigated in binary ethanol-water solutions, including the pure solvent systems. The relative uptake of each solvent was measured using quantitative ^{1}H-NMR (qNMR) spectroscopy. This study highlights the utility of qNMR as a rapid screening method for estimation of solvent selective fractionation in binary mixtures. The uptake properties of cellulose-EPI cross-linked polymers with ethanol and water were well described using the Sips isotherm model. Modeling shows that the monolayer surface coverage (Q_m) of adsorbates onto the polymer materials covered a range of values (1.13 - 2.44 g/g) with heterogeneous adsorption behaviour according to the Sips exponential fitting parameter ($n_s \neq 1$). The cellulose-EPI adsorbents display unique fractionation with water (W) and ethanol (E) from binary solutions, as evidenced by the relative selectivity ($R_{selectivity}$) value in binary W-E solvent systems. The $R_{selectivity}$ [$Q_m(W)/Q_m(E)$] values at saturative uptake conditions varied (1.10 to 2.03) and further illustrate that cellulose materials display molecular selective solvent fractionation in binary water-ethanol solutions. This study provides a greater molecular level understanding for the adsorptive uptake properties of cellulose that is relevant to developing cellulose-based adsorbent technology for the fractionation of biofuels and related chemical separations.

4.2 Introduction

Adsorption is ubiquitous to many natural, physical and biological processes and it is a key step in food processing,[1] environmental remediation,[2] and transport of pollutants in soil, groundwater, sediments, or aquatic environments. Pervaporative separation of alcohol fractions is a commonly used method for alcohol removal in beverages such as spirits. Water and ethanol removal is a key process for the food processing industry as well as alcohol and fuel production.[3-7] Production of natural flavour compounds through esterification requires continuous water removal[4] and some technologies such as pervaporation,[8] headspace evacuation, sparging of dry inert gas through the reaction medium have been studied.[9] Production of ethanol by fermentation of biomass feed stocks normally produces a mixture of ethanol and water[3] that often requires separation via solvent extraction or distillation which often demand significant material and/or energy inputs. By contrast, adsorptive-based methods represent an alternative chemical separation pathway that reduces the consumption of materials, energy, and operational costs. Solid-solution adsorption occurs when species such as adsorbates are transferred heterogeneously from the bulk of fluid phase to the surface of a solid phase adsorbent.[10-13] Adsorptive processes in many natural chemical and biological systems[14] are governed by various interactions that stabilize the adsorbent/adsorbate complex.[15] Thus, an understanding of such adsorptive interactions is fundamentally important for the design of new sorbent materials, especially for mixtures of adsorbates where molecular selective adsorption may occur.[16] Water-alcohol binary systems are of considerable interest in the fields of food chemistry and biofuel production because water removal enhances the market value of bioethanol and the longevity of food products' storage properties by resistance to microbes. In food and biofuel production, water removal from mixtures of esters with short chain acids and alcohols is very important in the production of fragrance compounds.[17] Esters are commonly produced by lipase enzymatic reactions in water[18] and the continuous removal of produced water is a key factor for achieving high product yields.[19]

Physical separation techniques such as distillation and membrane-based pervaporation have been reported to achieve separation of water from ethanol.[20-22] In general, high purity ethanol is often obtained by traditional separation methods such as distillation; however, significant infrastructure and energy inputs for distillation may approach 50-60% of the energy value content required to separate ethanol and water.[23] In some cases distillation is not feasible for thermally labile mixtures or when operational costs pose limitations. Thus, there is a need to develop more

sustainable methods for water/ethanol separation. Adsorption-based methods offer an efficient strategy for the separation of chemical mixtures that do not require differences in volatility for the separation of azeotropic components[21] and also offer a suitable alternative for pressure or temperature sensitive mixtures.[6]

The adsorption properties of naturally occurring adsorbents such as zeolites,[2] clay,[24] barley and wheat straw[25] have been reported. However, less effort has gone into the development of synthetically modified biomaterials such as modified cellulose.[26] Polysaccharide-based adsorbents and their modified gel-based materials[27] offer advantages over unmodified biopolymers.[10] In a recent study of modified polysaccharides, the swelling behaviour of these biomaterials in water, ethanol, and binary mixtures indicated that cellulose-based materials display molecular selective adsorption properties in water-alcohol mixtures.[28] Barley straw has relatively high cellulose content and this biomass sorbent displayed modest uptake selectivity between water and ethanol in binary mixtures.[25] To understand the molecular fractionation of such biosorbents, systematic uptake studies are required to further understand the molecular selective separation for binary water-ethanol systems.

In this paper, we report the utility of ^{1}H-NMR spectroscopy as a rapid screening tool to aide in the quantitative estimation of the fractionation properties of cellulose and its cross-linked forms in water-ethanol binary solutions.[28] The results of this study represent two key contributions to the field of energy production and chemical separation of biofuels, as follows: *i*) the development of a versatile NMR method for *in situ* quantitative analysis of biofuels mixtures, and ii) the elucidation of the role of cellulose materials for the adsorptive fractionation of water and ethanol. In this study, an investigation of the adsorptive properties of cellulose and its epichlorohydrin cross-linked polymers were evaluated in water-ethanol mixtures.[25] This research highlights the utility of a quantitative ^{1}H-NMR spectroscopy method for analytical *in situ* estimation of water and ethanol adsorption[28] and the role of cellulose materials in the molecular selective uptake of water and/or ethanol in binary solvent systems.

4.3 Experimental

4.3.1 Materials

Cellulose (CE) and its modified forms containing epichlorohydrin (EPI) were prepared and characterized, as reported recently.[28] Table 4.1 shows the product yield (%) and equilibrium swelling properties[28] in water (S_w) and in ethanol (S_E) for pure cellulose and cellulose-EPI at various cross-linking ratios and reaction temperatures (°C).

Table 4.1 Selected physicochemical properties of cellulose (CE) and its cross-linked polymers CE-X. Where X represents the relative mole content of epichlorohydrin.

*Polymer ID code	Mole ratio	Yield (%)	S_w (%)	S_E (%)
CE-1	Low (1:2)	58	244 ± 1	120 ± 1
CE-2	Medium (1:3.6)	42	205 ± 9	92 ± 8
CE-3	High (1:5.4)	45	161 ± 3	15 ± 5
CE	Not applicable	Not applicable	166 ± 9	2 ± 0.1

* Numerical descriptors used in the ID code refer to the various mole ratios of cross-linking as follows: CE = Cellulose; CE-1 = Low (1:2 mole ratio); CE-2 = Medium (1:3.6 mole ratio); and CE-3 = high (1:5.4 mole ratio) cross-linking of the CE-EPI biopolymers.

4.3.2 Methods

Anhydrous ethanol (reagent grade, Commercial Alcohols Inc. Brampton, ON, Canada) and Millipore water were used to prepare different weight ratios (w/w %) of ethanol-water solutions. Approximately 20 mg of adsorbent was added to a 4 dram glass vial with 10 g of a binary ethanol-water solution and shaken (Poly Science, Dual Action Shaker) at 160 rpm and room temperature for 24 h to achieve equilibrium. The samples were centrifuged (Precision Micro-Semi Micro Centricone, Precision Scientific Co.) at 1800 rpm for 1 h. Thereafter, 1 g of supernatant solution was added to 0.05 g mixtures of tetrahydrofuran (THF) and deuterium oxide (D_2O, 99.8%, both from Sigma-Aldrich). THF serves as an internal standard while D_2O serves as the deuterium field locking solvent, where the weight contents of these components were held constant for all NMR measurements. An adapted procedure using deuterated dimethyl sulfoxide (DMSO-d_6, 99.9%, from Sigma-Aldrich) was employed as a field locking solvent instead of D_2O. All ^{1}H-NMR spectroscopic measurements were obtained using a wide-bore (89 mm) 11.7 T Oxford superconducting magnet system (Bruker Bio Spin Corp; Billerica, MA, USA) equipped with 5 mm

PaTx1 probe. Spin-lattice relation times (T_1) of the pure solvents and their binary mixtures were measured by the inversion-recovery method.[29]

NMR operating parameters were controlled using a SSSC 500 console and workstation running X WIN-NMR 3.5. All measurements employed standard pulse programs available from the TopSpin 1.3 software. In this study, a quantitative NMR method (qNMR) was used to measure the relative water-ethanol (W-E) content in binary solutions by independent calibration curves derived from various standard binary W-E solutions at variable weight composition (w/w; %). Each solution contained an analytical internal standard (THF) and a locking solvent (D_2O or DMSO-d_6). The equilibrium time of the sorption process was evaluated by varying the incubation time of 20 mg samples of adsorbent with the binary W-E mixtures until no further change was observed. Quantitative evaluation of the relative amounts of adsorbed solvent at each time was evaluated using ^{1}H-NMR spectroscopy under fully relaxed and steady-state conditions.

4.3.3 Models and equations

The thermodynamic sorption behaviour of the polymer adsorbents in W-E binary solutions was analysed by fitting the adsorptive uptake for each solvent component (W or E) against the equilibrium concentration of each solvent (W and E) using various models (Langmuir, Freundlich, and the Sips isotherms).[30, 31]

The equilibrium sorptive uptake (Q_e) of the adsorbent material with ethanol, water, and binary (W+E) solvent systems was calculated using equation 4.1, where $W_{solution}$ is the weight of solution (W+E), $C_{0,i}$ is the initial solvent concentration of the i^{th} component (g), $C_{e,i}$ is the equilibrium concentration of the i^{th} component (W or E), and m is the mass of sorbent. The solvent concentration of the i^{th} component (W or E) is expressed on a relative fractional weight basis (w/w).

$$Q_{e,i} = \frac{\left(C_{0,i} - C_{e,i}\right)}{m} \times W_{Solution} \qquad \text{Equation 4.1}$$

Uptake data were presented as $Q_{e,i}$ (i= W or E), which can be analysed by different models such as Langmuir, Freundlich and Sips. The Langmuir model describes monolayer sorption between adsorbate and adsorbent. On the other hand, the Sips and Freundlich models account for

the relationship between the adsorbent surface and an adsorbate. Replacing D_2O by DMSO-d_6 as the NMR locking solvent was used to minimize exchange processes and to optimize spectral resolution of the ^{1}H-NMR spectral signatures for the various solvent mixtures. In D_2O, there are exchangeable protons in the binary W-E system such as OH that contributes to line broadening and spectral overlap due to chemical exchange effects. Isotherm models such as the Langmuir model provide the following parameters: Q_e (uptake of the respective i^{th} component; W or E), Q_m (monolayer adsorption capacity of sorbent) and C_e is the residual equilibrium concentration of the adsorbate (W or E) in a binary W-E solvent according to equation 4.2.[32]

$$Q_e = \frac{Q_m K_L C_e}{1 + K_L C_e} \qquad \text{Equation 4.2}$$

The Freundlich and Sips models provide heterogeneity factors, which are denoted as n_F and n_s according to equations 4.3 and 4.4, respectively.

$$Q_e = K_F C_e^{n_F^{-1}} \qquad \text{Equation 4.3}$$

The Sips model provides an estimate of the monolayer surface coverage of the adsorbate (Q_m) for W or E onto the adsorbent surface. Furthermore, the Sips model provides information on the heterogeneity of the adsorbent surface according to the heterogeneity factor (n_s) in equation 4.4. The Sips model accounts for a combination of Langmuir- and Freundlich-type sorption behaviour at certain limiting conditions. When n_s = 1, Langmuir isotherm behaviour (no heterogeneity) is predicted; whereas, Freundlich behaviour is predicted when $(K_s C_e)^{n_s} <<< 1$ ($n_s \neq 1$).

$$Q_e = \frac{Q_m (K_s C_e)^{n_s}}{1 + (K_s C_e)^{n_s}} \qquad \text{Equation 4.4}$$

The adsorption kinetics can be tested by three common types of models: the pseudo-first-order (PFO), pseudo-second-order (PSO) and pore diffusion models. PFO and PSO models have been tested to evaluate the adsorption mechanism. The non-linear Eqnuation 4.5 and linear equation 3.6 pseudo first-order kinetic models[33] are expressed as:

$$Q_e = Q_t(1-e^{-k_1 t}) \qquad \text{Equation 4.5}$$

$$\log\left(Q_e - Q_t\right) = \log\left(Q_e\right) - \frac{k_1 t}{2.303} \qquad \text{Equation 4.6}$$

k_1 is the rate constant of the PFO kinetic equation and where Q_e and Q_t are the uptake amounts of adsorbate (W or E) at equilibrium and variable time (t). The PFO kinetic model for adsorption is expressed as plots of $Q_t\ vs.\ t$ and $\log(Q_e - Q_t)\ vs.\ t$ for non-linear and linear PFO models, respectively. The values of K_1 and Q_e can be obtained from the slope and intercept of plots of $\log(Q_e - Q_t)$ *vs.* t. The non-linear equation 4.7 and linear equation 4.8 second-order kinetic models are defined by the following equations.[34, 35]

$$\frac{t}{Q_t} = \frac{1}{k_2 Q_e^2} + \frac{t}{Q_e} \qquad \text{Equation 4.7}$$

$$\frac{t}{Q_t} = \frac{1}{k_2 Q_e^2} + \frac{t}{Q_e} \qquad \text{Equation 4.8}$$

The parameter k_2 is the adsorption rate constant ($g.mg^{-1}.min^{-1}$) according to the PSO model. The PFO kinetic model for adsorption is expressed as a plot of $Q_t\ vs.\ t$ and $\frac{t}{Q_t} vs.\ t$ for non-linear and linear analyses, respectively. The k_2 and Q_e parameters can be obtained from the slope and intercept from plots of $t/Q_t vs.$ t. The pore diffusion equation is described by equation 4.9:

$$Q_t = K_d t^{0.5} \qquad \text{Equation 4.9}$$

K_d (mg/g $min^{-1/2}$) is the diffusion rate constant, and Q_t is the amount of adsorbate adsorbed at time (t). A plot of Q_t against $t^{1/2}$ yields a slope equal to the K_d term.

4.4 Results and Discussion

According to an NMR relaxation study,[31] the relaxation time (T_1) of the ^1H nuclei of ethanol increases nonlinearly with increasing ethanol concentration where the rate of relaxation (R_1) is defined by $R_1 = R_1^0(1 + B_1 m)$, where R_1 and R_1^0 are relaxation rates in D_2O and where the concentration of ethanol may be expressed on a weight basis (mole/kg or w/w). Therefore, the relaxation time is an important factor that should be considered in binary W-E mixtures. In such binary mixtures, D_2O and DMSO were used as NMR solvents. The CH_3 group of ethanol and the contribution of -OH groups of water and ethanol to T_1 were studied across a wide range of W-E compositions, where the results are shown to vary with increasing ethanol (w/w) content. The concentration dependence of T_1 is understood by the fact that the relative water mobility and structured water decrease as the ethanol content increases.[36] These factors together contribute to the relaxation time (T_1) where the results in Table 4.2 show that the T_1 values increased as the ethanol content increased for the W-E binary solutions.

^1H nuclear magnetic resonance (NMR) spectroscopy is a suitable technique for structure identification and quantification of organic compounds present in various states.[37] In this study, ^1H-NMR was evaluated to provide *in situ* quantitative estimates of the composition of components after the equilibrium sorptive uptake process in binary W-E mixtures, as described by equation 4.10.

$$\text{Sorbent}\,(s) + W_X/E_Y\,(soltn) \longleftrightarrow \text{Sorbent-}W_Z\text{-}E_{Z'}\,(s) + W_{X\text{-}Z}/E_{Y\text{-}Z'}\,(soltn) \qquad \text{Equation 4.10}$$

Table 4.2 Relaxation time (T_1) and relaxation delay (D_1) values of various nuclei in pure and binary W-E solvent systems. The -CH_3 group of ethanol was studied in D_2O, and the –-OH group of water was studied in DMSO-d_6 NMR locking solvents at 295 K.

$*T_{null}$[1]	T_1(**-CH_3**)[1]	D_1 (**-CH_3**)[1]	$*T_{null}$[2]	T_1(**–OH**)[2]	D_1 (**–OH**)[2]
100%H_2O (0.03s)	0.04 s	0.2 s	100% H_2O (0.5 s)	0.72 s	3.6 s
25% Ethanol (0.15 s)	0.22 s	1.1 s	25% Ethanol (2 s)	2.9 s	14.5 s
50% Ethanol (0.8 s)	1.16 s	5.8 s	50% Ethanol (1.9 s)	2.7 s	13.5 s
75% Ethanol (0.47 s)	0.68 s	3.4 s	75% Ethanol (1.8 s)	2.6 s	13 s
100% Ethanol (1.5 s)	2.1 s	10.5 s	100% Ethanol (0.5 ms)	0.72 ms	3.6 ms

$*T_{null}$ is the specific time for which the resonance signal is just passing through zero.
[1]Determined using DMSO-d_6 as the locking solvent
[2]Determined using D_2O as the locking solvent

This solid-solution system illustrates a physical separation of water (W) and ethanol (E) in a binary (W_X/E_Y) solution (soltn) according to an adsorption process at equilibrium. The limiting case presented above shows an arbitrary solvent uptake (Z and Z') by the sorbent relative to the original solvent composition of water and ethanol (X and Y). After phase separation of the solid adsorbent, the composition of ethanol and water in the liquid phase after sorption was calculated by comparison with the original solvent composition before sorption using qNMR. By carefully choosing an internal calibration standard, it is possible to avoid overlap of the ^{1}H-NMR resonance signals of the standard and respective solvent signatures. In this study, THF was chosen as the internal calibration standard because its chemical shift does not overlap with the ^{1}H-NMR signatures of water and ethanol (-CH_2 and –CH_3 groups) in the binary solution.

The ^{1}H-NMR spectra of 10% E in solution with THF/D_2O (Figure 4.1) show that chemical shift (δ) values for the THF standard occur at δ=1.60 ppm and δ=3.51 ppm, corresponding to the two nonequivalent methylene groups of THF. On the other hand, the chemical shifts for ethanol occur at 3.40 ppm, 0.90 ppm, and 4.60 ppm, corresponding to the –CH_2, -CH_3 and -OH groups, respectively. It is apparent from Figure 4.1 that the δ value for THF (δ=1.60 ppm) is well resolved from the –CH_3 group of ethanol and was used for the calculation of the ethanol content in the binary mixture by equation 4.11.

$$\frac{\text{peak area for THF at 1.60 ppm}}{\text{peak area for} -CH_3 \text{ ethanol}} = \frac{\text{concentration of THF}}{\text{concentration of ethanol}} \times \frac{n_{THF}}{n_{ethanol}} \qquad \text{Equation 4.11}$$

The n parameter terms refer to the number of moles of ^{1}H nuclei for ethanol and THF, respectively.

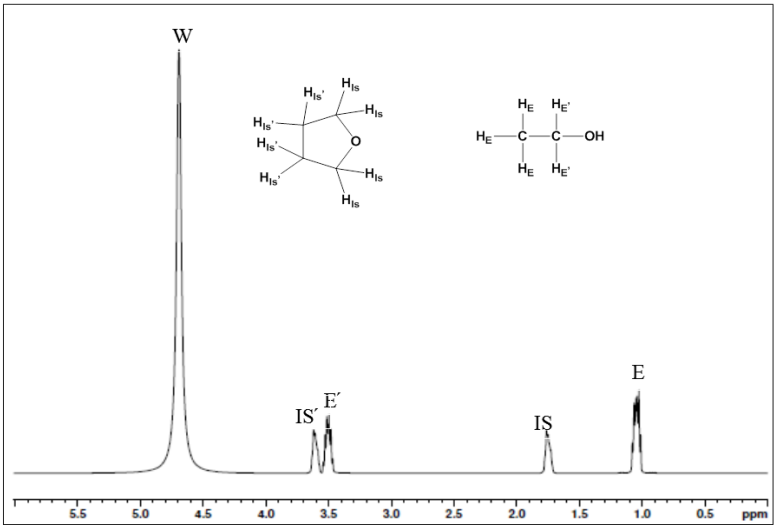

Figure 4.1 ^{1}H-NMR spectrum of ethanol (E and E') and water (W) in the W-E mixture where THF was the internal standard (IS and IS') and D_2O is the field-locking solvent at 295 K.

Equation 4.11 can be used since all other instrument parameters are held constant and the integrated ^{1}H-NMR signal is directly proportional to the concentration of the species giving rise to the signal of interest. The ^{1}H-NMR signal at δ=1.60 ppm is due to two methylene groups of THF and its integrated peak area is proportional to the number of ^{1}H nuclei. Therefore, the ratio of the relative peak areas for THF and the $-CH_3$ group of ethanol relates to the ratio of concentrations of each respective solvent component. The concentration of THF is known independently, which allows for the concentration of ethanol in the binary mixture to be calculated by equation 4.11.

In binary W-E solutions containing D_2O, the mixture cannot be calculated in the same way as the aliphatic groups of ethanol due to some uncertainty arising from exchange between the OH group of water and ethanol, including the overlapping signals of H_2O and HOD.[38] Water suppression experiments were investigated; however, it was not necessary for improvement of the

spectral signatures of ethanol since the $-CH_3$ signal was alternatively measured.[37] The concentration of water was calculated indirectly by mass balance of the binary mixture the CH_2 or $-CH_3$ groups of ethanol, as described by equation 4.12.

Ethanol (w/w; %) + water (w/w; %) +THF (w/w; %) =100% Equation 4.12

The use of a fixed amount of DMSO-d_6 as an NMR locking solvent instead of D_2O allows for quantification of the -OH group of water and ethanol binary mixtures due to the improved spectral resolution of each respective signature. This is attributed to solvent effects and anisotropic behaviour of DMSO-d_6 relative to D_2O.[32] Figure 4.2 shows the spectra of water and ethanol in binary mixtures indicating that there are two separate resonance lines for OH appearing at δ=4.50 ppm and δ=5.20 ppm for ethanol and water, respectively, including the reduced chemical exchange. The integrated peak areas of the signals W, E', and E are in a ratio of 1:2:3, in agreement with the relative number of the ^1H nuclei of the various groups (–OH, $-CH_2$, and $-CH_3$) for ethanol. The results are in good agreement with independent gravimetric estimates of solvent components (Table 4.3). The signal (W) is assigned to the –OH group of water. The peak area for the $-CH_3$ and –OH groups were used in the calculation of the ethanol and water content (w/w; %) in binary mixtures, according to the gravimetric value (n_W and n_E) by equation 4.13.

$$\frac{\text{Area(solvent)}}{\text{Area(THF)}} = \frac{^1\text{H}_{\text{nuclei}}\text{(solvent)}}{^1\text{H}_{\text{nuclei}}\text{(THF)}} \times \frac{\text{n}_{\text{solvent}}}{\text{n}_{\text{THF}}} \qquad \text{Equation 4.13}$$

The NMR parameters corresponding to the area (solvent) refer to the relative integrated peak areas for the ^1H-NMR signal of interest (W or E). The $^1H_{nuclei}$ refer to the number of ^1H nuclei of interest for the solvent, where $n_{solvent}$ is the moles of solvent (W or E), and n_{THF} refers to the number of moles of THF.

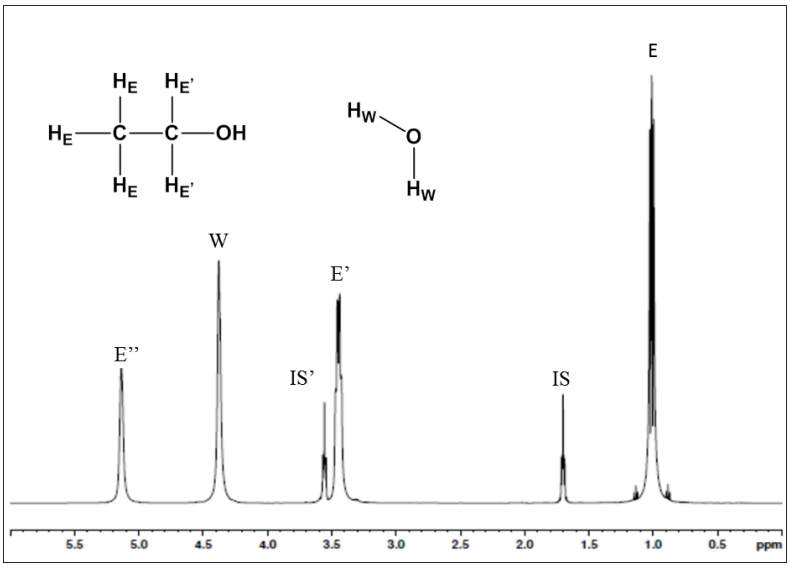

Figure 4.2 ^{1}H-NMR spectrum of ethanol (E, E', and E'') and water (W) in a binary mixture with THF as an internal standard (IS and IS') in DMSO-d_6 at 295 K.

Table 4.3 Comparison of water-ethanol content in binary mixtures by gravimetric (w/w; %) and quantitative ^{1}H-NMR (qNMR; w/w; %) spectroscopy at 295 K.

Ethanol (wt%)	**Ethanol from qNMR (C_0;wt%) (in D_2O)**	**Difference (wt-qNMR) %**	**Ethanol by qNMR (C_0;wt%) (in DMSO-d_6)**	**Difference (wt-qNMR) %**
5.00	4.32	0.67	5.03	0.03
10.00	8.89	1.10	9.19	0.81
15.00	14.85	0.15	13.30	1.70
20.00	16.50	3.50	14.40	5.60
25.00	23.10	1.90	22.10	2.90
30.00	23.54	6.46	28.90	1.10
35.00	25.74	9.26	33.70	1.30
40.00	33.66	6.34	39.60	0.40
45.00	44.99	0.01	43.00	2.00
50.00	46.75	3.25	48.60	1.40
55.00	50.27	4.73	55.50	0.50
60.00	58.52	1.48	59.50	0.50
70.00	64.68	5.32	70.50	0.50
75.00	67.54	7.46	74.90	0.10
80.00	69.63	10.37	80.00	0
85.00	79.53	5.47	84.70	0.30
90.00	89.87	0.13	90.10	0.10

In Table 4.3, the results for the difference (%) in composition show that the relative error for ethanol content obtained by qNMR (DMSO-d_6 as locking solvent) is less than the estimated error when D_2O was used as the solvent for field locking purposes. Therefore, the determination of the ethanol composition according to qNMR was preferred when DMSO was the locking solvent, as evidenced by the greater agreement between the gravimetric and qNMR values. The preferred use of DMSO-d_6 is related to the reduced exchange and better spectral resolution of NMR lines described above. Quantitative ^{1}H-NMR spectroscopy allows for simultaneous measurement of water and ethanol in binary mixtures. By comparison, techniques such as the Karl Fischer titration and chromatography (GC or HPLC) may resolve only one of the two components in binary solutions.[39, 40]

Based on the foregoing discussion of DMSO-d_6, the sorption isotherms were obtained using the qNMR method with DMSO-d_6 as the field locking solvent. The corresponding qNMR results using D_2O as the solvent system are provided in the supporting information (*cf.* Figure A4.1 in Appendix A4). Figure 4.3 shows the isotherm data for W-E mixtures adsorbed onto CE-EPI at 295 K. The results show that for mixtures with lower adsorbate (i.e. E or W) content, the uptake of ethanol is greater than water uptake for the same solvent composition. At greater adsorbate

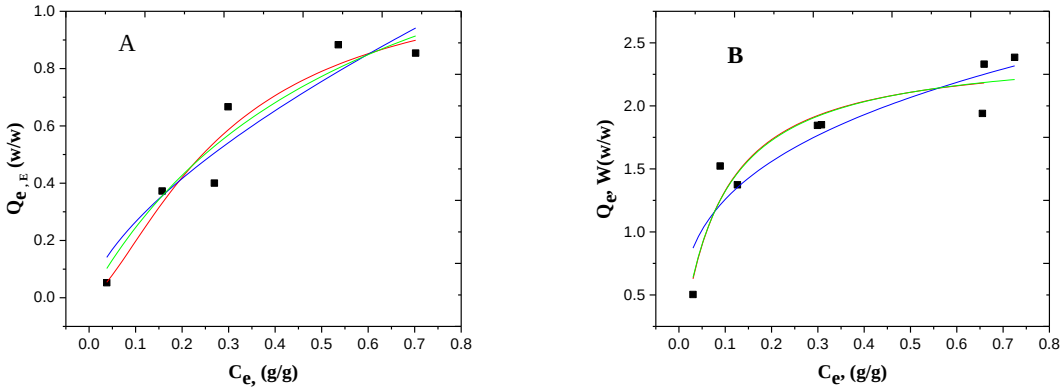

Figure 4.3 Adsorption isotherm for the uptake of solvent components with CE-3 in binary W-E solutions A) Ethanol uptake isotherm, and B) Water uptake isotherm in mixtures containing variable ethanol content at 295 K.

levels, the adsorption of water increases more than the uptake of ethanol, in accordance with equilibrium considerations. The results indicate a greater adsorptive affinity of water with cross-

linked cellulose than ethanol. The experimental results were modeled by the Langmuir (green), Freundlich (blue), and Sips (red) models. The quality of the best-fit lines reveals that the Langmuir and Freundlich models have lesser agreement with the experimental results (*cf*. Appendix A4, Figure A4.2), while the Sips model provided a better description of the results (R^2 =0.968).

Adsorption isotherms of such solid-solution systems provide an understanding of the sorption affinity and sorption capacity of cellulose materials. In the case of W-E binary solvent systems, the isotherms may reveal the relative uptake levels of solvent components (W and E) and the relative selectivity of the system. Tables 4.4 and 4.5 list the best-fit parameters for the Sips isotherm model. The ethanol and water uptake capacities (Q_m) of the cross-linked polymer (CE-3) display the highest uptake. The Q_m values for each sorbent are listed in descending order, as follows: CE-3 > CE-2 > CE-1 > CE. The heterogeneity parameter (n_s) is close to unity indicating a relatively homogeneous adsorbent surface with uniform adsorption sites. By comparison, the CE-EPI biopolymers (CE-1 and CE-3) have estimated values for n_s that deviate from unity, indicating some heterogeneity of the adsorbent surface. Among the cellulose materials studied, CE has a large value for n_s, which compares closely to the cross-linked sorbents (CE-1 and CE-3).

Table 4.4 Best fit model parameters for the Sips model for the uptake of ethanol at 295K with cellulose and its cross-linked polymers.

Cellulose ID Code	**K_s (g/g)**	**n_s**	**Q_m (g/g)**	**R^2**
CE	4.18 ± 0.67	3.18 ± 2.13	1.03 ±0.13	0.903
CE-1	5.34 ± 3.55	1.38 ± 0.67	1.02 ± 0.37	0.925
CE-2	6.57 ± 1.22	2.04 ± 0.47	1.09 ± 0.14	0.986
CE-3	3.47 ± 2.54	1.47 ± 0.97	1.13 ± 0.52	0.932

Table 4.5 Best model parameters for the Sips model for the uptake of water at 295 K with cellulose and its cross-linked polymers.

Cellulose ID Code	**K_s (g/g)**	**n_s**	**Q_m (g/g)**	**R^2**
CE	10.40 ± 3.19	1.15 ± 0.55	1.63 ± 0.244	0.937
CE-1	6.69 ± 2.62	1.18 ± 0.34	1.20 ± 0.206	0.968
CE-2	11.32 ± 8.97	1.08 ± 0.75	1.87 ± 0.63	0.858
CE-3	11.85 ± 4.93	1.03 ± 0.43	2.44 ± 0.39	0.912

Note: Statistic information (t-test values) was shown in Appendix A4, Tables A4.1and A4.2.

It follows that cross-linking of cellulose with epichlorohydrin may induce morphological variations and surface heterogeneities[41] that contribute to variable textural and surface chemistry effects[42] that agree with the known fibrillated structure of cellulose and the surface accessibility of it hydroxyl groups.

Favourable correlation coefficients (R^2) were observed for ethanol and water adsorbed by CE and its cross-linked polymers (CE-EPI). The use of DMSO-d_6 as a locking solvent provided better quality NMR spectra with greater analytical precision than D_2O as the locking solvent. Thus, DMSO-d_6 was preferred for quantitative analysis by qNMR for the uptake of solvent components for the binary W-E solutions. The reasonable agreement between experimental results and isotherm models was concluded from the smaller variation between gravimetric and NMR estimates. Notwithstanding the uncertainty in the *goodness-of-fit* between the experimental data and the isotherm models, the CE-EPI (high) adsorbent displayed more reliable results than the other materials [CE-EPI (low), CE-EPI (medium) and CE materials] for uptake of water and ethanol.

As seen in Figure 4.3, the relative uptake of water and ethanol differ across a range of compositions for the binary mixtures in the presence of the cross-linked polymer (CE-EPI; 1:5.4). To evaluate the performance of chemical separations of such adsorbents, the molecular selectivity for each respective solvent component was determined where the equilibrium uptake for W or E from a binary mixture is reflected by an average estimate expressed as a relative selectivity ($R_{selectivity}$) value, according to equation 4.14.

$$R_{selectivity} = \frac{Q_{m\,(Water)}}{Q_{m\,(Ethanol)}} \qquad \text{Equation 4.14}$$

Figure 4.4 illustrates the $R_{selectivity}$ values for cellulose and its cross-linked polymers that were estimated from equation 4.14 using the Q_m values for water and ethanol listed in Tables 4.4 and 4.5. The results illustrate that the cross-linked polymers have greater selective uptake toward water when compared with pristine cellulose (CE), except for CE-1. A maximum value for $R_{selectivity}$ was observed for CE-3 and this may relate to the level of cross-linking since fewer numbers of surface accessible -OH groups are present at this elevated level of cross-linking.[28] The cross-linking

reaction between cellulose and epichlorohydrin results in a net loss of one hydroxyl group for each cross-linker (epichlorohydrin) that undergoes complete reaction (*cf.* Scheme 1 in ref. 28).

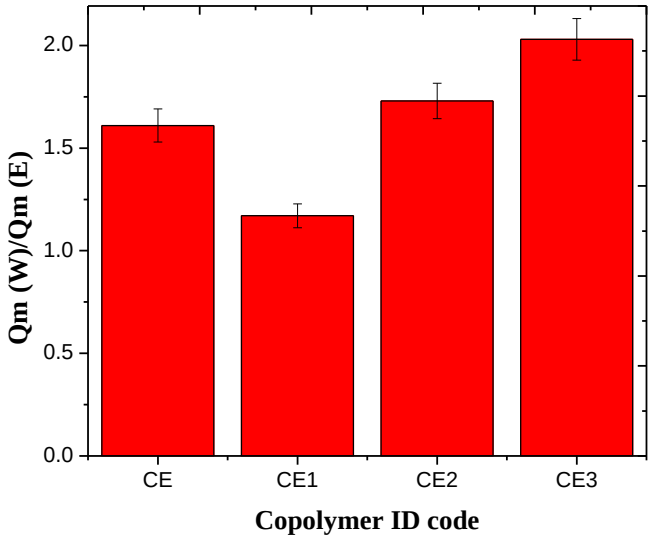

Figure 4.4 Equilibrium selectivity ratios ($R_{selectivity}$; Equation 4.14) of cellulose and its cross-linked polymers for uptake of ethanol and water in binary solvent systems at 295 K. The ID code corresponds to the sorbent materials listed in Table 4.1.

According to Table 4.1, the swelling behaviour of materials are not in agreement with the trends in isotherm adsorption results. The degree of swelling (%) measured for CE-1 was greater than CE-3 and CE-2. As the level of cross-linking increases, the -OH groups of cellulose may be less accessible, as evidenced by the attenuated solvent swelling. Therefore, the low EPI content of CE-1 does not favour ethanol adsorption due to the presence of abundant surface-accessible -OH groups of cellulose that offer active adsorption sites for water and ethanol uptake. The variation in $R_{selectivity}$ values may also be related to the surface accessibility of the -OH groups of cellulose for the cross-linked cellulose. Cross-linking alters the dipolar character of the polysaccharide surface by decreasing the overall number and accessibility of adsorption sites of cellulose. Cross-linking of cellulose results in steric effects of the adsorption sites and changes in the textural properties of the sorbent in a fashion consistent with the differences in morphology of native starch *vs.* cellulose,[43] in agreement with solubility differences in water. The foregoing is in agreement with the water uptake (*cf.* Table 4.5) and swelling behaviour in pure solvents (*cf.* Table 4 in ref. 28).

As indicated above, the heterogeneity parameter (n_s) estimated from the Sips model affords an assessment of the surface heterogeneity of the polysaccharide. The n_s values in Table 4.4 relate to uptake of ethanol while the values in Table 4.5 relate to water uptake. The n_s values in Table 4.4 for ethanol uptake exceed those listed in Table 4.5 for water uptake. The trend for n_s suggest that greater steric effects are more apparent due to apparent surface heterogeneities for the uptake of ethanol due to its greater molecular size and/or reduced polarity relative to water. The foregoing results provide insight on the variable adsorption properties of cellulose due to cross-linking by illustrating the role of surface functional groups and textural properties [25,45] in accordance with another independent study (*cf.* Figure 4 in ref. 46). In the case of biomaterials such as straw, there are adsorptive contributions arising from other biopolymer components besides cellulose. For example, additional components such as hemi-cellulose, lignin, low molecular weight organic compounds (oils), and inorganic species are likely to contribute to the overall uptake properties.[47] The greater uptake of water by barley straw[25] may relate to other components such as hemi-cellulose and starch since such biopolymers favour the sorptive uptake of water.[48] The reduced uptake of water in flax-PET fibre composites was attributed to the hydrophobic nature of PET; whereas, native flax fibres have greater water uptake capacity (*cf*. Figure 11 in ref. 49). The roles of surface functional groups and stabilizing interactions were evidenced by AFM and FE-SEM studies at the oil-water interface where dispersed and agglomerated nanofibrillated cellulose fibers contribute to the stabilization of emulsions by preventing the coalescence of droplets.[50]

The effective design of a practical sorption process depends not only on favourable interactions for the adsorbent-adsorbate system, efficient adsorption also depends on the kinetics of the uptake.[51] Figure 4.5 shows the amount of ethanol and water adsorbed by cellulose as a function of contact time where the ethanol and water uptake increases rapidly during an initial 6 h phase where it reaches saturation by *ca*. 24 h. The rapid initial uptake occurs due to the available vacant adsorption sites at the surface sites or micropore domains. Thereafter, the number of vacant adsorption sites decreases until the sorbent surface reaches saturation of the monolayer, as evidenced by the plateau region of the isotherm. The increase in the number of adsorbed sites from 12 h to 24 h is likely due to a slower kinetic process, where the gradual rise after the first 12 h may result from diffusion within narrow micropore sites or the fibril domains (crystalline and amorphous) of cellulose.

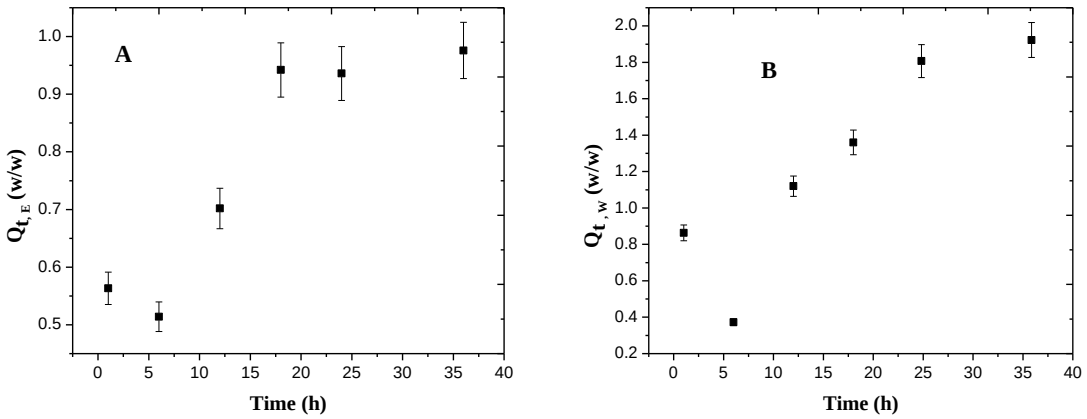

Figure 4.5 Determination of the equilibrium time for A) Ethanol uptake, and B) Water uptake from a binary W-E mixture containing 55% of ethanol with cellulose at variable time at 295 K.

The kinetics of adsorption were modeled using the PFO, PSO and the pore-diffusion models. The PSO kinetic model is more commonly used for describing the adsorption behaviour of adsorbents with homogeneous sorption sites, as shown by the best-fit data in Figure 4.5. In Figure 4.6, the PSO kinetic model provides a good description of the kinetic dependence (R^2 = 0.970 and 0.911) relative to the PFO and pore-diffusion models. The modeling details are provided in the Appendix A4 (*cf*. Figure A4.3) for the PFO and pore-diffusion models.

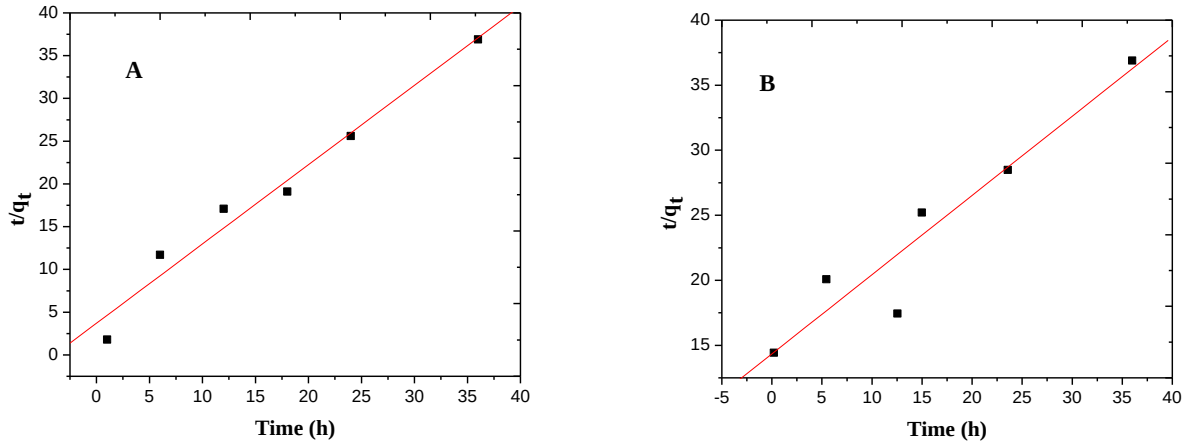

Figure 4.6 Pseudo-second-order plots for the uptake of ethanol from W-E mixtures: A) CE and B) CE-2 at 295 K.

The kinetic parameters, obtained by nonlinear regression analysis for the PSO model parameters, are listed in Table 4.6. CE-3 was predicted to have heterogeneous adsorption sites since this level of cross-linking exceeds the estimated number of available hydroxyl groups of cellulose if one neglects steric effects due to fibril formation. The uptake of ethanol and water from binary W-E mixtures was observed to follow the PSO profile. The role of EPI may serve to alter the surface chemistry or the textural microporous nature of native cellulose, as described above. Cross-linking of cellulose affects the number and surface accessibility of the hydroxyl groups[52] for inter- and intra- H-bonding interactions. In accordance with the traditional *two-phase* cellulose model, the ordered and amorphous domains are expected to vary, as shown in Scheme 4.1. It follows that cross-linking may contribute defect sites, which increase the overall surface area and pore structure by adulterating the expected hydrogen bond network of native cellulose.[53] Scheme 4.1 illustrates the amphiphilic properties of cellulose, which rely on its degree of amorphous *vs.* crystalline properties, in accordance with the variable solvent uptake (W and E) observed herein for binary solvent systems.

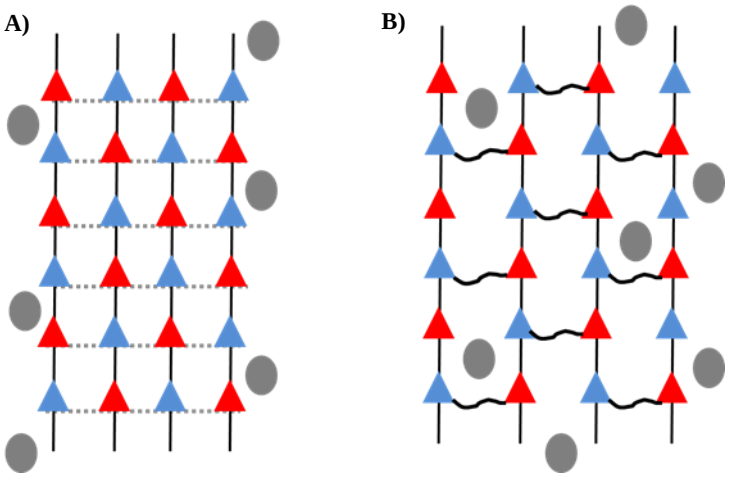

Scheme 4.1 Schematic illustration of the relative solvent accessibility according to the molecular structure of cellulose in two different forms: A) Native cellulose and B) cellulose with intermediate level of cross-linking. The β-1,4-linkages are shown as full straight line segments, inter-chain hydrogen bonding as dashed lines, and the EPI cross-linking as wavy bold lines. An arbitrary solvent (oval) is shown but it is not drawn to scale.

Table 4.6 Kinetic parameters of pseudo-second-order adsorption model for water and ethanol uptake by CE-3 in a binary solvent system at 295 K.

	Pseudo-second-order (PSO)			
Cellulose ID code	k_2 **(g.mg^{-1}.min^{-1})**	q_e**,(mg/g)**	R^2	χ^2
CE	0.928	3.69	0.970	0.007
CE-2	0.609	14.3	0.911	0.001

The rigid and pseudo-linear structure of cellulose is attributed to the β-1,4-glycosidic bonds and the presence of a combination of H-bond acceptors and donor groups for each cellobiose unit of this biopolymer. The occurrence of intra- and inter-chain hydrogen bonding is highly favoured, in agreement with the supramolecular framework of cellulose fibres, which are composed of 24-36 cellulose strands. The *fibril-like* structure of cellulose is consistent with the relative insolubility of cellulose in water and its high crystallinity index.[54] Cross-linking of cellulose will alter the hydrogen bonding network and van der Waals interactions among biopolymer chains, which are supported by the variable adsorption properties described herein. The lower uptake of ethanol over water agrees with the general notion of the lipophilic character of cellulose due to its unique supramolecular assembly according to Scheme 4.1. The changes in molecular structure of cellulose and its cross-linked forms are consistent with the unique $R_{selectivity}$ values reported herein, in agreement with the relative offset in polarity of water (16 D)[44] and ethanol (8.8). [44]

4.5 Conclusion

^{1}H-NMR spectroscopy represents a versatile analytical method for quantifying the level of water or ethanol in binary W-E solutions. The quantitative NMR (qNMR) method reported herein has advantages for the rapid screening and quantitation of binary solvents, as compared with other time consuming and labour intensive methods such as the Karl Fischer titration, gas chromatography, or high performance liquid chromatography. The qNMR method provides an *in situ* measure of the relative solvent uptake in binary solvent systems to afford analysis of the adsorption isotherms of cellulose and its cross-linked forms with water and ethanol in binary solvent systems. The tunable adsorption properties due to cross-linking effects was evidenced by the cellulose polymer (CE-3) according to its high uptake capacity for both ethanol and water, in comparison to reduced uptake for cellulose (CE) and cross-linked polymers (CE-1 and CE-2). Additionally, the uptake selectivity of water over ethanol ($R_{selectivity}$) was greater for the cross-

linked polymers relative to cellulose. CE-3 had an optimal $R_{selectivity}$ value and the equilibrium uptake results were further supported by the corresponding kinetic uptake properties.

Cross-linking of cellulose affects the accessibility of polysaccharide -OH groups, surface polarity, and the formation of micropore domains, according to the relative EPI content of the cross-linked biopolymer. This study has contributed to the development of a rapid *in situ* NMR method for assessing the relative solvent uptake in binary water-ethanol solutions and a molecular level understanding of the adsorption process. The cellulose materials investigated herein represent promising materials for the facile fractionation of water and ethanol in binary W-E solutions using an adsorptive-based process. Further work is underway[55] to explore the utility of these biopolymer materials for diverse types of adsorptive-based fractionation of waterborne organic contaminants in aqueous solution.

4.6 References

1. Foo, K. Y. *RSC Adv.* **2013,** *3,* 18248-18258.
2. Wilson, L, D.; Mohamed, M. H.; Headley, J. V. *Rev Environ Health.* **2014,** *29,* 1-8.
3. Ernest, R. Roth.; Villanova, Pa. Production of low-ethanol beverages by membrane extraction. U.S. Patent 4,306,884, Dec.22, **1981.**
4. Gubicza, L.; Kabiri-Badr, A.; Keoves, E.; Belafi-Bako, K. *J. Biotech.* **2000,** *84,*193–196.
5. Karlsson, H. O. E.; Trigirdh, G. *Trends Food Sci. Tech.* **1996,** *17,* 71-82.
6. Light, W. G.; Calif. S. D. Production of low alcoholic content beverages. U. S. Patent 4,617,127, Oct. 14, **1986.**
7. Stephen, L. M.; Harvard, M. Production of low-ethanol beverages by membrane extraction. U.S. Patent 4,778,688, Oct. 18, **1988.**
8. Van der Padt, A.; Sewalt, J. J. W.; Van't Riet, K. *J. Membr. Sci.* **1993,** *80,* 199–208.
9. Jeong, J. C.; Lee, S. B. *Biotechnol. Tech.* **1997,** *11,* 853–858.
10. Okewale, A. O.; Etuk, B. R.; Igbokwe, P. K. *IJET-IJENS.* **2011,** *11,* 81-91.
11. Baylak, T.; Kumar, P.; Hui Niu, C.; Dalai, A. *Energ Fuel* **2012,** *26(8),* 5226-5231.
12. Kim, Y.; Hendrickson, R.; Mosier, N.; Hilaly, A.; R. Ladisch, M. *Ind. Eng. Chem. Res.* **2011,** *50 (14),* 8678-8685.
13. Liu, Y-W.; Tang, T.; Chung, T. W.; Huang, Ch.; Lin, Y. S. *J. Chem. Eng. Data* **2010,** *55 (12),* 5807-5811.

14. Noll, K. E.; Gounaris, V.; Hou, W-S. Adsorption technology for air and water pollution control. Lewis. Pub., Michigan, **1991.**
15. Buszewski, B.; Bocian, S.; Rychlicki, G.; Vajda, P.; Felinger, A. *J. Colloid Interface Sci.* **2010,** *349,* 620-625.
16. Mohamed, M. H.; Wilson, L. D.; Headley, J. V. J. *Phys. Chem. B* **2013,** *117(13),* 3659-66.
17. Leblanc, D.; Morin, A.; Gu, D.; Zhang, X. M.; Bisaillon, J. G.; Paquet, M. Dubeau, H. *Biotechnol. Lett.* **1998,** *20,* 1127–1131.
18. Dhake, K. P.; Karoyo, A. H.; Mohamed, M. H.; Wilson, L. D.; Bhanage, B. M. *J. Mol. Catal. B: Enzym.* **2013**, *87,* 105-112.
19. Wehtje, E.; Svensson, I.; Adlercreutz, P.; Mattiasson, B. *Biotechnol. Lett.* **1993,** *12,* 873–878.
20. Al-Asheh, S.; Banat, F.; AL-Lagtah, N. *Chem. Eng. Res. Des.* **2004,** *82(A7),* 855-864.
21. Shih-Hsiung, Ch.; Kuang-Chang, Y.; Shiow-Shyung, L.; Dong-Jang, Ch.; Rey May, L. *J. Membr. Sci.* **2001,** *183,* 29-36.
22. Wah Koon, T.; Douglas, M, R. *Ind. Eng. Chem. Process Des. Dev.* **1986,** *25,* 17-21.
23. Huang, Z.; Wen, R.; Guo, Y.; Su, J.; Matsuura, T. *Sep. Purif. Technol*. **2006,** *51,* 126-136.
24. Ivanova, E.; Damgaliev, D.; Kostova, M. *J. Univ. Chem. Technol. Metallurgy* **2009,** *44,* 267-274.
25. Sun, N.; Okoye, Ch.; Niu, C.; Wang, H. *Int. J. Green Energy* **2007,** *4,* 623–634,
26. Mohamed, H. M.; Wilson, L. D.; Headley, J. V. *Carbohydr. Polym.* **2010,** *180,* 186-196.
27. Dabrowski, A. *Adv. Colloid Interface Sci.* **2001,** *93,* 135-224.
28. Dehabadi, L.; Wilson, L. D. *Carbohydr. Polym.* **2014,** *113,* 471- 479.
29. Claridge, T. D. W. High- Resolution NMR Techniques in Organic Chemistry. 2nd ed. Newnes: Elsevier, **2009,** 247-302.
30. Foo, K. Y.; Hameed, B. H. *Chem. Eng. J.* **2010,** *156,* 2-10.
31. Jiang, Y.; Huang, C.; Pang, H.; Liao, B. *Huaxue Tongbao Sci.* **2008,** *71(12),* 891-899.
32. Morin-Crini, N.; Crini, G. *Prog. Polym. Sci.* **2013,** *38,* 344-368.
33. Lagergren, *S. K. Sven. Vetenskapsakad. Handl.* **1898,** *24,* 1-39.
34. Ho, Y. S.; McKay, G. *Chem. Eng. J.* **1998,** *70,* 115-124.
35. Borah, J.; Sarma, M. J.; Mahiuddin, S. *Colloids Surf. A* **2011,** *387,* 50-56.
36. Tomoyoshi, S.; Takashi, M.; Ikuto, Y.; Akio, Sh.; Koichi, F.; Yoshihiro, T. *J. Mol. Liq.* **1996,** *70,* 1-9.

37. Ratanapariyanuch, K.; Shen, J.; Jia, Y.; Tyler, R. T.; Shim, Y. Y.; Reaney, M. J. T. *J. Agric. Food Chem.* **2011,** *59,* 10454-10460.
38. Hansen, F.; Led, J. J. *J. Magn. Reson.* **2003,** *163(2),* 215-27.
39. Ratanapariyanuch, K.; Shen, J.; Jia, Y.; Tyler, R. T.; Shim, Y. Y.; Reaney, M. J. T. *J. Agric. Food Chem.* **2011,** *59,* 10454-10460.
40. Dowd, M. K.; Reilly, p. j.; Trahanovsky, J. J.; Mustafa, A, F. *Cereal Chem.* **1993,** *70,* 204-209.
41. Gusev, S. S.; Kalutskaya, E. P.; Aleksandrovich, I. F.; Rozenberg, A. Y. *J. Polym. Sci.* **1978,** *20,* 88-93.
42. Pratt, D. Y.; Wilson, L. D.; Kozinski, J. A.; Mohart, A. M. *J. Appl. Polym. Sci.* **2010,** *116,* 2892-2989.
43. Y. Lee, J.; Westgate, P.; Ladisch, M. R. *AIChE J.* **1991,** *37,* 1187-1195.
44. Hynes, W. M. CRC Handbook of Chemistry and Physics, 92nd ed., CRC Press, Boca Raton, FL, USA, **2011.**
45. Olsson, A. M.; Salmén, L. *Carbohyd. Res.* **2004,** *339,* 813–818.
46. Okubayashi, S.; Griesser, U. J.; Bechtold, T. A. *Carbohyd. Polym.* **2004,** *58,* 293–299.
47. Kulp, K.; Ponte, J. G. J. Handbook of cereal science and technology. New York, **2000,** Marcel Dekker Inc.
48. Quintero, J. A.; Cardon, C. A. *Ind. Eng. Chem. Res.* **2009,** *48(14),* 6783–6788.
49. Gouanve, F.; Marais, S.; Bessadok, A.; Langevin, D.; Metayer, M. *Eur. Polym. J.* **2007,** *43,* 586–598.
50. Xhanari, K.; Syverud, K.; Chinga-Carrasco, G.; Paso, K.; Stenius, P. *J. Colloid Interface Sci.* **2011,** *356,* 58-62.
51. Okewale, A. O.; Babayemi, K. A.; Olalekan, A. P. *Int. J. Appl. Sci*. *Technol.* **2013,** *3,* 35-42.
52. Wilson, L. D.; Mohamed, M. H.; Headley, J. V. *J. Colloid Interface Sci.* **2011,** *357,* 215-222.
53. Mohamed, M. H.; Wilson, L. D.; Pratt, D. Y.; Guo, R.; Wu, C.; Headley, J. V. *Carbohydr. Polym.* **2012,** *87,* 1241-1248.
54. Jiao, Ch.; Xiong, J. *Bioresources* **2014,** *9(4),* 6504-6513.
55. Udoetok, I. A.; Dimmick, R. M.; Wilson, L. D.; Headley**,** J. V. *Carbohydr. Polym.* **2016,** *136,* 329–340.

CHAPTER 5

MANUSCRIPT 3: NMR Investigation of the Fractionation of Water–Ethanol Mixtures with Starch and Its Cross-Linked Forms

Leila Dehabadi, Lee D. Wilson∗

Description

Based on the results from the study of cellulose and its modified forms, the use of qNMR for the study of solvent-selective uptake in binary W-E mixtures was established. The study is focused on understanding the structure-adsorption property relationship between starch and its cross-linked forms in the presence of water-ethanol binary mixtures. In this research, different types of starch were evaluated according to the relative composition of amylose and amylopectin to gain insight on the role of linear and branched polysaccharide structures. The starch biopolymers were prepared and then characterized according to the cross-linking methodology described in Chapter 3 and was used as an adsorbent. The utility of qNMR enables the quantitative measurement of water or ethanol composition in binary mixtures and evaluation of the adsorption properties of the starch materials. The obtained results from the qNMR method for adsorption of ethanol over water evidenced the enhancement of the adsorption capacity using cross-linked starch materials. The variable solvent selective uptake ($R_{selectivity}$) of water over ethanol by starch-EPI adsorbents in binary W-E mixtures enhanced significantly and ranged from 3.8 to 80. The role of structure and textural properties of adsorbent materials among the different starch biopolymers can be related to the adsorption properties and water selectivity of the starch-based adsorbents along with comparison of biopolymer materials reported in literature.

Authors' Contributions

The project was conceived by the supervisor (L. D. Wilson) with input from L. Dehabadhi on the choice of variable types of starch with different amylose and amylopectin content. The experimental work and first draft of the manuscript were completed by L. Dehabadi. Subsequent revisions and edits were done by the supervisor and L. Dehabadi.

Relation of Manuscript contribution to Overall Thesis Objectives

This research builds upon the demonstrated utility of qNMR reported in Chapter 4 to further explore the adsorptive fractionation properties of starch-based materials as adsorbents in binary

W-E mixtures. While the results for cellulose presented in Chapter 4 reveal some measure of solvent selectivity of water over ethanol, where the use of starch and its modified forms is hypothesized to have greater solvent selectivity of water over ethanol in binary mixtures The systematic evaluation of the adsorption isotherms of starch and its modified forms in binary mixtures provides insight regarding the relationship of polysaccharide structure and adsorption properties, as outlined in Section 5.4.3. The use of qNMR revealed quantitative results concerning the $R_{selectivity}$ of starch-based materials that surpassed cellulose-based materials and other adsorbents. The variation in structure and the adsorptive fractionation properties reveal that the nature of the polysaccharide and the level of cross-linking play a key role in governing the adsorption properties of such materials. These results are anticipated to provide further insight on the adsorptive contributions of more complex polysaccharide biomasses that contain multi-component systems.

5. NMR Investigation of the Fractionation of Water–Ethanol Mixtures with Starch and its Cross-Linked Forms

Leila Dehabadi, Lee D. Wilson*

Department of Chemistry, University of Saskatchewan, 110 Science Place, Saskatoon, Saskatchewan, Canada S7N 5C9.

*Corresponding Author.

Supplementary Information (Appendix A, Chapter 5)

Graphical Abstract

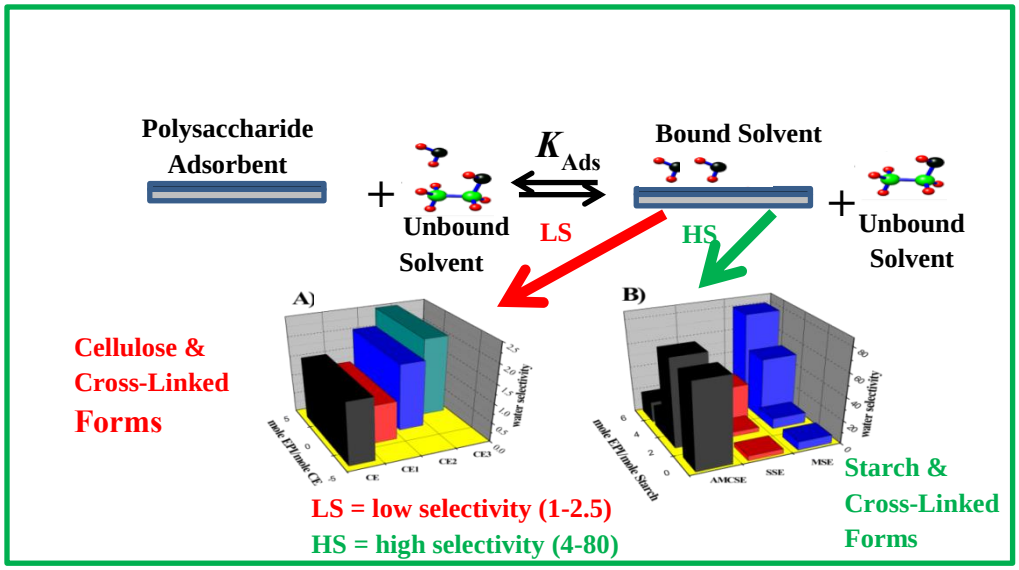

Research Highlights

- The uptake properties of different structural forms of starch (amylose and amylopectin) and their cross-linked forms were studied.
- Quantitative analysis of the relative water/ethanol uptake by starch materials was evaluated in binary mixtures using quantitative ^{1}H-NMR.
- The relative adsorptive selectivity ($R_{selectivity}$) of water over ethanol was obtained for different types of starch biopolymers and cross-linked forms.
- The $R_{selectivity}$ values for starch biopolymers exceeded those for cellulose and varied in an incremental manner according to the level of cross-linking.

5.1 Abstract

The development of low-cost and efficient methods for the fractionation of water and ethanol in binary mixtures is of great interest in the food processing and fuel production industries. Herein, we report a systematic study of a series of linear and branched starch-based biopolymers along with their modified forms *via* cross-linking with epichlorohydrin (EPI) at variable composition. The fractionation properties of these adsorbent materials were studied in binary ethanol-water solutions and compared with the neat solvents. ^{1}H-NMR spectroscopy was used to assess the binary solvent composition for the study of isotherms for the respective solvent components. The maximum adsorption capacities (Q_m) for starch and its cross-linked forms ranged from 0.01 to 2.70 $g.g^{-1}$ for water and ethanol in binary mixtures according to the Sips isotherm model. The fractionation selectivity [$R_{selectivity}$; $Q_m(W)/Q_m(E)$] of starch-EPI adsorbents for water (W) and ethanol (E) in binary mixtures range from 3.8 to 80. At saturative isotherm conditions, the $R_{selectivity}$ value reveals unique solvent selective uptake in binary W-E mixtures that depend on the amylose *vs.* amylopectin composition, along with the cross-linker content of the starch materials. The unique water uptake properties of starch and its cross-linked forms illustrate the role of textural properties and variations in the hydrophile-lipophile balance of the polymer network on the selective adsorption properties. Starch and its modified forms represent a promising class of adsorbent materials and a sustainable technology for the adsorptive-based fractionation of W-E binary mixtures.

5.2 Introduction

Bioethanol is often produced from agricultural waste through fermentation and is considered as a clean and sustainable biofuel with continued potential as a blending additive to conventional fossil fuels.[1] A key challenge associated with bioethanol production is achieving more effective and economical methods for water (W) removal. Techniques, including azeotropic distillation, extractive distillation, reactive distillation and adsorptive distillation, can be employed for the fractionation and enrichment of ethanol content in binary W-E mixtures.[2] Among these techniques, distillation is one of the commonly used separation methods used by the fine chemicals industry. However, there are some disadvantages with conventional distillation that employs the use of azeotropes like benzene to separate ethanol-water mixtures including high-energy consumption and costly operational requirements. Distillation relies on well-defined differences in the volatility and temperature stability of the components for adequate separation. Membrane-based pervaporation is gaining attention for the separation of labile liquid mixtures because of its safe operation, reduced energy footprint, and good efficiency.[3] However, there is a persistent enquiry for effective, green and environmentally friendly methods for the separation of water and ethanol in binary mixtures. Adsorption represents a relatively low cost, low energy input, and promising method for water removal in W-E mixtures,[4] especially in the condensed phase. Heterogeneous adsorption processes at the liquid-solid interface involving specific surface interactions may result in favourable fractionation of liquid mixture due to specific adsorbent/adsorbate interactions in a multi-component system.[5]

Recent efforts have been focused on the development of materials and methods to enrich the separation of W-E binary mixtures.[6] Diverse types of industrial adsorbents such as zeolites, clays, and biomass adsorbents have been employed for the separation of water in W-E mixtures.[4,7,8] An important class of inorganic adsorbents for gas phase separations is diatomaceous molecular sieves and zeolites because of their unique textural properties and extensive pore network structure. The lack of uniformity in size and tortuosity of various molecular sieves reveals a drawback that offsets the separation efficacy.[9,10] In contrast, biomaterials and their modified forms have advantages for the separation of liquid mixtures such as recyclability, high efficiency, and lower cost and energy consumption. In this respect, starch is an abundant and sustainable biopolymer adsorbent, which has attracted attention for the separation of W-E mixtures.[11-13] Starch biopolymers possess unique structural features such as abundant hydrophilic groups according to

their relative accessibility due to chain branching and variable morphology. Previous reports indicate that starch-based materials show evidence of solvent selective separations in the case of alcohol/water mixtures.[11] Chemical modification of polysaccharides via chemical cross-linking can be employed to modify the adsorption properties of adsorbents such as cellulose according to recent reports.[14,15] Cross-linked starch represents an important material with suitable properties for the fractionation of water in mixtures for the food processing industry.[16] Cross-linking of starch results in branching along with the formation of 3-D network structures that display enhanced swelling and gel formation in aqueous solution.[17] Thus, cross-linked starch may serve as an improved adsorbent for water in the fractionation processes for food and biofuels in the condensed phase. However, there are few reports in the literature describing the application of such biopolymers for the separation of W-E mixtures (ethanol dehydration), [18,19] while sparse reports that employed corn meal, corn grits and pristine starch are available.[20-24]

In a previous study, we reported the utility of cellulose and its cross-linked forms as adsorbents for the fractionation of W-E mixtures. These modified biomaterials, with molecular selectivity [$R_{selectivity;}Q_m(W)/Q_m(E)$] ranging between 1.10 to 2.03 at saturative conditions in binary W-E mixtures[15], demonstrated their promising potential utility for the fractionation of binary W-E systems.

Farhad *et al.*[25] recently reported that starch-coated surfaces have a higher affinity toward water vapour than silica gel coatings, which provides support that starch has good potential utility as a sorbent for water in the vapour state. In this study, we report on the adsorption properties of starch-based adsorbent materials for the fractionation of solvent components in W-E binary mixtures using ^{1}H-NMR spectroscopy as a quantitative analytical method. Structural variants of starch derived from corn, maize, and soluble starch were evaluated due to the variation in linear *vs.* branched polysaccharide content. The starch materials were further modified by cross-linking with epichlorohydrin at variable levels to evaluate the fractionation behaviour of starch with cellulose and its cross-linked forms.[15] This study contributes to the field of sustainable energy and biomass by revealing that starch materials display tunable adsorption behaviour in W-E systems that relate to the role of synthetic modification via cross-linking of such materials.

Generally, the objective for this study was investigation of new techniques and methods for separation of water and ethanol. The utility of the NMR method for the *in situ* quantitative analysis of W-E mixtures, the elucidation of the role of cross-linking of starch-based materials for the

adsorptive fractionation of water and ethanol, illustration of the remarkable water selective uptake behaviour of starch-based components, and finally the potential utility of such materials for the fractionation of W-E mixtures are among the most important aspects of this study. The outcome of this research would contribute to the field of energy production and chemical separation of biofuels.

5.3 Experimental

5.3.1 Chemicals and materials

Starch from various sources (corn or maize) containing variable levels of amylose and amylopectin was chosen as the polysaccharide material. Epichlorohydrin, sodium hydroxide and ethanol (reagent grade, Commercial Alcohols Inc. Brampton, ON, Canada) were purchased from Sigma–Aldrich (Oakville, ON, Canada) and used as received. The modified forms of starch containing different percentages of amylose/amylopectin (AM/AP) (such as SSE, 50% AM/AP, MSE, 98% AP, AMCE, 98% AM) and various mole ratios of EPI were prepared by a modified method reported in our previous work.[26,27]

5.3.2 Methods

To examine the sorption capacity of the starch materials with W-E in binary solvents, a batch adsorption method was used to obtain solid-solution isotherms for each adsorbent-solvent system. 20 mg of starch (or modified starch) was added to 10 g solvent with variable ethanol-water content in 4 dram glass vials. Samples of adsorbent and the solvent system were incubated with shaking (Poly Science, Dual Action Shaker) for 24 h at 160 rpm at ambient conditions to achieve equilibrium. Thereafter, the samples were separated from solutions by centrifuging (Precision Micro-Semi Micro Centricone, Precision Scientific C_o.) at 1800 rpm for 1 h. Thereafter, 1 g of supernatant solution was mixed with a 0.1 g mixture containing tetrahydrofuran (THF) with deuterated dimethyl sulfoxide (DMSO-d_6, 99.9%, from Sigma-Aldrich). THF serves as an internal standard and DMSO-d_6 serves as the field-lock solvent, where the weight content of THF in DMSO-d_6 was held constant for all measurements.

All ^{1}H-NMR spectra were recorded using a wide-bore (89 mm) 11.7 T Oxford superconducting magnet system (Bruker Bio Spin Corp; Billerica, MA, USA) equipped with 5 mm PaTx1 probe. NMR acquisition parameters were controlled using a SSSC 500 console and

workstation running X WIN-NMR 3.5. Standard pulse programs utilized were available from the TopSpin 1.3 software. In this study, the quantitative NMR method (qNMR) was used to analyse the relative solvent composition of water-ethanol (W-E) binary solutions by independent calibration curves derived from various standard binary W-E solutions prepared at variable W-E composition (w/w; %). Each solution contained an analytical internal standard (THF) and a locking solvent (DMSO-d_6). The recycle delay times were determined based on a previous T_1 relaxation study of analogous binary W-E mixtures and their neat solvents.

The equilibrium time of the adsorption process was evaluated by varying the contact times of 20 mg samples of adsorbent with the binary W-E mixtures. Quantitative determination of the respective solvent adsorbed at each mixing time was evaluated using ^{1}H-NMR spectroscopy under fully relaxed and steady-state conditions. The relaxation time (T_1) of the pure solvents and their binary W-E mixtures was measured by the inversion-recovery method.[15]

5.3.3 Models and equations

Adsorption isotherms were obtained by using equation 5.1 where $Q_{e,i}$ is the equilibrium sorption capacity (mg/g) of the adsorbent materials with the i^{th} solvent component (E or W) in a mixed binary (W+E) solvent system; $C_{o,i}$ and $C_{e,i}$ (mg/L) are the weight (g) of the initial solvent concentration before adsorption of the i^{th} component and $C_{e,i}$ is the weight-based equilibrium concentration after adsorption of the i^{th} component (W or E) The composition of the respective solvent components (W or E) were determined by their weight where the total weight of solution ($W_{solution}$; W+E), and m is the weight of polymer adsorbent (g). The equilibrium concentration ($C_{e,i}$) of ethanol and water in the supernatant solutions was estimated from the corresponding peak areas of E and W, before and after sorption.

$$Q_{e,i} = \frac{\left(C_{0,i} - C_{e,i}\right)}{m} \times W_{Solution} \qquad \text{Equation 5.1}$$

Finally, equilibrium adsorption was fitted to various isotherm models such as Langmuir, Freundlich, and Sips models[28,29] to evaluate the adsorption behaviour of the adsorbents in W-E binary solutions. The Langmuir model (Equation 5.2) describes monolayer sorption between adsorbate and adsorbent where Q_{max} represents the monolayer adsorption capacity and K_L

represents the Langmuir adsorption constant for the respective solvent component (W or E) in the binary W-E solvent system. The other terms ($C_{e,i}$ and $Q_{e,i}$) are defined by equation 5.1.[30]

$$Q_{e,i} = \frac{Q_m K_L C_{e,i}}{1 + K_L C_{e,i}} \qquad \text{Equation 5.2}$$

The Freundlich model (Equation 5.3) accounts for nonequivalent binding sites on heterogeneous surfaces. The heterogeneity factors are denoted by the exponential term (n_F) in equation 5.3.

$$Q_e = K_F C_e^{n_F^{-1}} \qquad \text{Equation 5.3}$$

The Sips isotherm is likened as a hybrid model with features described by the Langmuir and Freundlich isotherms at certain limiting conditions.[28] The Sips model provides an estimate of the monolayer surface coverage (Q_{max}) of the adsorbate (E or W) that depends on the uptake properties of the adsorbent. Equation 5.4 provides an understanding of multi-layer sorption processes. The Sips model accounts for adsorption processes that display surface heterogeneities according to the heterogeneity factor (n_s) in equation 5.4. When $n_s = 1$, Langmuir isotherm behaviour (no heterogeneity) is predicted; whereas, Freundlich behaviour is predicted when $(K_s C_e)^{n_s} <<< 1$ ($n_s \neq 1$).

$$Q_e = \frac{Q_m (K_s C_e)^{n_s}}{1 + (K_s C_e)^{n_s}} \qquad \text{Equation 5.4}$$

5.4 Results and Discussion

5.4.1 Selection of polysaccharide materials

The selection criteria for starch was based on commercially available structural forms which vary from linear (amylose) to increased branching (amylopectin), according to the source of the polysaccharide. The various structural forms of starch possess variable water solubility and

steric effects along with accessibility of primary *vs.* secondary hydroxyl groups due to branching.[31] Table 5.1 lists the various types of starch-based materials and the corresponding sample ID codes, where corn starch contains amylose, soluble starch contains *ca.* 1:1 amylopectin/amylose content, and maize contains a relatively greater fraction of amylopectin. Also, a summary of the modified starch yield (%) and equilibrium swelling properties in water (S_W) and in ethanol (S_E) for starch and its cross-linked forms (starch-EPI) at various compositions is listed in Table 5.1. Accordingly, the starch materials with variable levels of amylose/amylopectin were cross-linked using epichlorohydrin with low (1:2), medium (1:3.6), and high (1:5.4) levels of cross-linker to afford starch-based adsorbents variable framework structures and surface-accessible hydroxyl groups. Cross-linking of starch affords materials with variable textural properties (surface area and pore structure) and surface-accessibile hydroxyl groups that contribute to the solvent fractionation process in W-E binary solutions, according to the cross-linker content.[5,7,13-15,30]

Table 5.1 Selected physicochemical properties of starch and its cross-linked polymers Starch-X. where X represents the epichlorohydrin content at different levels (L, M, H)* of cross-linking.

PS-EPI biopolymers	*Polymer ID code	Yield (%)	S_W (%)	S_E (%)
Soluble starch-EPI (L)	SSE-L	93	35 ± 4	8 ± 3
Soluble starch-EPI (M)	SSE-M	91	67 ± 12	13 ±7
Soluble starch-EPI (H)	SSE-H	96	117 ± 18	27 ± 3
Soluble starch	SSE	ND	157 ± 21	8 ± 2
Maize starch-EPI (L)	MSE-L	86	25 ± 5	4 ± 2
Maize starch-EPI (M)	MSE-M	87	52 ± 7	4 ± 1
Maize starch-EPI (H)	MSE-H	85	107 ± 9	3 ± 2
Maize starch	MSE	NA	153 ± 9	2 ± 0.5
High amylose starch-EPI (L)	AMCE-L	89	63 ± 7	1 ± 0.3
High amylose starch-EPI (M)	AMCE-M	93	188 ± 11	2 ± 1
High amylose starch-EPI (H)	AMCE-H	90	307 ± 16	18 ± 4
High amylose starch	AMCE	NA	248 ± 12	14 ± 6
Cellulose-EPI (L)	CE-L	94	244 ± 1	120 ± 1
Cellulose-EPI (M)	CE-M	88	205 ± 9	92 ± 8
Cellulose-EPI (H)	CE-H	91	161 ± 3	15 ± 5
Cellulose	CE	NA	166 ± 9	2 ± 0.1

* L, M and H denotes for the mole ratios of Starch-EPI, as follows: L = Low (1:2 mole ratio); M = Medium (1:3.6 mole ratio); and H = high (1:5.4 mole ratio). NA denotes not applicable.

5.4.2 Quantitative analysis of water/ethanol components by qNMR

^{1}H nuclear magnetic resonance (NMR) spectroscopy is a unique method for the structural characterization and identification of organic compounds due to the relative abundance of ^{1}H nuclei and its sensitivity.[32] The ^{1}H-NMR method is a suitable technique for quantitative analysis of mixtures when suitable spectral signatures are well-resolved and instrumental conditions account for the relaxation dynamics of the accordant nuclei.[15]

The relaxation times (T_1) for specific nuclei in water and ethanol binary solvents were reported previously[15], facilitating qNMR analyses of starch-based systems in this study. qNMR

was used to estimate the solvent composition before and after the sorptive fractionation in binary W-E mixtures. Molecular selective adsorption for such systems indicates that the physical separation of one solvent component, such as water (W) over ethanol (E), occurs due to preferential uptake in a W-E solution. The composition of E and W in the liquid mixtures was calculated using calibration curves over a defined W-E composition range using qNMR. Tetrahydrofuran (THF) was chosen as the internal calibration standard because its ^{1}H spectral signatures do not overlap with those of water or ethanol (-CH_2 and –CH_3 groups) in the binary solution (*cf*. Figure 1 in ref. 15).

Among the various NMR solvents, DMSO-*d6* is an optimal choice as a field-locking solvent due to its miscibility in W-E mixtures and the spectral resolution it affords. Quantitative integration of the NMR spectra was achieved using the longest relaxation delay (D_1) as determined by the inversion-recovery determination of the relaxation time (T_1) of the various nuclei for E and W in pure and binary W-E mixtures.[33] The NMR spectra of W-E mixtures reveal resolved resonance lines for OH appearing at δ=4.50 ppm and δ=5.20 ppm for water and ethanol, respectively, as observed in (Figure 1 of ref. 15). Quantitative analysis of water and ethanol can be achieved by measuring the integrated signal intensity of relevant signatures (–OH, -CH_2, and –CH_3) for E and W. Favourable spectral resolution of the solvent signatures of fully relaxed spectra allow for the quantitative analysis by equation 5.5. The relative water content (w/w; %) in binary mixtures can be calculated according to the respective gravimetric (n_W and n_E) contributions by equation 5.5. Similarly, ethanol content was calculated according to the peak area for the –CH_3 group.

$$\frac{\text{Area (solvent)}}{\text{Area (THF)}} = \frac{^{1}\text{H}_{\text{nuclei}}\text{ (solvent)}}{^{1}\text{H}_{\text{nuclei}}\text{(THF)}} \times \frac{\text{n}_{\text{solvent}}}{\text{n}_{\text{THF}}} \qquad \text{Equation 5.5}$$

The relative area for each solvent component refers to the integrated peak area for the ^{1}H-NMR signals, $^{1}H_{nuclei}$ refers to the number of nuclei of the solvent (E or W), $n_{solvent}$ is the number of moles of solvent (ethanol or water), and n_{THF} refers to the mole content of THF. The results of such determinations were obtained in triplicate with standard deviations below 5%.

5.4.3 Sorption study

Based on the results in Table 5.1, it can be inferred that starch-based materials with greater amylose content display greater swelling in water over materials richer in amylopectin content. The swelling results for starch-based materials in neat ethanol are notably smaller by a factor of 5- to 10-fold compared with those in water. The amylose-based materials reveal comparable swelling in ethanol except those materials containing amylopectin, where the lowest swelling was observed in ethanol. The swelling of cellulose materials is relatively high in water and ethanol solvents, where this effect relates to the unique fibril structure of cellulose. Nitrogen adsorption results for cellulose show relatively high uptake when compared with starch-based materials, in accordance with the rigid nature and the micropore network structure of cellulose owing to its unique fibril morphology. Starch-based materials have lower surface area and reduced pore volume, which relate to the greater conformational entropy of amylose and amylopectin that results in denser packing and collapse of the starch framework, in agreement with the nitrogen adsorption and water swelling results.

In this study, the adsorption isotherms for three classes of starch (MSE, SSE, and AMCSE) with variable cross-linking are listed in Table 5.1. The value of $Q_{e,i}$ was calculated using equation 5.1 and analysed by several isotherm models. Estimates of the error contributions to $Q_{e,i}$ ($\Delta Q_{e,i}$) that relate to uncertainties in the solvent concentration ($C_{o,i}$ and $C_{e,i}$) and the mass error of the sorbent (Δm) were obtained by differential error analysis of equation 5.1. The adsorption isotherm of a solid-solution system describes the relationship between the bound and unbound adsorbate (W or E) at constant temperature and at equilibrium conditions. The corresponding adsorption isotherms for the uptake of water and ethanol in W-E binary solutions are illustrated in Figure 5.1. The isotherm parameters for the starch-based systems are listed in Tables 5.2 and 5.3, according to the best-fit results for the Langmuir, Freundlich and Sips models. The isotherm results show that starch-based materials display greater overall uptake of water over ethanol, in agreement with the swelling results in Table 5.1. The greater adsorptive affinity of water with cross-linked starch parallels the greater Q_m values relative to the parameters for ethanol. The Langmuir and Freundlich models show reduced R^2 values further illustrating that these isotherms show poorer agreement with the experimental results (Appendix A5, Figure A5); whereas, the Sips model provides a better description of the isotherm since the R^2 values are closer to unity.

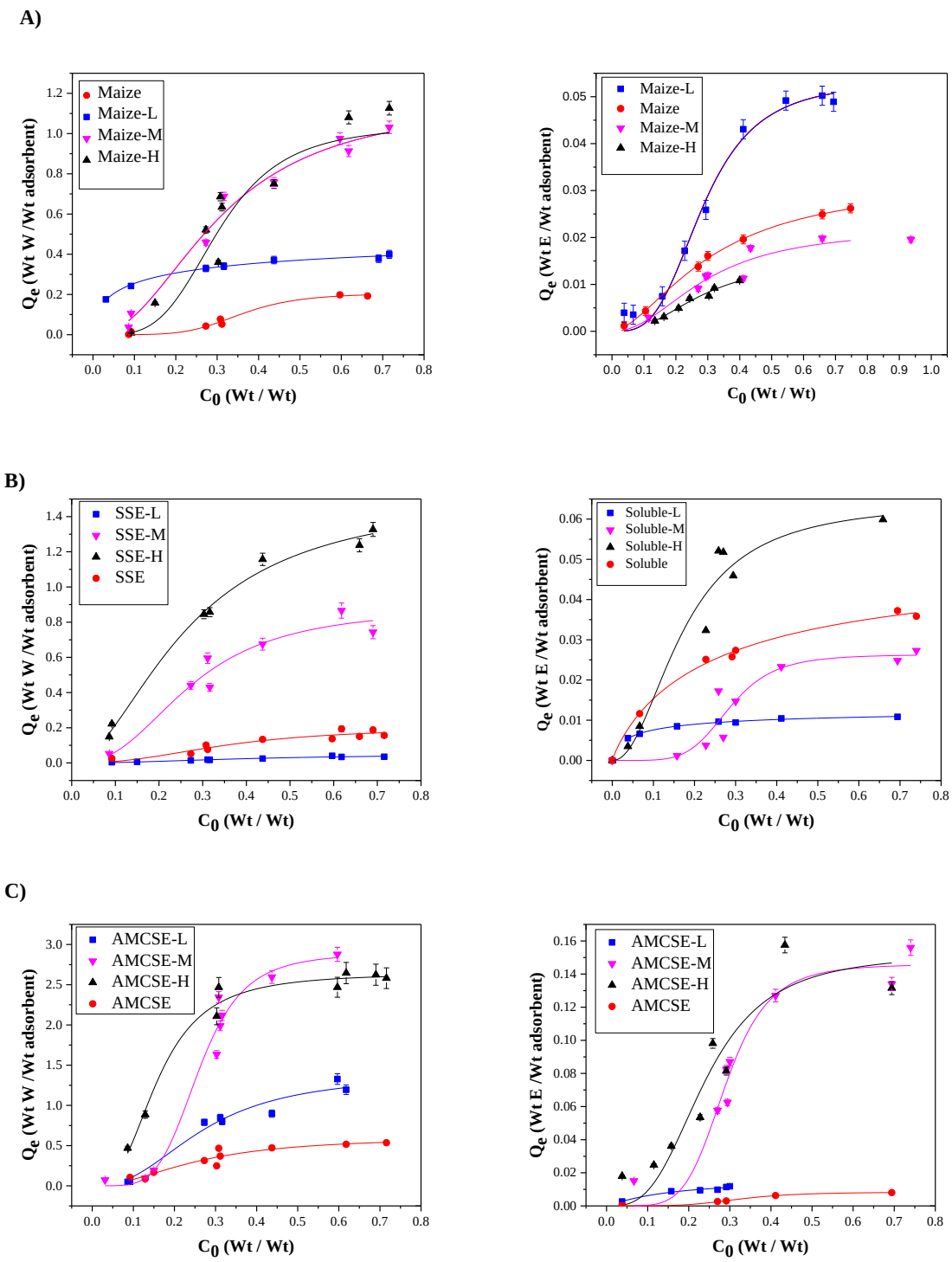

Figure 5.1 Adsorption isotherms for the uptake of water (W) and ethanol (E) A) MSE and its cross-linked polymers B) SSE and its cross-linked polymers and C) AMCSE and its cross-linked polymers in binary W-E solutions at 295 K. The error bars for the corresponding isotherm results denote the error contributions to equation 5.1 according concentration and mass.

A comparison of Q_m values of AMCE, SSE and MSE reveals that the cross-linked forms of starch show variable adsorption capacities for water. The greater uptake of water over ethanol can be related to differences in the physicochemical properties of each solvent. The greater polarity and smaller molecular size of water enables more efficient interaction with the polar hydroxyl groups of starch. In the case of cross-linked starch materials, the accessibility of hydroxyl groups within the polysaccharide framework varies due to steric effects and the net loss of one –OH group per cross-linked formed via Williamson etherification. Cross-linking of starch results in the formation of a network structure between adjacent starch polymer units (*cf.* Scheme 2 in Ref. 26). In the case of cellulose[14] and chitosan[34] materials, cross-linking results in a pillaring effect, as evidenced by the variable textural properties of pristine and modified materials. Evidence of changes in surface area and pore structure properties was observed by the variable dye uptake for *p*-nitrophenol and phenolphthalein in such systems at variable cross-linking. Adsorption isotherms of W-E binary solvent systems can be used to determine the relative uptake levels of each respective solvent component (W and E) and to estimate the relative solvent selectivity of the adsorbent systems. According to Figure 5.1 and Table 5.2, the uptake capacity (Q_m) of AMCE-H displays the highest value for water and ethanol. The Q_m values for the starch materials are listed in descending order for W and E, as follows: AMCE-H > SSE-H > MSE-H. According to the value of the heterogeneity parameter (n_s) in Tables 5.2 and 5.3, the surface of the starch materials is heterogeneous in nature since n_s deviates from unity overall. There are two factors that contribute to the heterogeneity of the starch surface: cross-linking effects and the disordered arrangement of the polysaccharide network due to branching or folding of the biopolymer. By contrast, cellulose is a more rigid polysaccharide with a linear morphology where the n_s values lie closer to unity for water uptake (*cf.* Table 5 in Ref. 26). Thus, cross-linking of starch contributes to an increase in the surface heterogeneity of starch materials for several reasons outlined below. The hydroxypropyl cross-linker contributes to surface heterogeneities[35] as follows: *i*) altering the morphology of the polysaccharide due to steric effects, *ii*) the formation of micropore domains, and *iii*) alteration of the HLB of the starch network due to an overall reduction in the overall number of –OH groups and iv) non-homogenous distribution of cross-linker in starch or cellulose. These heterogeneities affect the sorptive uptake and the solvent-selective uptake as compared with unmodified starch, according to the nature of each solvent (W or E) and the adsorptive interactions that govern the adsorption process.

In Tables 5.2 and 5.3, notable differences in the value of Q_m for each solvent (W or E) reveal that the starch materials show preferential uptake toward water over ethanol in binary mixtures. Molecular selective adsorption relies on differences in the physicochemical properties of the adsorbate (e.g., polarity) in order to achieve adsorptive fractionation of mixtures. The molecular selectivity of starch-based materials in W-E mixtures can be understood according to variation in the hydrophile-lipophile balance (HLB) of the adsorbent, according to the level of cross-linking and the type of starch biopolymer. The relative molecular selectivity ($R_{selectivity}$) value was calculated using equation 5.6.

$$R_{selectivity} = \frac{Q_{m(Water)}}{Q_{m(Ethanol)}} \qquad \text{Equation 5.6}$$

Table 5.2 Sips isotherm parameters for the uptake of ethanol at 295 K with variants of starch at variable levels of cross-linker content.

Starch ID Code	**K_s (g/g)**	**n_s**	**Q_m (g/g)**	***R^2***
AMCSE	3.08 ± 0.22	3.08 ± 1.4	0.0084 ±0.0025	0.803
AMCSE-L	4.14 ± 0.67	3.11 ± 1.3	0.0142 ± 0.0042	0.983
AMCSE-M	3.45 ± 0.13	5.51 ± 2.3	0.145 ± 0.0098	0.949
AMCSE-H	3.47 ± 2.24	1.14 ± 0.54	0.152 ± 0.026	0.884
SSE	3.91 ± 1.38	0.895 ±0.15	0.0509 ± 0.0079	0.993
SSE-L	15.4 ± 4.55	0.668 ±0.11	0.0134 ± 0.0011	0.988
SSE-M	3.49 ± 0.30	5.28 ± 2.6	0.0263 ± 0.0030	0.862
SSE-H	5.79 ± 1.1	2.11 ± 0.69	0.0643 ± 0.0089	0.943
MSE	3.21 ± 0.17	1.68 ± 0.10	0.0321 ±0.0012	0.999
MSE-L	3.50 ± 0.21	3.36 ± 0.60	0.0532 ±0.0031	0.984
MSE-M	3.39 ± 0.66	2.13 ± 0.87	0.022 ± 0.0037	0.869
MSE-H	3.59 ± 0.92	2.43 ± 0.63	0.0151 ± 0.004	0.966

Table 5.3 Sips isotherm parameters for the uptake of water at 295 K with variants of starch at variable levels of cross-linker content.

Starch ID Code	K_s (g/g)	n_s	Q_m (g/g)	R^2
AMCSE	3.91 ± 0.92	2.02 ± 0.66	0.608 ± 0.11	0.871
AMCSE-L	3.76 ± 0.57	2.40 ± 0.80	1.38 ± 0.20	0.952
AMCSEM	6.25 ± 0.45	2.76± 0.43	2.64 ± 0.093	0.977
AMCSE-H	3.84 ± 0.22	4.79 ± 0.22	2.89 ± 0.20	0.969
SSE	2.81 ± 1.0	2.44 ± 1.7	0.202 ± 0.075	0.848
SSE-L	2.40 ± 0.87	2.06 ± 0.74	0.0504 ± 0.015	0.944
SSE-M	3.64 ± 0.58	2.56 ± 1.4	0.885 ± 0.16	0.909
SSE-H	3.79 ± 0.41	1.85 ± 0.23	1.52 ± 0.11	0.978
MSE	2.78 ± 0.42	3.86 ± 1.2	0.206 ± 0.030	0.974
MSE-L	8.14 ± 5.2	0.555 ± 0.11	0.540 ± 0.087	0.993
MSE-M	3.26 ± 0.48	2.17 ± 0.51	1.16 ± 0.14	0.977
MSE-H	3.17 ± 0.32	2.76 ± 0.66	1.24 ± 0.12	0.974

The $R_{selectivity}$ values for starch materials were estimated using the Q_m values for water and ethanol from Tables 5.2 and 5.3. The value of the $R_{selectivity}$ varied according to the level of cross-linking and the nature of the starch biopolymer. Pristine and cross-linked starch materials show greater selective uptake behaviour toward water over ethanol, especially amylose-based materials where greater water selectivity ($R_{selectivity}$ = 4-80) was noted, except for SSE materials. SSE-L displays a maximum $R_{selectivity}$ value for ethanol. The highest $R_{selectivity}$ value was observed for MSE-H. By contrast, cellulose and its cross-linked forms show the lowest $R_{selectivity}$ value (*ca*. 1-2) relative to the starch-based materials. The $R_{selectivity}$ values in Tables 5.2 and 5.3 for starch-based adsorbents are among the highest reported in the open literature.

Table 5.4 $R_{selectivity}$ of water over ethanol for variable adsorbents.

Adsorbent	Selectivity	C_0	Ref
Canola meal	8-20	4-100 wt% (water)	36
Corn meal	0.6	15-75 wt% (Ethanol)	37
Protein-extracted canola meal	1.9	80-95 wt% (Ethanol)	38
Molecular Sieves	77.97	80-95 wt% (Ethanol)	38

The foregoing literature results, as shown in Table 5.4, provide indirect support for the role of surface accessibility of polar functional groups in the fractionation of W-E mixtures, along with the variable textural properties and surface chemistry of polysaccharides due to cross-linking effects.[26] In the case of cellulose with variable cross-linking, evidence of a reduction in the surface accessible hydroxyl groups and pillaring effects of the fibril structure was shown by variable decolourization efficacy of phenolphthalein at alkaline conditions (*cf.* Figure 6 in Ref.14).

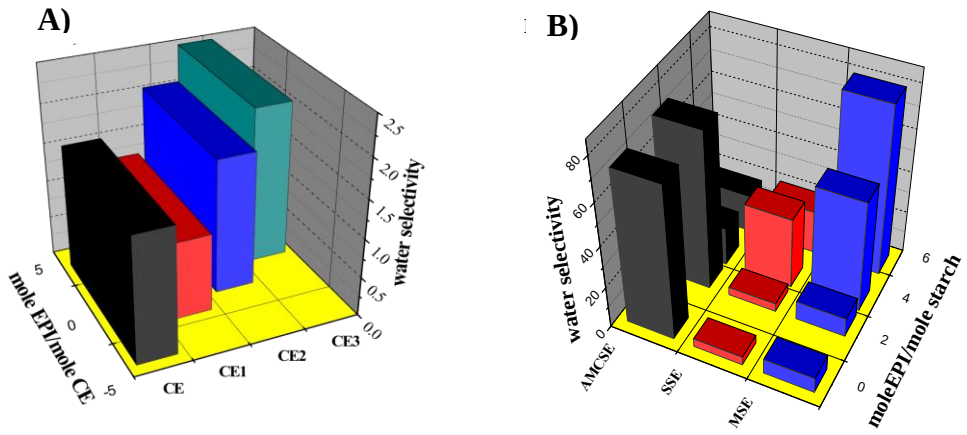

Figure 5.2 Equilibrium solvent selectivity ratios for cellulose and starch-based adsorbents in binary W-E systems at 295 K: A) native cellulose (CE) and its cross-linked forms, B) starch and its cross-linked forms. The sample ID code is defined in Table 4.1 (0: native biopolymer, 1: low, 2: medium and 3: high).

The equilibrium swelling properties of starch materials are a qualitative indicator of solvent uptake capacity of single component solvents at ambient conditions. Although the swelling parameters relate to the combined effects from adsorption and absorption (sorption), swelling enables solvent to permeate into polymer networks and membrane microstructures.[39] Biopolymer materials such as starch undergo swelling through expansion of the pore network due to the inclusion of solvent via physical interactions. Swelling depends on various factors including the pH of solution, ionic strength, temperature and so forth.[40-42] Cross-linked starch shows greater uptake of water over ethanol (*cf.* Table 5.1), along with the isotherm results in Figure 5.1, Tables 5.2 and 5.3. Furthermore, amylose-based polymers such as AMCSE showed the highest adsorption capacity for water, while SSE and SSE-L materials displayed greater uptake of ethanol over water.

Differences in the preferred uptake of water over ethanol for starch and its modified forms are illustrated in Figure 5.2. The observed trends in $R_{selectivity}$ relate to the effects of cross-linking due to surface heterogeneities (see below) that favour uptake of solvent (W or E) according to the relative accessibility of polar functional groups and textural properties of the adsorbent.[43] Increasing the cross-linker content resulted in an increase in the water uptake selectivity due to steric or pillaring effects, surface accessibility of polar functional groups, and textural properties (*cf.* Scheme 2 of Ref. 26). These factors contribute to the swelling and solvent selectivity of starch biopolymers; however, a detailed understanding of the role of cross-linking on the structure and function of these materials is the subject of ongoing and future studies. The greater uptake selectivity of water over ethanol for starch and its modified forms observed in this study finds support from other studies related to solvent selective uptake.[43,44] The physicochemical properties of the solvent such as the relative size and polarity of water and ethanol are key factors that influence the uptake of water over ethanol observed for starch-based materials. The offset in molar volume (V_m) of water (V_m=18 cm^3/mol) and ethanol (V_m=58.0 cm^3/mol) and relative polarity (H_2O: 16 D and C_2H_5OH: 8.8 D)[15] contribute to the observed fractionation of solvent species. The solvent physicochemical properties influence the variable kinetic and thermodynamic uptake properties of starch materials. The foregoing is consistent with the effects of cross-linking on the textural properties and HLB of the adsorbent materials, according to the observed $R_{selectivity}$ for starch- and cellulose-based adsorbents.

In general, starch shows greater uptake selectivity toward water over ethanol according to the greater accessibility of polar (-OH) groups in starch. Cellulose materials have reduced

accessibility of polar groups due to more extensive intra- and inter-molecular hydrogen bonding, owing to their fibril morphology and lower water solubility. Thus, the smaller solvents like water with greater polarity afford more stable binding interactions compared with ethanol over a range of surface accessible donor and acceptor groups at the polysaccharide surface. The variable $R_{selectivity}$ values for starch with different cross-linker content, along with variable amylopectin *vs.* amylose content account for a range of HLB in such starch materials.[44] Cross-linkers alter the HLB by introducing new functionalities and also increasing the carbon chain of the materials and amylopectin *vs.* amylose due to the variable lipid content effect on HLB. The stabilizing effect of hydrogen bonding with water and ethanol differs according to the level of cooperative interactions due to the structured nature of each solvent.[45] Thus, the role of molecular size, polarity, and adsorption site accessibility is highlighted in a study of the adsorption of apolar organics and water molecules using polysaccharides where the separation of smaller organic molecules, such as urea with molecular dimensions close to water, represent challenges in molecular selectivity.[46,47]

The relevance of polysaccharide structure on its kinetic adsorption properties is evidenced by the uptake of the adsorbate via three successive steps: *i*) transport of molecules from the bulk of the solution to the exterior surface of adsorbent particles through a boundary layer of two phases; *ii*) diffusion processes that relate to the transport of the adsorbate to the interior active sites of the adsorbent (intraparticle or internal diffusion); and *iii*) adsorption at the active sites within the micropore network of adsorbent. The specific adsorption capacity is often controlled by the third step and strongly relates to the role of pore structure and surface functionalization.[26] Crini[13] has suggested that polysaccharides display rapid adsorption kinetics due to the favourable solvation of the polar groups, in agreement with the swelling results for water over ethanol summarized in Table 5.1. The variable branching of amylose *vs.* amylopectin and its cross-linked forms (*cf*. Figure 5.3) influences the kinetics of adsorption in the above steps in agreement with the observed solvent selectivity in such starch materials.

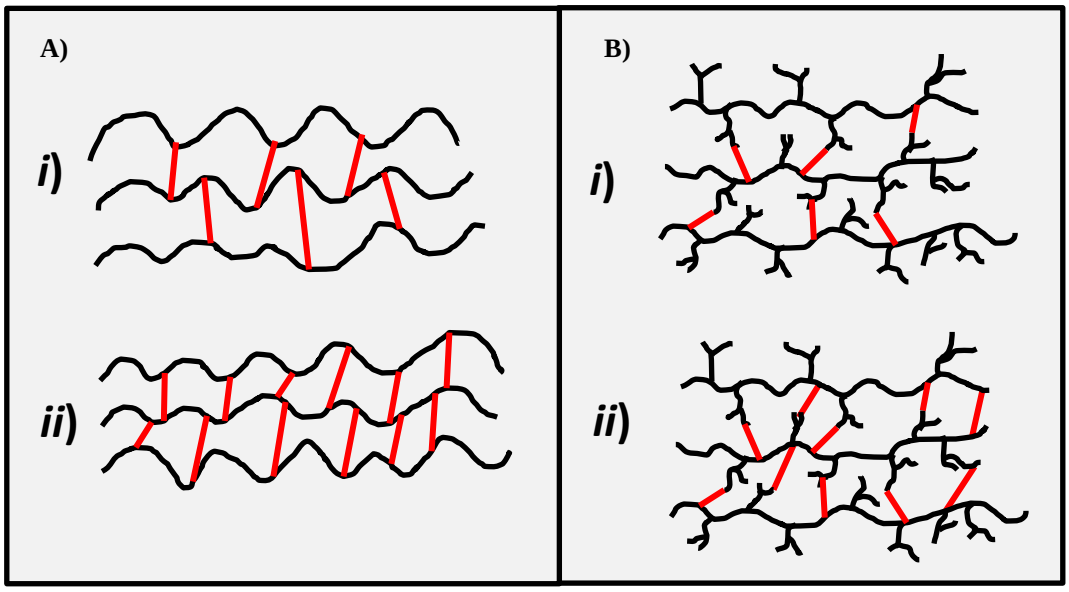

Figure 5.3 Conceptualized molecular structure of cross-linked polysaccharide materials: A) amylose, B) amylopectin, where *i*) denotes low cross-linking and *ii*) denotes higher cross-linking. The red bar represents the cross-linker and the black line is the polysaccharide backbone. The hydroxyl groups are not explicitly shown and the diagrams are not drawn to scale.

Among the various polysaccharides investigated, AMCSE showed notably higher adsorption performance and selectivity relative to SSE and MSE. Amylose is a linear starch based on α-1→4 glycosidic bonds with a molecular weight *ca.* 10^5–10^6 *amu* and a moderate degree of polymerization (n=600).[48] Amylopectin is a branched form of starch containing α-1→4 and α-1→6 glycosidic bonds with a relatively high molecular weight (*ca.* 10^7–10^9 *amu*). The linear and branched structural variants of starch influence the physical and biological properties of these materials that parallel the water and ethanol uptake properties of starch.[49] Highly branched amylopectin *vs.* linear starch variants influence the relative surface accessibility of the hydroxyl groups and their adsorptive interactions. The third step in the kinetic process of adsorption described above is influenced by cross-linking and the steric accessibility of polar functional groups; however, the structural details of such complex polysaccharides is currently lacking and require further dedicated studies. The fractionation properties of cellulose were reported for alkyl carboxylate anions and their mixtures in aqueous solution by Udoetok *et al.*[14] The fractionation

behaviour of cellulose paralleled the surface accessibility of polar functional groups since an alteration of the HLB and textural properties of the biopolymer was related to the level of cross-linking. Similarly, the high selectivity of Carboxymethylcellulose, and other polysaccharide polyelectrolyte membrane materials, for the dehydration of many aqueous/alcohol mixtures (under pervaporation conditions) is readily understood in terms of the HLB parameter, which is used to describe the selectivity of water or ethanol.[50] The findings presented by Reineke *et al.*[50] parallel the observed trends in solvent selectivity in this study. This is due to the effects of solvent size/polarity and the relative HLB of starch biopolymers and their modified forms, which is in agreement with the cross-linking effects illustrated in Figure 5.3.

5.5 Conclusion

^{1}H-NMR spectroscopy is a versatile and rapid screening technique for the estimation of solution composition in W-E binary mixtures for the study of fractionation in W-E binary mixtures using starch and its cross-linked forms. Starch-based materials show preferential uptake of water (2.68 g/g) over ethanol (0.152 g/g) in binary W-E solutions where selective solvent fractionation occurs at different levels of cross-linking using epichlorohydrin with starch- and cellulose-based materials. A cross-linked form of high amylose (AMCSE-H) starch revealed the highest uptake of ethanol and water when compared with starch materials such as MSE and SSE. The variable uptake selectivity of water over ethanol ($R_{selectivity}$) was attributed to the unique structure and textural properties of starch and its modified forms as shown in Figure 5.2. Overall, starch-based materials display greater selectivity ($R_{selectivity} \approx 80$) for water over ethanol. This research contributes significantly to the biofuels sector and sustainable energy production through the development of adsorbents with tunable solvent fractionation properties according to the nature of the polysaccharide and modification via a facile cross-linking method. Further studies are underway to develop a more detailed understanding of the structure-activity relationship related to the adsorption properties of these starch-based biopolymers.

5.6 References

1. Lu, L.; Shao, Q.; Huang, L.; Lu, X. *Fluid Phase Equilibria.* **2007,** *261,* 191–198.
2. Mccreadyan, R. M.; Hassid, W. Z. *J. Am. Chem. Soc.* **1943,** *65,* 1154-1157.
3. Magalad, V. T.; Gokavi, G. S.; Nadagouda, M. N.; Aminabhavi, T. M. *J. Phys. Chem. C* **2011,** *115,* 14731–14744.
4. Wang, Y.; Gong, Ch.; Sun, J.; Gao, H.; Zheng, S.; Xu, Sh. *Biores. Technol.* **2010,** *101,* 6170–6176.
5. Mohamed, M. H.; Wilson, L. D., Headley, J. V.; Peru, K. M. *Energy Fuels* **2015,** *29(6),* 3591–3600.
6. Jiang, L. Y.; Wang, Y.; Chung, T-S.; Qiao, X. Y.; Lai, J-Y. *Prog. Polym. Sci.* **2009,** *34,* 1135–1160.
7. Wilson, L. D.; Mohamed, M. H.; Headley, J. V. *Rev. Environ. Health.* **2014,** *29,* 5-8.
8. Ivanova, E.; Damgaliev, D.; Kostova, M. *J. Chem. Technol. Metall.* **2009,** *44,* 267-274.
9. Al-Asheh, S.; Banat, F.; Al-Lagtah, N. *Chem. Eng. Res. Des.* **2004,** *82(A7),* 855–864.
10. Kang, Q.; Huybrechts, J.; Bruggen, B. V.; Baeyens, J.; Tan, T.; Dewil, R. *Sep. Purif. Technol*. **2014,** *136,* 144–149.
11. Wu, P.; Gao, H.; Sun, J.; Ma, T.; Liu, Y.; Wang, F. *Biores. Technol.* **2012,** *107,* 437–443.
12. Hsu, S-H.; Hsu, W-C.; Chung, T-W.; Liao, C-C. *J. Taiwan Inst. Chem. Eng.* **2013,** *44,* 952–956.
13. Crini, G. *Prog. Polym. Sci.* **2005,** *30,* 38–70.
14. Udoetok, I. A.; Dimmick, R. M.; Wilson, L. D.; Headley, J. V. *Carbohydr. Polym.* **2016,** *136,* 329-340.
15. Dehabadi, L.; Wilson, L. D. *Energy Fuels* **2015,** *29,* 6512−6521.
16. Shukri, R.; Zhu, L.; Seib, P. A.; Maningat, C.; Shi, Y-C. *Bioact. Carbohydr. Dietary Fibre*. **2015,** *5,* 1-9.
17. Mostafa, K. M.; Samarkandy, A. R.; El-Sanabary, A. A. *Carbohydr. Polym.* **2011,** *86,* 491–498.
18. Ernest, R. R.; Villanova, P. Production of low-ethanol beverages by membrane extraction. U.S. Patent 4,306,884, Dec.22, **1981.**
19. Gubicza, L.; Kabiri-Badr, A.; Keoves, E.; Belafi-Bako, K. *J. Biotech.* **2000,** *84,*193–196.

20. Ladisch, M. R.; Voloch, M.; Hong, J.; Bienkowski, P.; Tsao, G. T. *Ind. Eng. Chem. Process Des. Dev.* **1984,** *23(3),* 437–443.
21. Chang, H. X.; Yuan, H. T.; Zeng, A. *Chem. Eng. Process. Process Intensif.* **2006,** *45,* 747-754.
22. Chang, H. X.; Yuan, T. H.; Zeng, A. *Ind. Eng. Chem. Res.* **2006,** *45,* 3916-3921.
23. Chang, H.; Yuan, X.; T. H.; Zeng, A. *Chem. Eng. Technol.* **2006,** *29,* 454-461.
24. Li, G.; Bai, P. *Ind. Eng.Chem. Res.* **2012,** *51,* 2723−2729.
25. Fathieh, F.; Dehabadi, L.; Wilson, D. L.; Besant, R.; Evitts, R.; Simonson, C. *ACS Sustainable Chem. Eng.* **2016,** *4(3),* 1262–1273
26. Dehabadi, L.; Wilson, L. D. *Carbohydr. Polym.* **2014,** *113,* 471- 479.
27. Ashish, P.; Khanderao, J.; Deelip, D. *Int. J. Pharm. Pharm. Sci.* **2013,** *5,* 391-397.
28. Foo, K. Y.; Hameed, B. H. *Chem. Eng. J.* **2010,** *156,* 2-10.
29. Jiang, Y.; Huang, C.; Pang, H.; Liao, B. *Huaxue Tongbao Sci.* **2008,** *71(12),* 891-899.
30. Morin-Crini, N.; Crini, G. *Prog. Polym. Sci.* **2013,** *38,* 344-368.
31. Lee, B.; D'Alessio, M.; Vissing, H.; Ramirez, F.; Steinmann, B.; Superti-Furga, A. *Am. J. Hum. Genet.* **1991,** *48(3),* 511-7.
32. Ratanapariyanuch, K.; Shen, J.; Jia, Y.; Tyler, R. T.; Shim, Y. Y.; Reaney, M. J. T. *J. Agric. Food. Chem.* **2011,** *59,* 10454-10460.
33. Schmitt, P.; Griswold, M. A.; Jakob, P. M.; Kotas, M.; Gulani, V.; Flentje, M.; Haase, A. *Magnet. Reson. Med.* **2004,** *51,* 661– 667.
34. Mohamed, M. H.; Udoetok, I. A.; Dimmick, R. M.; Wilson, L. D.; Headley, J. V. *RSC Adv.* **2015,** *5,* 82065-82077.
35. Singh, J.; Kaur, L.; McCarthy, O. J. *Food Hydrocoll.* **2007,** *21,* 1–22.
36. Ranjbar, Z.; Sun, N.; Niu, C. H.; Dalai, A. K. *CSBE/SCGAB* **2013,** Annual Conference, Saskatoon, Saskatchewan, July 7−10, 2013, Paper No. CSBE13-108, 1−10.
37. Chang, H.; Yuan, X.; Zeng, H. T. A. *Ind. Eng. Chem. Res.* **2006,** *45,* 3916-3921.
38. Ranjbar, Z.; Tajallipour, M.; Niu, C. H.; Dalai, A. K. *Ind. Eng. Chem. Res.* **2013,** *52(40),* 14429–14440.
39. Ying, W.; Kumar, R.; Herzberg, M.; Kasher, R. *Environ. Sci. Technol.* **2015,** *49,* 6815−6822.
40. Mandala, I. G.; Bayas, E. *Food Hydrocoll.* **2004,** *18,* 191–201.
41. Blazek, J.; Copeland, L. *Carbohydr. Polym.* **2008,** *71,* 380–387.
42. Démé1, F.; Peuvrel-Disdier, E.; Vergnes, B. *Ind. Crops Prod.* **2015,** *70,* 149–157.

43. Liu, Y-W.; Tang, T.; Chung, T-W.; Huang, C.; Lin, Y-S. *J. Chem. Eng. Data* **2010,** *55,* 5807–5811.
44. Wang, K-S.; Liao, C-C.; Chu, R. Q.; Chung, T-W. *J. Chem. Eng. Data* **2010,** *55,* 3334–3337.
45. Ladisch, M. R.; Voloch, M.; Hong, J.; Bienkowski, P.; Tsao, G. T. *Ind. Eng. Chem. Process Des. Dev.* **1984,** *23(3),* 437–443.
46. Westgate, P. J.; Ladisch, M. R. *Ind. Eng. Chem. Res.* **1993,** *32,* 1676-1680.
47. Xue, C.; Wilson, L. D. *Carbohydr. Polym.* **2016**, *135(1),* 180-186.
48. Ho, Y. S.; Porter, J. F.; Mckay, G. *Water Air Soil Pollut.* **2002,** *141,* 1–33.
49. Foo, K.Y.; Hameed, B. H. *J. Hazard. Mater.* **2009,** *172(2-3),* 523-31.
50. Reineke, C. E.; Jagodzinski, J. A.; Denslow, K. R. Hyghly *J. Membr. Sci.* **1987,** *32,* 207-221.

CHAPTER 6

MANUSCRIPT 4: Miscanthus biomass for the sustainable fractionation of ethanol-water mixtures

Leila Dehabadi, Mohammad H. Mahaninia, Majid Soleimani, and Lee D. Wilson*

Description

This research relates to the technological importance of biomass for the fractionation of binary solvent mixtures containing water and ethanol, as in the case of biofuels and beverage production. Chapters 4 and 5 report on the utility of qNMR as an analytical tool for quantifying the relative solvent uptake of cellulose and starch biopolymer systems. The results from Chapters 4 and 5 provided insight on the differential uptake of water and ethanol according to the nature of the biopolymer and the synthetic modification. In this study, an industrially relevant biomass material (Miscanthus) was used as an adsorbent containing different biopolymer compositions of cellulose and hemicellulose depending on the nature of the pre-treatment. The adsorption properties of this material toward uptake of water or ethanol in binary mixtures were analysed. Also, Miscanthus samples with physical treatment (different particle sizes) and chemical treatment were prepared and characterized. Quantitative ^{1}H-NMR spectroscopy was used for measurement of water or ethanol composition, before and after adsorption in binary mixtures. The adsorptive solvent selectivity ratios of these materials at equilibrium were estimated using the maximum adsorption capacity (Q_m) for water and ethanol from the adsorption isotherm model. The maximum adsorption capacities of water Q_m (W) and ethanol Q_m (E) fractions, determined using the best-fit Sips model, are listed in parentheses: raw Miscanthus biomass (Q_m (W) =8.93 and Q_m (E) =4.15) and pretreated Miscanthus biomass (Q_m (W) =4.73 and Q_m (E) =3.22, g.g-1). Finally, the regeneration of these materials was investigated to demonstrate their usability and durability. The relative uptake (W and E) for raw and pretreated Miscanthus decreased by *ca.* 12% after four adsorption-desorption cycles.

Authors' Contributions

The project was conceived by the supervisor (L. D. Wilson). The experimental work and data analysis was carried out by L. Dehabadhi, while the chemical treatment was done by Dr. Majid Soleimani from the Department of Chemical & Biological Engineering. L. Dehabadi prepared the

first draft with assistance from M. H. Mahaninia while subsequent editing was done by the supervisor, Dr. Wilson, and L. Dehabadi.

Relation of Manuscript 4 to Overall Objective of this Project

This study relates to an understanding of biopolymer components and their respective roles in adsorptive properties in the presence of binary solvents containing water and ethanol. The relationship of biomass treatment to the removal and/or enrichment of various biopolymer components provide insight on the relative role of such components in the overall adsorptive process for the removal of water and ethanol in binary mixtures. This work connects to the overall objective of this project as outlined in section 2.4 in Chapter 2. These objectives include evaluation of the relative water selectivity behaviour of biomaterials using quantitative NMR method and investigating the potential utility of native and treated biomass components of Miscanthus for the fractionation of water and ethanol mixtures. An outcome of this study relates to the utility of biomass adsorbents, their reusability, and an understanding of the physical and chemical treatment processes that enhance adsorption properties.

6. Miscanthus biomass for the sustainable fractionation of ethanol-water mixtures

Leila Dehabadi[1], Mohammad H. Mahaninia[1], Majid Soleimani[2], and Lee D. Wilson[1*]

[1]Department of Chemistry, University of Saskatchewan, 110 Science Place, Saskatoon, SK, Canada S7N 5C9

[2]Department of Chemical and Biological Engineering, University of Saskatchewan, 57 Campus Drive, Saskatoon, SK, Canada S7N 5A9

*Corresponding Author

Supplementary Information (Appendix A, Chapter 6)

Graphical Abstract

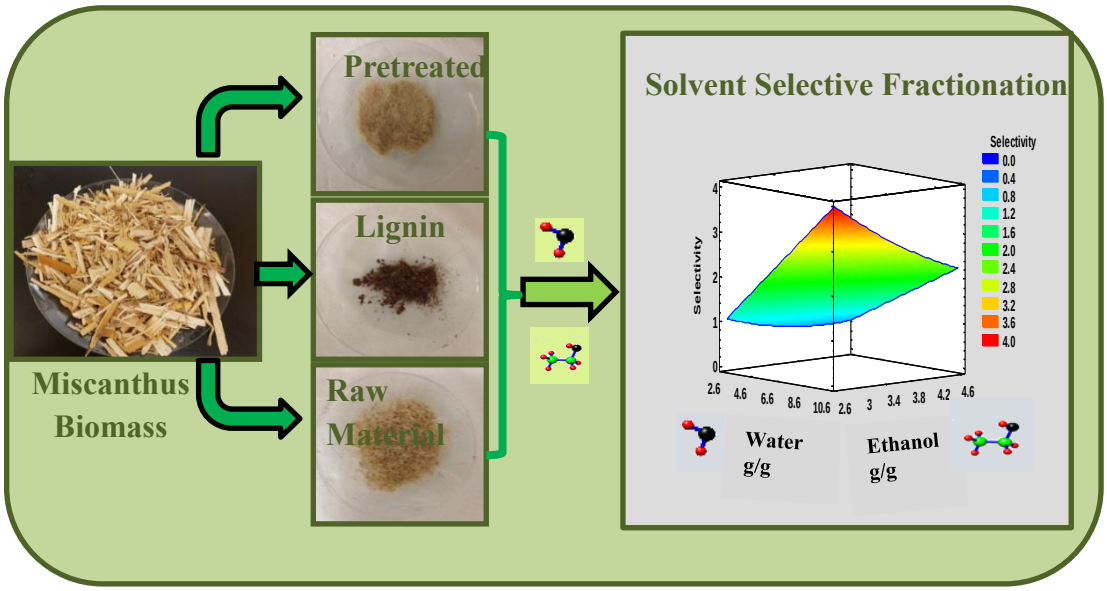

Research Highlights

- Miscanthus was modified by mechanical milling to vary the average particle size.
- The relative role of biomass and its respective components was evaluated as an adsorbent for the removal of water and ethanol from binary mixtures.
- Greater uptake of water over ethanol was observed for raw Miscanthus compared to chemically pretreated biomass.
- Regeneration and reusability of biomass using swelling tests was shown over four cycles.

6.1 Abstract

Miscanthus is a rich source of lignocellulosic biomass with low mineral content suitable for applications that range from biofuel production to value-added biomass-derived products such as a sustainable biosorbent. Herein, the utility of Miscanthus and its modified forms were used for the fractionation of water (W) and ethanol (E) mixtures using an *in situ* analytical method, referred to as quantitative NMR (qNMR) spectroscopy. Miscanthus was pretreated by hydrolysis and subsequent grinding to yield materials with variable biopolymer contents (cellulose and lignin) and particle sizes. The Miscanthus materials were evaluated as sorbents in binary water-ethanol (W-E) mixtures. The maximum biomass adsorption capacities (Q_m; $g.g^{-1}$) with water Q_m (W) and ethanol Q_m (E) fractions were determined by the best-fit Sips model parameters listed in parentheses: raw Miscanthus biomass (Q_m (W) =8.93 and Q_m (E) =4.15) and pretreated Miscanthus biomass (Q_m (W) =4.73 and Q_m (E) =3.22, $g.g^{-1}$). The fractionation properties of Miscanthus and its biopolymer constituents revealed a molecular selectivity [$R_{selectivity}= Q_m(W)/Q_m(E)$] between W and E. The $R_{selectivity}$ values are given in parentheses, as follows: untreated Miscanthus (3:1); pretreated Miscanthus (1.5:1); and lignin (1:5.4). The pretreated Miscanthus was prepared by acid and base hydrolysis for the removal of hemicellulose and lignin, respectively, leading to cellulose enrichment. The raw and pretreated Miscanthus have preferential water uptake properties that relate to their relative biopolymer composition such as cellulose. To test the reusability and regeneration of Miscanthus, the biosorbent was tested over four adsorption-desorption cycles. This work contributes to a greater understanding of chemical treatment effects on biomass and evaluation of the adsorptive contributions of biopolymer components for the fractionation of water-ethanol mixtures.

6.2 Introduction

Lignocellulosic biomass is an abundant, non-food, and inexpensive plant-based biomass that represents a renewable and sustainable source of cellulosic fibres suitable for the production of biofuels.[1] Among the commonly available biomass sources, Miscanthus has attracted great attention for the large-scale industrial production of bioethanol due to its abundant carbohydrate content.[1] A key challenge involving ethanol production for food and fuels is the ability to carry out efficient and low-cost separation of produced ethanol from water-rich fermentation media.[2–6] The traditional method of solvent separation by conventional distillation is energy intensive and requires specialized infrastructure that incurs high operating costs.[7] The recovery cost of ethanol by conventional distillation was estimated at *ca.* 50% of the caloric energy value of the produced ethanol. Thus, alternative and more sustainable strategies are required to address the fractionation of water and ethanol such as solid-phase adsorption processes. Adsorption phenomena are important in many natural, physical, and biological processes where phase separation occurs between the bulk and the adsorbent surface.[8–11] Differences in the adsorptive affinity of liquid phase components with an adsorbent in solid-liquid adsorption yields fractionation of mixtures. Studies concerning the research and development of cost-effective biosorbents for the fractionation of ethanol or other types of alcohols in water are known.[7, 12-14] Ranjbara *et al.*[13] report the use of canola meal for selective water (W) uptake in water-ethanol (W-E) mixtures, where a columnar material was developed for drying ethanol (E) with variable water content (4-90 %).[13] Two recent studies of polysaccharides and their modified forms report their fractionation efficacy in W-E binary mixtures, where the W/E solvent selectivity ($R_{selectivity}$) varied from 1.10 to 2.03 for cellulose materials.[14] By contrast, greater $R_{selectivity}$ (3.8 to 80) was reported for starch-based materials.[7] The current study was motivated by the unique properties of Miscanthus and its promising potential as a sustainable biosorbent alternative for the fractionation of W-E mixtures.[15] Miscanthus contains three major biopolymer components with variable composition: cellulose (40 to 60 wt %), hemicellulose (20 to 40 wt %) and lignin (10 to 30 wt %). It can be inferred that the adsorption properties of such biopolymers are variable in nature based on their structure and physicochemical properties.[16] The structural complexity of Miscanthus and its biopolymer components and the structure-function relationship to adsorption properties are poorly understood at the present time. Thus this research aims to contribute a bridge the knowledge gaps concerning the structure-function relationship to adsorption properties of Miscanthus and its modified forms in W-E

mixtures. This study will contribute significantly to the research and development of Miscanthus biomass as a sustainable alternative for the industrial fractionation of mixtures related to production of beverages, food, and fuels. Knowledge of the biopolymer components (cellulose, hemicellulose, and lignin) of Miscanthus and their roles can contribute to an understanding of the above knowledge gaps, especially for the case of adsorption properties in binary mixtures containing water-ethanol (W-E).

Surface chemistry and textural properties are posited to play important roles in the adsorption process of biomass such as Miscanthus.[17] Herein, we report on the adsorptive properties of Raw Miscanthus (RM) and Pretreated Miscanthus (PTM) in binary W−E mixtures using a quantitative NMR spectroscopy (qNMR) method. Miscanthus was chemically pretreated to remove biopolymers such as hemicellulose and lignin to afford biomass with modified composition and particle size. This study contributes to an understanding of Miscanthus biomass for adsorptive fractionation of W-E binary mixtures in several ways: i) establish the utility of the qNMR method for *in situ* estimation of biomass fractionation of W-E mixtures; ii) elucidate the effect of adsorbent particle size and chemical treatment on the adsorption properties; and iii) to evaluate the sorptive contributions of biopolymer components toward water and ethanol. This research contributes to a greater understanding of biopolymer components and pretreatment strategies for biomass sorbents and their utility for the fractionation of binary W-E solvent systems.[18]

6.3 Experimental

6.3.1 Materials

Miscanthus biomass with variable particle sizes was prepared by Richardson Milling Ltd., Martensville, SK, Canada. The raw biomass (Miscanthus) was cleaned by using a sieve (Link Manufacturing Company Inc., Fargo, ND). Thereafter, the Miscanthus biomass was separated by sieving through various mesh sizes (70, 40, and 16) to obtain variable sized particles for chemical pretreatment to alter the cellulose content. Miscanthus was treated to obtain products with variable lignin content, which were not further treated via sieving due to their fine particle size. Miscanthus was treated using alkaline and acidic conditions to vary the content of cellulose and lignin. To modify the raw material as a cellulose-enriched (cellulose 90%) fibre, a method reported by Soleimani *et al.*[19] was used. Briefly, the biomass was pretreated with a 1.2 N sulfuric acid solution

at atmospheric pressure and 100°C for 120 min to extract hemicellulose. Then, the acid-pretreated fibre was subjected to a 5% (w/v) NaOH solution at 100°C for 100 min. to remove lignin. Lignin isolation followed the method reported by Sluiter *et al.* [20] Briefly, the raw fibre was cold digested in a 72% (w/w) sulfuric acid at 30°C for 1 h. Then, the suspension was transferred to a larger vessel with dilution changing the concentration of acid to 4%, followed by digesting the solid fraction at 121°C for 1 h. Finally, the solid fraction obtained after two stages of digestion was separated and considered as lignin to be used for the adsorption study herein.[20] Table 6.1 shows the raw (as-received) and pretreated Miscanthus with variable particle sizes with solvent swelling at equilibrium[21] in water (S_W) and ethanol (S_E), respectively. The equilibrium uptake capacity of Miscanthus (raw and pretreated) was obtained in water and ethanol after immersing in each solvent for 24 h at 295 K. Swelling was reported by the difference in the weight before and after oven drying (at 60 °C). For the regeneration study, the sorption data for water and ethanol were obtained by repeating the adsorption-desorption cycles on raw and pretreated samples.

Table 6.1 Swelling properties of raw and pretreated Miscanthus with different particle sizes in water (S_W) and ethanol (S_E) neat solvents at 295 K.

Raw Miscanthus (RM) biomass	**ID code**	**S_W (%)**	**S_E (%)**
Miscanthus 16	RM-16	$(1.31\pm 0.03)\times10^3$	$(4.26\pm 0.02)\times10^2$
Miscanthus 40	RM-40	$(1.78\pm 0.01)\times10^3$	$(9.21\pm 0.03)\times10^2$
Miscanthus 70	RM-70	$(1.39\pm 0.01)\times10^3$	$(7.72\pm 0.02)\times10^2$
PTM (variable lignin, %)[1]	Lignin	$(1.91\pm 0.02)\times10^2$	$(6.44\pm 0.02)\times10^2$
PTM (variable cellulose, %)[1]	**ID code**	**S_W (%)**	**S_E (%)**
Miscanthus 16	PTM-16	$(1.30\pm0.01)\times10^3$	$(9.11\pm 0.01)\times10^2$
Miscanthus 40	PTM-40	$(1.39\pm 0.00)\times10^3$	$(8.14\pm 0.01)\times10^2$
Miscanthus 70	PTM-70	$(2.60\pm0.01)\times10^3$	$(8.78\pm 0.04)\times10^2$

RM: Raw Miscanthus; [1]**PTM:** Pretreated Miscanthus biomass; 16, 40 and 70 are mesh sizes of Miscanthus.

6.3.2 Characterization

The weight loss profiles of samples at variable temperature were measured using a thermogravimetric analyser (TGA; Q50 TA Instruments) using an open aluminum pan configuration. Samples were held isothermally at 30 °C and allowed to equilibrate for 5 min prior to heating at 5 °C/min up to 500 °C. The IR spectra were obtained with a Bio-RAD FTS-40 spectrophotometer where 6 mg of sample were mixed with 60 mg of spectroscopic grade potassium bromide (KBr) using a mortar and pestle followed by drying at 60 °C. The samples were analysed as powders in reflectance mode where the Diffuse Reflectance Infrared Fourier Transform (DRIFT) spectra employed multiple scans at 295 K against a background spectrum of KBr. The spectral resolution was 4 cm^{-1} over the 400–4000 cm^{-1} region. Nitrogen adsorption was obtained using a Micromeritics ASAP 2020 (Norcross, GA) to estimate the surface area (SA) and pore structure properties with an accuracy of ±5%. In brief, *ca.* 1 g of sample was degassed at an evacuation rate of 5 mmHg s^{-1} in the sample chamber until the outgas rate became stabilized (<10 mmHg min^{-1}), while the sample temperature was maintained at 100 °C for 48 h. Alumina (Micromeritics) with a known pore volume (PV) and SA was used to calibrate the instrumental parameters. The BET SA was calculated from the adsorption isotherm.[14, 21] The micropore SA was obtained using a *t*-plot (de Boer method). The Barret–Joyner–Halenda (BJH) method was employed to estimate the PV and pore diameter from the adsorption isotherm using the Kelvin equation, where the pores are assumed to be slit-shaped. The morphology of raw and pretreated Miscanthus was measured using a Hitachi S-3400N scanning electron microscope (SEM). The particle size was measured using a Mastersizer S Long Bench Particle Size Analyzer (PSA), Malvern Instruments. PSA detects particle size via measurement of the scattered diffraction pattern from the sample after passage through a laser beam.

The study of different weight ratios (wt %) of W-E solutions used anhydrous (100%) ethanol (reagent grade) obtained from Commercial Alcohols Inc. (Brampton, Ontario, Canada). Fixed amounts (*ca.* 150 mg) of each adsorbent (raw and pretreated Miscanthus with variable particle sizes) were mixed with 10 g of solution containing W-E (adsorbate) with variable wt% ratios in 4 dram vials. The samples were equilibrated at room temperature on a horizontal shaker table (SCILOGEX Model: SK-O330-Pro) for 24 h at 160 rpm. Next, the samples were centrifuged (Precision Micro-Semi Micro Centricone, Precision Scientific Co.) at 1800 rpm for 1h followed by adding 1 g of supernatant solution to 0.05 g mixture of tetrahydrofuran (THF) and dimethyl

sulfoxide (DMSO-d_6, 99.9%; Sigma-Aldrich). ^{1}H-NMR spectral analysis was conducted using a wide-bore (89 mm) 11.7 T Oxford superconducting magnet system (Bruker BioSpinCorp, Billerica, MA) equipped with a 5 mm PaTx1 probe. The NMR operating parameters were controlled by SSSC 500 console and workstation running X WIN-NMR 3.5 using the standard commercial pulse programs from the TopSpin 1.3 software library. Quantitative NMR analysis was carried out using an internal standard (dry THF) and a field-locking solvent (dry DMSO-d_6) that was added to each solution in fixed amounts. The inversion−recovery method enabled determination of the spin−lattice relation time (T_1) of each pure solvent and their binary mixtures.[22] Independent calibration curves of standard binary W−E solutions at variable composition (wt%) were used for qNMR determination of W−E content. As stated previously,[14] a solvent system (THF and DMSO-d_6) was used to evaluate the equilibrium time of the sorption process and incubation time of 150 mg of adsorbent in binary W−E mixtures. The relative solvent uptake at equilibrium was estimated by qNMR at fully relaxed conditions using a batch method. W-E composition was estimated before and after exposure of the sorbent in the binary W-E solutions.

6.3.3 Quantitative NMR (qNMR) spectroscopy

Quantitative NMR (qNMR) enables estimation of the solvent composition in binary W-E mixtures, especially for well-resolved NMR signatures in W-E mixtures. The relative uptake of solvents via adsorption in binary W-E solutions was estimated using qNMR. THF was selected as an internal standard since its NMR spectral signatures do not overlap with the W-E binary solvent (-CH_2, –CH_3, and -OH groups). DMSO-d_6 served as the NMR locking solvent and its anisotropic properties afford fully resolved lines for the -OH groups of binary W-E mixtures with negligible deuterium exchange.[14] The recycle delay (D_1) accounted for the relaxation time (T_1) of various nuclei using an inversion-recovery pulse sequence in neat and binary solvents. [14] The ^{1}H-NMR signatures for W and E show two separate signatures for OH at δ=4.50 ppm and δ=5.20 ppm, respectively.[14] Quantitative NMR was achieved by integration of the signal intensity of selected ^{1}H nuclei (–OH, -CH_2, and –CH_3) of the solvent components by equation 6.1.

$$\frac{\text{Area (solvent)}}{\text{Area (THF)}} = \frac{^1\text{H}_{\text{nuclei}}\text{(solvent)}}{^1\text{H}_{\text{nuclei}}\text{(THF)}} \times \frac{\text{n}_{\text{solvent}}}{\text{n}_{\text{THF}}} \qquad \text{Equation 6.1}$$

The water content (wt %) in the binary mixtures was calculated using gravimetric estimates (n_W and n_E) in equation 6.1. Similarly, the ethanol content was obtained by the peak area of the $-CH_3$ group. The relative area for each solvent component refers to the ^1H integrated peak area for the NMR signature in the mixed solvent (E or W), where $n_{solvent}$ is the number of moles (E or W), and n_{THF} refers to the mole content of THF.

6.3.4 Models and equations

The adsorption isotherm is shown as a plot of equilibrium uptake of adsorbate species (W and/or E) in a mixed binary (W+E) solvent system by an adsorbent. The uptake (Q_e; mmol/g or mg/g) by the sorbent phase is plotted *vs.* residual equilibrium concentration of unbound adsorbate (C_e; mmol/L or mg/L), according to equation 6.2.

$$Q_{e,i} = \frac{\left(C_{0,i} - C_{e,i}\right)}{m} \times W_{Solution} \qquad \text{Equation 6.2}$$

In equation 6.2, C_o and C_e (mg/L) are the initial concentration (wt %) of each respective solvent component (W or E), before and after adsorption. The relative weight content of each solvent component (W or E) was determined, where the total solution weight ($W_{solution}$) and the adsorbent mass (m) were measured. The Sips isotherm model was used to analyse the isotherm profiles to estimate thermodynamic parameters of adsorption (*cf.* Equation 6.3). In particular, the sorption capacity and sorption affinity constant of the adsorbent was evaluated in W-E binary solutions. [23]

$$Q_e = \frac{Q_m \left(K_s C_e\right)^{n_s}}{1 + \left(K_s C_e\right)^{n_s}} \qquad \text{Equation 6.3}$$

K_s is adsorption constant, n_s is the sorbent surface heterogeneity, C_e is the residual adsorbate concentration, and Q_m represents the monolayer adsorption capacity of sorbent. This equation provides an assessment of the heterogeneity of the adsorption process according to the exponential term (n_s).[23] Equation 6.3 accounts for Langmuir behaviour (n_s=1), while the Freundlich isotherm is inferred [24] when n_s deviates from unity.

6.4 Results and Discussion

6.4.1 Pretreatment of Miscanthus

The raw fibre content of Miscanthus (dry basis; wt%) is mainly composed of cellulose (48 %), hemicellulose (24 %), lignin (12 %), and inorganics (2 %). The Miscanthus biopolymer composition can be altered by applying an appropriate pretreatment technique such as hydrolysis to modify the fibre content, as illustrated in Scheme 6.1 (*cf*. Experimental section). Scheme 6.1 illustrates that the biopolymer content (hemi-cellulose and lignin) of Miscanthus can be modified by acid/base hydrolysis, along with mechanical treatment to yield fibre materials with variable composition and particle size, respectively.

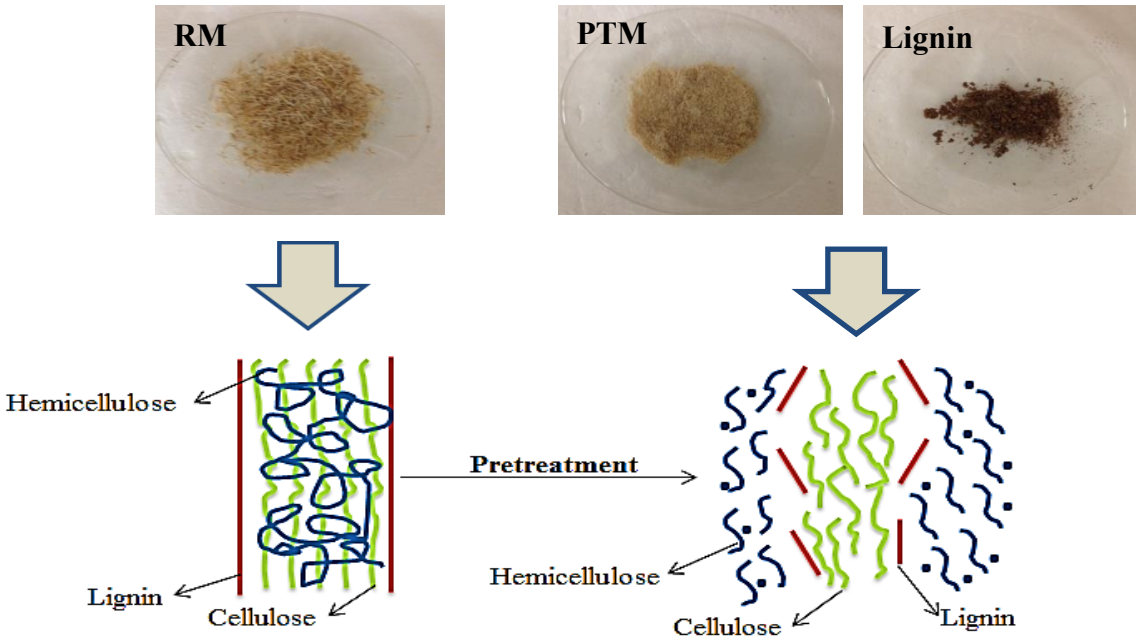

Scheme 6.1 Conceptual illustration for the pretreatment of raw Miscanthus to yield fibres with variable biopolymer content. The sample ID codes of the products are listed in Table 6.1.

6.4.2 Characterization

6.4.2.1 Particle size determination

The particle size distribution (PSD) and average particle size of raw and pretreated Miscanthus are shown in Table 6.2. The corresponding particle size distribution is provided in the Supporting Information (*cf.* Figure A6.1 in Appendix A6).

Table 6.2 Average particle size estimates for raw and pretreated Miscanthus.

Raw Miscanthus (RM) (untreated)	**Average particle diameter (μm)**
RM-16	1230
RM-40	483
RM-70	193
Pretreated Miscanthus (Increased Cellulose content)	**Average particle diameter (μm)**
PTM-16	1110
PTM-40	364
PTM-70	79.5

Note: Sample ID codes are defined in Table 6.1

Table 6.2 shows the particle size results for raw and pretreated Miscanthus, where a decrease in the average particle size occurs after pretreatment due to changes in the fibre composition. In Table 6.2, the reduced particle size of pretreated Miscanthus relates to a lower tendency to undergo aggregation due to greater wetting of the particle grains after hemicellulose removal. Cellulose is relatively insoluble in water in spite of the presence of hydrophilic polar hydroxyl groups on its surface. Cellulose is composed of D-glucopyranose attached together via β-(1,4) linkages that undergo extensive intra- and inter-strand hydrogen-bonding of biopolymer chains,[14] contributing to its unique mechanical strength and chemical stability. The particle size distribution shows a reduced full width at half maximum (FWHM) for the RM-40, and RM-70 materials (*cf.* Figure A6.1 in Appendix A). Physical treatment of Miscanthus such as mechanical grinding, milling, and sieving results in particle size variations, which affect aggregation and

wetting properties of biomass. The physicochemical properties of hydrophobic biopolymer components such as cellulose are affected by particle size and likely contribute to variable surface effects due to the aggregation effects described above. [25]

6.4.2.2 Nitrogen adsorption

Nitrogen adsorption is a technique that provides estimates of the surface area (SA) and pore structure properties of solid phase materials. Table 6.3 lists the accessible surface area (SA) and average pore size diameter (P_W) for different particle sizes of raw and pretreated Miscanthus estimated from N_2 adsorption isotherms (*cf.* Figure A6.2 in Appendix A6). The shapes of the isotherms resemble a Type II system according to the convention defined by the International Union of Pure and Applied Chemistry (IUPAC). A Type II isotherm can be shown for a range of pore size dimensions. This uptake profile is representative of sorbents with large macropores where the surface area of the pore is so large that multilayer adsorption can occur without any restrictions. As well, the Type II isotherm describes behaviour typical of nonporous materials where adsorption occurs mainly on the external surface.[24] The results obtained above show the saturation of an adsorbed monolayer at low relative pressure ($p/p^o \approx 0.2$). The isotherm displays low uptake of nitrogen up to greater relative pressure values ($p/p^o \sim 0.9$), while further adsorption occurs at higher ($p/p^o > 0.9$) values due to adsorption onto the powder grain boundaries.[21, 26] A large proportion (>90%) of the nitrogen uptake occurs at the grain boundary surface sites, while a smaller fraction occurs within the micropore sorbent domains. The absence of well-defined hysteresis loops for Miscanthus (raw and pretreated) provides additional evidence of reduced pore volume due to the reversible evaporation and condensation over the range of p/p^o values.[25] By contrast, the lignin shows evidence of mesopore structure according to the hysteresis loop near p/p^o above 0.9, along with greater uptake at higher values resulting from the greater SA of lignin. The results are in agreement with the more rigid and branched network structure of such polyphenolics relative to biomass rich with biopolymers with more densely packed domains such as cellulose and hemicellulose. The surface area (SA) of the raw/pretreated Miscanthus and lignin are listed in Table 6.3 where particles with similar size such as pretreated Miscanthus have greater SA and diameter relative to raw Miscanthus. The low SA values in Table 6.3 strongly suggest that the pore structure had collapsed upon drying and the SA estimated is due mainly to the external surface. Meng *et al.*[27] also reported increased surface area for chemically treated *Populus* fibre

when compared with the raw biomass. The greater SA of PTM relates to the removal of hemicellulose and lignin during the pretreatment steps that results in greater defibrillation effects due to chemical etching of the biopolymer network. The effect of pretreatment may be offset due to packing effects and/or shrinkage at 77 K during the adsorption process. A decrease in the particle size for both types of Miscanthus reveals an incremental rise in the SA of the biomass.

Table 6.3 Accessible surface area (SA) of raw and pretreated Miscanthus biomass with variable particle sizes.

Raw Miscanthus (RM)	**ID code**	**SA** (m^2/g)
Miscanthus 16	**RM-16**	0.43
Miscanthus 40	**RM-40**	0.56
Miscanthus 70	**RM-70**	0.74
PTM[1] (greater lignin, %)	**Lignin**	137
PTM[1] (greater cellulose content)	**ID code**	**SA** (m^2/g)
Miscanthus 16	**PTM-16**	0.71
Miscanthus 40	**PTM-40**	0.64
Miscanthus 70	**PTM-70**	0.96

[1]**PTM –** pretreated Miscanthus at variable hydrolysis conditions

6.4.2.3 Thermal gravimetry analysis (TGA) and FT-IR

Thermal gravimetry analysis is a commonly used method for materials characterization since it provides insight about the thermal stability and relative composition of multicomponent materials. Mohamed *et al.*[28] estimated the cross-linker content of cyclodextrin polymers using TGA, where individually resolved thermal events led to estimates of the relative polymer composition. The TGA curves are shown as weight-loss profiles *vs.* temperature at constant heating rate, along with derivative weight on the right hand ordinate (*cf.* Figure 6.1A). As noted above, TGA affords estimates of the biomass composition for well resolved thermal events.[21, 28] The TGA and IR for raw and pretreated Miscanthus are shown in Figure 6.1A-B.

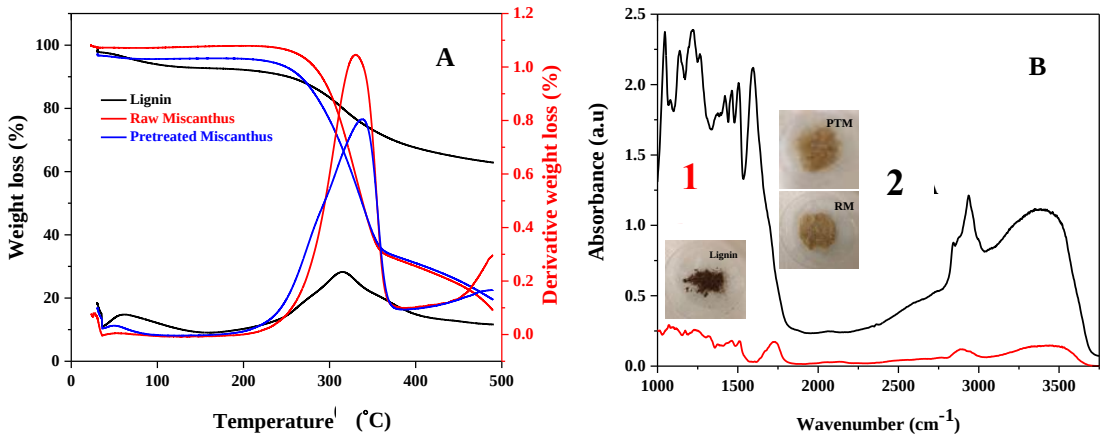

Figure 6.1 TGA profiles (A) and FT-IR spectral results (B) for Lignin (1) and raw/pretreated Miscanthus (2). The IR and TGA results for Miscanthus with different particle sizes are not shown. The results for mesh size 40 are shown to illustrate representative behaviour of the biomass.

The main thermal events observed for the Miscanthus materials are characterized by a broad thermal curve with similar shapes between 200 and 400˚C, as shown in Figure 6.1A. The thermal transitions observed below 100 ˚C relate to the loss of water.[21] A comparison of Miscanthus with a higher cellulose and hemicellulose content reveal that it undergoes decomposition more readily than materials with greater lignin content. The TGA results indicate that lignin is more stable and difficult to decompose relative to cellulose or hemicellulose biopolymers[29] due to its branched phenolic structure and reduced oxygen content as compared with polysaccharides. The thermal properties of Miscanthus are consistent with the variable lignin content of the biomass, since lignin content strongly depends on base hydrolysis pretreatment of the biomass.[29,30] The thermal profiles for the mass loss of cellulose and hemicellulose are similar. Thus, the TGA profiles for raw and pretreated Miscanthus are accounted for on the basis of differing biopolymer composition and the variable structure and thermal properties of each respective biopolymer.

In Figure 6.1B, the FT-IR results for Miscanthus and lignin are shown where the spectra for raw and pretreated Miscanthus show strong and broad IR absorption at 3300 cm^{-1} for OH stretching, where sharp and intense bands appear at *ca.* 2900 and 2800 cm^{-1} for the –CH stretching of the polysaccharide. The intense bands at 1460 cm^{-1} relate to skeletal bands/C-C bending

vibrations of alkyl and aromatic groups.[31] The band at 1750 cm^{-1} corresponds to the C=O stretching vibrations of a carbonyl group.[32] The band *ca.* 1370 cm^{-1} is assigned to the OH *in-plane* deformation of alcohols and phenols, while the band near 1200 cm^{-1} was assigned to the C-O vibrations of primary alcohols. The spectra for raw and pretreated Miscanthus and lignin are very similar with some minor differences, where the enhanced band appearing at 1500 cm^{-1} relates to the skeletal bands for the lignin-enriched material.

6.4.2.4 Scanning electron microscopy (SEM)

Scanning electron microscopy (SEM) was used to study the morphology and textural characteristics of raw and pretreated Miscanthus. SEM may provide estimates of the surface roughness, pore structure and accessible SA of biopolymer materials.[33, 34] Figure 6.2A shows the surface features of raw Miscanthus particles, which appear as flat and smooth domains. The SEM results show that the surface displays greater roughness with the presence of large cellulose fibres and pores due to the greater removal of hemicellulose and lignin (Figure 6.2B). Figure 6.2C shows the surface domains of lignin with a disintegrated loss of structure and pore features on the biopolymer surface, as compared with RM and PTM.[35,36] The rigid structure of lignin concurs with the branched and mesoporous nature of such materials due to inefficient packing of such polyphenolics. The greater SA of lignin is supported by the nitrogen isotherm results above, where similar trends in textural properties were noted for branched and rigid polymers according to swelling and dye adsorption results.[28]

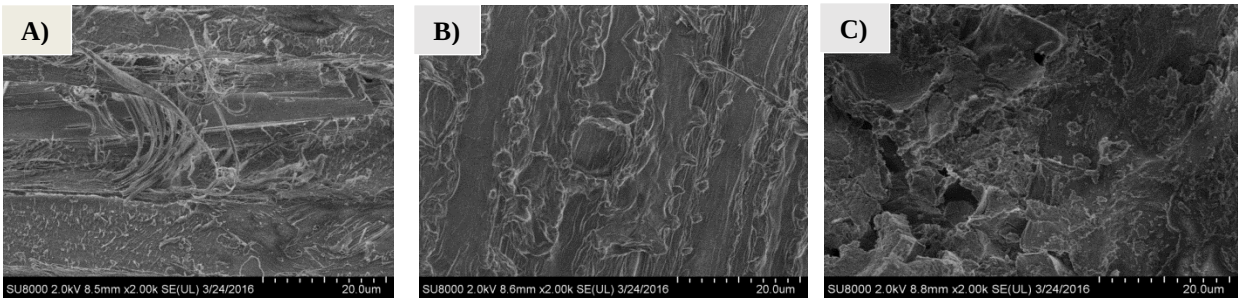

Figure 6.2 SEM images: A**)** raw Miscanthus, B**)** pretreated Miscanthus (greater cellulose content), and C**)** Lignin.

6.4.3 Equilibrium solvent swelling properties

Solvent uptake and swelling properties provide a measure of the potential utility of such materials as adsorbents. The relative uptake in neat solvents may be regarded as a proxy measure

of the relative equilibrium adsorption properties, as outlined in a recent report on starch and its cross-linked forms in water, ethanol, and binary (W-E) mixtures.[7] The relationship between swelling and sorption properties of materials has been reported where the role of solvent-swelling in the kinetic uptake processes is a key step in the overall adsorption process.[21] The equilibrium swelling data of particles with variable particle sizes for raw and pretreated Miscanthus are listed in Table 6.1 along with their relative solvent uptake (W or E) at ambient conditions. The sorbents besides lignin display high water affinity according to the greater uptake of W over E. RM-16 shows a greater selectivity towards water relative to raw Miscanthus 40, and 70. The observed effect may relate to variation in SA and pore volume (PV) effects according to the particle size (Table 6.3). The biomass solvent uptake capacity depends on the textural properties and surface-accessible polar functional groups of the biopolymers. Raw Miscanthus is likely to have similar surface chemical properties, while the SA may vary slightly due to textural properties. In the case of pre-treated materials, differences in the surface chemical properties are inferred relative to raw biomass due to the variable biopolymer content. The acid/base hydrolysis of Miscanthus alters various properties such as fibre structure, biomass composition, crystallinity, and textural properties, which can modify the adsorption affinity of solvents (W and E), according to hydrophobic effects.[37] The water uptake in materials with small pore sizes may display steric exclusion effects, especially in micropores with apolar surface domains.[38] It is interesting to note that Miscanthus 70 has a greater overall uptake capacity with W and E since particles with smaller size contain both small and large pores, which cannot discriminate uptake between water *vs.* ethanol.

6.4.4 Sorption study and selectivity

There is no direct relationship between crystallinity and particle size but mechanical milling and chemical hydrolysis of biomass may affect the solvent accessibility of the biopolymer surface.[39] Generally, the degradation of the crystalline regions of cellulose differ compared to the amorphous regions due to the presence of defects and ordered domains. In turn, the solvent accessibility of the biomass affects the cohesive interactions and aggregation properties of the biopolymer surface sites.[40, 41] Similarly, the sorption properties and accessibility of adsorption sites of Miscanthus can be related to particle size and textural properties (pore structure and SA).

In Table 6.1, the raw Miscanthus has greater adsorption capacity and swelling with water and ethanol relative to the pretreated materials. Raw Miscanthus has greater hemicellulose and lignin content when compared with the cellulose-enriched fibre materials. The adsorption properties of cellulose-enriched fibre materials are lower relative to RM and may relate to higher levels of crystalline cellulose, which prevent access of water molecules to the inner fibril structure [42, 43, 44] *vs.* materials with more amorphous domains of cellulose. The swelling results for raw and pretreated Miscanthus in ethanol are *10-fold* lower compared to the lignin isolates. Hemicellulose is naturally isotropic and amorphous in structure and is located within the cellulose fibril domains. The degree of hydrogen bonding with water and ethanol is higher at the external surface of cellulose and hemicellulose, as compared to the internal micropores due to the reduced pore volume. The presence of hemicellulose affords variable hydrogen bonding interactions within the cellulose fibril network and the surface sites since cellulose/hemicellulose may serve as donor and acceptor sites.[45]

The structural identification and characterization of organic components can be studied using qNMR due to the abundance of ^{1}H nuclei in such systems. ^{1}H-NMR spectroscopy is especially suitable for well-resolved signatures when instrumental conditions afford fully relaxed spectra. The latter relates to the spin lattice relaxation time (T_1) of selected nuclei in water (W), ethanol (E), and in binary (W+E) solutions.[14] In a previous report, qNMR was shown to be a suitable analytical method for estimating the W-E composition in binary systems.[14] This study uses qNMR for the analytical determination of solvent components before and after adsorption with modified and raw Miscanthus biomass. Sorption isotherms provide a detailed understanding of thermodynamic properties of adsorbate/adsorbent systems, especially where the structure of the sorbent varies in a systematic manner as shown for RM and PTM biomasses herein. Isotherm profiles describe the uptake of adsorbate (W or E) per unit mass of adsorbent at constant temperature *vs.* adsorbate concentration. Figure 6.3 illustrates the adsorption isotherms of Miscanthus materials and lignin in W-E binary systems, along with best-fit parameters as shown in Table 6.4. The Sips model provides a favourable description of the isotherm results according to the *goodness-of-fit* ($R^2 \approx 1$) criteria. The RM and PTM biomasses display greater uptake of water over ethanol. By contrast, lignin displays the opposite behaviour in agreement with the swelling results in Table 6.1. The greater adsorption of water over ethanol by Miscanthus concurs with the Q_m values in Table 6.4.

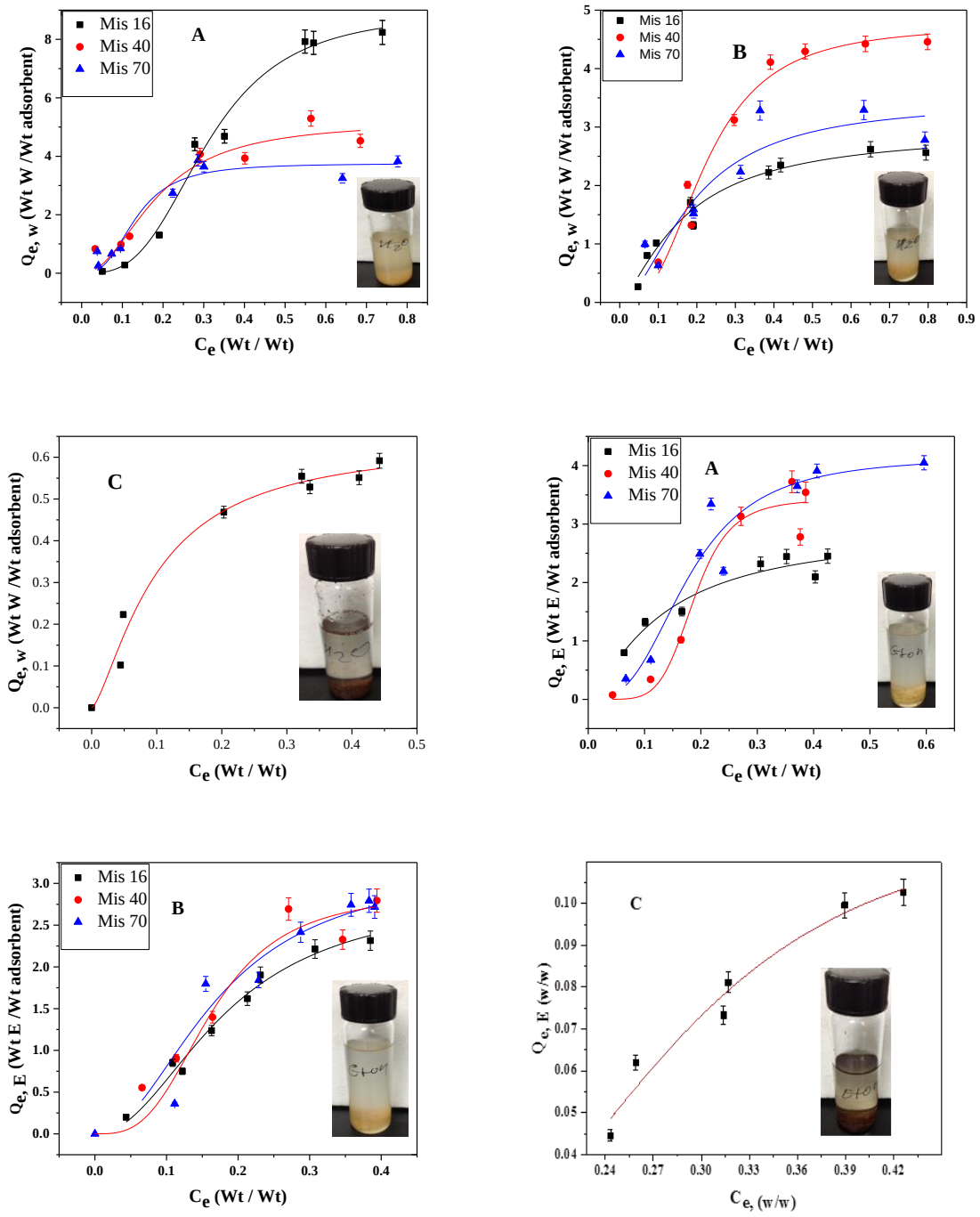

Figure 6.3 Adsorption isotherms of biomass and its modified forms for the uptake of water (W) and ethanol (E) in binary (W+E) solutions at 295 K: (A) Raw (RM), (B) Pretreated (PTM) and C) Lignin.

Table 6.4 Sips Isotherm parameters for the uptake of water (A) and ethanol (B) at 295 K with different particle sizes for raw and pretreated Miscanthus, and lignin.

A: Water uptake results for raw and pretreated Miscanthus biomass.

Raw Miscanthus	**K_s (g/g)**	**n_s**	**Q_m (g/g)**	***R^2***
RM-16	3.2 ± 0.30	3.1 ± 0.30	8.9 ± 0.70	0.97
RM-40	5.4 ± 1.6	2.1 ± 0.90	5.2 ± 0.80	0.92
RM-70	7.5 ± 1.3	2.83 ± 0.90	3.8 ± 0.30	0.92
Pretreated Miscanthus	**K_s (g/g)**	**n_s**	**Q_m (g/g)**	***R^2***
PTM-16	5.9 ± 1.3	1.4 ± 0.30	2.9 ± 0.30	0.90
PTM-40	4.5 ± 0.60	2.7 ± 0.60	4.7 ± 0.30	0.92
PTM-70	5.3 ± 1.8	1.76 ± 0.80	3.4 ± 0.70	0.86
Lignin	**K_s** (g/g)	**n_s**	**Q_m** (g/g)	***R^2***
Lignin	10.1 ± 3.5	1.4 ± 0.44	0.64 ± 0.095	0.95

B: Ethanol uptake results for raw and pretreated Miscanthus biomass.

Raw Miscanthus	**K_s (g/g)**	**n_s**	**Q_m (g/g)**	***R^2***
RM-16	7.2 ± 4.7	1.3 ± 0.70	2.9 ± 0.90	0.90
RM-40	5.3 ± 0.60	5.9 ± 3.1	3.4 ± 0.31	0.94
RM-70	5.6 ± 0.80	2.9 ± 1.0	4.2 ± 0.49	0.92
Pretreated Miscanthus	**K_s** (g/g)	**n_s**	**Q_m** (g/g)	***R^2***
PTM-16	5.5 ± 0.80	2.0 ± 0.40	2.9 ± 0.40	0.98
PTM-40	5.9 ± 2.4	2.1 ± 1.1	3.2 ± 0.99	0.90
PTM-70	6.1 ± 0.90	3.1 ± 1.4	2.9 ± 0.40	0.95
Lignin	**K_s** (g/g)	**n_s**	**Q_m** (g/g)	***R^2***
Lignin	3.7 ± 0.35	4.0 ± 1.5	0.12 ± 0.020	0.94

A comparison of the Q_m values for raw and pretreated Miscanthus reveal that raw Miscanthus has variable adsorption capacity toward water and ethanol that relates to its solvent affinity with the biopolymer components (cellulose, hemicellulose and lignin). It is noted that each respective biopolymer has variable surface functional groups that impart variable hydrophile-lipophile balance. For instance, lignin is apolar in nature relative to polysaccharides such as hemicellulose and cellulose with more polar character. While SA effects and accessibility of surface functional groups account for the uptake properties of Miscanthus materials, a detailed understanding is limited in the absence of a detailed knowledge of the biomass structure. Although Scheme 6.1 offers a simplified view of biomass structure and its biopolymer components, the actual structure is considerably more complex in nature.[46] Cellulose is a highly complex biopolymer owing to its unique fibril structure, along with its allotropes such as cellulose I and II.[47] Surface chemical groups at the biopolymer interface play a key role, especially H-bond donor/acceptor groups (e.g., –OH) on cellulose, as outlined in a report by Udoetok *et al.* (See Figure 4 in ref. 34).[34] The presence of more surface-accessible -OH groups relates to variable adsorptive uptake of alkyl carboxylate anions. [34] Similarly, the uptake of W-E in binary solvents by cross-linked starch correlates with the solvent polarity and solvent size, especially when adsorption occurs with surface accessible hydroxyl groups.[7] RM has a reduced SA and PV relative to PTM biomass (*cf.* Table 6.3). The Q_m values for water with each sorbent are listed in descending order, as follows: RM > PTM > lignin. Similarly, the Q_m values (ethanol) are listed in descending order: Lignin > RM ≈ PTM. In Table 6.4, the n_s parameter indicates heterogeneous surface character for RM and PTM since n_s deviates from unity, while the heterogeneity parameter is reduced for PTM due to the removal of hemicellulose. This effect may account for the lower adsorption of water and ethanol at the pretreated fibre surface. According to literature (*cf.* Table 5, in Ref. 21), cellulosic materials have adsorption sites with less heterogeneity as compared with modified celulose.[21] PTM biomass has lower heterogeneity of the sorbent surface according to the water uptake results ($n_s \approx 1$), in agreement with its greater cellulose content.[37] The pretreatment of Miscanthus likely alters the morphology of RM due to changes in the lignin (apolar) and the cellulose (hydrophilic) biopolymer contents. A lowering of the hemicellulose content due to pretreatment shows a lowering of the uptake of water and ethanol, in accordance with the abundant polar groups of this biopolymer. A key factor related to the preferential uptake of water over ethanol for RM, PTM, and lignin is attributed to the relative hydroxyl group accessibility. Lignin

has a branched and disordered structure compared to linear biopolymers (cellulose and hemicellulose) due to the dendritic nature of lignin.[47, 48] While lignin can form hydrogen bonds with water, the phenyl units are apolar and have reduced hydrogen bonding compared with cellulose and hemicellulose.[48, 49] The $R_{selectivity}$ values for RM and PTM were estimated using the Q_m values for water and ethanol (*cf.* Table 6.4). Figure 6.4 illustrates the $R_{selectivity}$ values for RM and PTM, which reveal remarkable differences based on the cellulose and hemicellulose content of the biomass. RM shows greater solvent-selective uptake ($R_{selectivity}$ = 1-3) of water over ethanol relative to PTM. By contrast, PTM has reduced solvent selectivity ($R_{selectivity}$ ≈1-1.5) due to the nature of the hydrolysis pretreatment.

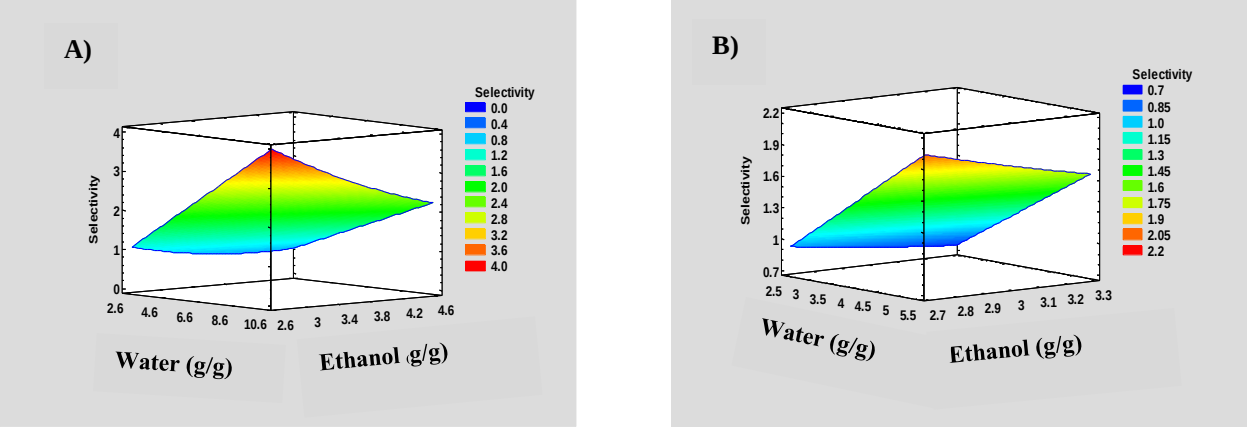

Figure 6.4 Equilibrium solvent selectivity ratios for A) Raw Miscanthus (RM) and B) Pretreated Miscanthus (PTM) in binary (W+E) systems at 295 K.

RM biomass has greater selectivity for water over ethanol. This may be understood on thermodynamic grounds according to differences in solvent affinity (W over E) due to variable textural properties and surface chemistry of RM. By contrast, the kinetic adsorption profiles of solid-solution systems are dependent on the role of textural properties and surface chemistry, in agreement with the three kinetic uptake steps of the overall process. In the case of water uptake, the first stage involves transport of solvent from bulk solution to the exterior surface of an adsorbent particle through a boundary layer of two phases. The adsorbate diffuses into the interior active sites of the adsorbent during the diffusion process. Finally, adsorption occurs onto the active surface sites at the adsorbent interior. The latter step governs the specific adsorption capacity, which relates to the role of textural properties and surface chemistry, in agreement with thermodynamic ($R_{selectivity}$) factors described above. The structure of Miscanthus (raw and

pretreated) and lignin have a significant effect on the adsorption properties of such materials, accounting for their solvent selectivity of water over ethanol.[50] Grewal *et al.*[51] have reported the use of oat hull biomass and hydrolysis for the preparation of the biocomposites containing cellulose and lignin, where the water absorption capacity and mechanical properties of the composites were investigated.[51] Lignin has a lower tendency for water uptake, in agreement with the results for RM and PTM biomasses reported herein. Biomass with greater cellulose content has a unique fibre structure owing to hydrogen bonding between adjacent biopolymer units that results in reduced surface accessible hydroxyl groups, as described above. On the other hand, the greater surface accessible polar groups of RM may relate to the presence of hemicellulose since it facilitates greater solvent selectivity (W over E), as noted above.

6.4.5 Regeneration

An important aspect of adsorption technology relates to the regeneration and reusability of the adsorbent for practical applications. Miscanthus samples were regenerated with pure water and ethanol after four cycles of adsorption-desorption, as shown in Figure 6.5. The relative uptake (W and E) for raw and pretreated Miscanthus decreased by *ca.* 12% and may relate to sintering effects during the intermediate drying process between cycles at elevated temperature. The RM and PTM biomass may undergo changes in biopolymer conformation, collapse, or shrinkage of the micropore sites during the loss of solvent upon drying. As well, sintering of the biomass network may occur upon heating due to fusing of the biopolymer components, which causes reduced pore structure and SA effects. An alternative to regeneration using pressure-drops instead of heating to remove solvent between cycles may reduce structural effects due to sintering. The structural effects of solvent removal are evidenced by the greater decline in regeneration efficiency in water *vs.* ethanol solvent (*cf.* Figures 6.5 A and B). Notwithstanding the sintering effects indicated above, the general utility of Miscanthus for the fractionation of solvent in binary water-ethanol mixtures over multiple cycles is shown in Figure 6.5, along with its general mechanical stability during the regeneration process.

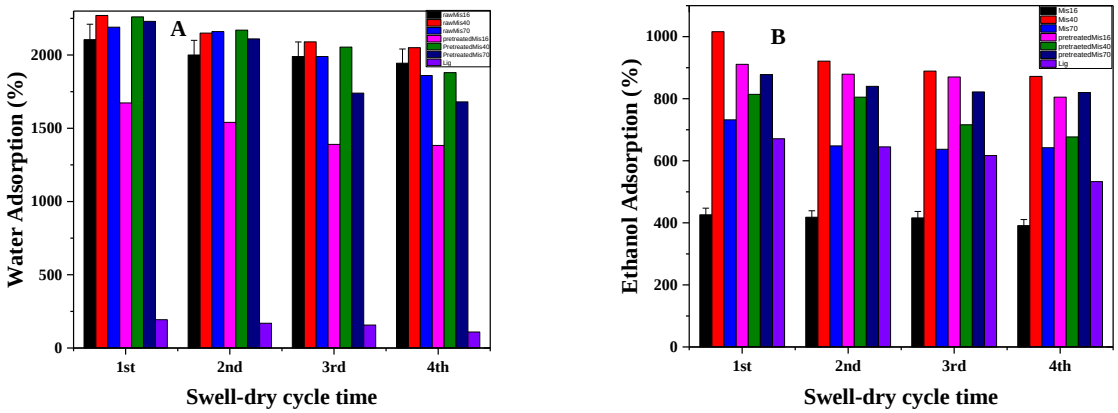

Figure 6.5 **A)** Water and **B)** Ethanol uptake results. Miscanthus materials and lignin are subjected to multiple adsorption-desorption cycles via drying at 60-80˚C for 24 h. (= RM16, = RM40, = RM70, = PTM16, = PTM40, =PTM70 and Lignin).

Comparison with other adsorbents

To provide a comparison of the uptake properties of Miscanthus obtained herein, a summary of selected examples of W-E adsorption selectivity results ($R_{selectivity}$) for various adsorbents from the literature are listed in Table 6.5. Among the biomaterials in Table 6.5, raw Miscanthus (RM) has the highest solvent selectivity of water over ethanol followed by canola meal with its protein extracted. Based on the relative abundance and sustainability of non-food commodities such as Miscanthus, its use as a biomass adsorbent offers significant advantages for the adsorptive fractionation of water-ethanol binary mixtures. The uptake and fractionation properties of Miscanthus rival that of cellulose biopolymers derived from cotton linters.[14]

Table 6.5 Solvent selectivity (R) of water (W) over ethanol (E) by different adsorbents.

Adsorbent	**Solvent Selectivity**	**C_0 (w/w %)**	**Ref**
Raw Miscanthus	3.0	4-85% (W)	This Study
Pretreated Miscanthus	1.5	45-87% (W)	This Study
Cellulose	1.10 - 2.03	4-75% (W)	14
Corn meal	0.6	25-85% (W)	52
Protein extracted canola meal	1.9	5-20% (W)	53

6.5 Conclusion

Raw Miscanthus (RM) biomass is a sustainable biomass with variable particle size. Various forms of chemical pretreatment (PTM) of this biomass yields modified biomass fractions with or without the lignin content. The isotherm adsorption properties of cellulose-enriched and lignin materials were evaluated in water (W), ethanol (E), and binary (W+E) mixtures, where variable solvent uptake was observed according to the nature of the chemical and physical treatment of Miscanthus. Particle size variation had a minimal effect on adsorption of water and ethanol. By comparison, chemical treatment had a greater effect according to the surface accessibility of the hydrophilic adsorption sites and micropore accessibility of the adsorbent. Quantitative NMR spectroscopy provided estimates of the solvent selective uptake in W-E binary mixtures. The adsorption capacity (g/g) of Miscanthus (RM-16) is listed in parentheses: water (8.93) and ethanol (4.15), where the solvent selectivity ratios in binary W-E solutions vary from 1 to 3. Regeneration studies were carried out using swelling tests over four cycles of regneration, where a moderate decrease (12%) in uptake was observed for Miscanthus. The fractionation properties of RM and PTM were variable in binary W-E systems, where RM biomass showed greater water uptake selectivity over ethanol. This research contributes to the field of advanced biomaterials and sustainability through an improved understanding of the role of biopolymer components for the adsorptive processing of beverages, food, and biofuels using sustainable and renewable biomass.

6.6 References

1. Hassan, E-S. R. E.; Mutelet, F.; Moïse, J-C.; Brosse, N. *RSC Adv.* **2015,** *5,* 61455-61464.
2. Ernest, R. R. Production of low-ethanol beverages by membrane extraction. U.S. Patent 4,306,884, Dec 22, **1981.**
3. Gubicza, L.; Kabiri-Badr, A.; Keoves, E.; Belafi-Bako, K. *J. Biotechnol.* **2000,** *84,* 193−196.
4. Karlsson, H. O. E.; Tragardh, G. *Trends Food Sci. Technol.* **1996,** *7,* 78−83.
5. Light, W. G. Production of low alcoholic content beverages. U. S. Patent 4,617,127, Oct 14, **1986.**
6. Stephen, L. M. Production of low-ethanol beverages by membrane extraction. U.S. Patent 4,778,688Oct 18, **1988.**
7. Dehabadi, L.; Wilson, L. D. *Energy Fuels* **2016,** *30(7),* 5684–5692.
8. Okewale, A. O.; Etuk, B. R.; Igbokwe, P. K. *Int. J. Eng. Technol.* **2011,** *11,* 81−91.
9. Baylak, T.; Kumar, P.; Niu, C. H.; Dalai, A. *Energy Fuels* **2012,** *26(8),* 5226− 5231.
10. Kim, Y.; Hendrickson, R.; Mosier, N.; Hilaly, A.; Ladisch, M. R. *Ind. Eng. Chem. Res.* **2011,** *50(14),* 8678−8685.
11. Liu, Y.-W.; Tang, T.; Chung, T. W.; Huang, Ch.; Lin, Y. S. *J. Chem. Eng. Data* **2010,** *55 (12),* 5807−5811.
12. Okewale, A. O.; Igbokwe, P. K.; Babayemi, K. A. *J. Chem. Eng. Process Technol.* **2015,** *6,* 1-8.
13. Ranjbara, Z.; Sun, N.; Niu, C. H.; Dalai, A. K. Adsorption of Water and Ethanol by Canola Meal in a Batch Liquid System. *CSBE – SCGAB,* **2013,** 1-10.
14. Dehabadi, L.; Wilson, L. D. *Energy Fuels* **2015,** *29,* 6512−6521.
15. Liu, Ch.; Xiao, L.; Jiang, J.; Wang, W.; Gu, F.; Song, D.; Yi, Z.; Jin, Y.; Li, L. *Food Energy Secur.* **2013,** *2(1),* 12-19.
16. Ale, M. T.; Mikkelsen, J. D.; Meyer, A. S. *Mar. Drugs* **2011,** *9,* 2106-2130.
17. Wang, H.; Shadman, F. *AIChE J.* **2013**, *59(5),* 1502–1510.
18. Li, H.; Liu, Y.; Gao, X.; Li, X. *J. Chem. Technol. Biotechnol.* **2016,** *91,* 977–984.
19. Soleimani, M.; Tabil, L.G.; Niu, C. *AICHE J.* **2015,** *61,* 1783-1791.

20. Sluiter, A.; Hames, B.; Ruiz, R.; Scarlata, C.; Sluiter, J.; Templeton, D.; Crocker, D. Determination of structural carbohydrates and lignin in biomass laboratory analytical procedure. National Renewable Energy Laboratory, Golden, Colorado, **2008.**
21. Dehabadi, L.; Wilson, L. D. *Carbohydr. Polym.* **2014,** *113,* 471−479.
22. Claridge, T. D. W. High-Resolution NMR Techniques in Organic Chemistry, 2nd ed.; Elsevier: Amsterdam, Netherlands, **2009,** 247− 302.
23. Morin-Crini, N.; Crini, G. *Prog. Polym. Sci.* **2013,** *38,* 344−368.
24. Karoyo, A. H.; Sidhu, P. S.; Wilson, L. D.; Hazendonk, P. *J. Phys. Chem. B* **2013,** *117,* 8269–8282.
25. Mohamed, M. H.; Udoetok, I. A.; Wilson, L. D.; Headley, J. V. *RSC Adv.* **2015,** *5,* 82065-82077.
26. Lowell, S.; Shields, J. E.; Thomas, M. A.; *J. Am. Chem. Soc.* **2005,** *127,* 14117-14120.
27. Meng, X.; Foston, M.; Leisen, J.; DeMartini, J.; Wyman, Ch. E.; Ragauskas, A. J. *Bioresource Technol.* **2013,** *144,* 467–476.
28. Mohamed, M. H.; Wilson, L. D.; Headley, J. V. *Carbohydr. Res.* **2011**, *346,* 219-229.
29. Gani, A.; Naruse, I. *Renew. Energ.* **2007,** *32,* 649–661.
30. Burhenne, L.; Messmer, J.; Aicher, T. Laborie, M. P. *J. Anal. App. Pyrol.* **2013,** *101,* 177–184.
31. Crini, G. *Prog. Polym. Sci.* **2005,** *30,* 38–70.
32. Wood, D. L.; Rabinovich, E. M. *Appl. Spectrosc.* **1989**, *43(2),* 263–267.
33. Mahaninia, M. H.; Wilson, L. D. *J. Applied Polym. Sci.* **2015,** *132,* 42949-42958.
34. Udoetok, I. A.; Dimmick, R. M.; Wilson, L. D.; Headley, J. V. *Carbohydr. Polym.* **2016,** *136,* 329-340.
35. Titirici, M-M.; Antonietti, M.; Baccile, N. *Green Chem*. **2008,** *10(11),* 1204–1212.
36. Zhu, Z.; Macquarrie, D. J.; Simister, R.; Gomez, L. D.; McQueen-Mason, S. J. *Sustain. Chem. Process* **2015,** *3(15),* 1-13.
37. Mittal, A.; Katahira, R.; Himmel, M. E.; Johnson, D. K. *Biotechnol. Biofuels.* **2011,** *4 (41),* 1-16.
38. Sasaki, T.; Matsuki, J. *Cereal Chem.* **1998,** *75,* 525–529.
39. Sannigrahi, P.; Miller, S. J.; Ragauskas, A. J. *Carbohyd. Res.* **2010,** *345,* 965–970.
40. Fan, L. T.; Lee, Y-H.; Beardmore, D. R. *Biotechnol. Bioeng.* **1980,** *22,* 177–199.

41. Hall, M.; Bansal, P.; Lee, J. H.; Realff, M. J.; Bommarius, A. S. *FEBS J.* **2010,** *227*, 1571–1582.
42. Bergenstrahle, M.; Mazeau, K.; Berglund, L. A. *Eur. Polym. J.* **2008,** *44(11)*, 3662−3669.
43. Matthews, J. F.; Bergenstrahle, M.; Wohlert, J.; Brady, J. W.; Himmel, M. E.; Crowley, M. F. *Biomacromolecules* **2015,** *16*, 2972−2978.
44. Wohlert, J.; Bergenstrahle-Wohlert, M.; Berglund, L. A. *Cellulose* **2012,** *19(6)*, 1821−1836.
45. Kulasinski, K.; Guyer, R.; Derome, D.; Carmeliet, J. *Biomacromolecules* **2015,** 16, 2972−2978.
46. Vårum, K. M.; Smidsrød, O. Structure-Property Relationship in Chitosans. In Polysaccharides: Structural Diversity and Functional Versatility; Dumitriu, S., Ed.; Marcel Dekker: NewYork, **2005,** 625-642.
47. Rojas, J. Effect of Polymorphism on the Particle and Compaction Properties of Microcrystalline Cellulose, Cellulose - Medical, Pharmaceutical and Electronic Applications, Theo van de Ven and Louis Godbout Pharmaceutical and Electronic Applications, L. B. T.-C.-M., Eds.; InTech: Rijeka, **2013,** p Ch. 02.
48. Olsson, A-M.; Salmen, L. *Carbohydr. Res.* **2004,** *339*, 813–818.
49. Rawat, S. P. S.; Khali, D. P. *Holz Roh. Werkst.* **1999,** *57*, 203-204.
50. Ding, Z.; Zhong, L.; Wang, X.; Zhang, L. *High Perform. Polym.* **2016,** *28*, 1–9.
51. Grewal, R. K.; Soleimani, M.; Tabil, L. G. Investigations on Biocomposites from Oat Hull and Biodegradable Polymers. In CSBE/SCGAB 2015 Annual Conference; **2015,** 1–9.
52. Chang, H. X.; Yuan, H. T.; Tian, H.; Zeng, A-W. *Ind. Eng. Chem. Res.* **2006,** *45*, 3916−3921.
53. Ranjbar, Z.; Tajallipour, M.; Niu, C. H.; Dalai, A. K. *Ind. Eng. Chem. Res.* **2013,** *52(40)*, 14429−14440.

CHAPTER 7

MANUSCRIPT 5: Spectroscopic and thermal methods for the study of biopolymer hydration

Leila Dehabadi, Abdalla H. Karoyo, and Lee D. Wilson*

Description

This study relates to the role of textural properties on the adsorption properties of biopolymer materials. It is revealed in Chapters 4 to 6 that variable uptake of water and ethanol was achieved according to the nature of the biopolymer and the level of synthetic modification. To achieve a greater level of understanding of the textural and surface chemical properties of various biopolymer systems and their hydration properties, a systematic materials characterization study using thermoanalytical and various spectroscopic techniques was undertaken to further characterize these biopolymer materials. As outlined in the previous chapters, the relationship between hydration effect and the mechanism of fractionation of water/ethanol in binary mixtures plays a key role on the adsorption properties. The results of this study showed that the swelling and sorption properties of polysaccharides depend strongly on the morphology and molecular structure as they relate to hydrophile-lipophile balance (HLB) and/or hydroxyl group accessibility.

Authors' Contributions

This project was conceived by the supervisor (L. D. Wilson) with input from L. Dehabadi on the hydration study of biopolymers. The structural characterization of these materials was done by L. Dehabadi. L. Dehabadi carried out the preliminary drafting of the manuscript with secondary assistance from A. Karoyo and editing provided by the supervisor throughout.

Relation of Manuscript 5 to Overall Thesis Objectives

This manuscript contributes to the knowledge gap and objectives introduced in section 2.4 of Chapter 2. The information presented in this manuscript is related to the role of structure and function of biopolymers and their adsorption properties. While this study is focused on the hydration properties, such processes play an integral role in understanding adsorption processes in aqueous solution. This study extends beyond the thermodynamic isotherm studies presented in Chapters 4 to 4 to yield further structural insight on the role of biopolymer structure. The role of

solvation effects in the adsorptive fractionation of water-ethanol (W-E) binary mixtures was examined by evaluating the accessibility of the -OH group and textural properties of biopolymers such as starch and cellulose. The results from this complementary and systematic study provide further insight concerning the role of hydroxyl group surface accessibility and the corresponding hydrophile-lipophile balance of the biopolymer structure in adsorption properties.

7. Spectroscopic and thermal methods for the study of biopolymer hydration

Leila Dehabadi[1], Abdalla H. Karoyo[1], Lee D. Wilson[1]*

[1]Department of Chemistry, University of Saskatchewan, 110 Science Place, Saskatoon, SK. Canada S7N 5C9

Supplementary Information (Appendix A, Chapter 7)

Graphical Abstract

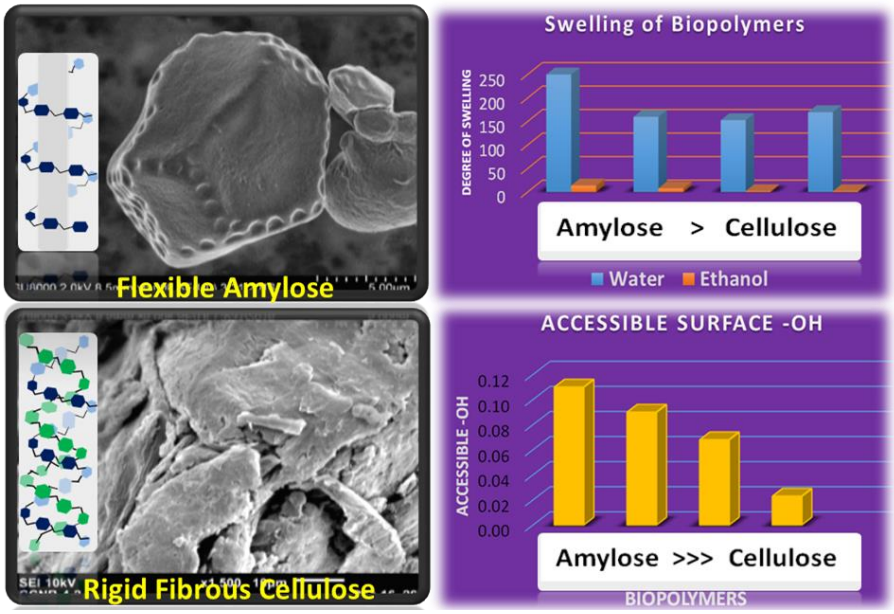

Research Highlights

- Understanding of the hydration properties of starch and cellulose through study of the morphological, thermal, swelling and rheological properties.
- To establish a molecular level understanding of the hydration phenomena of polysaccharide adsorbent/ solvent interactions by characterizing biopolymer structure.
- Study of the solvent-solvent and solvent-solute interactions on biopolymers in mixed solvents (water/ethanol).

7.1 Abstract

Solvent-selective adsorption processes in mixed solvent systems are poorly understood but are posited to relate to specific solute-solvent interactions at interfaces in accordance with the variable textural and surface chemical properties of biopolymer sorbent systems. To gain an improved understanding of the role of solvation effects and interfacial phenomena in mixed solvent (water-ethanol; W-E) systems, several types of polysaccharide sorbents (starches and cellulose) were studied by complementary analytical methods. Swelling of the polysaccharides was measured to ascertain the role of hydration and selective solvent uptake properties in binary W-E mixtures for cellulose (CE) and starch materials with variable amylopectin and amylose content. The hydration properties of the sorbents were further probed using differential scanning calorimetry (DSC) and Raman spectroscopy. Dye decolourization studies provided estimates of the surface-accessible hydroxyl (-OH) groups of the polysaccharides. The hydration properties of the biopolymer materials in W-E mixture are governed by the textural properties (pore structure and surface area) and accessibility of the polar –OH functional groups, in agreement with the isotherm results that reveal solvent-selective adsorption. This study contributes to a greater understanding of the role of structure and functional group accessibility governing biopolymers-solvent interactions. The trends in biopolymer solvation processes are further supported by scanning electron microscopy (SEM) results.

7.2 Introduction

Hydration phenomena at solid-solution interfaces play a key role in physical and biophysical processes in aqueous solutions.[1] In general, hydration has a large influence on the thermodynamics of processes involving the cleavage or formation of noncovalent bonds such as simple organic syntheses,[2,3] protein folding,[4] drug delivery systems,[5] and chemical separation processes.[6] In a previous study,[7,8] we reported the unique adsorption-based fractionation of water from water-ethanol (W-E) in binary mixtures using biopolymers and their modified forms. Adsorption processes involving biopolymer materials such as starch and cellulose enable a green strategy for the efficient separation of water and other organic molecules because the materials are abundant, low cost, require low energy inputs and basic infrastructure.[9] The adsorptive separation of solvents and organic mixtures has been reported previously using polysaccharide-based materials.[8,10,11] In particular, the fractionation of water from ethanol solution using starch- and cellulose-based adsorbents is well documented,[7,8,12–14] following the pioneering work of Ladisch and Dyck.[15] However, a molecular level understanding of the solvent selectivity in sorption-based processes of such biopolymer systems remains incomplete.

Various reports have investigated solvent-solvent interactions in W-E mixtures using theoretical [16] and spectroscopic [17] studies where the formation of H-bonded ethanol-ethanol clusters were suggested, in accordance with hydrophobic hydration phenomenon and the relative composition of ethanol in water. In cases where solid-phase polysaccharide adsorbent materials are employed to fractionate water from ethanol solution, biopolymer-solvent interactions are governed by the relative binding affinity between biopolymer surface sites and the solvent. Despite extensive research efforts, comprehension of the molecular-level details and hydration phenomena of biopolymer materials in W-E binary mixtures is limited. While a molecular level understanding is limited at present, recent adsorption studies [7,8] indicate that the physicochemical properties of biopolymers can be tuned via cross-linking methods to achieve variable solvent selectivity for modified biopolymers. Thus, it is posited that the textural properties and the role of surface-accessible functional groups play a key role in solvation phenomena. Gibbs surface energy and surface area models describing hydration phenomena can reliably predict Gibbs hydration energy, binding affinity, and hydration phenomena for well-defined molecular systems.[1] However, such models are limited in the case of large molecular assemblies with structural complexity as in the case of polysaccharides and macromolecular systems because of high computational demands.

While β-cyclodextrin (β-CD) is a structurally well-defined macrocyclic host system that has been studied by computational methods, high amylose starch poses greater challenges due to its higher molecular weight and greater degree of biopolymer chain entropy in solvent systems. By contrast, experimental methods that employ spectroscopic (FT-IR, NMR, and Raman) and thermoanalytical (DSC) methods provide tools to study the hydration properties of biopolymers with complex structures.[18–20] In particular, these techniques enable a detailed study of biopolymer/solvent interactions with consideration of their morphological, thermal, swelling and rheological properties.[18–20]

In this study, we report an investigation of the hydration properties of cellulose (CE) and several starch biopolymers derived from corn and maize and containing variable amylose (AM) and amylopectin (AP) contents. The starch materials used herein are maize starch (98% AP), soluble corn starch (50% AM) and high amylose starch (98% AM), and are denoted AP, AM50, and AM, respectively (*cf.* Table 7.1). The solvent-selective uptake properties of the biopolymers were investigated using batch sorption and swelling studies of neat solvents, water (W) and ethanol (E). The degree of decolourization of a model phenolphthalein (PHP) guest by the polysaccharide biomaterials provides a measure of the accessibility of the surface hydroxyl (-OH) functional groups of the biopolymers. The DSC and Raman spectroscopy results were compared with the solvent swelling and isotherm adsorption results that further reveal unique solvent selectivity in W-E binary solutions. The importance of this study is two-fold: i) to outline a systematic study of the structure and solvation characteristics of polysaccharide sorbents using complementary multi-instrumental methods, and ii) to provide a molecular level understanding of the structure-function relationship of the polysaccharide materials related to their hydration and sorption properties in W-E binary mixtures. This study contributes to an understanding of the hydration properties of biopolymers and the molecular level process of fractionation in W-E mixtures, where such hydration phenomena are the subject of ongoing scientific research for food processing, environmental remediation, and energy storage. Moreover, this research will catalyze further developments of green chemistry and engineering that employ platform biopolymers such as starch and cellulose materials because of their unique interfacial properties and increasing role as alternatives to petrochemicals in coatings, chemical synthesis, drug delivery, and catalysis.

7.3 Materials, chemicals and methods

7.3.1 Materials and chemicals

Cellulose (CE) and starches from various sources (corn or maize) containing variable amylose and amylopectin were chosen as the polysaccharide materials (*cf*. Table 7.1). All of the polysaccharides and ethanol (100% w/w) were purchased from Sigma Aldrich (Oakville, ON, Canada) and were used as received. Deionized and distilled water (Millipore) was used for the preparation of all aqueous solutions. Some of the physicochemical properties of the polysaccharides and the solvent components are listed in Table 7.1.

Table 7.1 Selected physicochemical properties of polysaccharides and solvents. NR = not recorded; ND = no data.

Polysaccharide	**Cellulose**	**Maize starch**	**Soluble starch**	**High Amylose Starch**
PS ID	CE	AP	AM50	AM
AP content (%)	-	98	50	2
Molar mass (g/mol)	($2.7x10^4$ - $9.0x10^5$)[21]	($5.30x10^7$) [22]	342.30	Average>$1.5x10^5$
Surface Area (SA; m^2/g)	0.96	1.52	NR	0.56
Water solubility (g/L)	Insoluble	10% soluble	Soluble	Negligible
Dielectric Constant (Ɛ)	1.2	3.6	ND	ND
Molar volume (V_m; ml/mol)	18.0		58.0	
Vapourization Enthalpy (ΔH_{vap}; kJ/mol)	40.6		38.6	

7.3.2 Methods

7.3.2.1 Swelling tests

The swelling properties of the polysaccharides were measured using 20 mg of the adsorbent equilibrated in 7 ml of Millipore water or neat ethanol for 48 h. The degree of swelling (S) in water (S_W) or ethanol (S_E) for the different materials was determined using the relationship in equation 7.1 below, where W_s is the wet sample, and W_d is the dry sample after oven drying at 60 °C:

$$S_W = \frac{(W_s - W_d)}{W_d} \times 100\% \qquad \text{Equation 7.1}$$

7.3.2.2 Phenolphthalein decolourization studies

The accessibility of the surface hydroxyl (-OH) groups of the polysaccharides were estimated based on the decolourization of phenolphthalein (PHP) in aqueous solution, according to a method that was previously reported.[10, 23] Seven mL of solution containing PHP in $NaHCO_3$ aqueous buffer at pH 10.5 was added to vials with variable mass (1 mg – 10 mg) of biopolymer material and allowed to equilibrate with shaking for 24 h at 295 K. This was followed by centrifugation (Precision Micro-Semi Micro Centricone, Precision Scientific Co.) at 1550 rpm and measurement of the absorbance using a double beam spectrophotometer (Varian CARY 100) at room temperature (295 ± 0.5 K) and λ_{max} of 552 nm.

7.3.2.3 Differential Scanning Calorimetry (DSC)

The DSC thermograms acquired from starch or cellulose samples were equilibrated with known amounts of water and ethanol solvents. Twenty mg of biopolymer were added to 4 dram glass vials containing 10 mg of solvent with variable water/ethanol (W-E) weight (%) content. The sample vials were incubated by shaking (Poly Science, Dual Action Shaker) for 24 h at 160 rpm at ambient pH and temperature to achieve equilibrium. Thereafter, the samples were separated from the solutions using a vacuum filter to obtain the solvated solids for analysis by DSC. The samples were added to DSC pans and sealed with a hole punched in the sample lid to allow for outgassing of vapour during heating over the temperature range 30 °C – 150 °C.

7.3.2.4 Raman spectroscopy

The samples for Raman spectroscopy were prepared as above (*cf.* Section 7.3.2.3), where the water content was isotopically mixed with 10% (w/w) D_2O/H_2O. The hydrated biopolymer samples were isolated by centrifuging (Precision Micro-Semi Micro Centricone, Precision Scientific Co.) at 1800 rpm for 1 h to obtain hydrated solids for analysis.

7.4 Results

7.4.1 Textural properties of polysaccharides

The textural properties (porosity and surface area) of sorbent materials play a key role in the relative accessibility of the active sorption sites in the case of biopolymers and their separation efficiency of W-E systems. Scanning Electron Microscopy (SEM) and Scanning Tunneling Microscopy (STM) provide important structural information regarding the morphology and pore structure of such polysaccharide materials.[24] The SEM images for AP, AM50, AM, and CE are shown in Figure 7.1. The starch materials display distinct particle-grain shapes and sizes that vary from large to small and oval to irregular, with variable diameters (5 – 50 μm). The SEM results for AP reveal minor surface pores (*cf*. Figure 7.1A); whereas, AM50 and AM display relatively smooth surface features that are nearly devoid of pores.[25] The SEM results of CE reveal the quaternary fibril structure of the biopolymer, as evidenced by the textural features in Figure 7.1D.

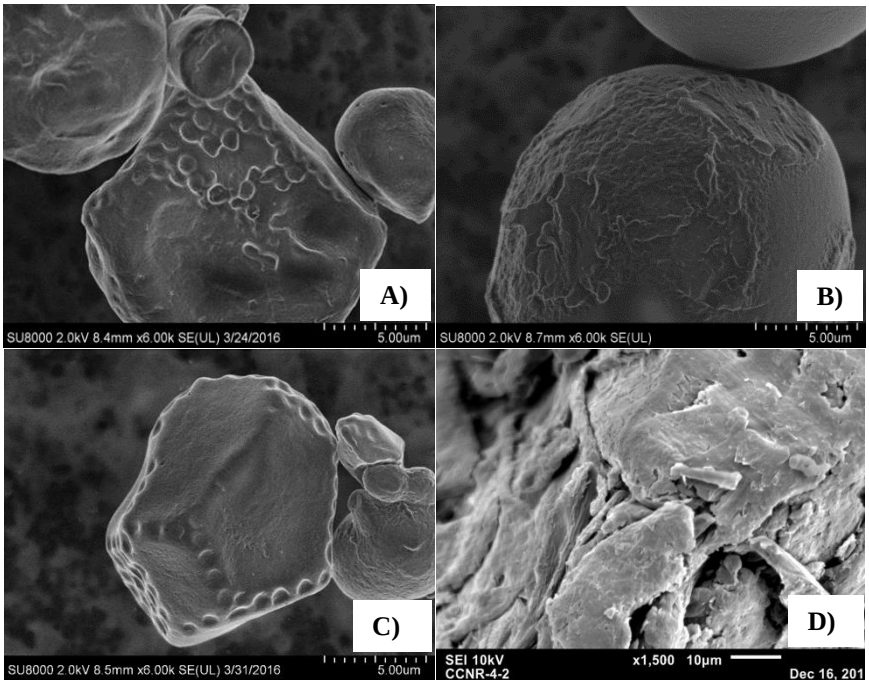

Figure 7.1 SEM micrographs for the various native biopolymers.

7.4.2 Swelling and uptake properties of sorbents

Solvent swelling is an important process in drug delivery systems [26,27] and contributes to the W-E separation in adsorptive fractionation processes.[28] Swelling phenomena at equilibrium conditions relate to adsorption and absorption processes, collectively referred to as sorption. The thermodynamics of solvent sorption processes by materials can be partly related to surface interactions that vary according to the textural porosity, according to Table 7.2. The degrees of swelling (%) of the polysaccharide materials in W-E generally decrease in the following order: AM (248) > CE (166) > AM50 (157) > AP (153). This trend in swelling parallels the monolayer uptake Q_m (W) properties of the biopolymers with water from binary W-E mixtures. The magnitudes of Q_m (W) (g of water per g of biopolymer) values vary as follows: CE (1.63) > AM (0.608) > AM50 (0.0202) ≈ AP (0.0206).[8]

Table 7.2 Swelling and uptake properties of biopolymers in water-ethanol mixtures.

MATERIALS	AP	AM50	AM	CE
$^{1}S_{E}$ (%)	2.1±0.5	8.0±2	14±6	2.0±0.1
$^{1}S_{W}$ (%)	153±10	160±21	250±12	170±10
$^{2}Q_{m}E$ (g/g)	0.032±0.001	0.051±0.008	0.0084±0.0025	1.03±0.13
$^{2}Q_{m}W$ (g/g)	0.21±0.03	0.20±0.08	0.61±0.11	1.6±0.2

[1] Swelling of biopolymers in Ethanol (E) and Water (W)
[2] Sorption capacities of Ethanol (E) and Water (W) in binary W-E mixtures of variable composition.

7.4.3 Phenolphthalein Decolourization Studies

The surface properties and dipolar character of the biopolymer surface were probed through the decolourization of phenolphthalein (PHP) dye as a model guest (*cf*. Appendix A7, Figure A7.1). The dye adsorption method provides an estimate of the surface-accessible hydroxyl (-OH) groups,[29] since PHP is known to interact with polysaccharides via ion-dipole interactions at alkaline pH.[30] In general, the level of dye decolourization correlates with the relative accessibility of the -OH groups of the biopolymer. Figure 7.2 illustrates the decolourization results obtained from the adsorption isotherm in the saturation region at a fixed level of biopolymer (*ca.* 30 mg) for each system. The extent of dye decolourization varies for the biopolymers as follows: AM > AM50 > AP >> CE, according to the relative absorbance change (ΔAbs) in Figure 7.2.

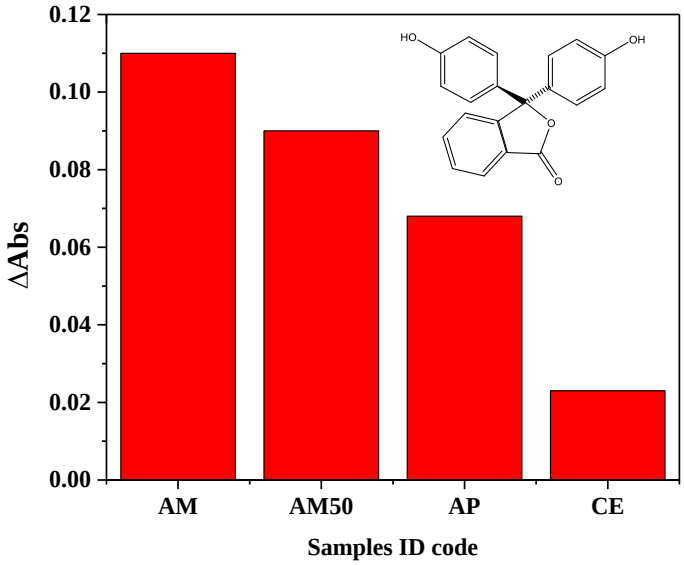

Figure 7.2 Dye decolourization of biopolymers in the presence of phenolphthalein (see inset denoting the structure of the non-ionized form of phenolphthalein).

7.4.4 Differential Scanning Calorimetry

DSC provides a measure of the degree and nature of the sorbed water by monitoring the dehydration temperature profile of the endotherms (ΔH_{vap}). DSC has been widely used to study the thermal properties of starch materials since its first use by Steven and Elton,[31] and its application for the study of macromolecular hydration was recently reviewed.[32] Moreover, the complex thermal behaviour of starch is known,[33] where numerous physicochemical changes can occur upon heating starch and its modified forms. Structural changes of this type involve dynamic processes and phase transitions such as gelatinization, melting, glass transition, and crystallization. DSC transition temperatures and gelatinization enthalpies of starch materials relate to properties such as the degree of crystallinity and solubility.[34,35] Stevens and Elton[31] observed an endotherm transition for starch-water mixtures at the 1:2 mole ratio in the temperature range between 54 and 73°C that was attributed to gelatinization. Other reports indicate two [36] and three [37] endotherms after heating wheat/potato starch to about 150 °C that contained 27% and 35-80% water content, respectively. Various studies [38,39] reveal the glass transition temperatures (T_g) of starch and its products differ markedly based on the water content.

Despite the complex structure of starch, DSC profiles provide important insight on the thermal properties for such materials, especially at variable hydration. The nature of biopolymer-solvent interactions can be inferred based on thermal events related to adsorbed solvent since samples of free (weakly bound), strongly bound, and desorbed water reveal unique DSC profiles with variable heat flow, intensity, and temperature shifts.[40] Figures 7.3A-D shows the DSC dehydration/gelatinization endotherms for polysaccharide systems with variable W-E content over the 30 – 140 °C temperature range. In Figure 7.3, the stability of the bound water generally varies in descending order: CE > AP ≥ AM50 > AM (*cf.* Figure 7.3). Amylose starch (AM and AM50) systems show a wide range of endothermic transitions (*ca.* 40–140 °C), especially at higher AM content.

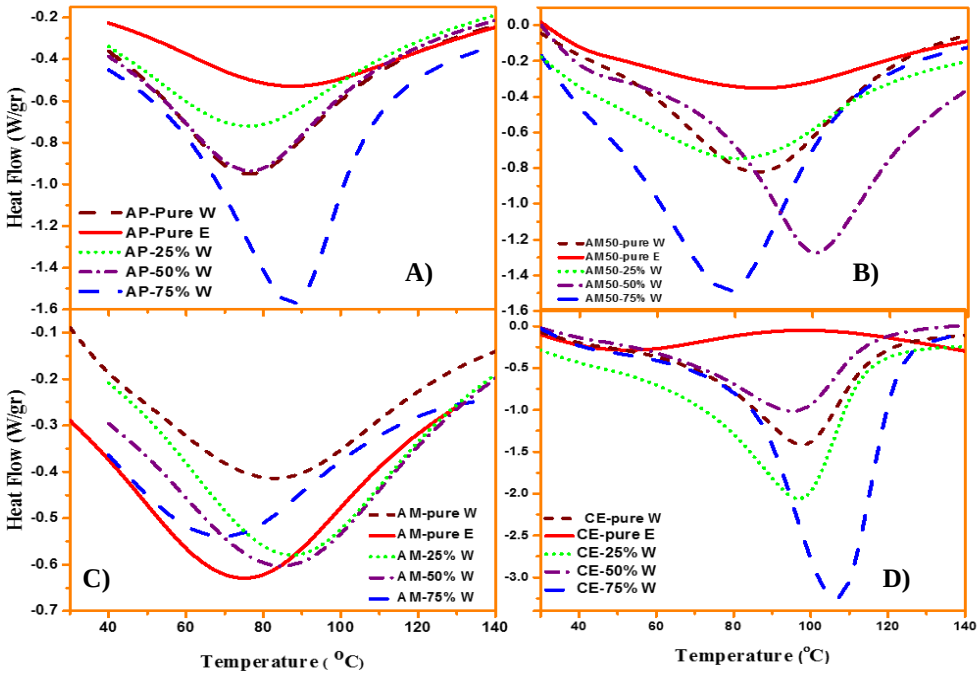

Figure 7.3 The differential scanning calorimetry results for the various biopolymer materials; A) AP, B) AM50, C) AM, and D) CE, with variable water/ethanol content.

In contrast, the DSC profiles for CE and AP cover a narrower range (*ca.* 80–120 °C). Variable water sorption affinity is shown by a decreasing trend in the thermal transitions: CE > AP ≥ AM50 > AM. Figure 7.4 summarizes the endotherm intensity and temperature shift for the systems, where variable trends occur according to the relative content of the W-E solvent. At 75%

W, the profiles reveal significant enthalpy change, whereas hydrated biopolymers with 100%W or with ethanol (0%W) display the lowest variation in endotherm intensity.

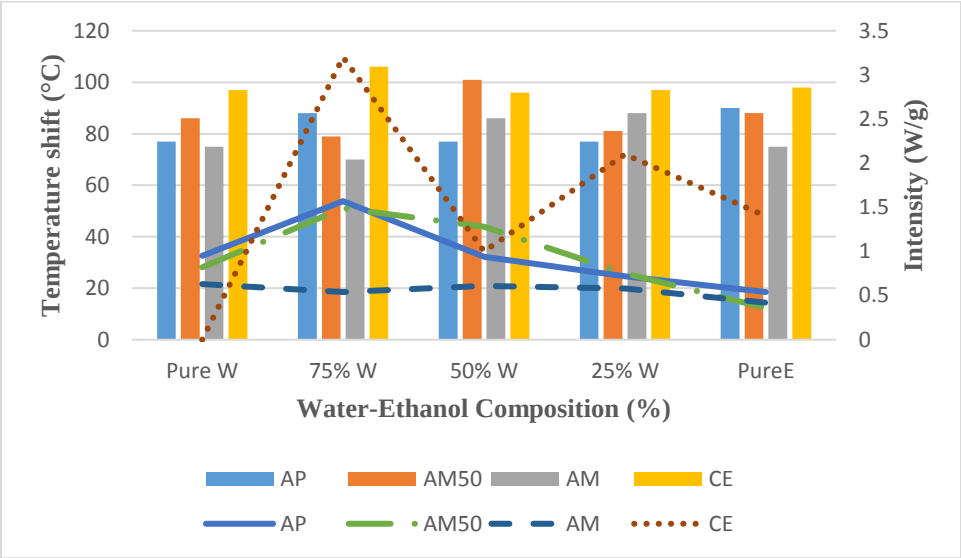

Figure 7.4 Temperature shift and intensity variations of the biopolymer-solvent systems at variable W-E content obtained from DSC results.

7.4.5 Raman Spectroscopy

Raman spectroscopy provides insight on the role of microenvironmental effects for macromolecules due to the sensitivity of Raman spectral intensity changes in polarization and noncovalent interactions.[41] The relatively low scattering cross-section of water aids in the study of hydration processes of biopolymers using Raman spectroscopy. Figure 7.5 illustrates the Raman spectra of various solid-phase biopolymers with variable levels of sorbed solvent (W or E). The Raman spectra of the solvated biopolymers were obtained between 2200 cm^{-1} – 3200 cm^{-1}, where the water fraction contains isotopic levels of D_2O (10% w/w), as described above. The variations in line-width/-shape of the uncoupled oscillator HOD Raman bands relate to microenvironmental effects such as biopolymers with bound *vs.* unbound water.[42,43]

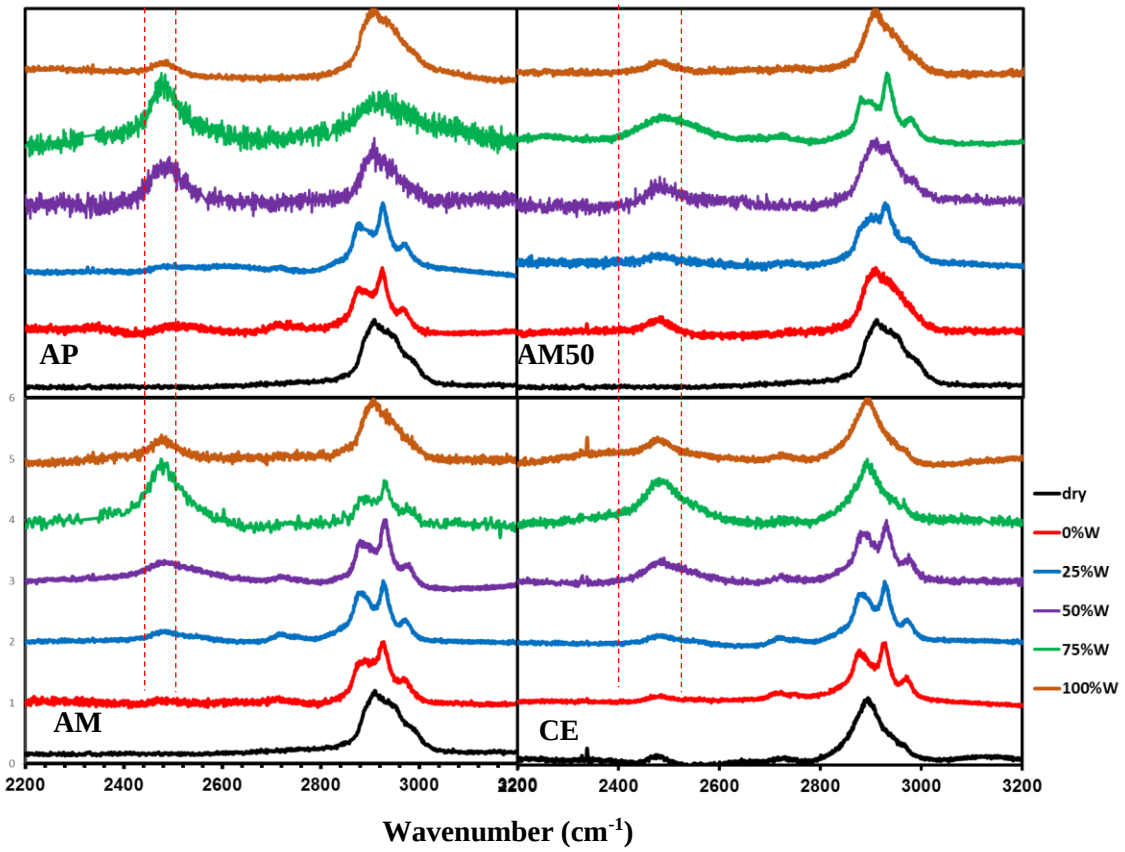

Figure 7.5 Raman spectra of biopolymer materials in W-E solvent systems containing D_2O (10% w/w), where the relative water (W) content is denoted by the inset.

The Raman spectra (Figure 7.5) are dominated by vibrational bands at ~2900 cm^{-1}. Polysaccharides typically display strong C-H stretching bands at ~2800 - 3000 cm^{-1} with broad O-H bands at ~3100 – 3600 cm^{-1}.[44,45] In the case of the Raman spectra of W-E mixtures, a characteristic sharp C-H band is observed for ethanol near 2900 cm^{-1}; whereas, the solvent O-H band appears *ca.* 3000-3400 cm^{-1}.[46] The C-H stretching bands (*ca.* 2900 cm^{-1}) relate to combined vibrational contributions from starch and ethanol and vary according to the solvent composition. The C-H band at 2900 cm^{-1} shows subtle red/blue Raman shifts up to ~15 cm^{-1}, indicative of microenvironmental effects at variable W-E content. While the Raman scattering cross-section of H_2O is low, the use of 10% D_2O/H_2O mixtures results in a band at 2500 cm^{-1} due to the HOD uncoupled oscillator contributions of the solvent. The spectroscopic features (intensity, FWHM, and shift) of this band are summarized in Table A7.1 of Appendix A7. The intensities of the HOD bands for these materials increase monotonically as the water content increases from 25%W to 75%W. Raman shifts of up to ~15 cm^{-1} are observed but do not appear to follow a well-defined

trend. Generally, the starch materials with greater amylose content (AM and AM50) show greater FWHM values and larger Raman shifts (Figure 7.5 and Table A7.1) *vs.* AP and CE.

7.5 Discussion

The hydration properties of starch and cellulose materials were compared because of the unique fractionation properties of such biopolymers and their modified forms in W-E mixtures.[7,8,47] While starch and cellulose are derived from glucose monomers,[48] the corresponding biopolymers have diverse molecular structure and complex morphology (*cf.* Figure 7.6). Starch is a semi-crystalline polymer linked by α(1→4) glycosidic bonds that consist of linear (amylose; AM) and branched (amylopectin; AP) forms that differ based on the position of the glycosidic bond (*cf.* Figures. 7.6A and B).[48,49] Cellulose (*cf.* Figure 7.6C) has β(1→4) glycosidic bonds and has greater rigidity and crystallinity over starch, attributed to the intra- and inter-molecular H-bonding between neighbouring glucosyl units and cellulose chains.[50,51] Cellulose is a supramolecular assembly because of the extensive intermolecular H-bonding between cellulose biopolymer chains, which can aggregate or self-assemble to form micro- and macro-fibrils.[51,52] The structural variability of starch and cellulose affects the textural (pore size distribution and surface area) properties and surface-accessible functional groups of these biopolymers.

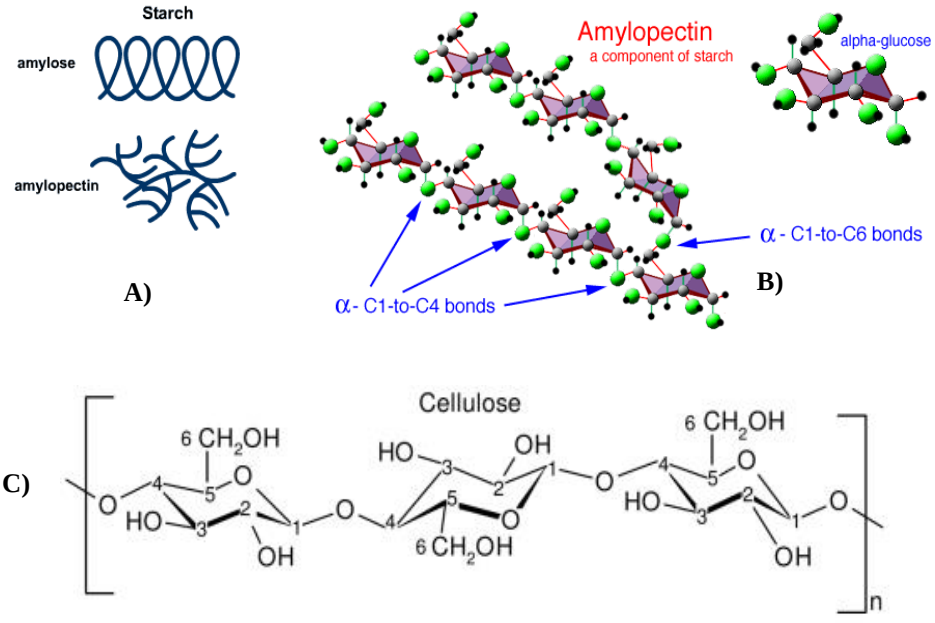

Figure 7.6 A) Schematic presentation of linear-chain amylose and branched amylopectin. Structures of B) starch and C) cellulose.[53]

The complementary techniques employed above reveal molecular level details regarding hydration properties of biopolymers in W-E binary mixtures. In particular, the trends in solvent swelling (AM > CE > AM50 > AP) in section 7.4.2 correlate well with solvent affinity for W-E systems (CE > AM > AM50 ≈ AP) with minor differences. Variable swelling occurs due to the role of polar functional groups, surface accessibility, the hydrophile-lipophile balance (HLB), and textural properties of the biopolymers, according to their physicochemical properties (*cf.* Table 7.1) and the SEM results (*cf.* Figure 7.1). Swelling behaviour is influenced by absorption and adsorption (sorption) processes that relate to the important role of hydrophilic biopolymer-solvent interactions in the W-E system.[53] In general, starch materials have greater hydrophilic character than cellulose (*cf.* Table 7.1) according to the surface accessibility of the hydroxyl groups. In the solid state, nitrogen adsorption isotherms reveal that cellulose has greater permanent surface area and pore volume over starch materials, in agreement with the rigid fibril structure of CE reported elsewhere.[8] In Table 7.2, the swelling of the starch materials appears to increase with amylose content (AM > AM50 > AP) of the biopolymer, and may relate to the polar group accessibility and amorphous regions of such materials.[20] The ability of such biopolymers to swell in aqueous solution contributes to the large differences in textural properties in their dry *vs.* hydrated state.[54] Non-amorphous *vs.* crystalline domains have variable hydrate content due to hydrogen bond donor/acceptor sites with variable accessibility. In the case of high amylose starch (AM), the linear topology and configurational entropy of AM contributes to greater O-H group accessibility, which contributes to greater swelling and increased Q_m (W) values in binary W-E solvents.[7,47]

The surface accessible –OH groups of the biopolymers were estimated using the PHP dye method, where variable decolourization occurs in descending order: AM > AM50 > AP >> CE. The surface-accessible active sites of various starch materials reported by Fannon *et al.*[25] and Gallant *et al.*[26,55] indicate that the relative accessibility of the starch-active sites in the quaternary level of granule organization influences the reactivity toward enzymatic reagents. Herein, biopolymers with greater –OH group accessibility such as AM and AM50 reveal greater dye decolourization, solvent swelling, and selective water uptake. It is noteworthy that dye decolourization is a surface-sensitive method that differs from the solvent swelling due to the combined effect of sorption (adsorption and absorption) especially for binary W-E mixtures with high water content. Biopolymers are anticipated to interact differently with water *vs.* PHP based on polarity, size, and steric effects. The notable water uptake, reduced accessibility of the surface

–OH groups (*ca.* 30%; *cf*. Figure 7.2),[56] and reduced water solubility of CE (*cf*. Table 7.1) are related to sorption phenomena due to the unique fibril structure of CE. The lower accessibility of PHP for the -OH groups of CE are in agreement with a recent study for CE and its cross-linked forms.[10] On the other hand, branched biopolymers such as AP have less rigidity with greater configurational entropy, accessibility, and favourable dye uptake compared with the rigid CE biopolymer. The single and double helical structures of starch are schematically illustrated in Scheme 7.1.

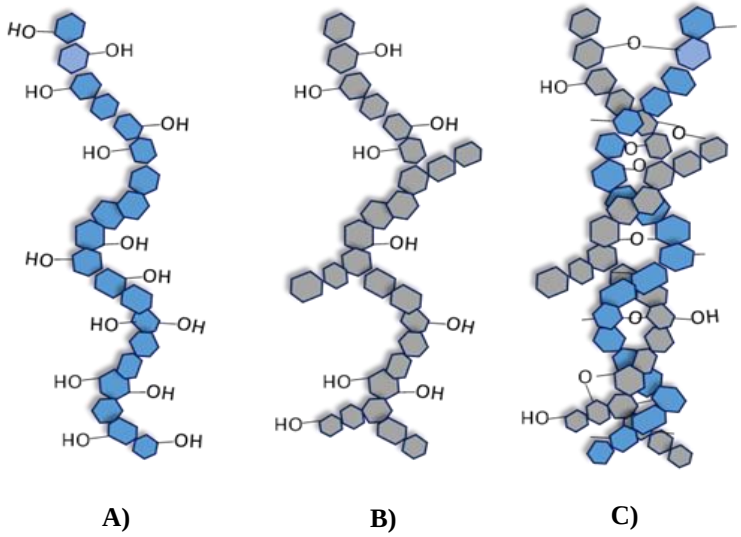

Scheme 7.1 Illustrative representation of biopolymer structure: A) single helical structure of amylose and B) amylopectin, and C) double helical structure of amylopectin. Note that the intra- and inter-molecular hydrogen bonding interactions are not shown.

It is noteworthy that similar decolourization results were observed for AM and AM50 (*cf*. Figure 7.2) despite the near linear morphology of AM and presence of branching in AM50. The presence of active sites such as surface pores, internal cavities, and channels is known to affect the binding properties of starch materials, according to light and fluorescence microscopy results.[53,57] However, the active sites and surface accessible -OH groups for these biopolymers are likely diminished, even under slight swelling conditions,[53] in accordance with hydration effects on the configurational entropy of the biopolymers (*cf.* Table 7.1). Evidence of surface accessibility on

dye decolourization was observed to increase for cross-linked cellulose and this may be understood due to "pillaring effects"[58] since cross-linking increases the surface accessible –OH groups.

In Table 7.2, AP displays favourable water uptake properties despite its reduced swelling, in agreement with its branched and conformational labile structure depicted in Scheme 7.1B. In general, the conformational degrees of freedom for starch contribute to its greater packing efficiency and reduced pore structure as compared with CE. CE has a more rigid structure with less swelling relative to the starch materials, in agreement with the nitrogen isotherm[8] and SEM results herein. In general, the swelling and water uptake results in Table 7.2 for starch and cellulose reveal that the uptake in pure water exceeds ethanol by an order of magnitude, and indicates the preferential solvent affinity of W over E, in agreement with the fractionation behaviour in W-E solutions.[7,47]

DSC, and Raman spectroscopy provide molecular level insight on biopolymer hydration processes. The DSC results indicate that the affinity of the biopolymers for water and the stability of the bound water are listed in descending order: CE > AP ≥ AM50 > AM, in agreement with the trend in DSC temperature and endotherm intensity (*cf*. Figure 7.3 and 7.4). The unique fibril assembly of CE accounts for unique uptake properties *vs.* starch according to the textural properties (pores, channels and cavities) illustrated in Scheme 7.2.

The accessibility of surface -OH groups for CE, and AP to a greater extent, allows them to participate actively in H-bonding interactions with water, leading to DSC transitions at higher temperature. Accessible free -OH groups present on the biopolymer surface are where the active sorption occurs in amorphous regions and micropore domains of the CE fibril bundles.

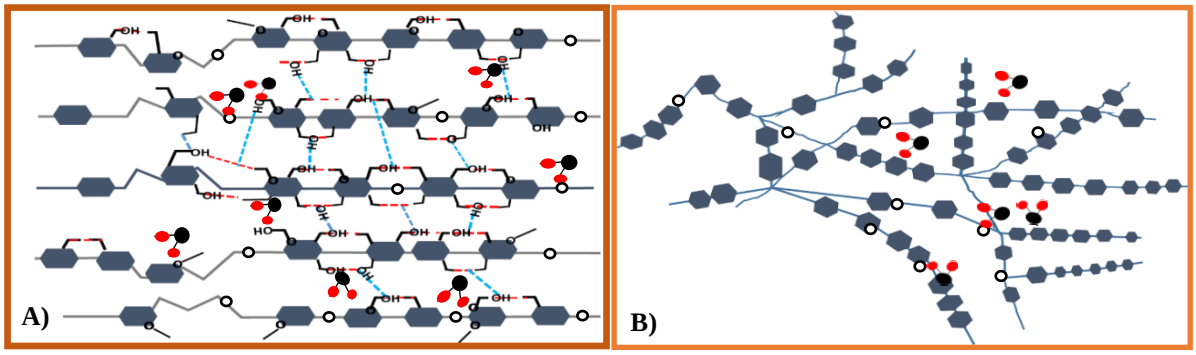

Scheme 7.2 A) Supramolecular structure of cellulose showing single strands (grey lines) connected by intra- (red dots) and inter-molecular (blue dots) hydrogen bonds to create fibrils with channels and cavities. The regions of zig-zag and straight lines are the amorphous and crystalline domains, respectively. B) Structure of starch showing highly branched amylopectin.

DSC gelatinization transitions are prominent in starch materials; such process was reported for corn starch at 190–200 °C for water content (11–30%).[59] Above 30% water content, the amorphous region of the starch gelatinizes at much lower temperature (~70 °C).[59] In the case of high amylose (AM and AM50) biopolymers, the occurrence of gelatinization is high, according to the greater swelling values (*cf.* Table 7.2) and in agreement with the broad DSC transition observed for these materials (*cf.* Figure 7.3). The DSC endotherm profiles of starch shift to higher temperature with greater AP content, as follows: AP > AM50 > AM (*cf.* Figure 7.4), in agreement with the thermal properties of linear *vs.* branched starch.[60–63] Starch materials containing greater AP content display higher dehydration temperature and enthalpy changes due to greater chain entanglement over AM starches.[60–62] The lower melting (gelatinization) temperature of AM starch is supported by its decreased crystallinity.[63] Therefore, solvent swelling, water uptake, and DSC results support the idea that starch hydration relates to the amount of double helical domains (AP) *vs.* single helical structures (AM),[20] as illustrated by Schemes 7.1 and 7.2. The ΔH_{vap} values undergo an increase when the samples are imbibed at higher water content (75 wt. %) in binary W-E mixtures, as evidenced by the greatest variation in DSC profiles (*cf.* Figure 7.4). The variable hydration for these biopolymers is observed from DSC temperature shifts and endotherm intensity variations at variable W-E solvent content. Hoogenboom *et al.*[64] have shown that physicochemical properties such as solubility, conformational entropy and self-assembly of polymers are strongly influenced by the solvent composition. In the case of pure ethanol, the endotherms of biopolymers

at ~80 °C in Figure 7.3 relate to the ethanol vapourization (ΔH_{vap}) of the solvent (*cf*. Table 7.1). By comparison, AM shows greater endotherm intensity due to its greater functional group accessibility, as described above.

In the case of the Raman results, attention was focused on the behaviour of the uncoupled OD vibrations and the FWHM since it was related to the nature of H-bonding of the biopolymer-solvent system.[42,43,65] The OD bands for AM and AM50 starch systems were broader with corresponding red shifts relative to AP and CE. The Raman results for the HOD bands with variable FWHM and intensity indicate greater sorbed water (solvent-solute) in microenvironments with weakly-bound/absorbed *vs.* strongly-bound/adsorbed water, especially in the case of AM and AM50. By contrast, AP and CE display attenuated OD bands with a reduced FWHM, and provide support of highly ordered water due to greater H-bonding within the micropore and fibril domains of CE. The Raman results provide support that variable H-bonding occurs for AP and CE due to absorbed *vs.* adsorbed water, as described above. The Raman spectra of hydration and bulk water consist of three components at ~2400 cm^{-1}, 2500 cm^{-1} and 2600 cm^{-1}, where the 2600 cm^{-1} band describes non-hydrogen bonded water (OD).[42] The broader bandwidths for AM and AM50 may be related to the weakly-bound water in the micropore domains, in agreement with their greater swelling and gelation properties.

7.6 Hydration Phenomena of the Polysaccharides

The hydration properties of the biopolymers vary due to three main factors: 1) structural factors related to the site accessibility of the polar functional groups of the biopolymer, 2) composition of the W-E solvent mixture, and 3) the physicochemical properties of water and ethanol. High amylose starches (AM and AM50) are characterized by broader endotherms with transitions at lower temperatures, providing evidence of weakly and strongly bound water. AP and CE display relatively sharp endotherms with shifts to higher temperatures, consistent with strongly bound water. The uncoupled OD Raman bands with red shifts, greater intensity, and bands with greater FWHM for AM starch systems provide support of weakly bound water, in agreement with DSC results.

Competitive solvation of biopolymers in mixed W-E systems is governed by the relative solvent affinity. The main driving force for selective solvation in mixed W-E systems may involve: i) the ability of the sorbent material to sorb water preferentially within its 3D network, ii) steric

effects and/or availability of the accessible sites of biopolymer for H-bonding interactions, and iii) the HLB of the biopolymer surface. High amylose (i.e. AM and AM50) starches' hydrophilic nature with abundant surface accessible –OH groups account for the solvent swelling and water uptake properties for these materials, in accordance with the textural properties of starch.

In the case of AP and CE, the variable textural properties are supported by the SEM results, which provide an account of the water uptake properties. The water swelling properties of CE (*cf.* Table 7.2) relate to its apolar character, which accounts for its reduced –OH group accessibility imparted by its quaternary fibril structure,[32] as compared with starch biopolymers that are more hydrophilic in nature. AP starch has favourable sorption properties due to its branched network structure that can undergo cooperative H-bonding with water. However, water uptake may occur within the voids and micropore domains of AP and CE via absorption, especially when the surface accessibility of the –OH groups is reduced due to steric effects. By contrast, AM biopolymers have more surface accessible –OH groups for H-bonding due to their linear morphology, in agreement with dye decolourization results in Figure 7.2. The surface accessibility of polar functional groups of the biopolymers governs the solvation processes in W-E mixtures. In turn, starch and cellulose possess variable HLB according to their structures, which relate to solvent affinities between W and E that differ according to the dielectric constant ($\varepsilon_W \approx 80$; $\varepsilon_E \approx 24$) and molar volume [V_m(W) = 18 cm^3/mole; V_m(E) = 58 cm^3/mole)] values in Table 6.1. The small molecular size of water and its large dielectric constant contribute to more efficient H-bonding over ethanol,[66] in agreement with its cohesive energy density and enclathration properties. By contrast the H-bond network of ethanol has a more 2D network character with a propensity to form hydrated clusters, where ethanol and water undergo favourable solvent-solvent interactions.[16] The hydration properties of the biopolymer systems studied herein are illustrated in Scheme 7.3.

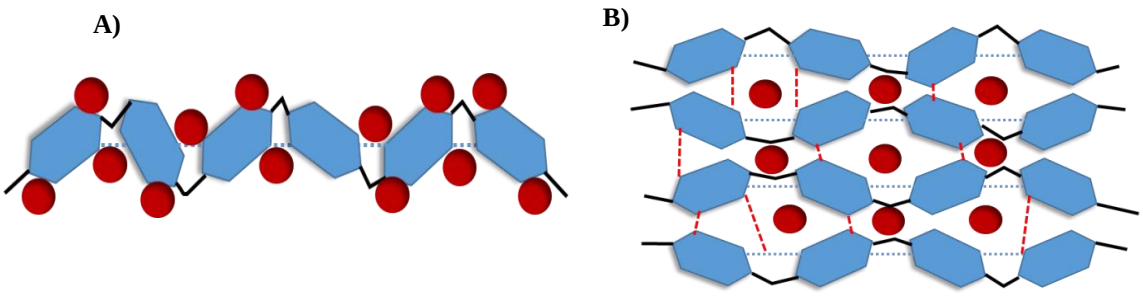

Scheme 7.3 The hydration phenomena for A) high amylose starches, where swelling and biopolymer surface-solvent hydrogen-bonding are anticipated, and B) cellulose and high amylopectin starch, where absorption and hydrogen-bonding occur within the cavities. The accessiblity of surface hydroxyl groups is reduced in cellulose due to massive intra- (blue dotted lines) and inter-hydrogen bonding (red dashed lines). The glycosidic linkages are shown by black lines.

7.7 Conclusion

The hydration phenomena of the various starch- and cellulose-based biopolymers (AP, AM50, AM, and CE) were studied using DSC, Raman spectroscopy, SEM, solvent swelling in neat/mixed systems, and adsorption isotherms. The swelling of the biopolymers was greater for high amylose (AM) and soluble starch (AM50) due to their flexible biopolymer backbone and increased fraction of surface accessible hydroxyl (-OH) groups. The conformational entropy of the starch materials (AM, AM50 and AP) accounts for their limited pore structure due to their high packing efficiency in the solid state; whereas, cellulose (CE) is more porous due to its rigid fibril structure, in agreement with the SEM results.

Variable surface accessibility of –OH groups for starch systems is supported by the decolourization results. In contrast to starch biopolymers, the surface –OH functional groups of CE are less accessible. Despite reduced surface –OH accessibility, CE and AP show similar hydration properties, in agreement with the DSC and Raman results and consistent with water uptake within the voids and micropore domains of these biopolymers via absorption. In contrast, high amylose (AM and AM50) and high amylopectin (AP) starches differ in their hydration properties due to variable branching and packing defects, which can offset the surface-accessible -OH groups in solution in the former due to swelling effects. The superior hydration properties of CE relate to the quaternary fibril structure that accounts for water uptake due to both absorption and adsorption processes, along with the small molar volume and dipolar nature of water. The

factors pertaining to the biomaterial and solvent that influence the hydration of polysaccharides are described, as follows: 1) the propensity of the biopolymer material to swell and ingress water within its 3D polymer network, 2) steric effects and/or availability of the accessible sites of biopolymer for H-bonding interactions, 3) the hydrophile-lipophile balance of the biopolymer surface, and 4) the nature and composition of the solvent in binary mixtures. An improved understanding of these factors will contribute significantly to awareness of the structure-property relationships of biopolymers and their modified forms in their use as sorbents for a diverse range of applications from food production and carrier systems to environmental remediation of waterborne contaminants.[71, 72]

7.8 References

1. Levy, R. M.; Zhang, L. Y.; Gallicchio, E.; Felts, A. K. *J. Am. Chem. Soc.* **2003**, *125*, 9523–9530.
2. Reichardt, C.; Welton, T. Solvents and Solvent Effects in Organic Chemistry; Wiley-VCH Verlag GMbH & Co. KGaA: Weinheim, Germany, **2011.**
3. Lubineau, A.; Auge, J. Modern Solvents in Organic Synthesis; Knochel, P., Ed.; Springer-Verlag: Berlin, Heidelberg, **1999.**
4. Privalov, P. L.; Makhatadze, G. I. *J. Mol. Biol.* **1993,** *232*, 660–79.
5. Bussemer, T.; Peppas, N. A.; Bodmeier, R. *Eur. J. Pharm. Biopharm.* **2003**, *56*, 261–270.
6. Llewellyn, P. L.; Bourrelly, S.; Serre, C.; Filinchuk, Y.; Férey, G. *Angew. Chemie - Int. Ed.* **2006**, *45*, 7751–7754.
7. Dehabadi, L.; Wilson, L. D. *Energy Fuels* **2015**, *29*, 6512–6521.
8. Dehabadi, L.; Wilson, L. D. *Carbohydr. Polym.* **2014**, *113*, 471–479.
9. Wang, Y.; Gong, C.; Sun, J.; Gao, H.; Zheng, S.; Xu, S. *Bioresour. Technol.* **2010**, *101*, 6170–6176.
10. Udoetok, I. A.; Dimmick, R. M.; Wilson, L. D.; Headley, J. V. *Carbohydr. Polym.* **2016**, *136*, 329–340.
11. Crini, G. *Prog. Polym. Sci.* **2005**, *30*, 38–70.
12. Beery, K. E.; Ladisch, M. R. *Ind. Eng. Chem. Res.* **2001**, *40*, 2112–2115.
13. Hsu, S. H.; Hsu, W. C.; Chung, T. W.; Liao, C. C. *J. Taiwan Inst. Chem. Eng.* **2013**, *44*, 952–956.

14. Wu, P.; Gao, H.; Sun, J.; Ma, T.; Liu, Y.; Wang, F. *Bioresour. Technol.* **2012**, *107*, 437–443.
15. Ladisch, M. R.; Dyck, K. *Science* **1979,** *205*, 898–900.
16. Lamoureux, G. *J. Phys. Chem B* **2005**, *109(14),* 6705–6713.
17. D'Angelo, M.; Onori, G.; Santucci, A. *J. Chem. Phys.* **1994**, *100*, 3107-3113.
18. Nakamura, K.; Hatakeyama, T.; Hatakeyama, H. *Text. Res.* **1981**, *51(9),* 607–613.
19. McCrystal, C. B.; Ford, J. L.; Rajabi-Siahboomi, A. R. *Thermochim. Acta* **1997**, *294*, 91–98.
20. Bogracheva, T. Y.; Wang, Y. L.; Hedley, C. L. *Biopolymers* **2001**, *58*, 247–259.
21. Immergut, E. H.; Ranby, B. G.; Mark, H. F. *Ind. Eng. Chem.* **1953**, *45*, 2483–2490.
22. Guo, C.; Zhou, L.; Lv, J. *Polym. Polym. Compos.* **2013**, *21*, 449–456.
23. Mohamed, M. H.; Wilson, L. D.; Headley, J. V. *Microporous Mesoporous Mater.* **2015**, *214*, 23–31.
24. Fannon, J. E.; Hauber, R. J.; Bemiller, J. N. *Cereal Chem.* **1992**, *69*, 284–288.
25. Gallant, D. J.; Bouchet, B. *Food Microstruct.* **1986**, *5*, 141–155.
26. Peppas, Nicholas A.; Reinhart, C. T. *J. Memb. Sci.* **1983**, *15*, 275–287.
27. Chen, S. X.; Lostritto, R. T. *J. Control. Release* **1996**, *38*, 185–191.
28. Chuang, W. *Polymer (Guildf).* **2000**, *41*, 8339–8347.
29. Mohamed, M. H.; Wilson, L. D.; Headley, J. V. *Carbohydr. Polym.* **2010**, *80*, 186–196.
30. Wilson, L. D.; Mohamed, M. H.; Guo, R.; Pratt, D. Y.; Kwon, J. H.; Mahmud, S. T. *J. Agromedicine* **2010**, *15*, 105–116.
31. Stevens, D. J.; Elton, G. A. H. *Starch/Stärke* **1971**, *23*, 8–11.
32. Dehabadi, L.; Udoetok, I. A.; Wilson, L. D. *J. Therm. Anal. Calorim.* **2016**, *126*, 1851–1866.
33. Yu, L.; Christie, G. *Carbohydr. Polym.* **2001**, *46*, 179–184.
34. Kim, S. Y.; Wiesenborn, D. P.; Orr, P. H.; Grant, L. A. *J. Food Sci.* **1995**, *60*, 1060–1065.
35. Krueger, B. R.; Knutson, C. A.; Inglett, G. E.; Walker, C. E. *J. Food Sci.* **1987**, *52*, 715–718.
36. Donovan, J. *Biopolymers* **1979**, *18*, 263–275.
37. Eliasson, A. . C. *Starch* **1980**, *32*, 270–272.
38. Slade, L.; Levine, H. Recent Advances in Starch Retrogradation. *In* Industrial Polysaccharides; Stivala, S. S.; Crescenzi, V.; Dea, I. C. M., Ed.; Gordon and Breach Publishers: New York, **1987,** 387–430.
39. Zeleznak, K. J.; Hoseney, R. C. *Cereal Chem.* **1987,** *64*, 121–124.

40. Karoyo, A. H.; Sidhu, P.; Wilson, L. D.; Hazendonk, P. *J. Phys. Chem. C* **2014**, *118*, 15460–15473.
41. Burikov, S.; Dolenko, T.; Patsaeva, S.; Starokurov, Y.; Yazhakov, V. *Mol. Phys.* **2010**, *108*, 2427–2436.
42. Bellavia, G.; Paccou, L.; Achir, S.; Guinet, Y.; Siepmann, J.; Hédoux, A. *Food Biophys.* **2013**, *8*, 170–176.
43. Mundy, W. C.; Gutierrez, L.; Spedding, F. H. *J. Chem. Phys.* **1973**, *59*, 2173–2182.
44. Kizil, R.; Irudayaraj, J.; Seetharaman, K. *J. Agric. Food Chem.* **2002**, *50*, 3912–3918.
45. Almeida, M. R.; Alves, R. S.; Nascimbem, L. B. L. R.; Stephani, R.; Poppi, R. J.; De Oliveira, L. F. C. *Anal. Bioanal. Chem.* **2010**, *397*, 2693–2701.
46. Burikov, S.; Dolenko, T.; Patsaeva, S.; Starokurov, Y.; Yuzhakov, V. *Mol. Phys.* **2010**, *108*, 2427–2436.
47. Fathieh, F.; Dehabadi, L.; Wilson, L. D.; Besant, R. W.; Evitts, R. W.; Simonson, C. J. *ACS Sustain. Chem. Eng.* **2016**, *4*, 1262–1273.
48. Eliason, A-C; Gudmundsson, M. Starch: Physicochemical and Functional Aspects. In Carbohydrates in Food; Eliasson, A.-C., Ed.; Taylor & Francis Group LLC: New York, **2006,** 391–431.
49. Buléon, A.; Colonna, P.; Planchot, V.; Ball, S. *Int. J. Biol. Macromol.* **1998**, *23*, 85–112.
50. Richardson, S.; Gorton, L. *Anal. Chim. Acta* **2003**, *497*, 27–65.
51. Habibi, Y.; Lucia, L. A.; Rojas, O. J. *Chem. Rev.* **2010**, *110*, 3479–3500.
52. Hayashi, A. Supermolecular Structure of Cellulose - Structural Memory Phenomena and its Causes. In Cellulose - Structural and Functional Aspects; Kennedy, J. F.; Philips, G. O.; Williams, P. A., Ed.; Ellis Horwood: Chichester, **1989,** 35.
53. Huber, K. C.; Bemiller, J. N. *Carbohydr. Polym.* **2000**, *41*, 269–276.
54. Wilson, L. D.; Mohamed, M. H.; Headley, J. V. *J. Colloid Interface Sci.* **2011**, *357*, 215–222.
55. Gallant, D. J.; Bouchet, B.; Baldwin, P. M. *Carbohydr. Polym.* **1997**, *32*, 177–191.
56. Tsuchida, J. E.; Rezende, C. E.; de Oliveira-Silva, R.; Lima, M. A.; d'Eurydice, M. N.; Polikarpov, I.; Bonagamba, T. J. *Biotechnol. Biofuels* **2014**, *7*, 127–134.
57. Fannon, J. E.; Schull, J. M.; BeMiller, J. N. *Cereal Chem.* **1993**, *70*, 611–613.

58. Mohamed, M. H.; Udoetok, I. A.; Wilson, L. D.; Headley, J. V. *RSC Adv.* **2015**, *5*, 82065–82077.
59. Jang, J. K.; Pyun, Y. R. *Starch - Starke* **1996**, *48*, 48–51.
60. Franco, C. M. L.; Cabral, R. A. F.; Tavares, D. Q. *Starch/Stärke* **2002**, *54*, 469–475.
61. Jane, J. *Cereal Chem.* **1999**, *52*, 629–637.
62. Van Hung, P.; Macaulay, T. G.; Marsh, S. P. *Aust. J. Agric. Resour. Econ.* **2007**, *51*, 195–211.
63. Gupta, M.; Bawa, A. S.; Semwal, A. D. *Int. J. Food Prop.* **2009**, *12*, 587–604.
64. Hoogenboom, R.; Thijs, H. M. L.; Wouters, D.; Hoeppener, S.; Schubert, U. S. *Soft Matter* **2008**, *4*, 103–107.
65. Corcelli, S. A.; Skinner, J. L. *J. Phys. chem A* **2005**, *109(28)*, 6154–6165.
66. Khazraj, A. C.; Robert, S. *J. Nanomater.* **2013**, *2013*, 1–9.
67. Hua, G; Odelius, K. *ACS Sustainable Chem. Eng.* **2016**, *4(9)*, 4831–4841.
68. Liang, H.; Liu, B.; Yuan, Q.; Liu, J. *ACS Appl. Mater. Interfaces* **2016**, *8(24)*, 15615–15622.

CHAPTER 8

8.1 Integrated discussion of manuscript chapters

The overall objective of this PhD research was to rationalize the relationship between the structure and surface chemistry of biomaterials and their modified forms as it relates to adsorption-based phenomena. The use of pure and cross-linked biomaterials for adsorption in mixed solvent systems is poorly understood. Hence, there is a knowledge gap for adsorption processes of such systems especially in the case of biofuels, though many studies have been reported for vapour phase separations. In this PhD thesis, further study was carried out in this research area to address the above knowledge gaps that would advance the field of adsorption science and chemical separations. In chapter 1and 2, a detailed overview and background of different biopolymer materials, characterization methods and relevant adsorption models was investigated. Starch granules (linear and branched polymers refer to Table A8.1 in Appendix A8), natural cellulose fiber, and cotton linter, (*cf.* Table A8.2) were chosen due to their unique physicochemical properties and their structural variability. This thesis was focused on biomaterials such as cellulose and starches in their native and modified forms along with studies of their related physicochemical properties using various complementary methods (chapters 3). Chapter 3 discusses the importance of the cross-linking process for altering the textural properties (surface area, and porosity) and surface chemistry (polarity, and functional groups) in detail for these biomaterials. Thereafter, the adsorption properties of these biomaterials were evaluated where the uptake properties for water (W) and ethanol (E) in binary mixtures were studied (chapters 4-6). The study related to the hydration phenomena of the native biomaterial adsorbents provided a molecular level understanding of the sorptive behaviour of such materials for W, E, and binary (W+E) solvents (Chapter 7).

Among the biomaterials, starch granules, natural cellulose fiber, cotton, and modified and unmodified Miscanthus were chosen due to their unique physicochemical properties and structural variability. Each of the biomaterials possess unique physicochemical properties which affect their adsorptive properties in aqueous solution. In the case of cellulose, its fibril structure differs from starch which affects the accessibility of the hydroxyl groups and its corresponding adsorption affinity to polar *vs.* nonpolar adsorbates.[1] The helical and rigid fibril structure of cellulose differs from that of starch mainly due to the presence of β- *vs.* α-linkages. The presence of β-linkages in cellulose allows for this biopolymer to fold in a fully extended conformation to form a sheet–like

secondary structure that is stabilized by intra- and inter-molecular hydrogen bonding. On the other hand, starch is a mixture of α–amylose and amylopectin (linear *vs.* branched polymers) with variable composition (low to high). While α–amylose adopts an irregular aggregating helical-coiled conformation that contains regular left–handed helix regions.[2] Linear starch (amylose) can form stable complexes with polar and nonpolar species such as triiodide and lipids, according to previous reports.[3] One study using X-ray diffraction indicated that starch with higher amylose content form more stable complexes.[4] Amylopectin by comparison, has a tree– or brush–like dendritic structure due to branching effects.[5] This difference in the structure of starch and cellulose has shown approximately 30% lower accessibility of the hydroxyl groups for cellulose (*cf*. Figure 7.2 for determination of accessibility of the biopolymer hydroxyl groups using the PHP decolourization method). This fact also can be supported by differences in water retention values (WRV) (*cf*. Table A8.3 in Appendix A8) and solvent swelling properties (*cf*. Table 3.4). The water retention value (WRV) test provides an indication of a fibers' ability to absorb solvent. By using a centrifuge, determination of the WVR is possible since it facilitates water detachment from the surface and therefore, the remaining water molecules are associated with submicroscopic pores within the spaces adjacent to the sheet's surface (absorption).[6] The analyzed data for water retention values suggests a decrease in absorption according to the level of cross-linking. In turn, a solvent swelling test measures the total contribution of absorption and adsorption properties together. This method is useful for understanding the sorption process involving biopolymer-based materials (e.g., cellulose, starch, alginate), as they favour processes involving both adsorption on surface and diffusion within the polymer network.[7] The analyzed data of water swelling showed an increasing water uptake from 63% for native starch to 307 % for modified high amylose starches. The disparity between results of water retention values and the water swelling test originates from processes such as adsorption and absorption behavior of the materials that contribute differently.

The surface and textural characterization of biopolymer based materials was carried out using N_2 gas adsorption/desorption isotherms, where Type II isotherm was noted, according to the IUPAC classification system. In addition, the adsorption results suggested that completion of the monolayer saturation profile takes place at a low relative pressure (p/p^o) near 0.2. Greater adsorption of N_2 gas occurred at $p/p^o = 0.8$, since nitrogen gas molecules can access the grain boundaries and surface sites of the modified materials.[8] The Barret−Joyner−Halenda (BJH) and

the t-plot (de Boer method) methods provide a means to estimate the pore volume/pore diameter and micropore surface area (SA), respectively. The BET method provides estimates for the textural properties, where the SA (*ca.* 1 m^2 g^{-1}) and average pore size (*ca.* 10 nm) varied for these biomaterials. This data infers that the pore types in the sorbent materials remained mesoporous even after modification. However, the calculated SAs by the BET method does not ideally reflect the actual values of SA in different microenvironments such as water media due to the occurrence of water swelling and the size of N_2 molecules. It can be concluded that variation in the apparent SA of cellulose and starches using N_2 gas adsorption and water vapor sorption do not arise from presence of pores. Instead, the absorption of water molecules into the biopolymer structure where solvent interactions with anhydroglucose units result in structural changes to due strong dipolar interactions. As a result of the smaller size of a water molecule (~ 0.2 nm) as compared with a nitrogen molecule (~ 0.43 nm), water vapour sorption measurement can serve as a complementary technique for analysis of materials with narrow pores that nitrogen molecules cannot access. Additionally, the water vapour isotherm enables an independent measurement of the SA and pore size distribution (for details see Figure A8.1 and Table A8.4 in Appendix A8). It is found that, the water vapour sorption process in cellulose and starch are alike due to the presence of similar functional groups in their structures. However, due to presence of variability in crystalline nature of starch and cellulose, they behave differently toward water and ethanol. The results of studies on starch indicated that water vapor uptake in starch was higher than cellulose and zeolites.[9] However, due to steric effects of highly branched amylopectin molecule in the structure of starch and the larger molecular size of ethanol relative to water, the reported ethanol adsorption capacity (20 $mg \cdot g^{-1}$) is lower compared to zeolite 3Å (40.9 $mg \cdot g^{-1}$).

In this thesis research, both cellulose and starch were modified by cross-linking with epichlorohydrin (EPI) at variable synthetic feed ratios (polysaccharide monomer/cross-linker mole ratio; 1:2 [low], 1:3.6 [medium], and 1:5.4 [high]), although EPI cross-linker suffers from some disadvantages like its low water solubility,[10,11] and its related toxicity. The use of EPI with low ratio was generally approved for food-grade modified starch, as reported by Acˇkar *et al.*[12] The importance of controlling the ratio of the cross-linking finds support by the research reported by Crini's group.[13-16] These mole ratios (low, medium, and high) were chosen to provide the means to investigate the effect of the level of cross-linking on the structure of the modified products. Since each monomer unit of cellulose and starch consists of three hydroxyl groups, the cross-

linking feed ratios enable a study of the effect of cross-linker content on the product yield and structure of the materials. The yield (%) for cross-linked reaction was calculated based on equation 8.1 as follows:[17]

$$\text{yield}\% = \frac{\text{dry weight of cross - linked polymers (g)}}{\text{dry weight of polymers (g)}} \times 100 \qquad \text{Equation 8.1}$$

Furthermore, in the case of cross-linking with epichlorohydrin, the amount of cross-linker is very critical since the excess amount of cross-linker to biopolymer reactant leads to self-polymerization, where blocks the hydroxyalkyl sites and forms bridges and side chains within the network.[18] On the other hand, the cross-linking of starch with epichlorohydrin at the right stoichiometric ratio may take place on the surface and interior of the starch granules. This is because the cross-linker has the ability of the diffusing into the structure of the polysaccharides and is affirmed by previous results, where the thermogram of a cross-linked biopolymer demonstrated variable thermal stability for polymers with interior *vs.* exterior cross-linking.[19-21]

SEM has been used to relate granule morphology to the starch type and its physicochemical properties, such as pore structure.[22] The starch granule materials displayed distinct shapes and sizes with diameter ranging between 5 – 50 μm according to analysis of the SEM results (*cf.* Figure. A8.2 in Appendix A8). The maize starch was characterized using SEM and revealed variable surface pores in the native and EPI-cross-linked states (*cf.* Figure A8.2A in Appendix A8) and particularly, the modified maize starch AP-EPI displayed surfaces with enhanced textural properties. In turn, the SEM of soluble (AM50), high amylose (AM) starches and cellulose displayed smooth and non-porous surface. The SEM micrographs of AM50 and AM are generally characterized by heterogeneous surface and small size granules,[23] as shown in Appendix A8, Figures A8.2B and A8.2C. The SEM results of cellulose and its cross-linked forms (CE-EPI) are illustrated in Figure A8.2D. The micrograph of cellulose (*cf.* A8.2D) implies that the fibril structures of cellulose resemble bundles of long fibers.[24-26] probably, the presence of intramolecular hydrogen bond interactions results in the entanglement of cellulose fibrils to form a sheet-like topology. As illustrated in the SEM of modified cellulose, the collapse and disintegration of the fibril structures occur after modification due to fragmentation of the long

fibers.[27] However, SEM results in a study on EPI-cross-linked cellulose showed that the condition of reaction lead to a smoother surface with slight collapse of the fibril structure.[17]

Differential scanning calorimetry (DSC) was used to indicate effect of EPI cross-linking on the structure of cellulose and starch at variable stage of reaction. The term "gelatinization" in DSC analysis refers to the phase transition where a highly-ordered structure of materials, e.g., starch granules, transfers into disordered structure due to heating in the presence of excess water.[28,29] Gelatinization can be used for the evaluation of starch granule properties before and after gelatinization. The ratio of amylose/amylopectin and the structure of starch granules affect the physicochemical properties and the phase transition of starch.[30] Although both amylopectin and amylose in starch granules can undergo cross-linking reaction, it is believed that the amylopectin has a greater reactivity.[31] Herein, determination of the thermal properties of the samples using DSC revealed that the gelatinization temperature of the cross-linked starch increased relative to that of native starch. The results are shown in Figure A8.3 (Appendix A8) which are in agreement with the results reported by Singh *et al.*[32] This observation can be explained according to the reduced mobility of the amorphous chains created by the intermolecular cross-linking. According to the findings by Chen *et al.*,[29] the enthalpy of gelatinization depends on the factors like intermolecular bonding, degree of crystallinity, and presence of impurities. For instance, the waxy wheat starch with high amylopectin content requires higher energy for gelatinization due to its higher crystallinity compared with the normal wheat starch. Acquarone *et al.*[33] found that the cross-linking process adds intra- and intermolecular bonds that stabilize the structure of granule. Based on the study by Hirsch *et al.*[34] on the cross-linking of several starch materials, greater cross-linking resulted in smaller granule volume due to creation of higher aggregation. Therefore, the viscosity observed for the cross-linked starches with higher ratio of cross-linkers is lower than the more highly cross-linked starches.

Structural variation of the biopolymers (e.g., branching, molecular weight, and relative amylopectin (branched)/amylose (linear) content) was confirmed to contribute to the variable solvent uptake in neat solvents (i.e. water *vs.* ethanol) using gravimetric-based solvent swelling at equilibrium conditions. The trends for water swelling showed an increase with greater levels of cross-linking for high amylose starch. These results led to a better understanding of the adsorptive behaviour of the materials with pure water and ethanol, respectively. These results provided background information to devise further experimental studies (adsorption isotherm, etc.), as

outlined in Chapter 4. The N_2 adsorption isotherms provided information about textural properties of the adsorbents according to a solid-gas adsorption process.[35] As well, the application of a phenolic dye (PNP) as an adsorbate was used to characterize the adsorptive capacity and textural properties in aqueous solution to account for the role of solvent and swelling effects. The results of PNP adsorption isotherm study provided estimates of the textural properties of cellulosic materials (e.g., SA and pore volume). In a study by Udoetok *et al.*, [36] the calculated SA of native cellulose and its modified forms according to adsorption isotherms with PNP varied from 9.83 to 38.6 m^2/g. A similar range of SA values was obtained for starch and its cross-linked forms according to the minor variation in PNP uptake as revealed for amylose (1.22 mg/g to 1.44 mg/g) and amylopectin (1.31 mg/g to 1.55 mg/g). A dye-based method using PNP (*cf.* Figure 3.5) also was used to assess the effects of cross-linking on the surface chemistry and textural properties of cellulose and its cross-linked forms. The results indicate that the Q_e values for cellulose as 1.11 mg/g and 1.32 mg/g for its cross-linked forms. Increased cross-linking provides an incremental change in the surface chemistry and textural properties that are inferred to influence adsorption properties. The findings indicated that the cross-linked materials have tunable sorption properties as evidenced by their adsorptive capacity toward model dye (PNP), as compared to the unmodified biopolymer. In addition, the textural properties (i.e. surface area and porosity) and surface modification due to the presence of functional groups and cross-linker units for these adsorbent materials were probed using dye adsorption (PNP at pH 6) in aqueous solution. The value of pH at the *point of zero charge* (pH_{zpc}) provided a means for understanding the electrostatic interactions between surfaces of the adsorbent materials and charged adsorbate species (Figure A8.4 in Appendix A8).[37-39] As an example, the surface of cellulose is negatively charged due to deprotonation of hydroxyl groups at pH above ~3 when $pH > pH_{zpc}$. In turn, the cellulose surface has excess positive charge at $pH < pH_{zpc}$, due to adsorption of H^+ ions. The neutral form of cellulose (R-OH) or its protonated forms can interact with ionic forms of PNP as an adsorbate (pK_a of PNP=7.15) via ion-dipole or ion-ion interactions, according to speciation of such a system. Variable surface protonation occurs for cross-linked *vs.* unmodified cellulose according to the observed trends in the pH_{zpc} values as the level of cross-linking varies.

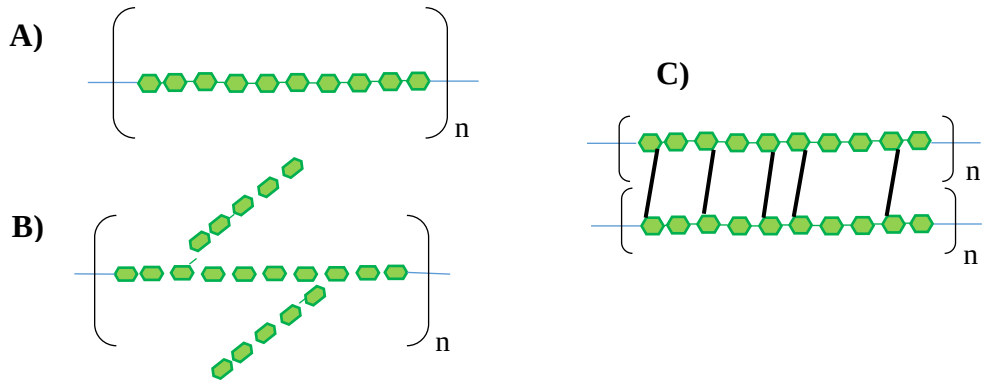

Scheme 8.1.1 A) Linear, B) Branched and C) cross-linked structure of biomaterials (dark line segment).

The presence of numerous hydroxyl groups in the 3D polymer network alter the hydration properties and vary the intensity of the biopolymers according to the level of cross-linking. The resuls obtained using ^{13}C solid state NMR spectroscopy (*cf.* Figure 3.2) and differential scanning calorimetry (*cf.* Figure 7.3) showed that the 3D biopolymer networks possess amorphous structure, with limited or the complete absence of ordered networks. The results of this thesis research reveal that there is no clear relationship between the level of cross-linking and adsorptive capacity of the biopolymer materials for PNP since the biopolymers are too polar, whereas; PNP would require surfaces with more apolar character to be adsorbed. These results indicate that several different factors govern the adsorption process such as steric hindrance and relative accessibility of the active binding sites. Therefore, this study contributes to a greater understanding of the connection between the adsorption properties and structure of biopolymers and their modified forms in aqueous solutions. Thus, systematic studies related to the study of the structure and adsorption properties of such systems are warranted for future work. The swelling and PNP uptake results provide limited insight on the adsorption properties based on the use of single point adsorption results. Additionally, the changes in water and PNP uptake capacity of modified adsorbents provided a rationale to conduct adsorption experiments for the separation of water from ethanol.

To enable a systematic study of the adsorption properties in mixed solvent systems (W+E), a suitable method for the analytical detection of water and ethanol in a binary mixture was required. Chapters 4 and 5 were focused on the development of qNMR for quantification of the uptake of solvent components for estimation of isotherm uptake parameters for such polymer/solution

systems. The qNMR technique is an analytical method that is versatile and rapid compared to other techniques for quantification of water and ethanol over a range of water contents (4-95%) in binary (water-ethanol) mixtures. ^{1}H-NMR spectroscopy was used to provide *in situ* quantitative estimates for the composition of water/ethanol components when adsorptive uptake reached an equilibrium condition in binary W-E mixtures, as depicted by equation 8.2.

$$\text{Sorbent (s)} + W_X/E_Y \text{ (soltn)} \rightleftharpoons \text{Sorbent-}W_Z\text{-}E_{Z'} \text{ (s)} + W_{X\text{-}Z}/E_{Y\text{-}Z'} \text{ (soltn)} \qquad \text{Equation 8.2}$$

This solid-solution system illustrates a physical separation of water (W) and ethanol (E) in a binary (W_X/E_Y) solution (soltn) corresponding to adsorption at equilibrium. The limiting case presented above shows an arbitrary solvent uptake (Z and Z') by the sorbent relative to the original binary (W+E) solvent mixture at variable composition (X and Y).

In order to provide quantitative data to allow for analytical estimation of concentration from peak area of the NMR signals, a longer time for T_1 was chosen to obtain fully relaxed spectra. The optimized conditions were used to obtain fully relaxed spectra (*cf.* Table 4.2). In chapter 4, cellulose and its modified forms with different levels of cross-linking were also used as adsorbents for separation of water and ethanol in binary mixtures. The qNMR method was developed to estimate the relative composition of water and ethanol in binary W-E mixtures. Deuterated DMSO was used as the NMR solvent in W-E mixture rather than D_2O as it results in better resolution for the respective water-ethanol NMR signals (*cf.* Table 4.3). The results of isotherms at equilibrium conditions by use of dye uptake studies were evaluated using the Sips isotherm model to obtain the adsorption parameters (*cf.* Equation 2.7 in chapter 2). As well, these results were used to estimate the potential of such sorbents for the separation of water from ethanol in binary (W+E) mixtures. The Sips model is a three-parameter equation that gives a better fit than two-parameter isotherm models such as the Freundlich and Langmuir equations. Nevertheless, the Langmuir and Freundlich isotherms have been used for the study of various adsorption isotherms. Karimi *et al.*[40] applied both Langmuir and Freundlich models satisfactory on adsorption isotherm of starch and cellulose in water/ethanol system. During the adsorption in the water/ethanol system, both species may be adsorbed on the surface regardless of their affinity toward the adsorbents; therefore, either may play role in the adsorption of another. For this reason, several theoretical models for adsorption isotherms have been derived. Although application of a dual- mode isotherm model for

fitting the water/ethanol isotherms (equation 8.3) seems more relevant to obtain realistic values due to role of potential interference of adsorbate in multi-component systems. Herein, the interpretation of the uptake results was conducted by considering the uptake of water and ethanol independently. Indeed, a study of multicomponents in solution is essential for understanding the interactions between components since surface charge, structure, size, and functional groups of adsorbates play an important role in the adsorption process. However, in this study, water was considered as a solvent and adsorption of ethanol was modeled using the Sips model. Nonetheless, since the measurement of unbound fraction of water and ethanol is possible using NMR spectroscopy due to differences in the coupling pattern (i.e. coupling doesn't occur between equivalent hydrogens), reliable spectra of ethanol were used to achieve two mutually exclusive isotherms. The modified Sips isotherm for multicomponent system is:

$$Q_{e,i} = \frac{Q_{m,i} K_{s,i} C_{e,i}^{m}}{1 + \Sigma K_{s,i} C_{e,i}^{m}} \qquad \text{Equation 8.3}$$

Where $Q_{e,i}$ represents the equilibrium adsorption capacity for component i (mg/g), $C_{e,i}$ represents the equilibrium concentration of component i (mg/L), $Q_{m,i}$ is the monolayer adsorption capacity for component i (mg/g) , $K_{e,i}$ is a constant for Sips isotherm $(L/mg)^m$, and m is the Sips model exponent. The Sips constants are taken from the isotherm data of respective solvent components (W *vs.* E).

Chapter 5 describes a study that builds upon the results obtained from chapter 4 for cellulose-binary solvent isotherm studies. Chapter 5 is focused on an adsorption study of various starches (maize, corn starch, soluble starch) and their modified forms in water/ethanol binary system. Based on the variable structure of starch in relation to cellulose, the study in Chapter 5 was focused on developing an understanding of the structure-adsorption property relationship between starch (linear and branched forms) and modified forms in the presence of water/ethanol in binary mixtures. The structure of the starch consists of α–linkages (*cf*. Figure 1.1), whereas; cellulose has β–linkages between monosaccharide units in the biopolymer structure (*cf*. Figure 1.3). This structural variability affords variable characteristics to these polysaccharides including crystallinity, rigidity, and solubility. In addition, the unique water uptake properties (higher

$R_{selectivity}$ values) of starch and its modified forms relative to the cellulose materials illustrate the role of textural properties and relative hydrophobic character of the polymer network according to the selective adsorption properties (*cf.* Figure 5.2) in W-E binary mixtures. Among different types of starch (linear and branched forms), high amylose starch had the highest water selectivity (*ca.* 72) compared to the branched amylopectin starch (*ca.* 6.4). This is due to the presence of variable numbers of surface –OH groups with different surface accessibility that influence favourable interactions between the biopolymer and solvent components.[41,42] Generally, starch based materials show greater water selectivity (*cf.* Figure 5.2 B) over ethanol when compared with cellulose-based materials (*cf.* Figure 5.2.A) and their cross-linked forms, as follows: $R_{selectivity}$ (water: ethanol) was 2.5:1 (cellulose) and 80:4 (starch). These results confirmed that the dehydration of the binary W-E mixtures can be achieved by adsorptive fractionation at ambient conditions. Based on the given information in Table 5.4, for values of $R_{selectivity}$, starch can compete as an alternative dessicant as compared with molecular sieve adsorbents.[43]

As indicated before (in Chapter 4), cellulose materials have reduced accessibility of polar groups because of extensive intra- and intermolecular hydrogen bonding which is in agreement with the supramolecular framework structure of CE fibers. This fibril structure of CE has an effect on the accompanying adsorption properties and selectivity.[44] It can be inferred from the isotherm results (*cf.* Figure 4.3) that cross-linking of cellulose expose the hydroxyl groups and influence the relative accessibility due to "pillaring effects" that occur upon cross-linking.[45] Although epicholorohydrin (EPI) has been used commonly as cross-linker for modification of cellulose,[46] cross-linking likely takes place at the surface rather than core of the fibers since the linkages between the anhydroglucose units of the cellulose chains could hinder the formation of inter-fiber hydrogen bonds.[47]

Powder X-ray diffraction (PXRD) analysis serves as a non-destructive analytical technique that enables evaluation of the crystalline nature of materials. The XRD pattern indicates two main diffraction signatures at *ca.* $2\theta = 20$ and 30° which can be assigned to the crystalline region of cellulose. (*cf.* Figure A8.5, Appendix A8) The slight broadening of the diffraction pattern of modified cellulose by EPI indicates that crystallinity is decreased slightly after modification probably due to presence of less ordered structure because of the disruption of intra hydrogen bonding. The XRD patterns of a study by Majzoobi *et al.*[20] indicated that cross-linking reaction reduces the distance between starch chains without changing the crystalline pattern. This

observation is confirmed in another study by Koo *et al.*[48] where they reported that no big difference in crystallinity pattern has been found after modification of the corn starch compared to the native starch. This infers that the process of cross-linking mainly occurs in the amorphous region of starch granules showing no alteration in the XRD patterns for the crystalline domains of the starches.

^{13}C solid state NMR spectroscopy revealed useful structural information related to the framework of the carbon in the structure of cellulose and its modified forms, as illustrated in Figure A8.6, Appendix A8. The main signals of cellulose and its cross-linked forms were observed between 62 and 105 ppm, in accordance with previous studies.[49-52] Generally, the signals at 104.9 ppm (C1), 88.7 ppm (C4) and 64.7 ppm (C6) can be assigned to ^{13}C nuclei in the crystalline domains where signals at 83.8 ppm (C4) and 63 ppm (C6) can be related to the amorphous domains of cellulose. The similar chemical shifts of cellulose and its modified forms enable one to infer that the cellulose skeleton was preserved after cross-linking, in agreement with previous reports.[46-49] Important spectral features for cross-linked cellulose is its reduced intensity for the amorphous domains where signal splitting also occurs at 104.9 ppm and 70–87 ppm. The reduced intensity and splitting suggest that the carbons corresponding for these signals are involved with cross-linking.[7] In addition, NMR studies[53-55] for materials cross-linked with EPI revealed ^{13}C NMR signatures between 69 and 73 ppm for the EPI linker unit, in accordance with the NMR results in Figure A8.6, Appendix A8.

According to the results in chapter 4, the uptake properties of cellulose and its modified forms rely on the nature of the cross-linking. This feature was evidenced by a dependence of the uptake capacity of these biopolymer materials (*cf.* Tables 4.4 and 4.5) on the textural properties and surface chemistry. The high uptake capacity for both ethanol and water was observed in cellulose with higher level of cross-linking because of the incremental effects of cross-linking of the modified materials (*cf.* Tables 4.4 and 4.5). Besides, the relative selectivity of water over ethanol was greater for modified forms of these materials relative to native cellulose (*cf.* Figure 4.4). This research addressed the second objective of the thesis that related the development of the qNMR technique for study of the adsorptive fractionation of water/ethanol using cellulose materials.

In addition, these studies (chapters 4 and 5) resulted in a greater understanding of the role of structure and surface chemistry on the adsorptive behaviour of biopolymers for fractionation of water-ethanol mixtures. With respect to the trends in the adsorption properties for starch and

cellulose biopolymers for the separation of water-ethanol mixtures, the results from Chapters 4-5 may provide insight on the adsorption properties of biomass that contain similar biopolymer components. One such biomass is Miscanthus since it is composed of cellulose and hemicellulose biopolymers among other components (40-60% cellulose, 20-40% hemicellulose, and 10-30 % lignin).[56] In Chapter 6, the adsorption properties of Miscanthus and its modified forms were evaluated according to variable types of chemical pretreatment and mechanical milling to yield materials with variable particle size. The resulting Miscanthus adsorbents were studied for their adsorptive fractionation properties of water and ethanol in binary (W+E) mixtures. The chemical pretreatment of Miscanthus was carried out to generate biomass with modified levels of cellulose and lignin content. Subsequently, the adsorption properties of cellulose-enriched and lignin materials were evaluated using qNMR in binary mixtures of water and ethanol. The adsorption results obtained for water and ethanol indicated that cellulose enriched materials had lower water uptake (Q_m = 2.9-3.4 g/g). By comparison, the raw Miscanthus biomass displayed higher water uptake compared to lignin (Q_m = 0.64g/g). In raw Miscanthus biomass, the hemicellulose is located within the cellulose fibril domains.[57] The presence of hemicellulose affords variable hydrogen bonding interactions within the cellulose fibril network and the surface sites because cellulose/ hemicellulose may serve as donor and acceptor sites for the respective solvent components (water and ethanol). Moreover, the solvent selectivity ratio of these materials showed that this selectivity ratio is similar to the selectivity ratio reported above for pure cellulose and its modified forms (*ca.* 2.5:1 for water over ethanol). The results of this research uncovered that the particle size variation (16, 40, 70 μm) has significant effect for raw Miscanthus with water (Q_m = 3.7-8.9 g/g). In the case of raw Miscanthus, there may be a waxy outer layer on the biomass that becomes removed upon grinding to variable particle size. Reduction in particle size via grinding may result in some degree of removal or exposure of the waxy regions that contributes greater access of water to the adsorption sites (cf. Scheme 8.1.2).[58] Particle size effects on the modified forms of Miscanthus show a minimal impact on the overall adsorption capacity toward water (Q_m = 2.9-4.7 g/g) and ethanol (Q_m = 2.8-3.2 g/g). This observation indicated that the impact of chemical treatment was more significant since it generates more access to the hydrophilic sites (e.g., hydroxyl groups) and pores in the structure of the biomass.

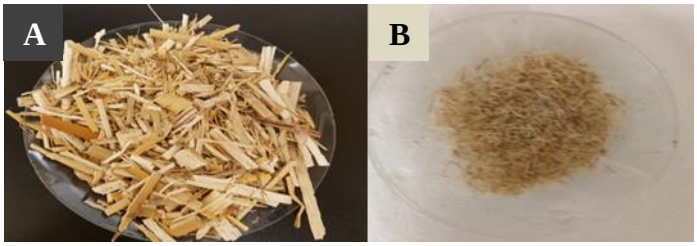

Scheme 8.1.2 Photograph of miscanthus A) before grinding and B) after grinding.

One of the critical aspects of the adsorption process relates to the regeneration and reusability of the adsorbent materials. Regeneration of sorbent materials enables an enhancement of the efficiency of the system for multiple cycles of application. To meet this requirement, a regeneration study was conducted on modified and unmodified Miscanthus toward water/ethanol by applying four cycles of adsorption-desorption. The results of regeneration studies showed *ca.* 12% decrease for the relative uptake of water/ethanol due to sintering effects during the intermediate drying process at high temperature. The results of this study contribute to the development and application of biomass alternatives such as Miscanthus for adsorptive processing of solvent mixtures due to their relative abundance and low cost over the use of synthetic adsorbents or isolated biopolymers such as cellulose and hemicellulose.

The results reported by Crini's group suggest that there are sparse studies directed towards development of a systematic understanding of the interactions between the components of the adsorption process (i.e. the bioadsorbent, adsorbates and solvents).[59,60] Although the characteristics of the cross-linked biomaterials have been studied widely, investigation of the solvation phenomena are sparsely reported in the literature.[61,62] Based on the results outlined in the previous chapters (e.g., swelling test, and dye uptake results), solvent effects play a key role on the adsorption process that influence the uptake capacity and molecular selectivity in the case of mixed systems. The use of dye uptake studies not only provided a tool for measuring the adsorption properties, but also provided estimates of the textural properties of adsorbents. The estimation of the surface area by the dye-based method gives complementary insight on the textural properties that may be compared to the nitrogen adsorption results due to the role of solvent swelling effects in aqueous solution. To achieve a more comprehensive understanding about the adsorption process for the separation of water-ethanol mixtures, it was essential to study the role of solvent contributions and its role to the overall sorption process.

The final objective of this thesis was addressed in Chapter 7 which focused on the role of hydration effects (i.e. biopolymer-solvent interactions) to gain further insight on the adsorption properties of starch and cellulose biopolymers. For this reason, chapter 7 was focused on a study of the molecular details of the solvent effect (hydration effects) on starch and cellulose with respect to their adsorption properties. In Chapter 7, thermoanalytical (e.g., DSC), spectroscopic techniques (e.g., Raman spectroscopy), SEM, and dye (i.e. PNP and PHP) adsorption methods were used to evaluate solvent effects. The results provided supporting evidence for the key role of water adsorption for variable types of starch (i.e. maize, corn starch, soluble starch) and cellulose. The hydration effect refers to interactions of the solvent with the adsorbent surface. Based on that, the variable HLB properties of starch and cellulose contributed to variable solvent affinity between water and ethanol according to the differing dielectric constant ($\varepsilon_W \approx 80$; $\varepsilon_E \approx 24$) of each solvent component. The results of this study indicated the solvent effects due to hydration phenomena are more pronounced for the adsorption properties of cellulose/water/ethanol system compared to the other systems studied in this chapter (*cf.* Figures 7.4 and 7.5). In this regard, cellulose has a quaternary fibril structure that may lend to its unique hydration properties, in agreement with the results of water uptake (*cf.* Table 4.5 in Chapter 4). The water swelling results (*cf.* Table 7.2) are unique owing to the small molar volume (V_m=18 ml/mol) and dipolar nature of water (μ=1.85 D) compared to ethanol (V_m =58 ml/mol, μ =1.66 D), as depicted in Scheme 8.1.3.

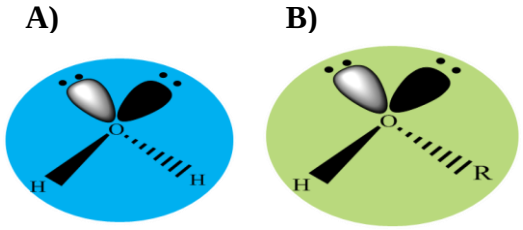

Scheme 8.1.3 Molecular structure of A) Water and B) Ethanol (R= CH_3CH_2-).

Note: Water has 30% smaller molar volume relative to that of ethanol.

It is well-accepted that adsorption properties of an adsorbent depend strongly on the physicochemical characteristics such as the textural and surface chemical properties. However, the process of adsorption is the consequence of balanced interactions between the adsorbent, adsorbate and solvent. These adsorptive interactions are well correlated to the textural properties,

morphology, and surface chemical nature of the adsorbents and the physicochemical properties of the solvent. Various intermolecular forces including van der Waals, induction and/or dispersion), electrostatic interactions, hydrogen bonding, and hydrophobic interactions affect the adsorption processes. The study outlines the importance of solvent effects which provide an understanding of the role of interactions between the biopolymer and solvent in the adsorption process.

8.2 Conclusion

In this PhD research project, the adsorption properties of native and modified polysaccharides toward liquid mixtures of water/ethanol were studied by characterizing their structural and adsorption properties. This work has yielded several unique outcomes that relate to new knowledge of biopolymer materials and their utilization in applications such as the food and fuel industry. The results provide an in depth understanding for the relationship of polysaccharide structure and hydration phenomena, along with the selective adsorption properties of such materials in water/ethanol binary mixtures.

The outcomes of this study demonstrated that biomaterials such as cellulose, starch, and their modified forms have variable adsorption properties in aqueous solution, according to their diverse macromolecular structure. The synthetic modification of biopolymers including starch and cellulose were carried out by cross-linking at variable synthetic feed ratios. A study of the dye uptake properties using *p*-nitrophenol at equilibrium conditions and the swelling properties in water and ethanol revealed that the modified biopolymers had tunable physicochemical (i.e. textural and sorption) properties. The tunable adsorption properties of these biopolymers was correlated with the cross-linking method employed according to the different ratios of the cross-linking agent (epichlorohydrin), and variable synthesis conditions (e.g., nature of the biopolymer, stirring rate and temperature) to form cross-linked materials. The characterization of the materials according to TGA and FT-IR spectroscopy confirmed the structure of the modified cross-linked biopolymers. The adsorption studies for the modified biopolymers reveal an improvement relative to the native biopolymer materials. The variation in adsorption properties was attributed to *pillaring effects* and changes in surface functionality that arise due to cross-linking of the biopolymer network. Solvent swelling in the presence of ethanol or water was evaluated and a significant increase in water/ethanol uptake capacity was observed, especially for cross-linked polysaccharides. In addition, equilibrium sorption properties of the cross-linked polysaccharides was evaluated using a dye-based method with *p*-nitrophenol (PNP) as a model organic compound

for estimating the textural properties.[64] The cross-linked materials with EPI and high amylose content display decreased sorption as the EPI ratio increased, whereas; biopolymers with greater amylopectin (AP) content display greater uptake of PNP as the EPI ratio increased. These observations provided supporting evidence for variable adsorptive uptake properties according to the level of cross-linking. In this regard, the development of a suitable quantitative method for analytical detection of water and ethanol reveal that methods such as the Karl Fischer titration and chromatography (GC and HPLC) have some drawbacks mainly due to their need for longer analysis time. This research focused on the development of a quantitative ^{1}H-NMR (qNMR) spectroscopy as a technique to measure the water and ethanol levels in binary (W+E) solutions. qNMR enabled the characterization of the solid-solution adsorption isotherms through the detection of residual water and ethanol in binary solvent mixtures. It was concluded that qNMR was suitable for *in-situ* quantitative analysis of solvent components (water and ethanol), especially for the quantification of the adsorption properties in binary mixtures for each respective solvent component (W and E). The outcome of this research project indicated that qNMR is suitable for the detection of water and ethanol over a range of 4-95% water content in binary mixtures, based on studies of solid-solution adsorption isotherms. The study of isotherms using the Sips model provided thermodynamic parameters that give insight on the structure and adsorption properties of the biopolymers and their modified forms. The effect of biopolymer cross-linking was shown for starch and cellulose materials, in accordance with the high uptake capacity for both ethanol and water. Furthermore, the variable solvent uptake selectivity of water over ethanol ($R_{selectivity}$) for these biopolymers and their cross-linked forms was revealed by the nature of biopolymer, degree of cross-linking, and textural properties of the adsorbent. Likewise, the results showed that the uptake selectivity of water over ethanol ($R_{selectivity}$) was greater (4:80) for the cross-linked starch *vs.* the native starch. These observations confirmed that cross-linked biopolymers have greater uptake of water and ethanol in mixed solutions. Cross-linking was inferred to alter the surface area and porosity as well as surface chemistry via accessibility of the biopolymer –OH groups in an incremental manner. This trend is supported by results obtained using N_2 adsorption (e.g., collapse in N_2 adsorption-desorption diagram of starch) and FT-IR spectral results.[64]

To understand the kinetic process of water/ethanol adsorption, the kinetic uptake results were evaluated using the PSO model for the solvent uptake (water and ethanol) for cellulose and its cross-linked forms. In the case of cellulose/solvent systems, a relatively rapid kinetic uptake

[0.6-0.9 $g.mg^{-1}.min^{-1}$] was observed as noted in Figure 4.6 in chapter 4. The PSO model assumes that the overall adsorption rate is limited by the rate of adsorbate diffusion into the pores of sorbent. Thus, it was indicated that increased biopolymer cross-linking had a positive effect on the uptake properties.

To extend the study and provide a means for comparison with starch-based materials, an understanding of the fractionation properties of variable types of starch and its cross-linked forms were evaluated. As a result, a modified form of high amylose starch was shown to display the highest uptake of ethanol and water (*cf.* Figure 5.2 in chapter 5), when compared against other types of starch. Overall, starch based materials display greater solvent selective uptake of water over ethanol, where values of $R_{selectivity}$ (*ca.* 4:80) exceed that for cellulose-based materials. The differences between starch and cellulose at variable cross-linking ratios are attributed to the variable types of glycosidic linkages (α-linkage for starch and β-linkage for cellulose), macromolecular structure, and textural properties of these biopolymers.

The adsorption studies for simple biopolymers (e.g. cellulose and starch) provided motivation for the study of a Miscanthus biomass adsorbent because of its greater structural complexity. Therefore, an investigation of the solvent selective uptake in W-E mixtures for raw Miscanthus (RM) and pretreated Miscanthus (PTM) biomass was conducted to understand the role of various biopolymer components on the adsorption properties in a comparative manner. The difference in RM and PTM materials relate to the variable effects of chemical pretreatment to yield modified biomass with variable biopolymer composition (cellulose, hemicellulose and lignins). The adsorption isotherm model showed variable solvent uptake with water (W), ethanol (E), and in binary mixtures using PTM. The solvent uptake results showed that particle size difference (16-70μm) has a negligible effect on the adsorption of W-E in binary solvent mixtures (*cf.* Table 6.2 in chapter 6). Furthermore, chemical treatment indicated an effect related to the surface accessibility of the hydrophilic adsorption sites and micropore accessibility of the biomass adsorption sites. The adsorption capacity (g/g) of raw Miscanthus was evaluated with water (8.93) and ethanol (4.15) using qNMR spectroscopy. The results showed that the solvent selectivity ratios in binary W-E solutions are greater for RM (*ca.* 1:3) compared with PTM (*ca.* 1:1.5), and may be ascribed to changes in the composition of cellulose and hemicellulose due to the treatment. A key aspect of this study was focused on regeneration of the biomass for multiple adsorption-desorption cycles. Regeneration studies were investigated using swelling tests as a model process over four

cycles of adsorption and desorption in neat solvents (water *vs.* ethanol). The results show that Miscanthus has a moderate decrease (12%) in uptake. Overall, RM biomass showed greater water uptake selectivity over ethanol compared to PTM in binary W-E systems. This study presents a molecular level understanding of the role of biopolymer components in solvent swelling and selectivity. The study on Miscanthus also motivated a more detailed study of the hydration properties of biopolymer components as described below. Adsorption processes are strongly influenced by choice of solvents (water and ethanol) which also influence the hydration phenomena of the biopolymer. To gain a further understanding of the role of hydration phenomena in adsorption processes involving water/ethanol mixtures, a research study was focused on the hydration properties of biopolymers. The use of thermoanalytical and various spectroscopic techniques were employed to investigate the hydration of various biopolymer materials in a comparative manner. The hydration phenomena of the various starches with different structural forms according to the content of amylose (linear) *vs.* amylopectin (branched), and cellulose-based biopolymers were studied using DSC, Raman spectroscopy, SEM, solvent swelling in single component and mixed solvent systems, along with adsorption isotherms with various dye-based probes. This multi-instrumental approach was pursued to develop a molecular level understanding to gain insight why high amylose (AM) and soluble starch (AM50) display greater solvent swelling in water and ethanol relative to other biopolymers. The observed variation in hydration properties were attributed to the flexible biopolymer backbone and the greater fraction of surface accessible hydroxyl (-OH) groups. Variable surface accessibility of the –OH groups for starch and CE are supported by the dye decolorization results, as indicated by the use of phenolphthalein (PHP) as a dye probe (*cf.* Figure 7.2 in section 7.4.3). The PHP dye decolorization method reveals that the surface –OH functional groups of CE are less accessible compared to starch biopolymers. CE and AP show similar hydration properties, in agreement with the DSC and Raman spectral results, despite the reduced surface –OH accessibility of CE. The reduced surface –OH accessibility of CE is related to its fibril structure which are bound by strong inter/intra molecular hydrogen bonding. In addition, the hydration properties of high amylose (AM), soluble starch (AM50) and high amylopectin (AP) starches differ because of variable branching and packing defects of their tertiary structures. Structural effects of this type are hypothesized to affect the adsorbate permeability and surface accessibility due to the variable proportion of -OH groups on the biopolymer surface.[65] In aqueous solution, the quaternary fibril structure of CE influences the hydration properties due to

the reduced accessibility of the surface hydroxyl groups on the solvent uptake and swelling phenomena. The accessibility of polar functional groups such as biopolymer –OH groups contribute to an increase in the sorption properties. This is especially true in the case of CE due to changes in surface area and pore structure properties due to the greater role of biopolymer-solvent interactions *vs.* biopolymer-biopolymer interactions. The small molar volume and dipolar nature of water affects the hydration properties of polysaccharides in several ways: 1) the tendency of the biopolymer material to swell due to solvent uptake within its 3D polymer network, 2) H-bonding interactions of the biopolymer can occur to variable extents because of steric effects and/or availability of the active binding sites (e.g., -OH groups). A better understanding of these factors will contribute a further understanding of the *structure-property* relationships of biopolymers and their modified forms as sorbents for applications that range from food to fuel production. To summarize, this PhD research study addressed the following knowledge gaps in the field of polysaccharide materials:

1- The study on polysaccharides contributed to a greater understanding of factors related to water-ethanol adsorptive separation, where such studies were sparsely reported in terms of liquid phase separation at the start of this PhD thesis research. This study characterized the structural, physicochemical, textural and adsorption properties of cellulose and starch as biosorbents for separation of water from ethanol in binary mixtures.

2- Modification of cellulose, starch, and Miscanthus was carried out to alter their chemical and textural properties. This PhD research study employed variable types of surface chemical modifications (e.g., cross-linking and physical/chemical treatments) to alter the type of surface functionality of the biopolymer materials.

3- Limited studies have evaluated the effect of cross-linking degree in a systematic fashion. Herein, variable stoichiometric ratios for cellulose and starch with epichlorohydrin as cross-linker (1:2, 1:3.6, 1:5.4) was employed in an incremental manner to a series of structurally related polysaccharides to investigate the effects of cross-linking and its role on surface accessibility and textural properties.

4- Structural and physicochemical characterization of these polysaccharides was carried out to gain a greater understanding of the effect of cross-linking on the adsorptive properties of modified adsorbents. This PhD research study employed the combined use of several

types of spectroscopic and analytical methods to investigate the *structure-property* relationships of biopolymers in a systematic manner.

5- The application of native forms of biomass (Miscanthus) as an adsorbent was used for the controlled uptake of chemical species and separations from aqueous solution. This PhD research study contributes to an improved understanding of the role of biopolymer components in Miscanthus biomass and the potential use of such materials for the adsorptive processing of water-ethanol binary mixtures by adsorption-based separations.

6- Application of alternative methods such as quantitative NMR (qNMR) for detection of water/ethanol has not been widely reported for the study of adsorptive fractionation in binary mixtures. The qNMR technique overcomes the need for chromatographic separation and offers *in situ* detection when there is no spectral overlap of the NMR signatures of interest). As well, this approach results in shorter analysis times relative to chromatographic methods.

8.3 Future work

Based on my research projects during the PhD program, the utility of biopolymers, such as cellulose, starch (linear and branched forms) and their modified forms were reported as suitable adsorbents in binary (water and ethanol; W+E) solution mixtures at variable W+E composition.[66] A key hypothesis in my PhD research focused on the controlled variation of the physicochemical properties of native biopolymers and biomass through synthetic modification of the biopolymer structure. Cross-linking of polysaccharides with epichlorohydrin (EPI) serves as a promising technique to achieve this goal. Judicious choice of cross-linker offers specific features including rigidity, flexibility, and variable HLB. The cross-linking of polysaccharides with different types of cross-linkers is a recommended area of proposed research for the design of new adsorbents. The cross-linker introduces intermolecular bridges or cross-links units between biopolymer units that may serve to alter the overall textural properties and surface chemistry of the framework. In addition, the modular design by doping other components such as metal ions or introduction of other elements as chelator sites represents a facile approach for tuning the sorption capacity especially for polysaccharides. Metals that incorporate modular binding sites when combined with polysaccharides are predicted to enhance their water and/or ethanol adsorptive properties.[67]

In this research, additional study has revealed that the utility of biomass such as Miscanthus offers a cost-effective and sustainable adsorbent material with suitable adsorbent properties that may fulfill the requirements for adsorptive fractionation in ethanol-water mixtures. Experimental studies on the fractionation of water or ethanol in binary (W+E) mixtures illustrate the unique hydration and physicochemical properties of biopolymers and their modified forms due to their ability to undergo molecular selective adsorption in solution.[68] Moreover, the ability to tune the hydration and textural properties of biomass through synthetic modification is supported by results from recent publications.[64,69,70] The present study was focused on solid-liquid (s/l) adsorption processes; however, biopolymers and their modified forms can be extended to solid-gas (s/g) adsorption phenomena. The systematic study of solid-gas isotherms can provide further insight on the role of solvation phenomena by comparing each type of process (s/l *vs.* s/g). The study of thermodynamics of adsorption can be further evaluated using immersion calorimetry to evaluate heats of adsorption to further understand the role of structure and the nature of the adsorptive interactions between the biopolymer-adsorbate systems. Also, the systematic studies using dynamic vapour sorption can be done at variable temperature to obtain enthalpic data or heats of adsorption.[71] Furthermore, complementary measurements such as surface sensitive measurements using Attenuated Total Reflectance (ATR), and measurement of water *vs.* D_2O along with more detailed evaluation of the uncoupled oscillator bands using Raman spectroscopy may be useful to understand the interactions between the active site of adsorbent and the mode of adsorption for such solid adsorbent-vapour phase systems.[72] As well, these studies may provide insight on the role of biopolymer surface modification and its effect on the thermodynamics and kinetics of the adsorption process. In terms of application, the use of other biomass sources for water-ethanol separation in aqueous media can be considered since the key factors (e.g., biomass composition, particle size) that govern the adsorptive selectivity in mixed solvents can be applied to other biomass sources. Generally, biomass is amenable to further chemical modification which offer potential suitability as biomaterial platforms through synthetic modification for wider use as adsorbent materials in various technological applications. For example, biomass-based desiccant materials are widely used due to their strong affinity for uptake of water vapour, which have potential utility in devices for controlling relative humidity and/or gas separation. Desiccants are widely used in food products, nutritional supplements, and the packaging industry (nutraceuticals, textiles, pharmaceuticals, and electronic equipment), ventilation and drying systems, solvent

purification, and air separation due to different technical demands for each type of application. Silica gel, molecular sieves, activated alumina, activated carbon, and zeolites are common industrial adsorbents in the global market. With the increased demand in drying processes and desiccant materials, a recent study revealed that the global market for adsorbents is projected to reach $4.3 billion (USD) by 2020.[73] In the past few decades, research activity has focused on sustainable and advanced desiccant material and/or desiccant based technology, especially for porous silica and carbon.[74] Research efforts on the development of new types of desiccant have resulted in materials with promising desiccant properties. The field of adsorption science and technology has witnessed increasing attention toward the use of biomaterial adsorbents due to their unique adsorption properties that can be altered upon synthetic modificaiton. However, comparatively few studies have evaluated biomaterials as alternative desiccants.[375] Improved biopolymer desiccant materials have been developed with greater sorption capacity, regeneration ability, and long-term stability. Among the various polysaccharide sorbent materials available, starch and cellulose are renewable resources of great interest due to their biodegradability, structural variability, relative and synthetic versatility. A recent study has revealed that starch biopolymer desiccants displayed enhanced sorption capacity and regeneration ability when compared against commercial silica desiccant materials for air conditioning applications.[67] The potential use of polysaccharides and their modified forms as adsorbents for solid-gas (s/g) adsorption processes has been demonstrated. For example, polysaccharides as desiccants have been studied as coatings for enthalpy wheels due to their high surface area, low cost, and low regeneration temperature.[73] A schematic of an energy wheel channel with coating is shown in Figure 8.3.1, where hot and humid air passes through the wheel channels and the latent heat is mainly stored upon condensation onto the metallic substrate. As the wheel rotates and the channels are exposed to the cold and dry airstreams, the accumulated heat and moisture in the wheel matrix are released into the airstream. As a result of the continuous rotation of the wheel, heat and moisture are transferred between the supply and exhaust airstreams, periodically. The commercial wheels in the market are capable of transferring up to 80-85% of heat and 70-75% moisture between the airstreams.[76] Studies of the performance of a starch-coated energy wheel indicates that the abundant hydrophilic groups and the unique structure of polysaccharide-based materials possess unique adsorption properties towards water vapour. With the same amount of desiccant coated on the energy wheel matrix, the moisture recovery effectiveness of the starch-coated wheel

was improved by up to 13% compared to the silica gel-coated wheel. Future work on modified biopolymers (cellulose, starch) and biomass desiccants (flax and oat hulls) as alternative desiccants for energy wheels are proposed herein. It should be mentioned that the biomass candidates can be chemically treated to increase the surface accessibility of the samples to enhance their water uptake capacity. A key research issue with such systems is how to optimize adsorption from the gas phase at ambient conditions without the need for cooling to initiate condensation of the vapour. Thus, the study of materials with controlled surface chemical and textural properties is warranted and may be achieved by controlled modification of biopolymers using a cross-linking strategy. The effect of the cross-linking on efficiency of the heat exchanger system coated using these biomaterials can be investigated systematically.[67] Controlling the HLB and textural properties through synthetic modification are key parameters of the adsorbent and developing an understanding of its role on water vapour adsorption is an important scientific goal. The development and use of calorimetric methods such as immersion calorimetry may offer a new screening method for understanding the thermodynamics of adsorbed vapours (water and ethanol) onto new types of adsorbents in s/g systems. Therefore, developing an understanding of the adsorbent-adsorbate enthalpic interactions is a key thermodynamic parameter; especially when used in conjunction with a sensitive method such as ATR spectroscopy to address the knowledge gaps and objectives described above.

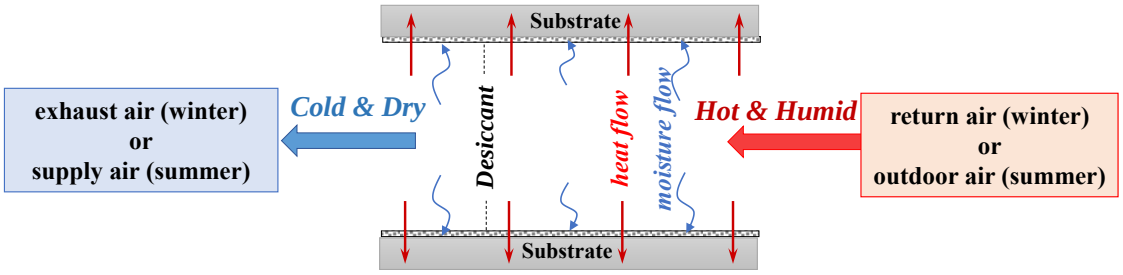

Figure 8.3.1 Schematic of heat and moisture transfer in a desiccant-coated channel of an energy wheel.

Knowledge gaps and specific objectives:

- To carry out screening of biopolymers, biomass, and their modified forms through characterization of their physicochemical properties for adsorption of water/ethanol vapours at variable conditions (monolayer *vs.* multilayer adsorption).
- To devise and develop a practical synthetic modification method for preparing biomaterial-based desiccants suitable for application in vapour phase adsorption of water.
- To evaluate the role of particle morphology and surface chemistry of polysaccharides and their modified form on adsorption kinetics and thermodynamics of water vapour.
- Calorimetric studies can provide a molecular-level understanding of the water vapour adsorption process by examination of such processes in a systematic manner.
- AT-IR and Raman spectroscopy can serve as potentially useful spectroscopic technique to establish the modality of interaction (monolayer *vs.* multilayer adsorption) to yield molecular level information concerning the interactions at the adsorbent surface.

8.4 References

1. Alcázar-Alay, S. C.; Meireles, M. A. A. *Food Sci. Technol, Campinas* **2015,** *35(2),* 215-236.
2. Bertoft, E. *Agronomy* **2017,** *7,* 56-85.
3. Immel, S.; Lichtenthaler, F. W. *Starch – Stärke* **2000,** *52(1),* 1-8.
4. Hanna, A. M.; Bhatnagar, H. *Cereal Chem.* **1994,** *71(6),* 582-587.
5. Kasaai, M. R. *Curr. Trends Polymer Sci.* **2012,** *16,* 49-63
6. Ehrhardt, A.; Groner, S.; Bechtold, T. *Fibers Text. East Eur.* **2007,** 15(5-6), 46-48.
7. Pratt, D. Y.; Wilson, L. D.; Kozinski, J. A.; Mohart, A. M. *J. Appl. Polym. Sci.* **2010,** *116,* 2982–2989
8. Mohamed, M. H.; Udoetok, I. A.; Wilson, L. D.; Headley, J.V. *RSC Adv.* **2015,** 5, 82065–82077.
9. Wang, K-Sh.; Liao, Ch-Ch.; Chu, R. Q.; Chung, T-W. *J. Chem. Eng. Data*, **2010**, *55* (9), 3334–3337.
10. Shiftan, D.; Ravenelle, F.; Mateescu, M. A.; Marchessault, R. H. *Starch/Stärke* **2000,** 52,186–195.
11. Singh, J.; Kaur, L.; McCarthy, O. J. *Food Hydrocoll.* **2007,** *21(1),* 1-22.
12. Acˇkar, D.; Babic´, J.; Šubaric´, D.; Kopjar, M.; Milicˇevic, B. *Carbohyd. Polym.* **2010,** *81,* 76–82.

13. Vecchi, C.; Bertini, S.; Crini, G.; Naggi, A. M.; Torri, G. *Rivista Combust.* **1998,** *52,* 231–236.
14. Bonenfant, D.; Niquette, P.; Mimeault, M.; Furtos-Matei, A.; Hausler, R. *Water Res.* **2009,** *43,* 3575–3581.
15. Bonenfant, D.; Niquette, P.; Mimeault, M.; Hausler, R. *Water Sci. Technol.* **2010,** *61,* 2293–2301.
16. Bonenfant, D.; Niquette, P.; Mimeault, M.; Hausler, R. *Water Sci. Technol.* **2012,** *66,* 224– 230.
17. Udoetok, I. A.; Wilson, L. D.; Headley J. V. *Ultrason. Sonochem.* **2018,** *42,* 567–576.
18. Morin-Crini, N.; Crini, G. *Prog. Polym. Sci.* **2013,** *38,* 344–68.
19. Smith, A. M. *Biomacromolecules,* **2001,** *2(2),* 335-341.
20. Majzoobi, M.; Radi, M.; Farahnaky, A.; Jamalian, J.; Tongdang, T. *Iran Polym. J.* **2009,** *18(6),* 491-499.
21. Horianski, M. A.; Peralta, J. M.; Brumovsky, L. A. *Nutr. Food Sci.* **2016,** *46(4),* 517-528.
22. Fannon, J. E.; Hauber, R. J.; Bemiller, J. N. Surface pores of starch granules. *Cereal Chem.* **1992,** *69,* 284–288.
23. Gallant, D. J.; Bouchet, B. Ultrastructure of maize starch granules - a review. *Food Microstruct.* **1986,** *5,* 141–155.
24. Chinga-Carrasco, G. *Nanosc. Res. Lett.* **2011,** *6,* 417-424.
25. Ding, S-Y.; Zhao, S.; Zeng, Y.; *Cellulose,* **2013,** *21,* 863–871.
26. Sumari, S.; Roesyadi, A.; Sumarno, S. *Sci. Study Res.* **2013,** 14, 229-239.
27. Li, W.; Wang, R.; Liu, S.X. *Bioresources* **2011,** *6,* 4271–4281.
28. Wang, L.; Xie, B.; Xiong, G.; Du, X.; Qiao, Y.; Liao, L. *Carbohydr. Polym.* **2012,** *87(2),* 1038–1044.
29. Chen, P.; Yu, L.; Kealy, T.; Chen, L.; Li, L. *Carbohydr. Polym.* **2007,** *68(3),* 495–501.
30. Liu, H.; Yu, L.; Xie, F.; Chen, L. *Carbohydr. Polym.* **2006,** *65(3),* 357–363.
31. Jane, J.; Xu, A.; Radosavljevic, M.; Seib, P. A. *Cereal Chem.* **1992,** *69,* 405-409.
32. Singh, J.; Kaur, L.; McCarthy, O. J. *Food Hydrocoll.* **2007,** *21 (1),* 1-22.
33. Acquarone, V. M.; Rao, M. A. *Carbohydr. Polym.* **2003,** *51,* 451–458.
34. Hirsch, J. B.; Kokini, J. L. *Cereal Chem.* **2002,** *79(1),* 102–107.
35. Sanz-Perez, E. S.; Arencibia, A.; Sanz, R.; Calleja, G. *RSC Adv.* **2015**, 5, 103147–103154.
36. Udoetok, I. A.; Dimmick, R. M.; Wilson, L. D.; Headley, J. V. *Carbohydr. Polym*. **2016**, 136, 329–340.

37. Alexandrino, J. S.; Peres, A. E. C.; Lopes, G. M.; Rodrigues, O. M. S. *REM: R. Esc. Minas, Ouro Preto,* **2016,** *69(2),* 193-198.

38. Hubbe, M. A.; Beck, K. R.; Gilbert O'Neal, W.; Sharma, Y. Ch. Bioresources **2012,** *7(2),* 2592-2687.

39. Kosmulski, M. *J. Colloid Interface Sci.* **2002,** *253,*77–87.

40. Karimi, S.; Ghobadian, B.; Omidkhah, M-R.; Towfighi, J.; Tavakkoli Yaraki, M. *J. Adv. Res.* **2016**, 7, 435–444.

41. Klucinec, J. D.; Thompsonref, D. B. *Cereal Chem.* **1999,** *76(2),* 282–291.

42. Tester, R. F. Morrison, W. R. *Cereal Chem.* **1990,** *67(6),* 551-557.

43. Simo, M.; Sivashanmugam, S.; Brown, C. J.; Hlavacek, V. *Ind. Eng. Chem. Res.* **2009,** *48,* 9247-9260.

44. Mardis, K. L.; Brune, B. J.; Vishwanath, P.; Giorgis, B.; Payne, G. F.; Gilson, M. K. *J. Phys. Chem. B* **2000,** *104,* 4735-4744.

45. Rojas, J.; Azevedo, E. *Int. J. Pharm. Sci. Rev. Res.* **2011,** *8(1),* 28-36.

46. Lee, Sh-H.; Kim, M-J.; Park, H. *J. Appl. Polym. Sci.* **2010,** *117,* 623–628.

47. Lesas, C. H.; Pierre, M. Cross-linked cellulose fibers. U.S. Patent 4204055A, May.20, 1980.

48. Koo, S.H.; Lee, K.Y.; Lee, H.G. *Food Hydrocoll.* **2010,** *24,* 619–625.

49. Aloulou, F.; Boufi, S.; Labidi, J.; *Sep. Purif. Technol.* **2006,** *52,* 332–342.

50. Moulthrop, J. S.; Swatloski, R. P.; Moyna, G.; Rogers, R. D. *Chem. Commun.***2005,** *28(12),* 1557-1559.

51. Tran, C. D.; Duri, S.; Delneri, A.; Franko, M.; *J. Hazard. Mater.* **2013,** *252,* 355–366.

52. Tang, L. R.; Huang, B.; Lu, Q. L.; Wang, S.Q.; Ou, W.; Lin, W.Y.; Chen, X. R. *Bioresour. Technol.* **2013,** *127,* 100–105.

53. Sing, K. *Colloids Surf. A: Physicochem. Eng. Aspects* **2001,** *187–188,* 3–9.

54. Broekhoff, J. *J. Catal.* 1968, 10, 153–165.

55. Mohamed, H. M.; Wilson, L. D. *Nanomaterials* **2015,** *5,* 969–980.

56. Henniges, U.; Veigel, S.; Lems, E-M.; Bauer, A.; Keckes, J.; Pinkl, S.; Gindl-Altmutter, W. *Cellulose* **2014,** *21,* 1601–1610.

57. Arnoult, S.; Brancourt-Hulmel, M. *Bioenerg. Res.* **2015,** *8,* 502-526.

58. Moiceanu, G.; Voicu, G.; Paraschiv, G.; Voicu. P. Engineering for Rural Development, Jelgava, **2013,** 23.509-515.

59. Szejtli, J.; Fenyvesi, É.; Zsadon, B.; Szilasi, M. *Starch/Stärke* **1978,** *30*, 127–131.
60. Szejtli, J. *Starch/Stärke* **1982,** *34*, 379–85.
61. Tekin, K.; Karagöz, S.; Bektas¸ S. *Renew Sust. Energy Rev.* **2014,** *40,* 673–87.
62. Oleinikova, A.; Brovchenko, I. *J. Phys. Chem. B* **2012,** *116(50),* 14650–14659.
63. Wilson, L. D.; Mohamed, M. H.; Headley, J. V. *J. Colloid Interface Sci*. **2011**, 357, 215-222.
64. Dehabadi, L.; Wilson, L. D.; *Carbohyd. Polym.* **2014,** *113,* 471-479.
65. Mohamed, M. H.; Wilson, L. D. *Adsorption* **2016,** *22,*1025–1034.
66. Zheng, X.; Ge, T. S.; Wang, R.Z. *Energy,* **2014,** *74*, 280–94.
67. Fathieh, F. Dehabadi, L.; Wilson, L. D.; Besant, R. W.; Evitts, R. W.; Simonson, C. J. *ACS Sustainable Chem. Eng.* **2016,** *4(3),* 1262–1273.
68. Dehabadi, L.; Wilson, L. D. *Energy Fuels* **2016,** *30,* 5684-5692.
69. Dehabadi, L.; Wilson, L. D. *Energy Fuels* **2015,** *29,* 6512-6521.
70. Fathieh, F.; Besant, R. W.; Evitts, R. W.; Simonson, C. J. *Int. J. Heat Mass Transf.* **2015,** *87,* 312–326.
71. Harley,; S. J. Glascoe, E.; A. Maxwell, R.; S. *J. Phys. Chem. B* **2012,** *116,* 14183−14190.
72. Belhadj, H.; Hakki, A.; Robertson, P. K. J.; Bahnemann, D. W. *Phys. Chem. Chem. Phys.* **2015,** *17,* 22940-22946.
73. www.marketsandmarkets.com/Market-Reports/adsorption-market-1173.html.
74. Zheng, X.; Ge, T. S.; Wang, R. Z. *Energy* **2014,** *74,* 280–294.
75. Westgate, P. J.; Lee, J. Y.; Ladisch, M. R. *Trans. ASAE* **1992,** *35,* 213-219.
76. ASHRAE, **2008,** ASHRAE, HVAC Systems and Equipments, ASHRAE, Atlanta, GA.

Supplementary Data and Appendices

1. Appendix A (Chapter 2)

A2.1 Selection of pulse sequence for quantitative NMR

One of the most common ways to employ qNMR spectroscopy for the detection of small molecules is the use of the single-pulse NMR technique,[1] which is comprised by a relaxation delay (RD) and a 90° hard pulse followed by acquisition of signals.

In one study, the limit of detection was indicated as 0.02 g/L for ethanol.[2] If the concentration of the analyte is low, it could affect the quantitative accuracy and precision owing to the presence of a strong solvent signal. This issue is known as *dynamic range* and emerges in the presence of a very strong solvent peak (typically water) for recording of very weak signals. To overcome this obstacle, solvent-suppression techniques are used to achieve an acceptable *signal-to-noise ratio* (S/N) that results in improved quantitative accuracy and precision. For instance, to observe the hydrogen nuclei for an amide, the spectra of proteins and peptides requires a solution of 90% H_2O /10% D_2O. In this solvent mixture, a good solvent detection of hydrogen atoms is not possible before applying a solvent-suppression technique. Solvent-suppression techniques need some consideration in the pulse sequence, which can be executed before the 90° hard pulse by pre-saturation of the solvent spectral frequency.

A2.2 Acquisition parameters

A2.2.1 Excitation pulse

For recording the spectra, a 90° or lower angle pulse can be used and the excitation bandwidth of the hard pulse should be uniform throughout the entire spectral width. The success of this method varies with offset as repetition time is dependent on the design of the low-pass frequency filter (eclipsed or brick-wall shaped), resulting in an erroneous signal intensity.[3] Success with 90° pulses might also differ depending on the physicochemical properties of the sample. Calibration of the pulse length should be done to obtain acceptable precision and accuracy. Although a 90° pulse should provide maximum intensity, sometimes applying a smaller pulse angle can assist in reaching a complete spectral relaxation.

A2.2.2 Repetition time (RT)

Repetition time can be defined as the total time required to acquire a single-scan spectrum, which also includes a relaxation delay (RD) and acquisition time. RT depends on the longest T_1 present in the sample and in order to measure 99% of the equilibrium magnetization, the RD should be five times greater than the longest T_1,[4,5] according to the following equation:

$$M_z = M_0 . (1 - e^{\frac{-\tau}{T_1}}) \qquad \text{Equation A2.1}$$

Calculation of the amount of relaxation for a specific resonance at a fixed T_1 is possible where M_z and M_0 are the magnetization in the z-axis dimension after the repetition time (τ) and at full relaxation, respectively. T_1 is considered as the longitudinal relaxation time of the resonance signal.

A2.2.3 Integration

Integration of the spectral peak area is one of the most critical steps when using qNMR spectral analysis because the range of the integral region of the spectral signal and the setting of the slope and the bias are known to strongly influence the precision of the quantitative measurement.[6] During integration, greater accuracy is probable if a number of sources of errors such as *signal to noise*, saturation effects (the decrease in the intensity of a spectral line with increasing power of the external resonant electromagnetic radiation), and digital resolution (equal to [acquisition time]$^{-1}$) are properly controlled. To cover 100% of the peak area, infinite integration is required. In order to cover 99% of the total area, the integral region should be extended in a way that it becomes 20 times longer than the peak width in both directions. By performing an adequate baseline correction, slope and bias corrections are unnecessary as integrals are highly sensitive to baseline imperfection. Sometimes, for obtaining accurate quantitation, manual slope and bias corrections are required.[6]

The information above provides background to define the objectives of this PhD thesis research. Descriptions of the different separation and quantitation techniques enhance an understanding of the utility of NMR spectroscopy for the quantitative analysis, in adsorption processes, of binary solvent mixtures containing water/ethanol.

A2.3 References

1. Becker, E. D. High Resolution NMR: theory and chemical applications, 2nd ed. Academic, New York: **1980,** 1-417.
2. Zailer, E. Diehl, B. W. K. *J. Pharm. Biomed. Anal.* **2016,** *119,* 59–64.
3. Saude, E. J.; Slupsky, C. M.; Sykes, B. D. *Metabolomics* **2006,** *2,* 113-123.
4. Ernst, R. R.; Anderson, W. A. *Rev. Sci. Instrum.* **1996,** *37,* 93-102.
5. Bharti, S.; Sinha, N.; Joshi, B.; Mandal, S.; Roy, R.; Khetrapal, C. *Metabolomics* **2008,** *4,* 367-376.
6. Bharti, S. K.; Roy, R. *Trends Anal. Chem.* **2012,** *35,* 5-26.

2. Appendix A (Chapter 3)

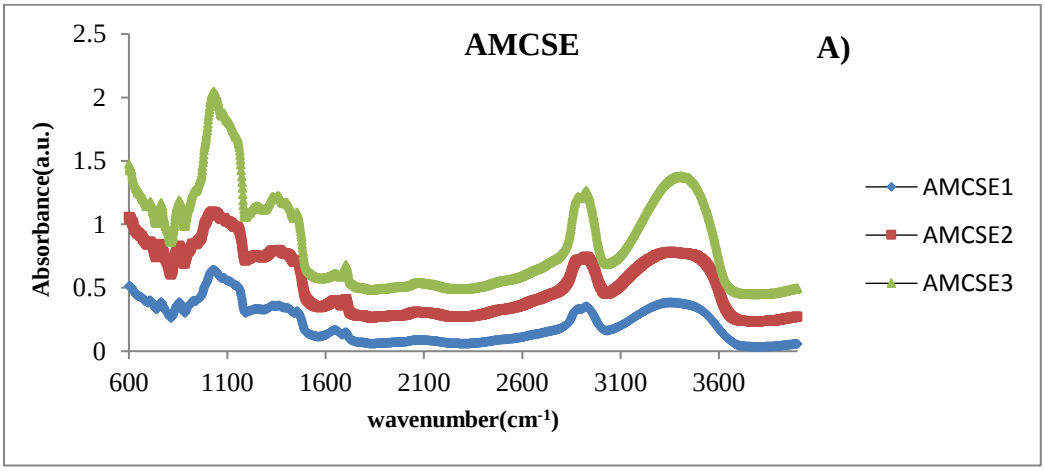

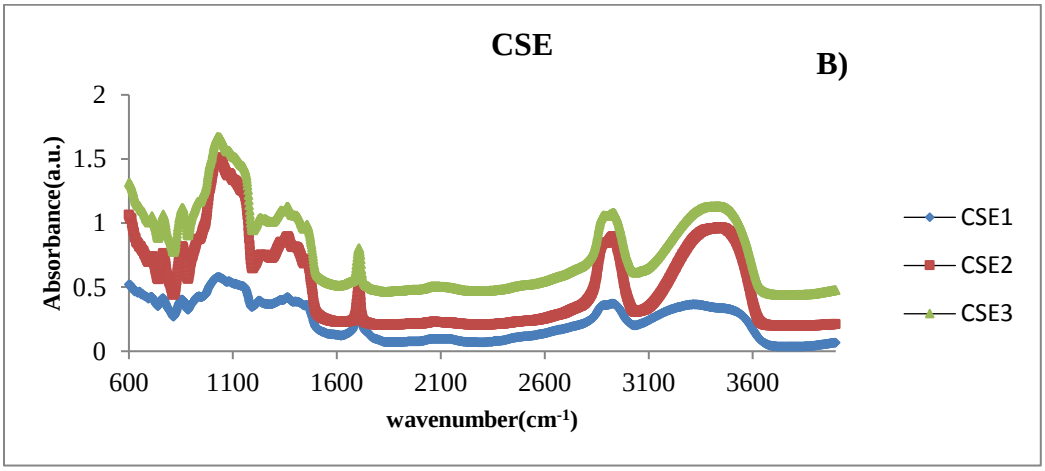

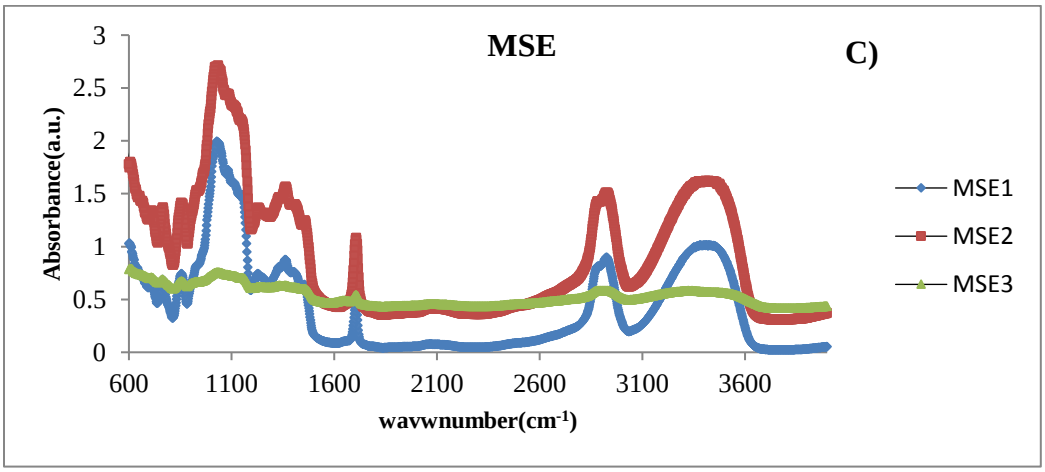

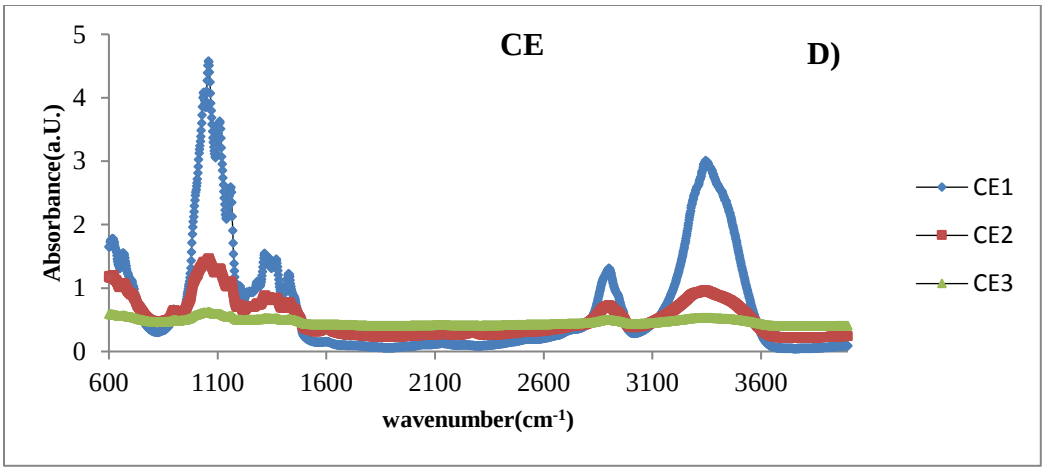

Figure A3.1 FT-IR spectra of starch and its PS-EPI biopolymers: A) AMSE-1, -2, and-3; B) CSE-1, -2, -3; C) MSE-1, -2, and -3; and D) CE-1, -2, -3.

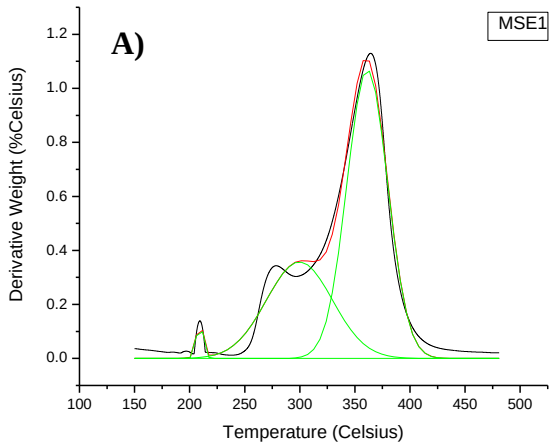
A)
MSE1
Derivative Weight (%Celsius)
Temperature (Celsius)

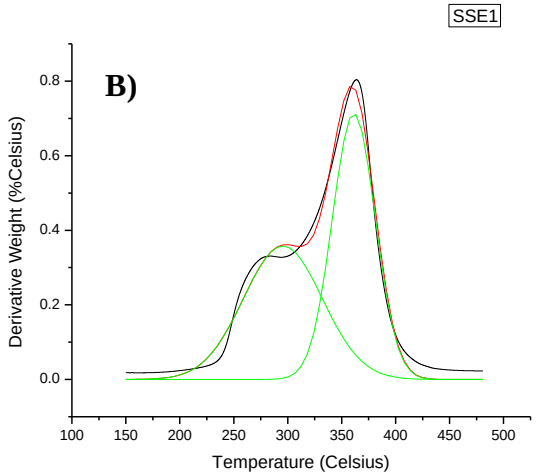
B)
SSE1
Derivative Weight (%Celsius)
Temperature (Celsius)

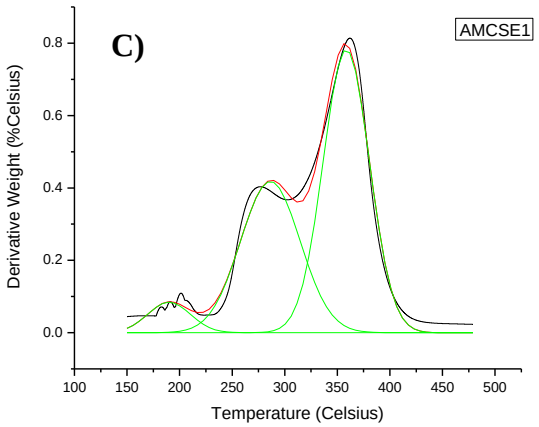
C)
AMCSE1
Derivative Weight (%Celsius)
Temperature (Celsius)

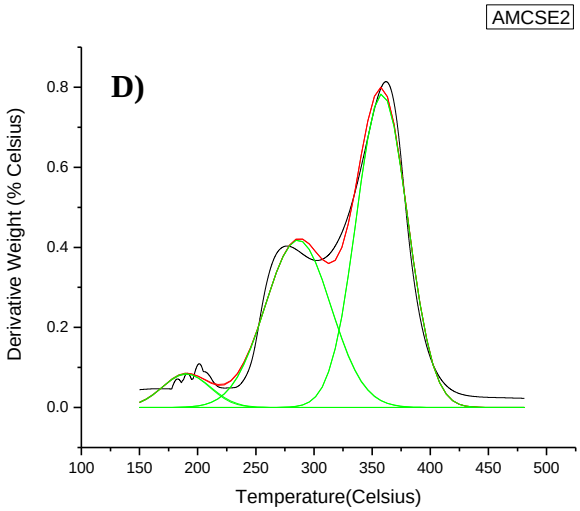
D)
AMCSE2
Derivative Weight (% Celsius)
Temperature(Celsius)

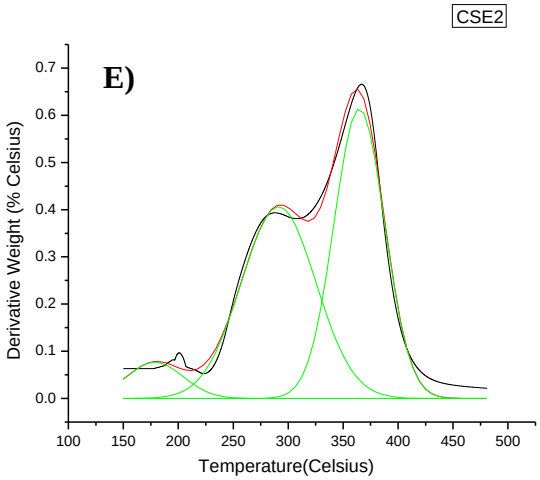
CSE2
E)
Derivative Weight (% Celsius)
Temperature(Celsius)

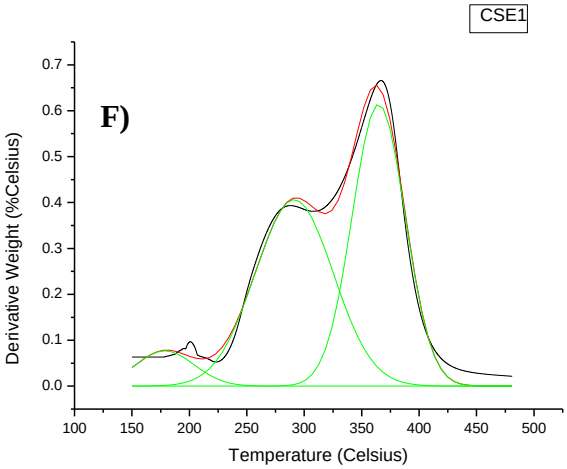
CSE1
F)
Derivative Weight (%Celsius)
Temperature (Celsius)

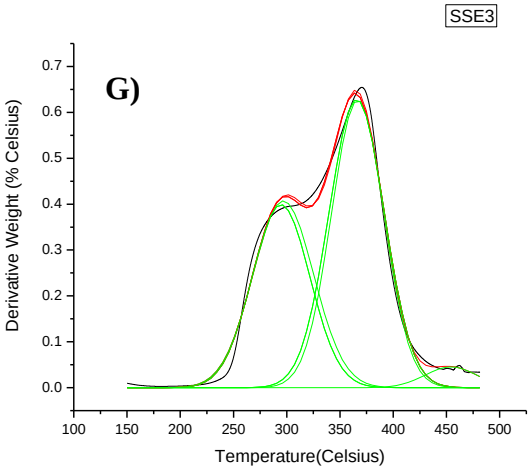
SSE3
G)
Derivative Weight (% Celsius)
Temperature(Celsius)

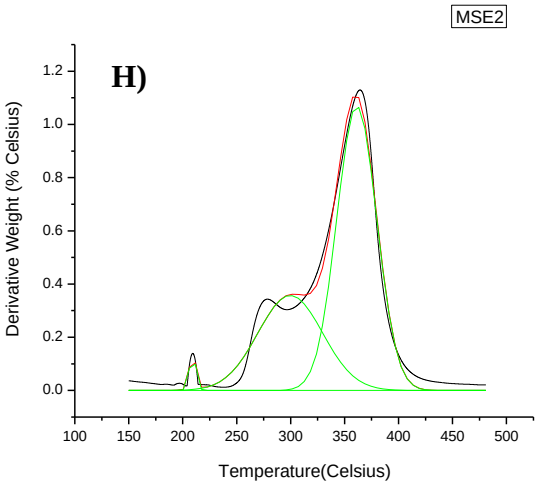
MSE2
H)
Derivative Weight (% Celsius)
Temperature(Celsius)

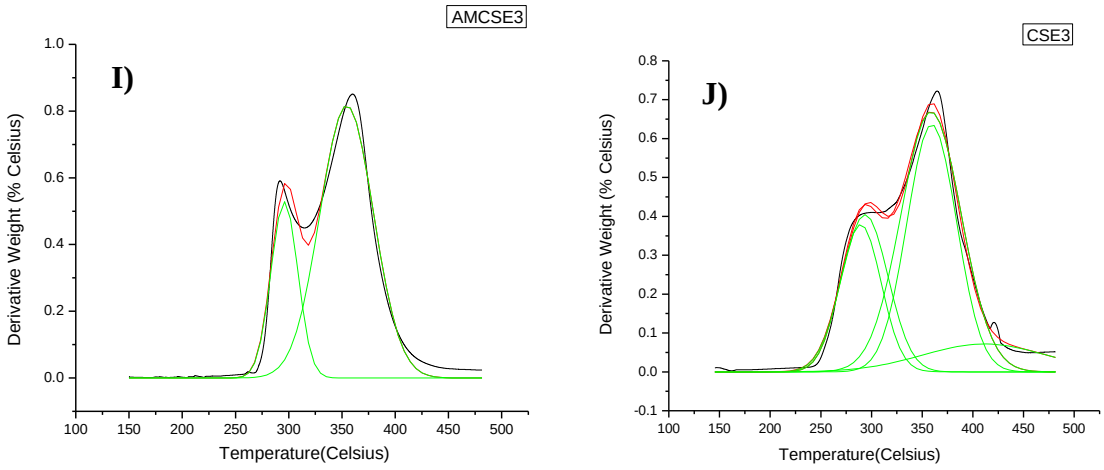

Figure A3.2 First derivative plots of weight loss with temperature against temperature (°C) for PS-EPI biopolymers. A) MSE-1; B) SSE-1, C) AMCSE-1, D) AMCSE-2, E) CSE-2, F) CSE-1, G) SSE-3, H) MSE-2, I) AMCSE-3, and J) CSE-3. The fitted lines represent Gaussian functions of the respective components for the DTG profile.

3. Appendix A (Chapter 4)

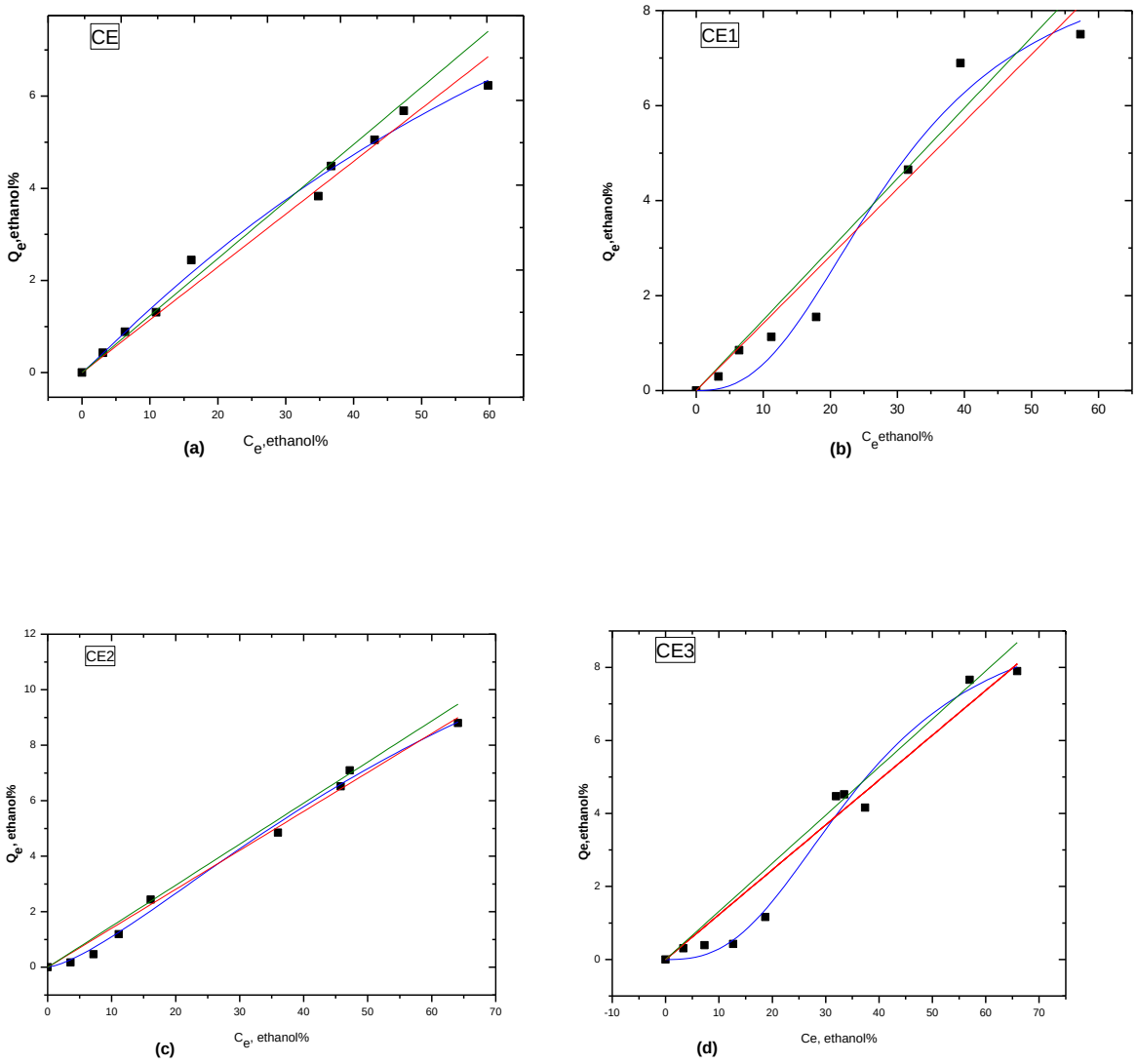

Figure A4.1 The Sorption isotherms Sips (blue), Langmuir (green) and Freundlich (red) fitting results for uptake of ethanol with cellulose and its cross-linked forms with D_2O as NMR solvent at 295 K.

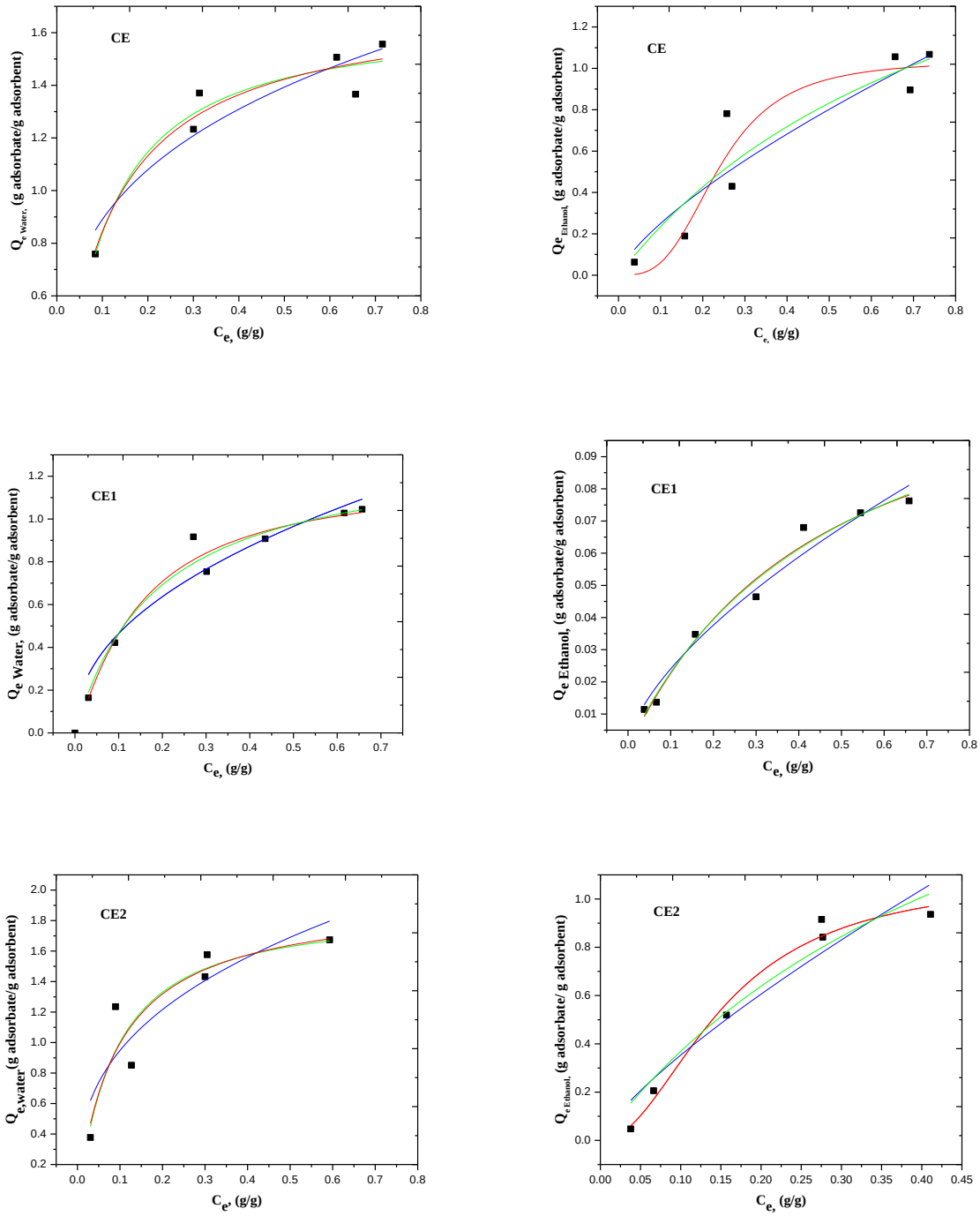

Figure A4.2 Uptake of solvent components (water and ethanol) in binary W-E solutions at 295 K. Best-fit lines according to the Sips (blue) and Langmuir (green) and Freundlich (red) isotherm models for cellulose and its cross-linked polymers.

Table A4.1 Sample descriptives using t-test for equality of means. (Water)

Cellulose ID Code	**K_s (g/g)**	**Q_m (g/g)**
CE	4.18 ± 0.67	1.03 ±0.13
CE-1	5.34 ± 3.55	1.02 ± 0.37
CE-2	6.57 ± 1.22	1.09 ± 0.14
CE-3	3.47 ± 2.54	1.13 ± 0.52
Mean	4.89	1.07
Standard Deviation	1.36	0.052
t-test	0.011	

Table A4.2 Sample descriptives using t-test for equality of means. (Ethanol)

Cellulose ID Code	**K_s (g/g)**	**Q_m (g/g)**
CE	10.40 ± 3.19	1.63 ± 0.244
CE-1	6.69 ± 2.62	1.20 ± 0.206
CE-2	11.32 ± 8.97	1.87 ± 0.63
CE-3	11.85 ± 4.93	2.44 ± 0.39
Mean	10.1	1.80
Standard Deviation	2.02	0.45
t-test	0.0045	

A') Pore diffusion

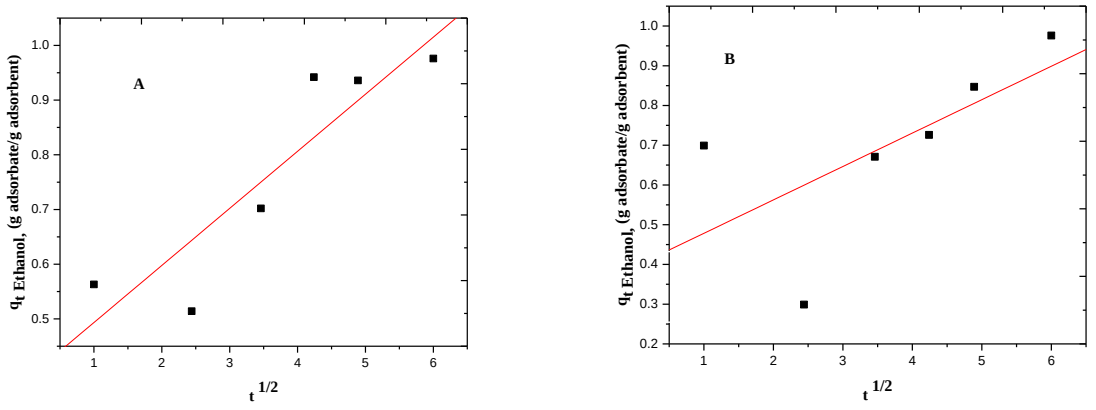

B') Non-Linear Pseudo-first order

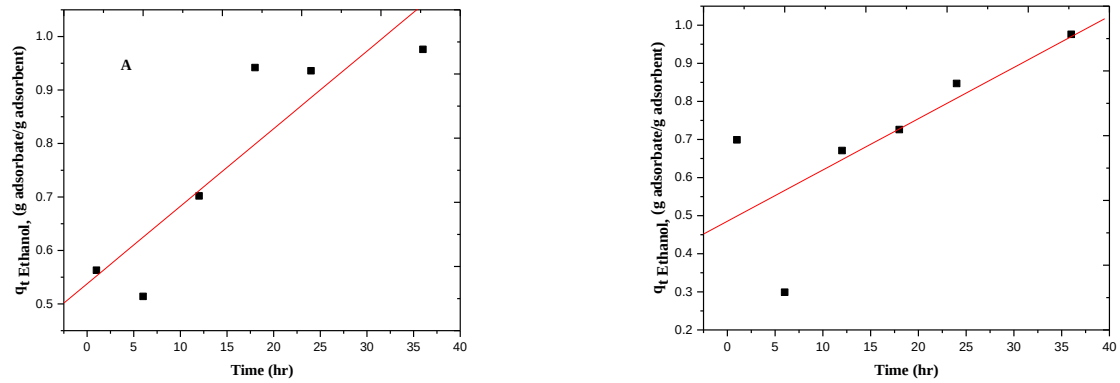

Figure A4.3 Kinetic uptake of ethanol from water-ethanol mixtures A) CE and B) CE-2 at 295 K.

4. Appendix A (Chapter 5)

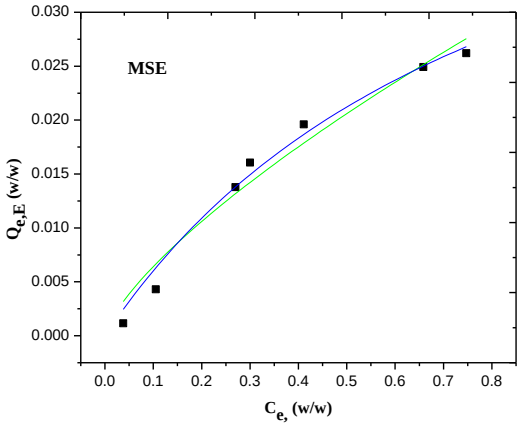

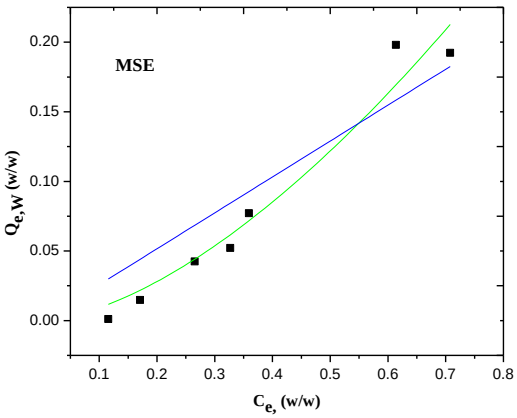

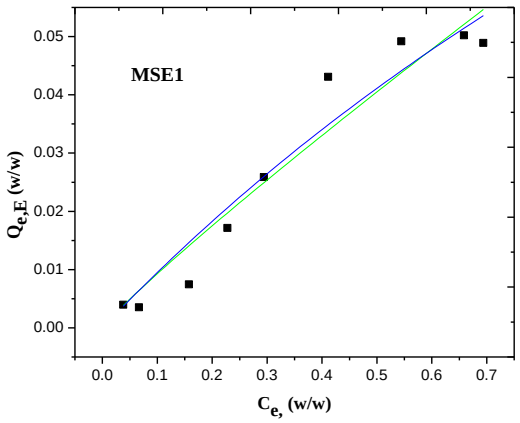

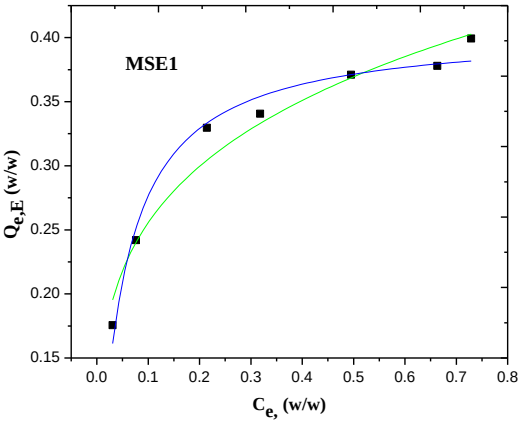

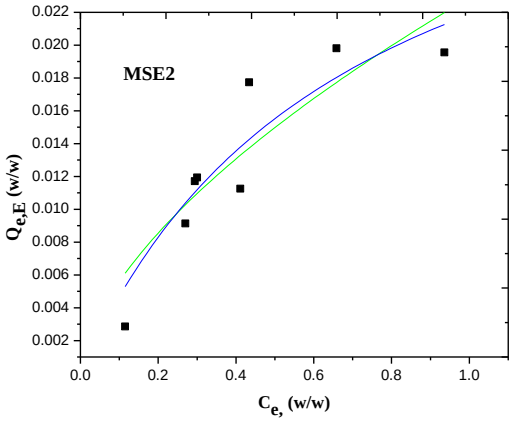

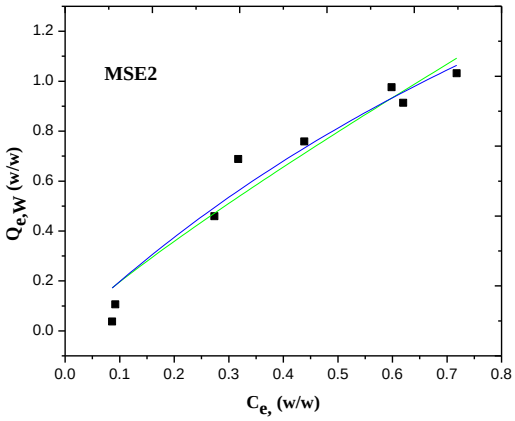

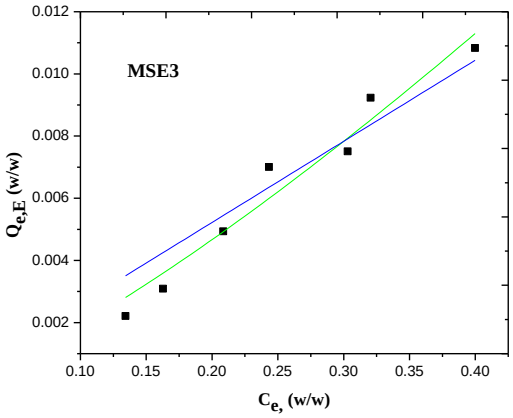
MSE3
Qe,E (w/w)
Ce, (w/w)

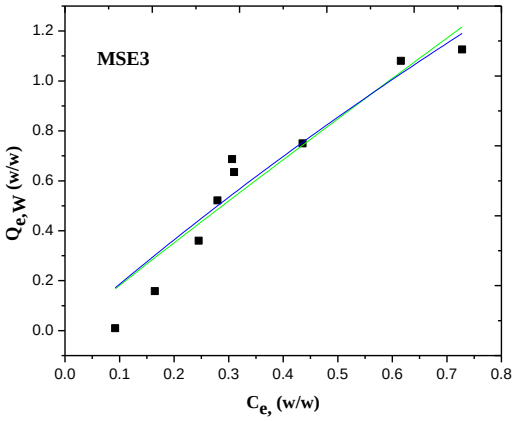
MSE3
Qe,W (w/w)
Ce, (w/w)

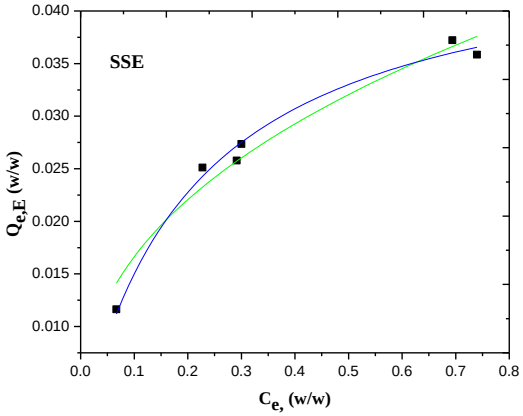
SSE
Qe,E (w/w)
Ce, (w/w)

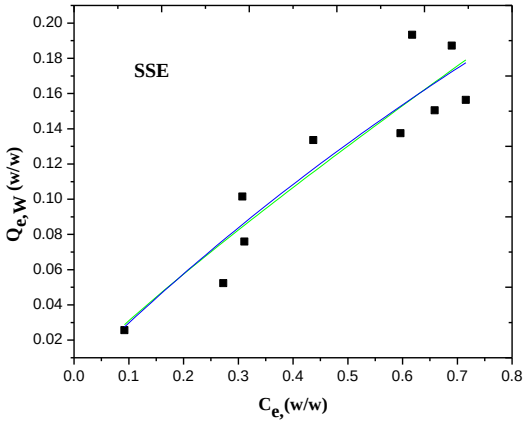
SSE
Qe,W (w/w)
Ce,(w/w)

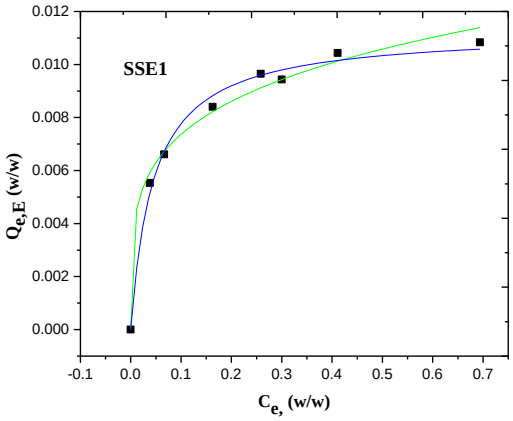
SSE1
Qe,E (w/w)
Ce, (w/w)

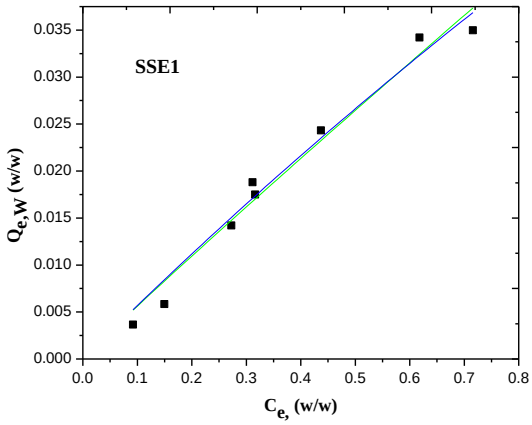
SSE1
Qe,W (w/w)
Ce, (w/w)

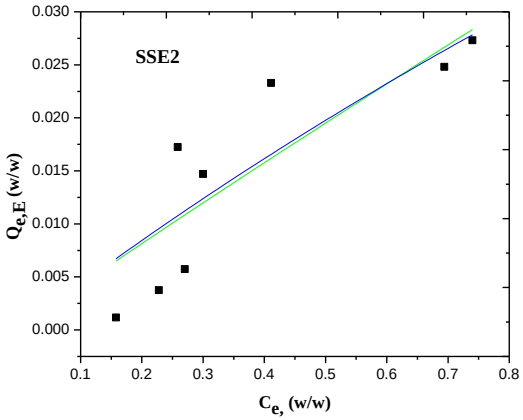
SSE2
$Q_{e,E}$ (w/w)
C_e, (w/w)

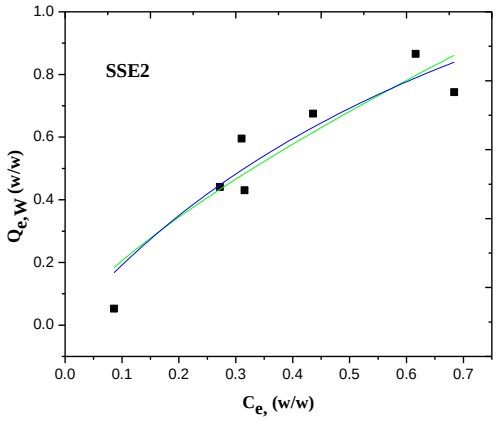
SSE2
$Q_{e,W}$ (w/w)
C_e, (w/w)

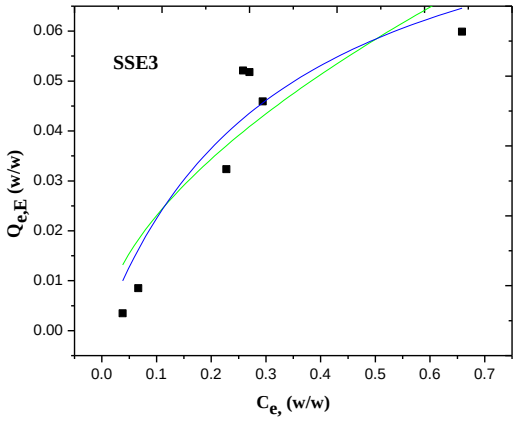
SSE3
$Q_{e,E}$ (w/w)
C_e, (w/w)

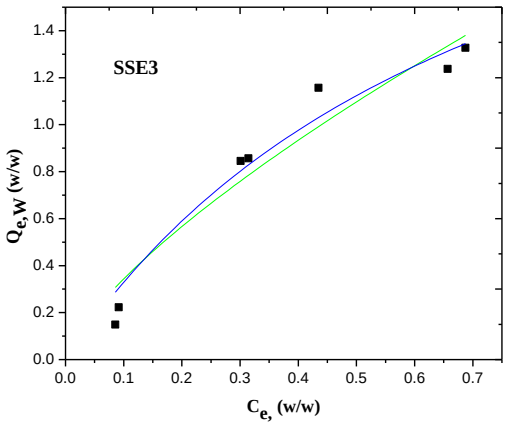
SSE3
$Q_{e,W}$ (w/w)
C_e, (w/w)

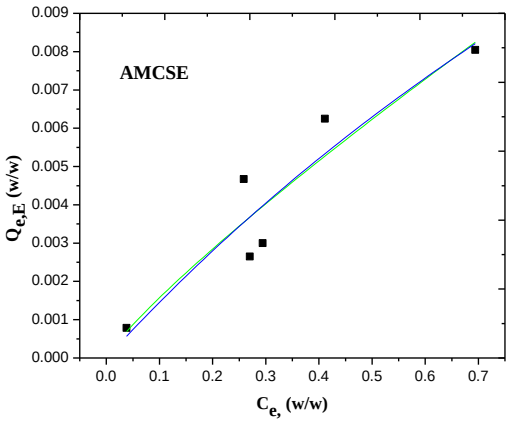
AMCSE
$Q_{e,E}$ (w/w)
C_e, (w/w)

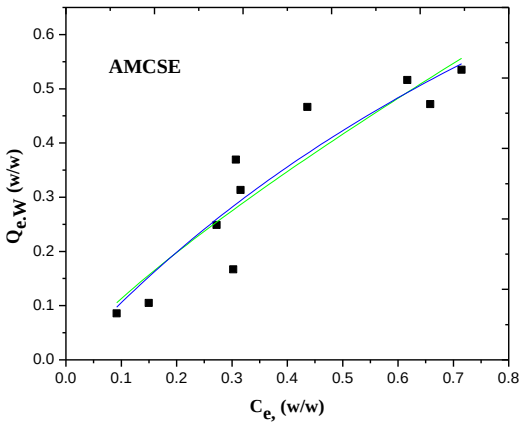
AMCSE
$Q_{e,W}$ (w/w)
C_e, (w/w)

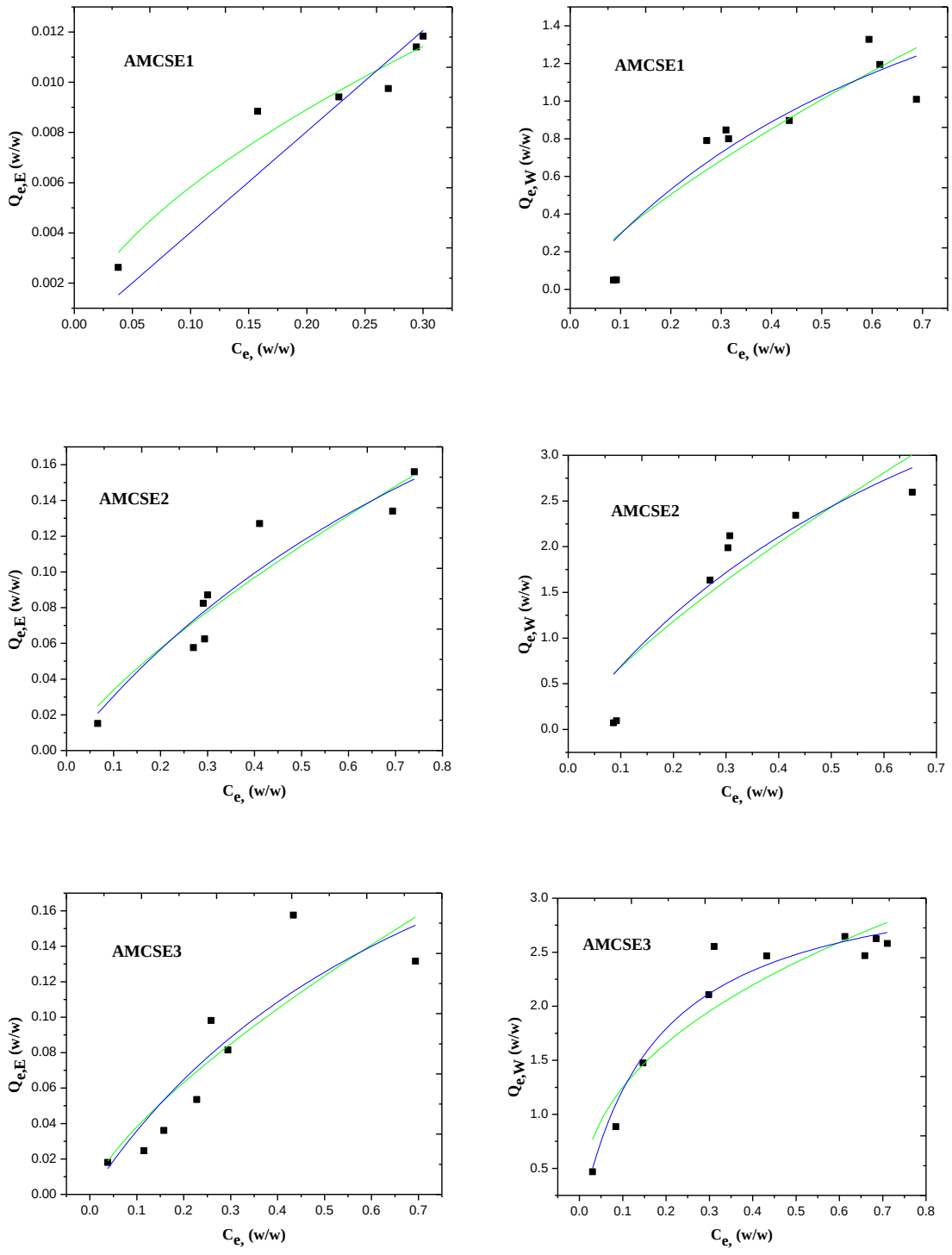

Figure A5 The Sorption isotherms Langmuir (blue) and Freundlich (green) fitting results for uptake of ethanol and water with starch and its cross-linked forms with DMSO-d_6 as NMR solvent at 295 K.

5. Appendix A (Chapter 6)

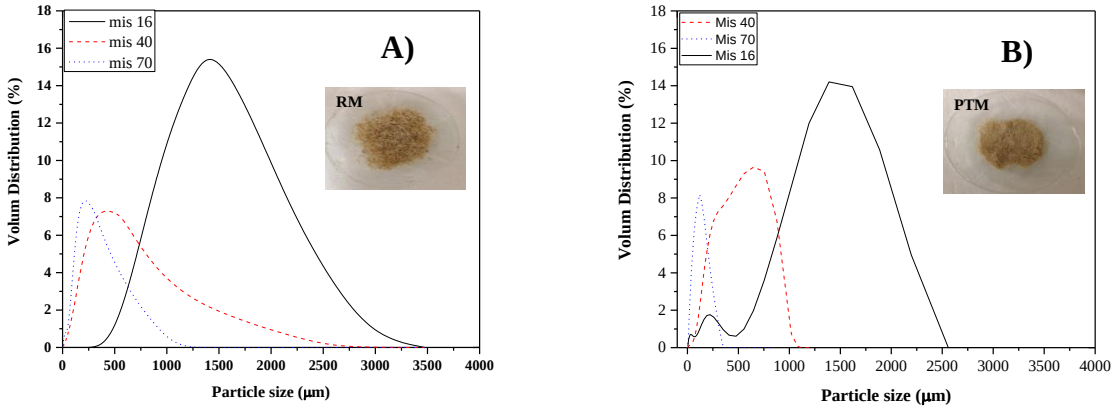

Figure A6.1 Particle size distribution and estimation of raw Miscanthus (A) and pretreated Miscanthus (B).

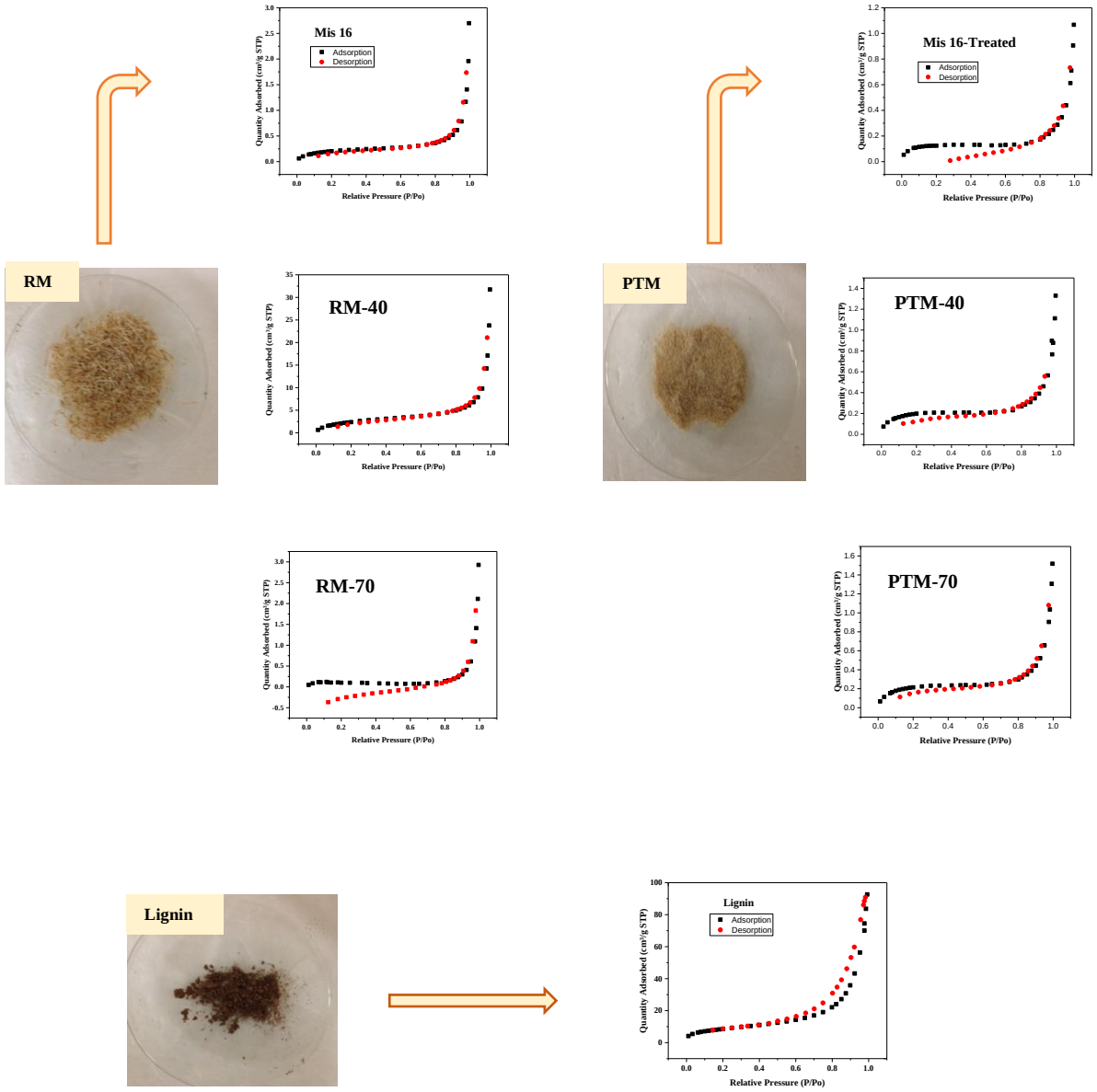

Figure A6.2 Nitrogen adsorption-desorption isotherm at 77 K for Raw Miscanthus (RM), Pretreated Miscanthus (PTM; greater cellulose content), and Lignin. The sample ID codes are defined as in Figure 6.1 above. Adorption profile (black) and desorption profile (red) is defined in lower panel.

Table A6.1 Textural characteri zation of Raw Miscanthus (RM), Pretreated Miscanthus (PTM; greater cellulose content), and Lignin using N_2 adsorption isotherms.

Surface Area	RM 16	RM 40	RM 70
Single point surface area at P/Po = 0.200388621 (m^2/g)	0.71	0.56	0.35
BET Surface Area (m^2/g)	0.80	0.61	0.32
Langmuir Surface Area (m^2/g)	1.1	0.87	0.42
t-Plot External Surface Area (m^2/g)	0.92	0.59	0.00
BJH Adsorption cumulative surface area of pores between 17.000 Å and 3000.000 Å width (m^2/g)	0.62	0.35	0.31
BJH Desorption cumulative surface area of pores between 17.000 Å and 3000.000 Å width (m^2/g)	0.65	0.41	0.45

Surface Area	PTM 16	PTM 40	PTM 70
Single point surface area at P/Po = 0.200388621 (m^2/g)	0.43	0.69	0.75
BET Surface Area (m^2/g)	0.44	0.74	0.82
Langmuir Surface Area (m^2/g)	0.60	1.05	1.18
t-Plot External Surface Area (m^2/g)	0.25	0.68	0.79
BJH Adsorption cumulative surface area of pores between 17.000 Å and 3000.000 Å width (m^2/g)	0.19	0.35	0.43
BJH Desorption cumulative surface area of pores between 17.000 Å and 3000.000 Å width (m^2/g)	0.35	0.55	0.49

Surface Area	Lignin
Single point surface area at P/Po = 0.200388621 (m^2/g)	29
BET Surface Area (m^2/g)	31
Langmuir Surface Area (m^2/g)	44
t-Plot External Surface Area (m^2/g)	32
BJH Adsorption cumulative surface area of pores between 17.000 Å and 3000.000 Å width (m^2/g)	33
BJH Desorption cumulative surface area of pores between 17.000 Å and 3000.000 Å width (m^2/g)	40

Pore Volume	RM 16	RM 40	RM 70
Single point adsorption total pore volume of pores less than 817.635 Å width at P/Po = 0.975739151(cm^3/g)	0.0018	0.022	0.0017
t-Plot micropore volume (cm^3/g)	0.00	0.00	0.00030
BJH Adsorption cumulative volume of pores between 17.000 Å and 3000.000 Å width (cm^3/g)	0.0042	0.050	0.0045
BJH Desorption cumulative volume of pores between 17.000 Å and 3000.000 Å width(cm^3/g)	0.0041	0.048	0.0045

Pore Volume	PTM 16	PTM 40	PTM 70
Single point adsorption total pore volume of pores less than 817.635 Å width at P/Po = 0.975739151(cm^3/g)	0.00095	0.0012	0.0014
t-Plot micropore volume (cm^3/g)	0.000086	0.0000090	0.00
BJH Adsorption cumulative volume of pores between 17.000 Å and 3000.000 Å width (cm^3/g)	0.0015	0.0019	0.0022
BJH Desorption cumulative volume of pores between 17.000 Å and 3000.000 Å width (cm^3/g)	0.0016	0.0021	0.0023

Pore Volume	Lignin
Single point adsorption total pore volume of pores less than 817.635 Å width at P/Po = 0.975739151(cm^3/g)	0.11
t-Plot micropore volume (cm^3/g)	0.00
BJH Adsorption cumulative volume of pores between 17.000 Å and 3000.000 Å width (cm^3/g)	0.14
BJH Desorption cumulative volume of pores between 17.000 Å and 3000.000 Å width (cm^3/g)	0.14

Pore Size	RM 16	RM 40	RM 70
Adsorption average pore width (4V/A by BET) (A°)	90.0	92.0	208
BJH Adsorption average pore width (4V/A) (A°)	268	209	577
BJH Desorption average pore width (4V/A) (A°)	254	211	402

Pore Size	PTM 16	PTM 40	PTM 70
Adsorption average pore width (4V/A by BET) (A°)	86.0	63.0	68.0
BJH Adsorption average pore width (4V/A) (A°)	326	220	206
BJH Desorption average pore width (4V/A) (A°)	189	151	184

Pore Size	Lignin
Adsorption average pore width (4V/A by BET) (A°)	137
BJH Adsorption average pore width (4V/A) (A°)	171
BJH Desorption average pore width (4V/A) (A°)	141

6. Appendix A (Chapter 7)

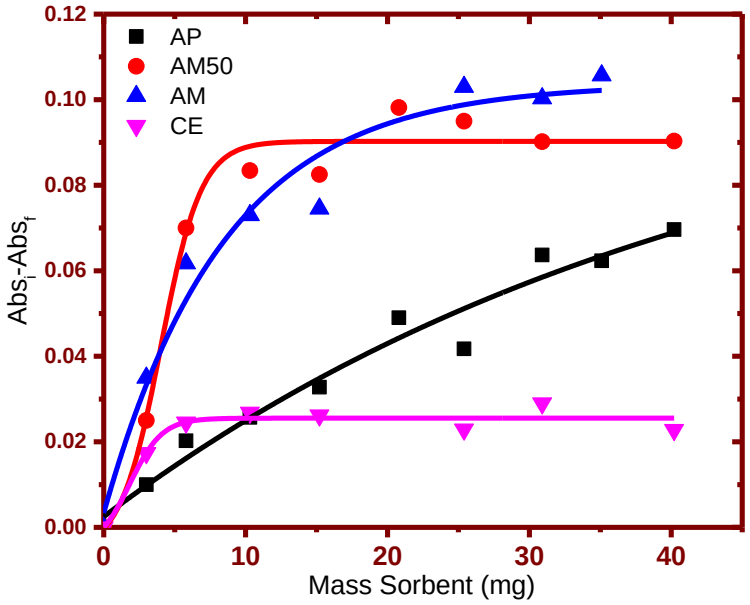

Figure A7.1 The decolorization isotherm of phenolphthalein dianion species in the presence of the various biopolymers with phenolphthalein dye at pH 10.5 in $NaHCO_3$ buffer.

Table A7.1 Spectroscopic Raman features of the different polysaccharides in variable compositions of ethanol and water (in 10% (w/w) D_2O).

Polysaccharide	HOD Band	25%W	50%W	75%W	100%W
AP	FWHM	-	85.48±0.023	74.73 ±0.018	59.49 ±0.032
	Height	-	0.5500±0.011	0.7000±0.012	0.1600±0.0070
	shift	**-**	**2488**	**2485**	**2474**
AM50	FWHM	89.69±0.041	89.40±0.036	117.53±0.013	54.99±0.021
	Height	0.1100±0.0041	0.2500±0.081	0.3200±0.0028	0.1300±0.0043
	Shift	**2480**	**2493**	**2499**	**2483**
AM	FWHM	105.1±0.023	122.7±0.019	87.17±0.013	68.85±0.018
	Height	0.1300±0.0022	0.2400±0.0027	0.8000±0.0092	0.2700±0.0058
	Shift	**2492**	**2494**	**2481**	**2480**
CE	FWHM	82.42±0.021	45.21±0.019	92.99±0.014	59.34±0.020
	Height	0.1100±0.0022	0.2900±0.010	0.5500±0.0063	0.2200±0.0060
	Shift	**2488**	**2482**	**2488**	**2479**

7. Appendix A (Chapter 8)

Table A8.1 Particle size distribution and estimation of different types of starch granules.

Types of starch	AM	AP	AM50
Particle size distribution (μm)	1.221	0.734	1.118

Table A8.2 Sample analysis of natural cellulose fiber. (Each assay was run in duplicate and was repeated if standard error was >3%).

Sample ID	CE
Ash (%)	0.00
Lignin (%)	0.10
Hemicellulose (%)	0.00
Cellulose (%)	99.90

Table A8.3 Water retention value of cellulose and its cross-linked forms.

Sample ID	Water Retention Value %
CE	55.92
Low CE-EPI	32.71
Medium CE-EPI	20.80
High CE-EPI	16.57

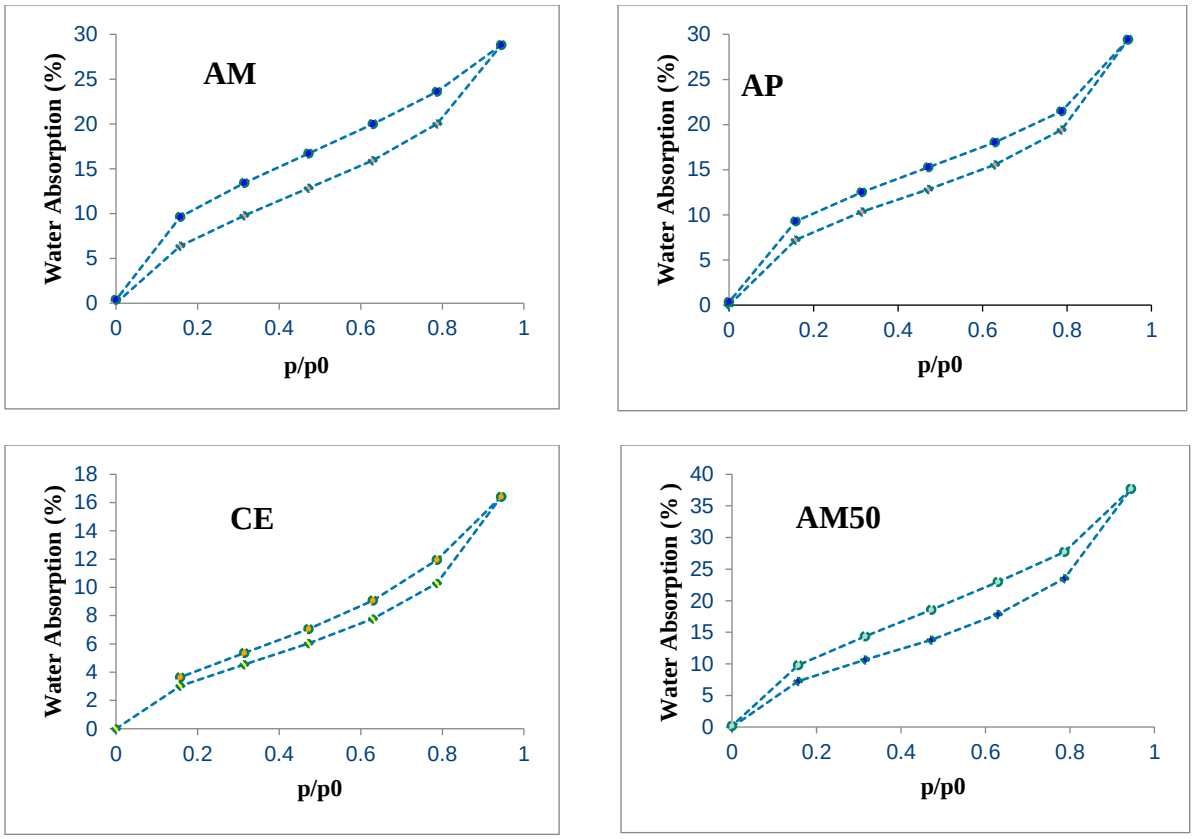

Figure A8.1 Water vapor adsorption isotherm for biopolymers at 298 K.

Table A8.4 Water vapor adsorption isotherm for biopolymers. (The parameters values represent best-fit values estimated from the BET model).

parameters	**AM**	**AP**	**CE**	**AM50**
Q_m (g/g)	9.390	8.370	4.050	14.42
K_{BET} (L/g)	13.02	29.17	14.50	13.79
C	1.380	1.320	1.250	1.500
R^2	0.9900	0.9900	0.9900	0.9900
Reduced Chi-Sqr	0.1700	0.3600	0.03500	0.2500
Surface Area (m^2/g)	329	239	142	506

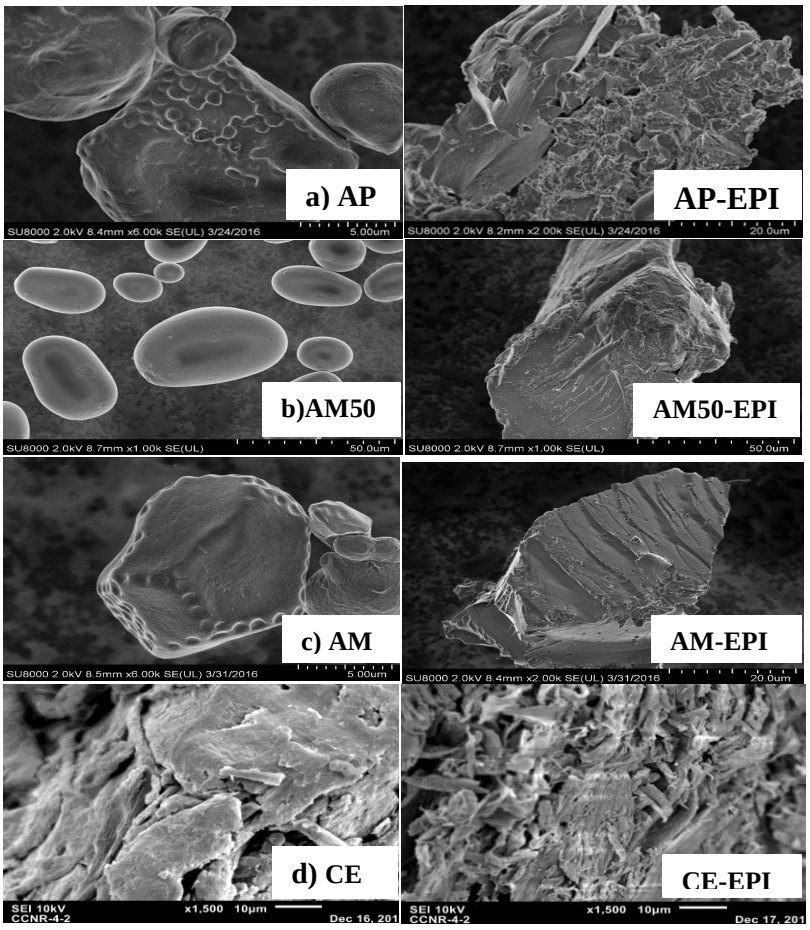

Figure A8.2 The SEM micrographs of the different starch materials and cellulose in the native and cross-linked form with epichlorohydrin (EPI).

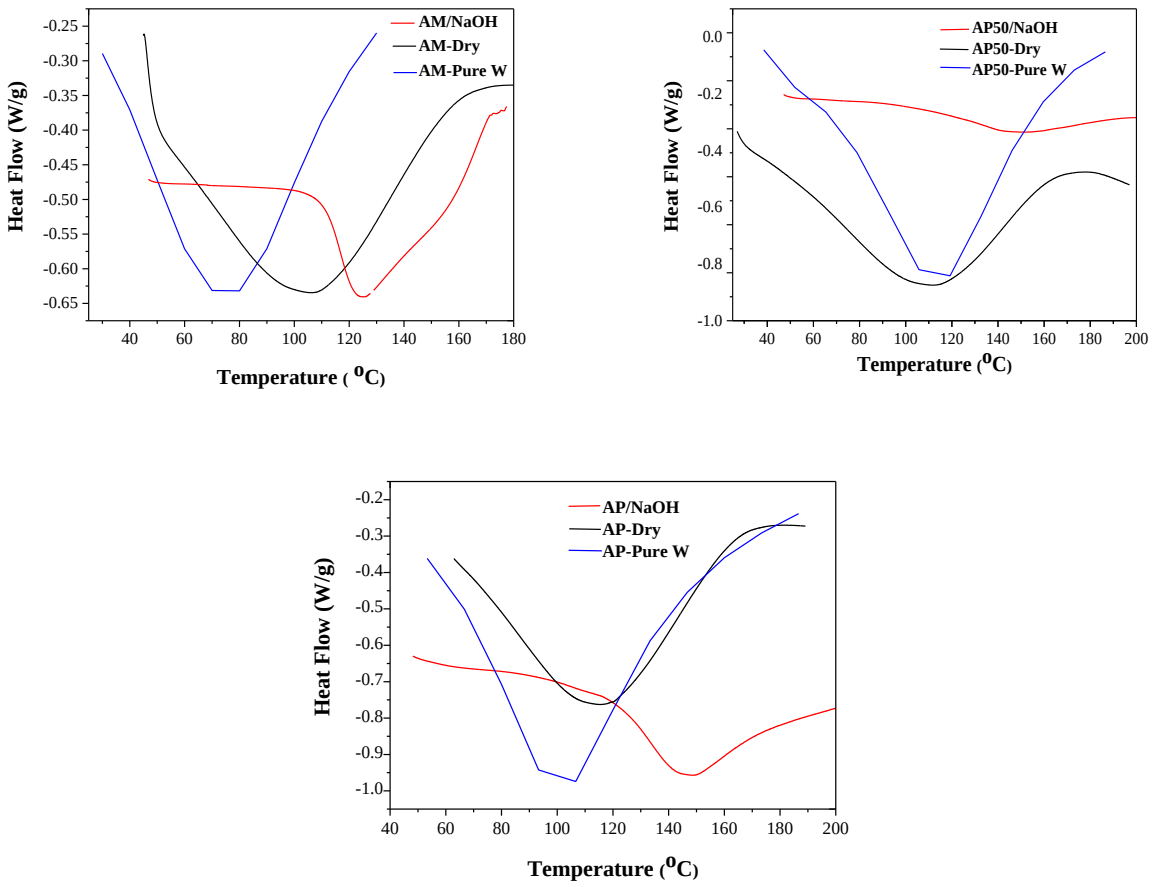

Figure A8.3 The DSC thermograms of the different starch materials in the presence and in the absence of solvent systems (H_2O, NaOH solution).

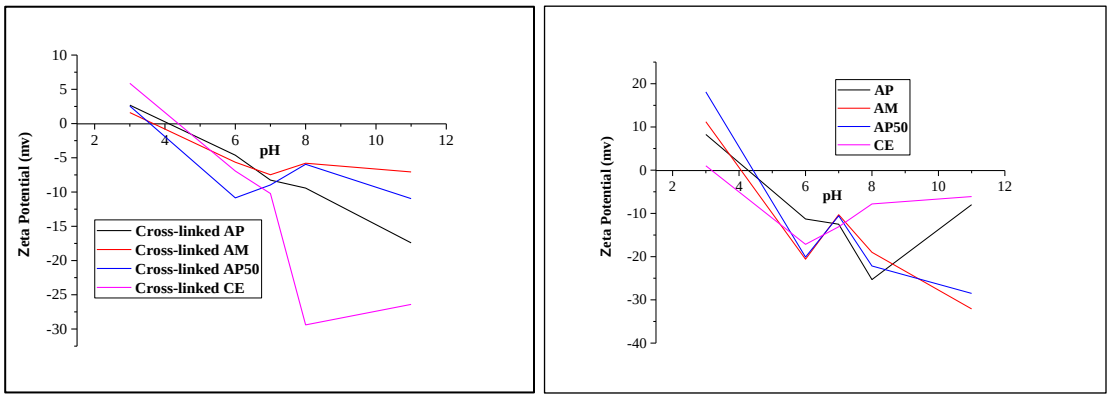

Figure A8.4 Point of zero charge (pzc) of A) polysaccharides and B) modified forms using aqueous sodium chloride at variable pH.

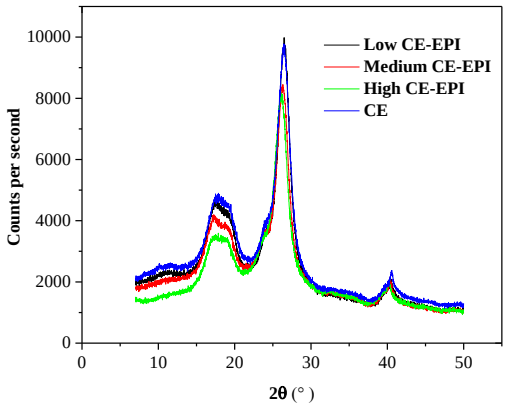

Figure A8.5 The XRD results of modified and unmodified cellulose.

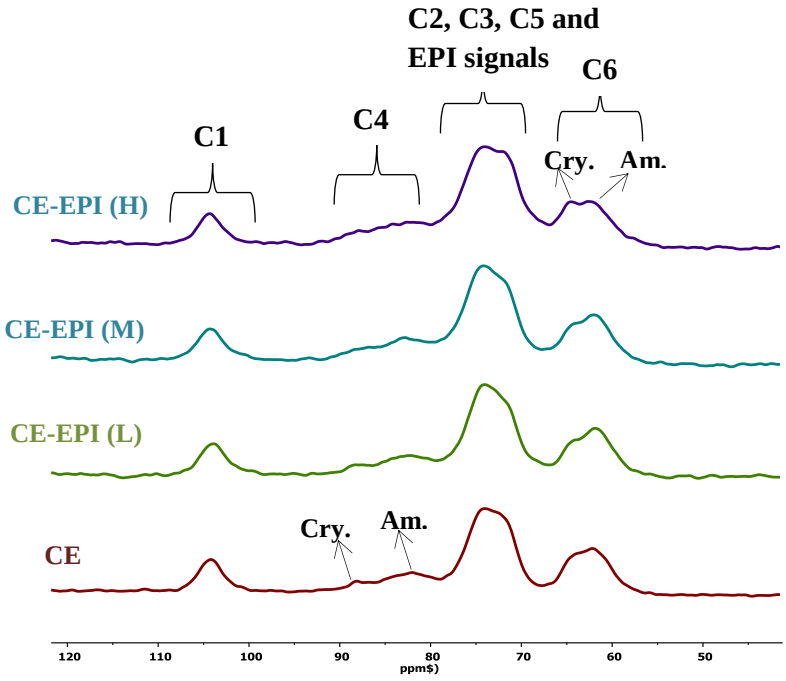

Figure A8.6 The ^{13}C solids CP-MAS NMR spectra of modified and unmodified cellulose (CE).[1-4] [The assignment of crystalline and amorphous domains is based on a literature assignment][3]

Table A8.5 Sample analysis of raw Miscanthus.
Note: Each assay was run in duplicate and was repeated if standard error was >3%.

Sample ID	Method Used	CE
Ash (%)	AOAC 942.05	2.30
NDF (%)	ANKOM Method 6	85.4
ADF (%)	ANKOM Method 5	60.9
Lignin (%) or ADL (%)	ANKOM 08/05	12.5
Hemicellulose (%)	NDF (%) – ADF (%)	24.4
Cellulose (%)	ADF (%) – ADL (%)	48.4

Table A8.6 Sample analysis of pretreated Miscanthus.
Note: Each assay was run in duplicate and was repeated if standard error was >3%.

Sample ID	Method Used	CE
Ash (%)	AOAC 942.05	0.00
NDF (%)	ANKOM Method 6	95.8
ADF (%)	ANKOM Method 5	89.3
Lignin (%) or ADL (%)	ANKOM 08/05	7.10
Hemicellulose (%)	NDF (%) – ADF (%)	6.50
Cellulose (%)	ADF (%) – ADL (%)	82.2

Experimental and methods

A8.7 Particle size Distribution and Zeta-Potential

The particle size and zeta potential measurement were obtained using a Malvern Zetasizer Nano ZS instrument (Malvern Instruments Ltd, Malvern, Worcestershire, UK). The size distribution of the samples were obtained by measuring the light scattered ($\theta = 173°$) by particles (dynamic light scattering, DLS) illuminated with a laser beam, using the CONTIN algorithm to analyze the decay rates that are a function of the translational diffusion coefficients of the particles, D. Size distribution values were derived from three measurements, each consisting of a minimum of ten individual runs.

Zeta potential caution measurements were based upon laser Doppler electrophoresis and phase analysis of light scattering.[5-7] The initial pH of the starch suspensions (40 mg starch in 7 mL) of adsorbent in Millipore water was adjusted over a range of values (pH 3–12) using HCl (0.01 M) or NaOH (0.01 M). After the equilibrium pH, aliquots of the suspension were taken for measurement of zeta potential. The reported zeta potential results are the average of three measurements, each derived from a minimum of ten individual runs.

A8.8 Chemical treatment of cotton linter cellulose fiber

Cellulose was considered using alkaline and acidic conditions to vary the content of cellulose, hemicellulose and lignin. Briefly, the cellulose from cotton linter was analyzed with a 1.2 N sulfuric acid solution at atmospheric pressure and 100 °C for 120 min to extract hemicellulose. Then, the acid was subjected to a 5% (w/v) NaOH solution at 100 °C for 100 min to remove lignin. Lignin isolation followed the method reported by Sluiter *et al.*[8] The cellulose from cotton linters was cold digested in a 72% (w/w) sulfuric acid at 30 °C for 1 h. Then, the suspension was transferred to a larger vessel with dilution reaching the concentration of acid to 4%, followed by digesting the solid fraction at 121 °C for 1 h. Finally, the solid fraction obtained after two stages of digestion was separated and considered as lignin to be studied for adsorption process.

A8.9 Water Retention Value

40 mg of cellulose and its modified forms were immersed in deionized water for 1 h until equilibrium, and then centrifuged (Precision Micro-Semi Micro Centricone, Precision Scientific Co.) at 4000 rpm for 1h. They were weighed (m_3), and next dried in a conventional oven at 105 °C. Finally, they were placed over night in a desiccator and weighed (m_4). Each measurement had triplicate and the water retention value was calculated using equation F8.2. Where WRV = water retention value in %, m_3 is the mass in g after centrifuging and m_4 is the mass in g after drying.

$$\%WRV = \frac{m_3 - m_4}{m_3} \times 100 \qquad \text{Equation A8.1}$$

A8.10 Adsorption Isotherms

Sorption Analyzer is a high resolution vapor sorption analyzer for precisely characterizing vapor-solid interactions. The measurements of adsorption isotherms were obtained using the Intelligent Gravimetric Analyzer system IGA-002 (Hiden Isochema, UK). 40 mg of the adsorbent sample was put in a stainless steel container, which was suspended to the balance. The sample was placed in thermostat reactor that allowed for achieving ultra-high vacuum. The IGA system basing on values of pressure inside the chamber automatically controlled the input and output valves in order to achieve the set point of pressure. After reaching equilibrium of the mass value, the IGA system passed to the next point of isotherm (next the set point of pressure). The temperature was held isothermally at 25°C and pressure was incremented by values of 10 mbar.

A8.11 Scanning Electron Microscopy

The morphology of Different types of starch and cellulose were examined using a Hitachi S-3400N SEM system, where the average diameter of the materials were calculated by the *Image J* software with a differentiation threshold set to be consistent with the image scale.

A8.12 Differential Scanning Colorimetry

The DSC thermograms acquired from starch or cellulose samples were equilibrated with known amounts of water. Biopolymer (*ca.* 20 mg) was added to 4 dram glass vials containing 7

ml of the solvent. The sample vials were incubated by shaking (Poly Science, Dual Action Shaker) for 24 h at 160 rpm at ambient pH and temperature to achieve equilibrium. Thereafter, the samples were separated from the solutions using a vacuum filter to obtain the solvated solids for analysis by DSC. The biopolymer/sodium hydroxide solutions have been prepared by dissolving 1 g of the samples in a 4 ml of sodium hydroxide (2 M) under mechanical stirring. The samples were added to DSC pans and sealed with a hole punched in the sample lid to allow for outgassing of vapour during heating over the temperature range 30 $^{\circ}$C – 150 $^{\circ}$C.

A8.13 X-ray Diffraction

The X-ray diffraction patterns of cellulose and cellulose-based materials were obtained using a PANalytical Empyrean powder X-ray diffractometer. A monochromatic Co−Kα1 radiation was used while the applied voltage and current were set to 40 kV and 45 mA, respectively. The samples were mounted in a horizontal configuration after evaporation of methanol films. The XRD patterns were measured in continuous mode over a 2θ range, where 2θ = 7−50° with a scan rate of 3.2° min^{-1}. The crystallinity index (CrI) was calculated from the height ratio between the intensity of the crystalline peak (I_{cr}) and amorphous peak (I_{am}).

A8.14 Solid state ^{13}C NMR spectroscopy

The ^{13}C solid state NMR experiments of the cellulose and its modified forms were done using a 4 mm DOTY CP-MAS probe on a Bruker AVANCE III HD spectrometer running at 125.77 MHz (^{1}H frequency at 500.23MHz) with magic angle spinning (MAS), where the sample rotation occurs about the axis orientated at a 54.7° angle with respect to the applied external magnetic field (B_o). The ^{13}C CP/TOSS (Cross polarization with Total Suppression of Spinning Sidebands) spectra were acquired using a 6 kHz spinning speed with a ramp pulse on the ^{1}H channel and a 1 ms contact time. The CP MAS experiments were acquired using the EASY pulse sequence[1] (removing background signal) at a spinning speed of 7.5 kHz. A ^{13}C 90°- pulse of 3.2 μs and a recycle delay of 20 s were used. 2800 – 3100 scans were accumulated for different samples. During data acquisition, all samples were recorded using a 71 kHz SPINAL-64 decoupling technique. The reference sample which is used in this experiment, is the low field signal of adamantane (38.48 ppm).

A8.15 Analysis of Miscanthus

The lignocellulosic composition was tested at the Department of Animal and Poultry Science Laboratory, University of Saskatchewan, Saskatoon, SK, Canada. In the analysis, total ash content was determined by AOAC standard method 942.05 (2000).[9] Lignin content, ADF and NDF were determined as per ANKOM method 08/05 (2005), ANKOM Method 5 (2006a) and ANKOM Method 6 (2006b) on a dry matter basis.[10] Cellulose content was calculated as ADF minus lignin content and hemicellulose content was calculated as NDF minus ADF.[11]

A8.16 Analysis of porosity and pore structure

Brunauer, Emmett, and Teller model which is an extension of the Langmuir model of monolayer adsorption to multilayer adsorption.[12] This model is used to quantify pore size and pore volume by assuming that pores are filled with liquid adsorbate, total pore volume can be derived from the amount of vapour adsorbed at a relative temperature. In equation A8.3, V_{ads} represents volume of adsorbed gas, V_{liq} is volume of liquid N_2 in pores V_m = molar volume of liquid adsorbate (N_2=34.7cm^3/mol), Pa is the ambient pressure, and T is the ambient temperature.

$$V_{liq} = \frac{P_a V_{ads} V_m}{RT} \qquad \text{Equation A8.3}$$

The average pore size can be estimated from the pore volume. Assuming cylindrical pore geometry (type A hysteresis) average pore radius (r_p) can be expressed as:

$$r_P = \frac{2\ V_{liq}}{S} \qquad \text{Equation A8.4}$$

Where S is the specific surface area (S) of the pores that obtained using the BET model.

A8.17 References

1. Lee, Sh-H.; Kim, M-J.; Park, H. *J. Appl. Polym. Sci.* **2010,** *117*, 623–628.
2. Lesas, C. H.; Pierre, M. Cross-linked cellulose fibers. U.S. Patent 4204055A, May.20, 1980.
3. Koo, S.H.; Lee, K.Y.; Lee, H.G. *Food Hydrocoll.* **2010,** *24*, 619–625.
4. Aloulou, F.; Boufi, S.; Labidi, J.; *Sep. Purif. Technol.* **2006,** *52*, 332–342.
5. Kirby, B. J.; Hasselbrink Jr, E. F. *Electrophoresis* **2004**, *25*, 187-202.
6. Vanerek, A.; Alince, B.; van de Ven, T.G.M. *J. Pulp and Paper Sci.* **2000,** 26(4), 135-139.
7. Yang, H.; Chen, D.; van de Ven, T. G.M. *Cellulose* **2015,** *22*, 1743–175.
8. Sluiter, A.; Hames, B.; Ruiz, R.; Scarlata, C.; Sluiter, J.; Templeton, D.; Crocker, D. Determination of Structural Carbohydrates and Lignin in Biomass Laboratory Analytical Procedure; National Renewable Energy Laboratory: Golden, CO, **2008.**
9. Official Method of Analysis of the Association of Official Analytical Chemists. 15th ed., **1990,** *70.* Arlington, VA, AOAC method 942.05—Ash in Animal Feeds. In: Helrick K, editor. Association of Official Analytical Chemists.
10. Official Method of Analysis of the Association of Official Analytical Chemists, 15th ed., **1990,** *82.* Arlington, VA, AOAC method 973.18—Fiber (Acid Detergent) and Lignin in Animal Feeds. In: Helrick K, editor. Association of Official Analytical Chemists.
11. Mani, S., L.G. Tabil and S. Sokhansanj. 2006. *Biomass Bioenergy* **2006,** *30*, 648-654.
12. Cole, D. R. *Rev. Mineral. Geochem.* **2015,** *80*, 61-164.

8. Appendix B

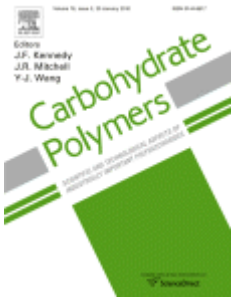

Title: Polysaccharide-based materials and their adsorption properties in aqueous solution
Author: Leila Dehabadi,Lee D. Wilson
Publication: Carbohydrate Polymers
Publisher: Elsevier
Date: 26 November 2014

Logged in as:
Leila Dehabadi
Account #: 3000975980
LOGOUT

Order Completed

Thank you for your order.

This Agreement between Leila Dehabadi ("You") and Elsevier ("Elsevier") consists of your license details and the terms and conditions provided by Elsevier and Copyright Clearance Center.

Your confirmation email will contain your order number for future reference.

Printable details.

License Number	4159570931706
License date	Jul 31, 2017
Licensed Content Publisher	Elsevier
Licensed Content Publication	Carbohydrate Polymers
Licensed Content Title	Polysaccharide-based materials and their adsorption properties in aqueous solution
Licensed Content Author	Leila Dehabadi,Lee D. Wilson
Licensed Content Date	Nov 26, 2014
Licensed Content Volume	113
Licensed Content Issue	n/a
Licensed Content Pages	9
Type of Use	reuse in a thesis/dissertation
Portion	full article
Format	both print and electronic
Are you the author of this Elsevier article?	Yes
Will you be translating?	No
Title of your thesis/dissertation	Development of biopolymers and their modified forms as sustainable sorbent materials
Expected completion date	Dec 2017
Estimated size (number of pages)	200
Requestor Location	Leila Dehabadi 110 Science place

	saskatoon, SK S7N 5C9 Canada Attn: Leila Dehabadi
Total	0.00 CAD

Title: Metal–organic frameworks for the control and management of air quality: advances and future direction

Author: Pawan Kumar,Ki-Hyun Kim,Eilhann E. Kwon,Jan E. Szulejko

Publication: Journal of Materials Chemistry A

Publisher: Royal Society of Chemistry

Date: Nov 17, 2015

Quick Price Estimate

The reuse of up to three figures is granted free of charge for academic/educational requestors. Payment is required for the reuse of four or more figures.

I would like to... reuse in a thesis/ dissertation

I am a/an... academic/ educational

The portion I would like to use is... figures/ tables/ images

Number of figures/tables/images requested 1

My format is... print and electronic

My distribution is 1

Field is required.

I will be translating... no

No content delivery. This service provides permission for reuse only. Once licensed, you may copy and paste the text-only portion of the content according to the terms of your license.

My currency is... USD - $

Quick Price Click Quick Price

QUICK PRICE CONTINUE

To request permission for a type of use not listed, please contact Royal Society of Chemistry contracts-copyright@rsc.org.

Copyright Clearance Center RightsLink®

Home Create Account Help

ACS Publications Most Trusted. Most Cited. Most Read.

Title: Nuclear Magnetic Resonance Investigation of the Fractionation of Water–Ethanol Mixtures with Cellulose and Its Cross-Linked Biopolymer Forms

Author: Leila Dehabadi, Lee D. Wilson

Publication: Energy & Fuels

Publisher: American Chemical Society

Date: Oct 1, 2015

LOGIN

If you're a copyright.com user, you can login to RightsLink using your copyright.com credentials.

Already **a RightsLink user** or want to learn more?

PERMISSION/LICENSE IS GRANTED FOR YOUR ORDER AT NO CHARGE

This type of permission/license, instead of the standard Terms & Conditions, is sent to you because no fee is being charged for your order. Please note the following:

- Permission is granted for your request in both print and electronic formats, and translations.
- If figures and/or tables were requested, they may be adapted or used in part.
- Please print this page for your records and send a copy of it to your publisher/graduate school.
- Appropriate credit for the requested material should be given as follows: "Reprinted (adapted) with permission from (COMPLETE REFERENCE CITATION). Copyright (YEAR) American Chemical Society." Insert appropriate information in place of the capitalized words.
- One-time permission is granted only for the use specified in your request. No additional uses are granted (such as derivative works or other editions). For any other uses, please submit a new request.